ADVANCES IN CHITIN SCIENCE

Volume XII

Organizers

Telma T. Franco
State University of Campinas, Brazil

Martin G. Peter
University of Potsdam, Germany
and
State University of Campinas, Brazil

ADVANCES IN CHITIN SCIENCE

Volume XII

Proceedings of the
5th Iberoamerican Chitin Symposium

06 – 09 June 2010
Santiago do Chile
– Extended Abstracts –

Organized by

Dr. Telma T. Franco

Professor of Chemical Engineering

V SIAQ Chair and President of SIAQ

State University of Campinas, Brazil

Dr. Martin G. Peter

Emeritus Professor of Natural Products

University of Potsdam, Germany

and

Visiting Professor

State University of Campinas, Brazil

Published by FEQ-UNICAMP

Campinas, Brazil, 2010

ISBN 978-85-64131-00-2

Preface

The 5th Symposium of the Sociedad Iberoamericana de Quitina (SIAQ) was held in Santiago do Chile, June 06 – 09, 2010. It was organized under the SIAQ presidency of Telma Franco, with Gustavo Cabrera (Santiago do Chile) as chairman, and Galo Cardenas (Concepcion), Paola Anaya (Los Angeles), and Edelio Taboada (Temuco) as members of the local organization committee. The recently founded private university "Aldofo Ibanez", located in beautifully designed buildings in the foothills of the Andes, not only offered splendid views over the city and the nearby snow-capped mountains, but also excellent auditoriums and technology available for the oral presentations.

Ca. 90 delegates attended the conference, with an impressive number of 29 students. Besides Spanish and Portuguese Iberian members of SIAQ, a few participants came from other European countries and also from Asia.

The scientific programme included six plenary lectures, 23 oral presentations and 111 posters, documenting the lively scientific activity of SIAQ. The topics were divided into classical thematic areas, i.e. production, enzymes, applications in the various areas, covering also nanotechnology and biomaterials. Plenary talks were given by D. Laurent (Lyon) on hydrogels, biomaterials, and tissue engineering, R.H Chen (Taipei) on kinetic reaction parameters and physicochemical properties of chitosan prepared with different regimes, C. Peniche (La Habana) on nanomaterials and applications in medicine, A. Heras (presented by B. Miralles, Madrid) on protein-chitosan composite materials, A. Gandini (Aveiro) on chitosan-cellulose composites, and S. Campana (Sao Carlos) on ultrasound deacetylation of chitin. Oral presentations and posters gave a comprehensive overview on production of chitin/chitosan from organisms of South and Central America, on fungal enzymes, preparation of various materials and applications in technology, food, medicine, and agriculture.

An invitation to authors to publish an extended abstract resulted in submission of 40 short manuscripts which are now presented in this Volume, *Advances in Chitin Science*, Vol. XII. We greatly acknowledge Rodrigo da Silveira Franco for valuable help in preparing the PDF web version.

Campinas, S.P., Brazil, August 2010

Telma T. Franco
franco@feq.unicamp.br

Martin G. Peter
Martin.Peter@uni-potsdam.de

Table of Contents

Plenary Lecture

Page

Degradation kinetics difference among sonolysis, microfluidization, and shearing treatment and the rationale of applying those physical methods in practical chitosan production 1
R.H. Chen, M.L. Tsai, L.Z. Tseng, C.H. Hsu

Sources, Production and Technological Processes

USAD process applied to β-chitin: influence of ultrasound irradiation on the resulting chitosan 9
J.A. de M. Delezuk, M.B. Cardoso, A. Domard, S.P. Campana-Filho

Characterization of chitin isolated from legs, pincers and carapace of *Aegla chol chol* crab 14
P. De Los Ríos, A. Hernández, P. Dantagnan, R. Oliva, E. Taboada, L. Becherán, P. Bernabé, M. Gidekel, G. Cabrera

Characterization of chitosan arising of waste exoskeleton shrimp 20
F.V.C. Kock, E.A Silva Filho, E.V.R. de Castro

Enzymology and Biochemistry, Biological and Ecological Aspects

Structure and function of glycoside hydrolase family 19 chitinases 24
W. Ubhayasekera

Evaluation of different protocols for isolation of chitin from the mushroom *Ganoderma lucidum* 30
S.P. Ospina, D.A. Ramírez, D.N. Mesa, D.M. Escobar, C.P. Ossa, L. Atehortúa, P. Zapata

Production and activity of chitinases and hydrophobins obtained from solid and liquid cultures of *Lecanicillium lecanii* 38
Z. Rocha-Pino, K. Shirai

Evaluation of antifungal activity of chitosan coating on cut apples by image analysis technique 42
O.B.G. Assis, D. de Britto

Chitosan production by S*yncephalastrum racemosum* using low cost media 47
A.C.L. Batista, M. Lopes, V.A. Santos, C.D.C. Albuquerque, R.V.S. Amorim, G.M. Campos-Takaki

Antifungal effect of chitosan on the growth of *Aspergillus parasiticus* and production of aflatoxin B1 52
O. Cota-Arriola, M.O. Cortez-Rocha, Y.L. López-Franco, A. Burgos-Hernández, E.C. Rosas-Burgos, M. Plascencia-Jatomea

Solid state fermentation for chitosan hydrolysing enzymes producing bioactive chitosan oligomers 56
T.L Honorato, F. Granuso, S. Rodrigues, B.M. Moerschbacher, T.T. Franco

Formulation of fermentation medium for aquatic species residues for the production of xanthan gum 64
E.C.A Reis, Y.L.F Maia-Araujo, C.B.Z. Oliveira, J.L. Rodrigues, J.C Cardoso, J.I. Druzian, F.F Padilha

Biotechnological process for the production of chitin from the fungus *Ganoderma lucidum* 68
S.P. Ospina, D.A. Ramírez, E.J. Obando, C.P. Ossa, L. Atehortúa, P. Zapata

Analysis of a polyelectrolyte complex formed with jicama pectin and water soluble chitosan 75
A.M. Ramos-de-la Peña, A.M. Rangel-Rodrigeuz, N. Balagurusamy, A. Carillo-Castillo, J.C. Contreras-Esquivel

Microbial treatment of shrimp waste for recovery of chitin and astaxanthin 80
P. Islas-Enríquez, M. Gimeno, E. Rodríguez-Huezo, K. Shirai

Potential of chitosan from *Mucor circinelloides* as alternative natural compound to inhibit *Aspergillus* 85
S.R. Cabral de Alcântara, T.C.M. Stamford, A.K. Nishida, N.P. Stamford, L. de Oliveira Franco, M.C. da Silva, G.M. Campos-Takaki

Chemical and Physicochemical Properties

Characterization by FT-IR of chitosan oligomers produced by enzymatic sequential treatments 89
E.M. Del Aguila, L.P. Gomes, C.I.R. de Oliveira, M.C. Silva, C.T. Andrade, J.T. Silva, V.M.F. Paschoalin

Physico-chemical characterization of chitosan from *Absidia corymbifera* 93
M.C.F. da Silva, T.C.M. Stamford, L.R.R. Berger, T.M. Stamford, S.R.C. de Alcântara, G. Campos-Takaki

Effects of starch gelatinization and oxidation on the rheological behavior of chitosan/starch blends 98
M.M. Horn, V.C.A. Martins, A.M.G. Plepis

Addition of chitosan to apple juice: a sanitising treatment before pasteurization. 103
F.A. Greco, M.A. Cubitto, M.S. Rodríguez

Chemical Modifications and Advanced Materials

Optimization of the *N,N,N*-trimethyl chitosan (TMC) synthesis by factorial design 106
D. de Britto, F.R. Frederico, O.B.G. de Assis

Jumbo squid collagen-chitosan composites 112
J.M. Ezquerra-Brauer, J.L. Arias-Moscoso, M. Plascencia-Jatomea, H. Soto-Valdez, R.L. Vidal-Quintanar, O. Rouzaud-Sández

New method for chitooligomers preparation by oxidative degradation 115
L. Albertengo, A. Debbaudt, M. Montero, M.S. Rodríguez

Applications in Life Sciences (Medicine, Pharmacy, Agriculture, Food, Biotechnology, Environment)

Chitosan coated nanoparticles for heparin administration: development and evaluation for asthma treatment 119
F.A. Oyarzun-Ampuero, J. Brea, M.I. Loza, D. Torres, M.J. Alonso

Hydrogel beads based chitosan employed in protein delivery systems 124
R. Torelli-Souza, J. Lopes-Ferreira, T. Batista-Lins, L. Monteiro, R. Amorim

Antimicrobial analysis of gels and films from chitosan and *N,N,N*-trimethyl chitosan 129
R.C. Goy, D. de Britto, O.B.G. Assis

Chitosan blend biofilms: structural analysis, mechanical properties, thermic stability, and fungistatic acitivity against *Aspergillus niger* 133
A.P. Martinez-Camacho, M.O. Cortez-Rocha, J.M. Ezquerra-Brauer, A.Z. Graciano-Verdugo, E.I. Diaz-Rojas, M. Plascencia-Jatomea

Extruded chitosan/polyethylene composite films: physicochemical and fungistatic properties 137
A.P. Martínez-Camacho, A.Z. Graciano-Verdugo, J.M. Ezquerra-Brauer, M.O. Cortez-Rocha, M.M. Castillo-Ortega, H.C. Santacruz-Ortega, M. Plascencia-Jatomea

Microspheres of chitosan conjugates covalently attached to steroids with potential biological activity as agrochemicals. 142
J. Pérez, R. Szopko, C. Schmidt, C. Peniche

Chitosan activity on *Ramularia cercosporelloides* isolated from infected safflower leaf in Mexico 149
E.A. Quintana-Obregón, M. Plascencia-Jatomea, M.O. Cortez-Rocha

Removal of 2,4-dichlorophenoxyacetic acid herbicide from water using chitosan 153
A. Nunes, A. Moura, M. Holanda, A.G.S. Prado

Use of inoculants with chitin for the bioremediation of hydrocarbon-contaminated soils 158
A. Gentili, M. Cubitto, M. Rodríguez

Immobilization of calcium oxide onto chitosan beads as a heterogeneous catalyst for biodiesel production 162
C.-C. Fu, T.-C. Hung, C.-H. Su, D. Suryani, W.-T. Wu, W.-C. Dai, Y.-T. Yeh

TiO_2 immobilized on microspheres of chitosan for heterogeneous photocatalysis of 2,4-dichlorophenoxyacetic acid herbicide from water 166
G.W. Tavares, M.S. Holanda, A.R. Nunes, A.O. Moura, A.G.S. Prado

Applications in Material Science (Biosensors, Composites, Textile, etc)

Chitosan intelligent film: a fast detection of H_2S 169
E.T. Kator Jr., C.M.P. Yoshida, T.T. Franco

Chitosan intelligent film: time-temperature indicator 176
V.B.V. Maciel, C.M.P. Yoshida, T.T. Franco

Effects of chitosan coating on kraft barrier properties 186
A.B. Reis, C.M. P. Yoshida, T.T. Franco

Effect of chitosan on growth and settlement of highbush blueberry plants 191
G. Cabrera, D. González, C. Silva, Y. Bernardo, M. Gidekel, J. Osorio, E. Taboada, J.C. Cabrera

Characterization of quaternized chitosan-stabilized iron-oxide nanoparticles as a novel potential MRI contrast agent for cell tracking 196
C.-R. Shen, S.-T. Wu, Z.-T. Tsai, T.-C. Yen, J.-S. Tsai, C.-L. Liu

Platelet lysate formulation based on chitosan for the treatment of buccal lesions: in vitro evaluation 200
C.M. Caramella, F. Ferrari, M.C. Bonferoni, S. Rossi, G. Sandri, M. Mori, C. Perotti, C. Delfante

Author Index

Albertengo, L. 115
Albuquerque, C.D.C. 47
Alonso, M.J. 119
Amorim, R. 124
Amorim, R.V.S. 47
Andrade, C.T. 89
Arias-Moscoso, J.L. 112
Assis, O.B.G. 42, 129
Atehortúa, L. 30, 68
Balagurusamy, N. 75
Batista, A.C.L. 47
Batista-Lins, T. 124
Becherán, L. 14
Berger, L.R.R. 93
Bernabé, P. 14
Bernardo, Y. 191
Bonferoni, M.C. 200
Brea, J. 119
Burgos-Hernández, A. 52
Cabral de Alcântara, S.R. 85
Cabrera, G. 14, 191
Cabrera, J.C. 191
Campana-Filho, S.P. 9
Campos-Takaki, G. 93
Campos-Takaki, G.M. 47, 85
Caramella, C.M. 200
Cardoso, J.C. 64
Cardoso, M.B. 9
Carillo-Castillo, A. 75
Castillo-Ortega, M.M. 137
Chen, R.H. 1
Contreras-Esquivel J.C. 75
Cortez-Rocha, M.O. 52, 133, 137, 149
Cota-Arriola, O. 52
Cubitto, M. 158
Cubitto, M.A. 103
da Silva, M.C. 85
da Silva, M.C.F. 93
Dai, W.-C. 162
Dantagnan, P. 14
de Alcântara, S.R.C. 93
de Assis, O.B.G. 106
de Britto, D. 42, 106, 129
de Castro, E.V.R. 20
De Los Ríos, P. 14
de Oliveira Franco, L. 85
de Oliveira, C.I.R. 89
Debbaudt, A. 115
Del Aguila, E.M. 89
Delezuk, J.A. de M 9
Delfante, C. 200
Diaz-Rojas, E.I. 133
Domard, A. 9
Druzian, J.I. 64
Escobar, D.M. 30
Ezquerra-Brauer, J.M. 112, 133, 137
Ferrari, F. 200
Franco, T.T. 56, 169, 176, 186
Frederico, F.R. 106

Fu, C.-C. 162
Gentili, A. 158
Gidekel, M. 14, 191
Gimeno, M. 80
Gomes, L.P. 89
González, D. 191
Goy, R.C. 129
Graciano-Verdugo, A.Z. 133, 137
Granuso, F. 56
Greco, F.A. 103
Hernández, A. 14
Holanda, M. 153
Holanda, M.S. 166
Honorato, T.L. 56
Horn, M.M. 98
Hsu, C.H. 1
Hung, T.-C. 162
Islas-Enríquez, P. 80
Kator Jr., E.T. 169
Kock, F.V.C. 20
Liu, C.-L. 196
Lopes, M. 47
Lopes-Ferreira, J. 124
López-Franco, Y.L. 52
Loza, M.I. 119
Maciel, V.B.V. 176
Maia-Araujo, Y.L.F. 64
Martinez-Camacho, A.P. 133, 137
Martins, V.C.A. 98
Mesa, D.N. 30
Moerschbacher, B.M. 56
Monteiro, L. 124
Montero, M. 115
Mori, M. 200
Moura, A. 153
Moura, A.O. 166
Nishida, A.K. 85
Nunes, A. 153
Nunes, A.R. 166
Obando, E.J. 68
Oliva, R. 14
Oliveira, C.B.Z. 64
Osorio, J. 191
Ospina, S.P. 30, 68
Ossa, C.P. 30, 68
Oyarzun-Ampuero, F.A. 119
Padilha, F.F. 64
Paschoalin, V.M.F. 89
Peniche, C. 142
Pérez, J. 142
Perotti, C. 200
Plascencia-Jatomea, M. 52, 112, 133, 137, 149
Plepis, A.M.G. 98
Prado, A.G.S. 153, 166
Quintana-Obregón, E.A. 149
Ramírez, D.A. 30, 68
Ramos-de-la Peña, A.M. 75
Rangel-Rodrigeuz, A.M. 75
Reis Elisiane, C.A. 64
Reis, A.B. 186
Rocha-Pino, Z. 38
Rodrigues, J.L. 64

Rodrigues, S. 56
Rodríguez, M.S. 103, 158, 115
Rodríguez-Huezo, E. 80
Rosas-Burgos, E.C. 52
Rossi, S. 200
Rouzaud-Sández, O. 112
Sandri, G. 200
Santacruz-Ortega, H.C. 137
Santos, V.A. 47
Schmidt, C. 142
Shen, C.-R. 196
Shirai, K. 38, 80
Silva Filho, E.A. 20
Silva, C. 191
Silva, J.T. 89
Silva, M.C. 89
Soto-Valdez, H. 112
Stamford, N.P. 85
Stamford, T.C.M. 85, 93
Stamford, T.M. 93
Su, C.-H. 162
Suryani, D. 162
Szopko, R. 142
Taboada, E. 14, 191
Tavares, G.W. 166
Torelli-Souza, R. 124
Torres, D. 119
Tsai, J.-S. 196
Tsai, M.L. 1
Tsai, Z.-T. 196
Tseng, L.Z. 1
Ubhayasekera, W. 24
Vidal-Quintanar, R.L. 112
Wu, S.-T. 196
Wu, W.-T. 162
Yeh, Y.-T. 162
Yen, T.-C. 196
Yoshida, C.M.P. 186, 169, 176
Zapata, P. 30, 68

Species Index

Absidia corymbifera 93
Aegla chol chol 14
Agaricus bisporus 68
Anomalocardia brasiliana 64
Aspergillus flavus 85
Aspergillus fumigates 85
Aspergillus niger 85, 133, 137
Aspergillus ochraceus 85
Aspergillus parasiticus 52, 85
Crassostrea brasiliana 64
Escherichia coli 75
Fusarium oxysporum 56
Ganoderma lucidum 30, 68
Grifola frondosa 68
Kluyveromyces marxianus 103
Lactobacillus spp. 80
Lecanicillium lecanii 38
Lentinus edodes 68
Litopenaeus vanamei 80
Loligo sp 9
Lucina pectinata 64
Mucor circinelloides 85
Pachyrhizus erosus 75
Panulirus argus 142
Ramularia cercosporelloides 149
Rhodococcus corynebacterioides 158
Saccharomyces cerevisiae 89
Solenocera prominentis 1
Staphylococcus aureus 75
Syncephalastrum racemosum 47
Trichoderma harzianum 56
Trichoderma polysporum 56
Ucides cordatus 64
Verticillium fungicola 38
Vitis vinifera L. 89
Xanthomonas campestris 64

Subject Index

2,4-D 166
2,4-D adsorption 153
Aflatoxin B1 52
agrochemical 142
amino-oligosaccharides 56
anthocyanin 176
Antibacterial activity 129
Antifungal activity 42
antifungal property 85
Apple Juice 103
Asthma 119
barrier properties 186
Bioaugmentation 158
Biodegradable 169
Biodiesel 162
Biopolymer 20, 93
Biotechnological Process 68
Bivalve 64
BSA 124
by-products 112
Calcium oxide 162
Carboxymethyl-β-cyclodextrin 119
Cassava wastewater 47
cell tracking 196
Chitin 14, 20, 30, 68, 80, 89, 158
chitin deacetylase 89
chitinase 89
chitinases 38
chitooligomers 115
Chitosan 9, 20, 42, 47, 52, 85, 98, 103, 112, 115, 119, 124, 129, 153, 158, 162, 166, 186
chitosan blend films 137
chitosan conjugates 142
Chitosan film 169, 176
chitosan intelligent films 176
chitosanases 56
chitosans 89
coating 186
collagen 112
colloidal chitin 38
Colorimetric indicator 169
contrast agent 196
Corn steep liquor 47
Crustacea 64
crystallographic properties 93
Deacetylation 9, 89, 93
Degree of deacetylation 20
delivery systems 124
drug delivery 142
Edible coating 42
Endochitinase 24
Enzyme mechanism 24
extrusion 137
factorial design 106
Fermentation 64, 80
films 112
food preservative 85
FT-IR spectroscopy 89
fungal pathogen 85

Fungal Source 68
Fungi 149
glass transition temperature 133
GPC 106
Hyaluronic acid 119
Hydrocarbon-degrading bacteria 158
hydrogel 124
hydrogen peroxide 115
hydrophobins 38
Immobilization 158, 162
Intelligent packaging 169
Inverting mechanism 24
iron-oxide 196
jumbo squid 112
Kraft paper 186
lactic acid bacteria 80
lipid 186
Loop movements, 24
low density polyethylene 137
Mastocytes 119
microfludization 1
microwave irradiation 115
Minimally processed fruit 42
molecular weight 1, 106
MRI 196
Mycelial Biomass 30
N,N,N-trimethyl chitosan 106
Nanoparticles 119
nanoparticles 196
oxidation 98
pectic substances 75
photodegradation 166
physical methods 1
pomace 75
Primacor 1430 137
Protein content 14
quaternized chitosan 196
radial growth 133, 149
Rheology 64, 98
Sanitizing Procedure 103
Scanning Electron Microscopy 14
Serum milk 47
shearing 1
Shrimp 20
shrimp shells 56
shrimp waste 80
Soil bioremediation 158
solid culture 38
sonolysis 1
sorbitol 133
spore diameter 133
spores 149
starch 75, 98
steroids 142
Submerged Culture 30
synthesis optimization 106
thermal analysis 93
Thermogravimetry 14
time-temperature indicators 176
Ultrasound 9
USAD process 9
viscosity 149

water solubility 115
Water-soluble chitosan 129
β-Chitin 9

Degradation kinetic differences among sonolysis, microfluidization, and shearing treatment, and their application in practical chitosan production

Rong Huei Chen,[1,2*] Min Lang Tsai,[1*] Lan Zang Tseng[1] and Chu Hsi Hsu[1,3]

[1] Department of Food Science, National Taiwan Ocean University, 2 Pei-Ning Road, Keelung 20224, Taiwan
[2] R & D Center, Seaparty International Co., LTD, Rm 201, 2F, Building B, Huang Kong Street, Keelung, 20248. Taiwan.
[3] Department of Food and Beverage Management, Yuanpei University, 306, Yuanpei Street, Hsinchu 30015, Taiwan
*E-mail: rhchen@mail.ntou.edu.tw, tml@mail.ntou.edu.tw

Abstract
Solution concentration, temperature, reaction time, and use or nonuse of concurrent ultrafiltration treatment for fragment removal are factors that affect the degradation rate constant in sonolysis, microfluidization, and shearing treatments. The cause of these operation conditions and their effect on the chitosan degradation rate constant were compared. Conditions studied for each treatment resulted in various solution viscosities, ease in dissipation of cavitation, entanglement and stretching, in turn resulting in different rates of effectiveness of degradation by different degradation mechanisms. The reasons for applying these physical methods in practical chitosan production was proposed.

Keywords: physical methods; sonolysis; microfluidization; shearing; molecular weight

INTRODUCTION

The functional properties of chitosan such as rheological properties,[1,2] antimicrobial capability,[3-6] antioxidation activity,[7,8] immunoadjuvant activity,[9,10] hypercholesterolemic activity,[11,12] blood coagulation activity[6,13] etc. depend on intrinsic factors such as molecular weight (MW), polydispersity, degree of deacetylation (DD), distribution of acetyl groups, etc.[2,14] Therefore, it is important to develop an easy method to manipulate the MW while preserving their integrated structure, and to be able to scale up for mass production.

Chitosans of different MWs are usually prepared by different methods, including: chemical method acid hydrolysis[15-17] or alkali hydrolysis,[18] and the oxidative degradation method.[19-21] Acid or alkali treatment at elevated temperatures is a very common, effective method used to produce various MWs and DDs in chitinous materials. However, acid or the alkali depolymerization procedure creates environmental problems.[20] The enzymatic method uses chitinase or chitosanase in hydrolyzing higher MW chitin or chitosan, respectively, to smaller MW ones.[22-26] Physical methods are energy-saving, environmentally friendly, and effective methods, including: the ultrasonic method,[27-32] the microfluidization method,[33-35] and mechanical shearing.[36-40] High energy radiation of an X-ray or γ-ray has been reported.[41,42] Chemical methods are difficult to manipulate with the MWs of resultant chitosan. Enzymatic methods cannot be feasible for use in mass production, whereas the physical methods have the advantages of low cost, ease of access and operation, and it is apparently suitable in mass production with relative efficiency.

The mechanism of a microfluidization process accelerated the solution stream to a very high speed and forced it into a reaction chamber with high pressure air. The process stream separates into two, changes direction, and collides forming a single stream again, generating a powerful shear force, turbulence, impaction, and cavitation forces. Those forces cause the disintegration of the particles or the degradation of the polymers.[34,43,44] Microfluidization has

been applied in cell rupture, homogenization or preparing the unilamellar vesicle.[45] Kasaai et al.[34] reported that chitosan degraded by a microfluidization process will narrow the polydispersity of the resulting product. The DD of the resulting chitosan increased when 0.1 M of acetic acid was used as a solvent, whereas the DD of the resulting chitosan did not change when 0.04 M of hydrochloric acid was used as a solvent. They revealed that the average number of chain scissions increased with increased operational pressure. This may be because increasing the operational pressure enhances the fluid velocity and increases the energy flow, thereby enhancing the efficiency of degradation.

The mechanism of sonolysis dissipates ultrasonic energy into the solution, resulting in cavitations. Cavitation produces vibrational wave energy, shear stresses at the cavitation interphase, and local high pressure and temperature. These are the major factors causing the degradation of polymers.[46] Popa-Nita[32] reported the distribution of ultrasound waves depends on the geometries in the reactor. The separated "active zones" were located in the axial direction (parallel to the probe), however, in the radial direction (perpendicular to the probe) the intensity of the ultrasound waves decreased steeply. In general, the configuration of the reactor (liquid level, immersed probe height, probe and reactor diameter, etc.) is a key factor in determining energy distribution. The rate constant increased with the input power- the probe diameter; while it decreased with the solution concentration- the reactor diameter.

The mechanism of the polymer shearing degradation proposed is such that during the high rate of shearing, the strong elongated flow encountered by the polymer may bring sufficient energy to disrupt the molecules.[39] Besides, the polymer shearing along the direction of the shearing flow, Casale and Porter[47] reported that the entangled molecules facilitated the degradation reaction during the shearing treatment; therefore, the length of the polymer has to be long enough to be entangled and stretched by the shear force.[48] Muzzarelli[36] reported that mechanical shearing can be used to prepare special MW chitosan, and the polydispersity was narrowed. Austin et al.[37] employed mechanical shearing and a chemical method to prepare microcrystalline chitin. Chen et al.[38] reported that chitosan was degraded by mechanical shearing at different shear rates, reaction temperatures, chitosan concentrations, and shear time; polydispersity was narrowed.

MATERIALS AND METHODS

Chitosan preparation: Chitin was prepared from shrimp (*Solenocera prominentis*) waste via a modified method by Stanley et al.[49] and Chen et al.[50]

Mechanical shearing: The shearing treatment referred to methods of Tsai et al.[40]

Ultrasonic treatment: The ultrasonic treatment referred to methods of Tsaih et al.[30]

Microfluidization treatment: The microfluidization treatment referred to methods of Tsai et al.[35]

Concurrent removal of smaller degraded molecules during mechanical treatments: The concurrent removal of small fragments with UF during mechanical treatment referred to methods of Tsai et al.[30,35,40]

Molecular weight determination: MW were determined by HPSEC.[51]

Rate constant calculation: The rate constant of degradation reaction referred to methods of Tsai et al.[30,35,40]

RESULTS AND DISCUSSION

Effect of operation conditions on the degradation rate constant

Solution concentration: Results in Fig. 1 show that the rate constant increase is inversely proportional to the solution concentration in all three different physical methods, at different solution temperatures studied, and with or without concurrent UF treatment for removal of degraded fragments during treatments. This is because the degradation energy received by

each molecule during treatment is inversely proportional to the solution concentration. The energy received by each chitosan molecule is less in higher concentration solutions than that in lower concentration ones. It may also be because the higher the solution concentration, the higher the solution viscosity. A high viscous solution retards the cavitation formation and transportation,[52] or shearing effect, therefore rendering the higher concentration solution to have a lower degradation rate constant.

However, from the mass production point of view, solutions of the highest concentrations possible have to be used to decrease costs by shortening the total operation time, and lessening the facility, utility, and labor costs. Fig. 2 shows the effect of chitosan concentrations on the degrading efficiency of different physical methods at their optimal solution temperatures. The degradation efficiencies were 3.0, 4.1, and 5.1 times higher for 0.8%, 1.4% and 2.0% solutions respectively, compared to a 0.2% solution for microfluidization treatment at 30°C. With the same range of concentration elevation, the efficiency increases were 2.4, 3.6, and 3.8 times greater for ultrasonic treatment at 30°C. For mechanical shearing at 50°C, the efficiency increases were 2.8, 3.1, and 3.6 times higher with the same range of concentration elevations. The results showed that the higher the concentration of chitosan solution used, the better the degradation efficiency that resulted in the concurrent UF treatment. Among the three physical methods studied, the microfluidization treatment resulted in the highest efficiency by using higher solution concentrations.

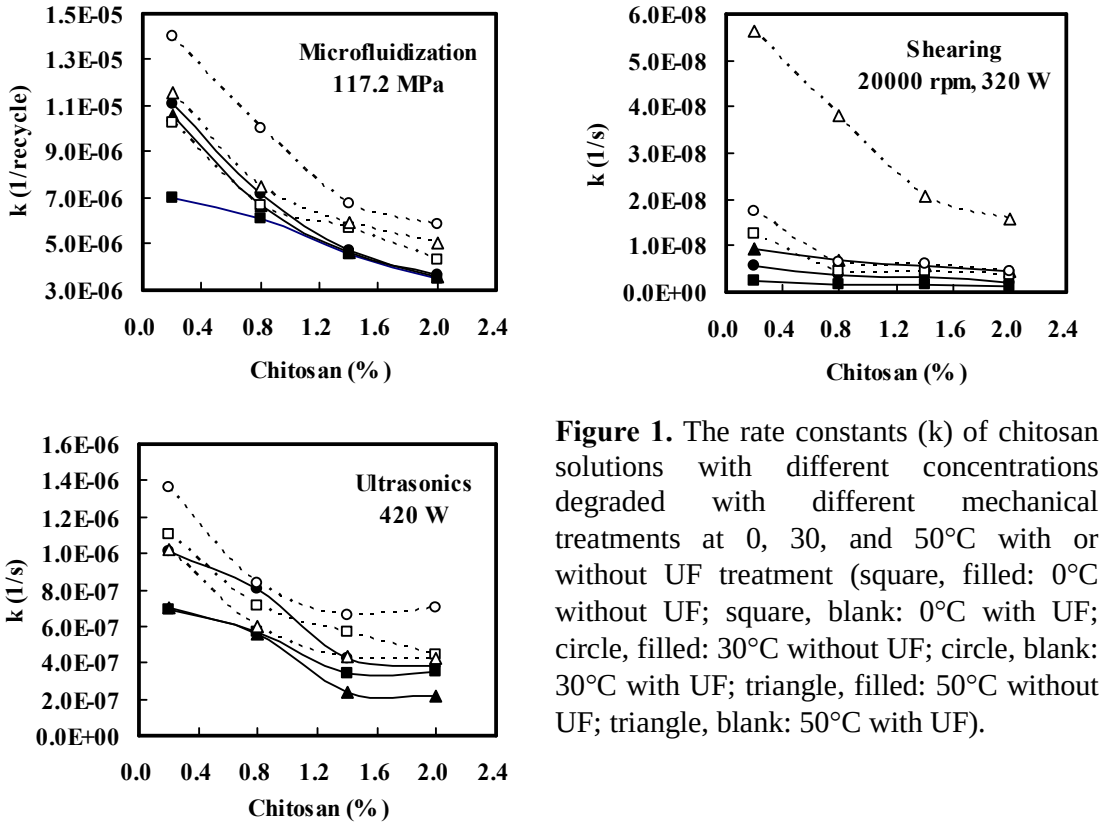

Figure 1. The rate constants (k) of chitosan solutions with different concentrations degraded with different mechanical treatments at 0, 30, and 50°C with or without UF treatment (square, filled: 0°C without UF; square, blank: 0°C with UF; circle, filled: 30°C without UF; circle, blank: 30°C with UF; triangle, filled: 50°C without UF; triangle, blank: 50°C with UF).

Solution temperature: Results in Fig. 1 and Fig. 3 show the rate constants increased with solution temperatures for those degraded with mechanical shearing, with or without concurrent UF treatment, between 0 and 50°C. However, the rate constant was higher for those treated at 30°C than those treated at 0 or 50°C, with or without concurrent UF treatment

by ultrasonic or microfluidization treatments.

This may be due to different disintegration mechanisms of chitosan molecules by different mechanical treatments. Cavitation energy resulting from ultrasonic energy dissipation in solution[46] is from ultrasonic treatment. Entanglement and stretch effects is from shearing.[39,47] Whereas, entanglement and stretch effects plus cavitation energy is from a microfluidization process.[43-45] Therefore, the rate constant was higher for those treated at 30°C than those treated at 0 or 50°C for both ultrasonic or microfluidization treatments, because of an elevated temperature, facilitating the loss of cavitationalenergy.[28,53] Therefore, reaction rates were higher at 30°C than at 50°C. Lii et al.[52] reported that highly viscous solutions hindered the effect of cavitation energy because solutions at lower temperatures had viscosities higher than those at higher-temperatures, thus the reaction rate at 0°C was lower than that at 30°C. The rate constant did not differ significantly between the earlier and later periods at three solution temperatures studied in ultrasonic treatment. However, in the microfluidization treatment, the rate constant differed significantly between the earlier and later periods at the three solution temperatures studied. Results indicate that the facilitated effect of entanglement and tearing of high MW species resulted in a pronounced increase in rate constant in earlier stages of microfluidization treatment. However, in earlier stages of ultrasonic treatment it did not show any facilitated effect of entanglement and tearing of high MW species. The difference indicates entanglement and stretch effects plus cavitation energy contribute to the microfluidization process, however, only cavitation energy contributes to ultrasonic treatment.

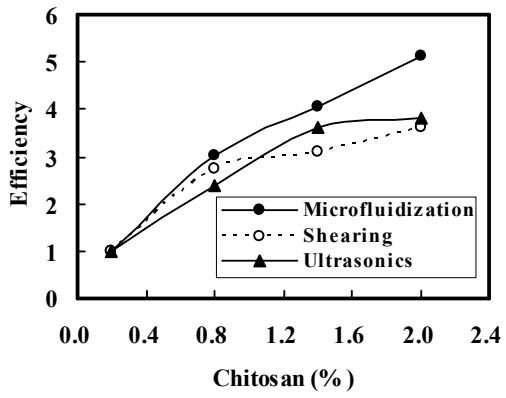

Figure 2. Effect of chitosan concentration on degraded efficiency of microfluidization (30°C), ultrasonics (30°C), and Shearing (50°C) treatments combined with UF treatment.

The degradation rate constant increased along with increasing solution temperatures for all solution concentrations studied, with or without concurrent UF treatment in shearing treatments. Results indicate the contribution of acid hydrolysis occurred at higher solution temperatures.[40]

Reaction time: Results in Fig. 3 show that the degradation rate constant in the earlier period ($k_{0,5}$, first 5 cycle) is significantly higher than that in the middle and/or in the later period ($k_{5,25}$, the 5^{th} to 25^{th} cycle) either with or without concurrent UF treatment by microfluidization treatment. Kasaai et al.[34] reported similar result,s this may be because in the earlier stages (higher degradation rate), the rate constant was the sum of the results of cavitation, free radical effect, and entanglement tearing force. However, in the later stages (lower degradation rate), the rate constant was the sum of the results of cavitation and free radical effect only[40], because the higher MW chitosan species were consumed in the earlier stage. The mechanism of polymer entanglement tearing most likely occurred in the earlier state of degradation during the high rate of shearing, via the strong elongated flow encountered by the polymer which may entail sufficient energy to disrupt the molecules.[47]

The results indicate that entanglement plus cavitation/free radicals are major contributions to the degradation of the polymer during earlier periods of microfluidization.
Without concurrent UF treatment, the degradation rate constants are not significantly different between the earlier period and later period of a shearing treatment. The results imply the entanglement and stretch are the only players in disintegrating the molecule during shearing. However, with concurrent UF treatments, the rate constant of those in the later period was higher than those at the beginning period of shearing treatment. This may be due to the detrimental effect of lowering the mass transfer coefficient by concurrent UF treatments overweighing the facilitating effect of increasing the concentration of high MW species remaining in the retention. The higher MW species increase the viscosity of the solution and reduce the mass transfer coefficient during concurrent UF treatments.
Results show that the degradation rate constant at the beginning period ($k_{0,1}$) are not significantly different than that of the later period ($k_{1,2.5}$) for either with or without concurrent UF treatment, at three temperatures studied by sonolysis treatment. The result implies only the cavitation and free radical contribution to the degradation reaction during sonolysis.

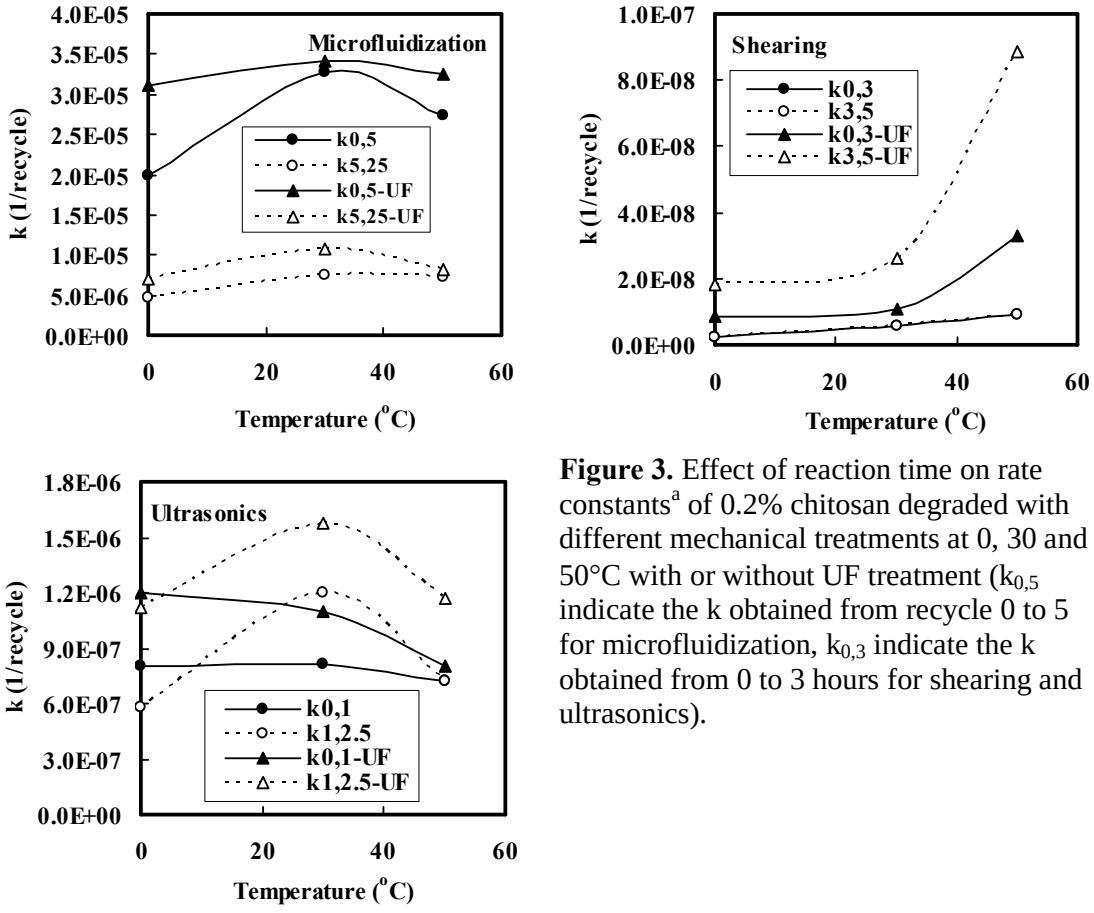

Figure 3. Effect of reaction time on rate constants[a] of 0.2% chitosan degraded with different mechanical treatments at 0, 30 and 50°C with or without UF treatment ($k_{0,5}$ indicate the k obtained from recycle 0 to 5 for microfluidization, $k_{0,3}$ indicate the k obtained from 0 to 3 hours for shearing and ultrasonics).

Facilitated by concurrent UF treatment

Data in Fig. 4 shows the rate constant of 0.2% to 2.0% chitosan solutions treated with microfluidization at 0, 30, and 50°C with concurrent UF treatment increased from 1.1 to 1.6 times higher than that without UF treatment. The rate constant for 0.2% to 2.0% chitosan solutions was increased between 1.0 to 2.0 times by sonolysis at 0, 30, and 50°C with UF treatment than without UF treatment. The rate constant for 0.2% to 2.0% chitosan solutions

increased between 1.8 to 6.0 times by mechanical shearing. In general, the facilitate effect was more pronounced for higher concentrated solutions with sonolysis or microfluidization treatment. Results also indicated the enhancing effect was more prominent for lower concentrated solutions with shearing treatment/UF than for sonolysis/UF or microfluidization/UF treatment. Results indicate the degradation through the entanglement and tearing occurred more frequently among higher chain length species (earlier stage), however degradation through cavitation or free radical occurred with an equal chance among long or short chain length species (earlier and later stages).

Energy saving strategy

A combined method of using mechanical shearing/UF treatment at 50°C during the earlier stage and microfluidization/UF treatment at 30°C at a later stage is proposed for industrial scale production of chitosan. The proposed method has the merits of a MW of chitosan, is able to be controlled, can save input energy, and will have a relatively high efficiency. The reasons are as follows:

A decrease in solution viscosity limits the undesirable color changes as well as enhancing acid hydrolysis reactions accompanied by increasing temperatures to 50°C, thus improving the degradation rate constant for mechanical shearing/UF treatment at 50°C in earlier stages. Decreased solution viscosity will enhance the inter-molecular entanglements to elevate the tearing efficiency and increase the degradation rate, thus saving in operational costs. The highest ratio of "with concurrent UF treatment" to "without concurrent UF treatment" in the earlier periods of mechanical shearing was superior to the other two treatments (Fig. 4) and is another reason to propose shearing/UF treatment at 50°C at earlier stages.

The reason for using microfluidization/UF treatment at 30°C at later stages is that the detrimental effects of high viscous solutions (due to high concentration and high MW of solute) on the cavitational effects in the earlier periods of microfluidization/UF treatment no longer exist. Besides, the proportion of high MW species inside the reactor is not high enough to generate high effective shearing reaction (reason to shift to microfluidization/UF, at 30°C). The rate constant of microfluidization/UF treatment at 30°C was higher than that at 0, or 50°C for ultrasonic or microfluidization treatment (Fig. 1 and Fig. 3) and we can avoid the discoloration problem. Data in Fig. 2 shows that enhancing efficiency of using microfluidization/UF at 30°C is significantly higher than that for ultrasonic/UF at 30°C. This is another reason to propose microfluidization/UF for the later periods of operation.

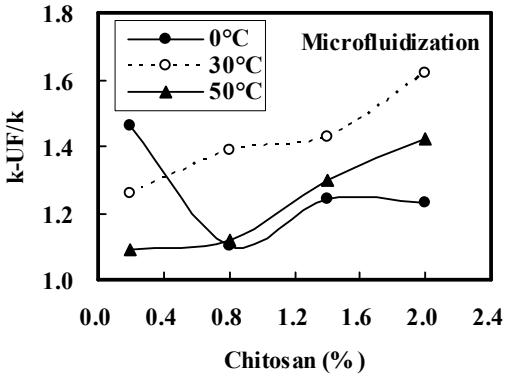

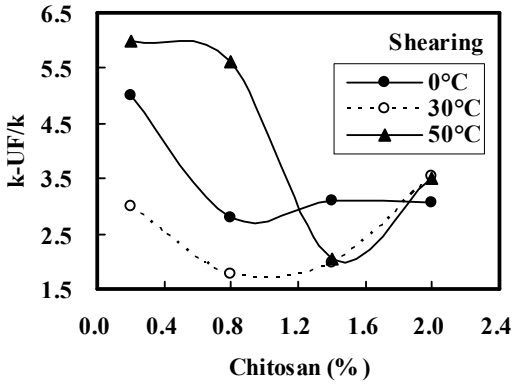

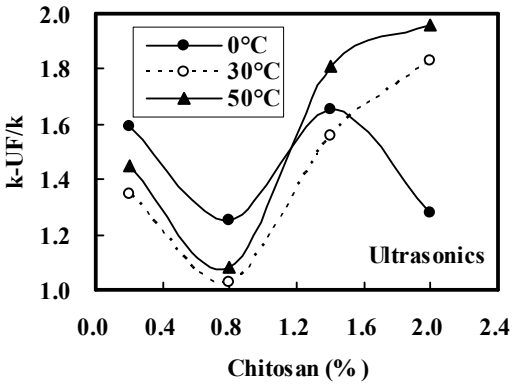

Figure 4. The ratios of rate constants (k-UF/k) of different concentrations of chitosan solutions degraded with different mechanical treatments with or without UF treatment at 0, 30, and 50°C

CONCLUSIONS

Degradation mechanisms among the three physical methods studied are all different - entanglement and stretch for shearing, cavitation for sonolysis, entanglement and stretch plus cavitation for microfluidization. A combined method of using mechanical shearing/UF treatment at 50°C in the earlier stage and microfluidization/UF treatment at 30°C in the later stages is proposed for industrial scale production of chitosan.

REFERENCES

1 Chen RH, Lin WC and Lin JH, *Acta Polym* **45**:41-46 (1994).
2 Tsaih ML and Chen RH, *Int J Biol Macromol Sci* **20**:233-240 (1997).
3 Tsai GJ, Zhang SL and Shieh PL, *J Food Prot* **67**:396-398 (2004).
4 Tsai GJ and Hwang S-P, *Fish Sci* **70**:675-681 (2004).
5 Jeon YJ, Park PJ and Kim SK, *Carbohydr Polym* **44**:71-76 (2001).
6 Ong SY, Wu J, Moochhala SM, Tan MH and Lu J, *Biomaterials* **29**:4323-4332 (2008).
7 Feng T, Du Y, Li J, Hu Y and Kennedy JF, *Carbohydr Polym* **73**:126-132 (2008).
8 Chen SK, Tsai ML, Huang JR and Chen RH, *J Agric Food Chem* **57**:2699-2704 (2009).
9 Wu GJ and Tsai GJ, *Fish Sci* **70**:1113-1120 (2004).
10 Wu GJ and Tsai GJ, *Taiwanese J Agric Chem Food Sci* **44**(4):228-234 (2006).
11 Ikeda I, Sugano M, Yoshida K, Sasaki E, Iwamoto Y and Hatano K, *J Agric Food Chem* **41**:431-435 (1993).
12 Baker WL, Tercius A, Anglade M, White CM and Coleman CI, *Ann Nutr Metab* **55**:368-374 (2009).
13 Muzzarelli RAA, Lough C and Emanuelli M, *Carbohydr Res* **164**:433-442 (1987).
14 Ottøy MH, Vårum KM and Smidsrød O, *Carbohydr Polym* **29**:17-24 (1996).
15 Holme HK, Foros H, Pettersen H, Dornish M and Smidsrød O, *Carbohydr Polym* **46**:287-294 (2001).
16 Vårum MK, Ottøy MH and Smidsrød O, *Carbohydr Polym* **46**:89-98 (2001).
17 No HK, Kim SH, Lee SH, Park NY and Prinyawiwatkul W, *Carbohydr Polym* **65**:174-178 (2006).
18 Tsaih ML and Chen RH, *J Appl Polym Sci* **88**:2917-2923 (2003).
19 Chang KLB, Tai MC and Cheng FH, *J Agric Food Chem* **49**:4845-4851 (2001).
20 Huang QZ, Zhuo LH and Guo YC, *Carbohydr Polym* **72**:500-505 (2008).
21 Yue W, Yao P, Wei Y, Li S, Lai F and Liu X, *Food Chem* **108**:1082-1087 (2008).
22 Ilyina AV, Tatarinova NY and Varlamov VP, *Process Biochem* **34**:875-878 (1999).
23 Ilyina AV, Tikhonov VE, Albulov AI and Varlamov VP, *Process Biochem* **35**:563-568 (2000).

24 Zhang H, Du Y, Yu X, Mitsutomi M and Aiba SI, *Carbohydr Res* **320**:257-260 (1999).
25 Zhang H and Neau SH, *Biomaterials* **22**:1653-1653 (2001).
26 Li J, Du YM, Liang HB, Yao PJ and Wei YA, *J Appl Polym Sci* **102**:4185-4193 (2006).
27 Muzzarelli RAA and Rocchetti R, *Carbohydr Polym* **5**:461-472 (1985).
28 Chen RH, Chang JR and Shyur JS, *Carbohydr Res* **299**:287-294 (1997).
29 Tsaih ML and Chen RH, *J Appl Polym Sci* **90**:3526-3531 (2003).
30 Tsaih ML, Tseng LZ and Chen RH, *Polym Degrad Stab* **86**:25-32 (2004).
31 Baxter S, Zivanovic S and Weiss J, *Food Hydrocolloids* **19**:821-830 (2005).
32 Popa-Nita S, Lucas JM, Ladavière C, David L and Domard A, *Biomacromolecules* **10**:1203-1211 (2009).
33 Lagoueyte N and Paquin P, *Food Hydrocolloids* **12**: 365-371 (1998).
34 Kasaai MR, Charlet G, Paquin P and Arul J, *Innovative Food Science and Emerging Technologies* **4**:403-413 (2003).
35 Tsai M-L, Tseng L-Z and Chen R-H, *Carbohydrate Polymers* **77**:767-772 (2009).
36 Muzzarelli RAA, Pergamon Press, Oxford, (1977).
37 Austin PR, Brine CJ, Castle JE, Zikakis JP, *Science* **212**(15):749 (1981).
38 Chen R-H, Chang J-R, & Shyur J-S, *Journal of the Fisheries Society of Taiwan* **25**:219-229 (1998).
39 Floury J, Desrumaux A, Axelos MAV and Legrand J, *Food Hydrocollids* **16**:47-53 (2002).
40 Tsai ML, Tseng LZ, Chang HW and Chen RH, *J Appl Polym Sci* (accepted) (2010).
41 Ulanski P, Wojtasz-Pajak A, Rosiak JM and von Sonntag C, Radiolysis and sonolysis of chitosan - two convenient techniques for a controlled reduction of the molecular weight. in *Advance Chitin Science,* Vol. 4. ed by Peter MG, Domard A and Muzzarelli RAA. University of Potsdam, pp 429-435 (2000).
42 Kume T, Radiation degradation of chitosan and induction of biological activites, in *Chitin and Chitosan-Chitin and Chitosan in Life Science,* ed by Uragami T, Kurita K and Fukamizo T. Kodansha Scientific, pp 190-193 (2001).
43 Silvestri S, Gabrielson G and Wu LL, *Int J Pharm* **71**:65-71 (1991).
44 Cencia-Rohan L and Silvestri S, *Int J Pharm* **95**:23-28 (1993).
45 Masson G, *Food Microstructure* **8**:11-14 (1989).
46 Grönroons A, Pirkonen P, Heikkinen J, Ihalainen J, Mursunen H and Sekki H, *Ultrason. Sonochem* **8**:259-264 (2001).
47 Casale A and Porter P, *Polymer Stress Reactions* Vol. 1, Academic Press, New York (1978).
48 Tsai ML, Bai SW and Chen RH, *Carbohydr Polym* **71**:448-457 (2008).
49 Stanley WL, Watters GG, Chan BG and Mercer JM, *Biotechnol Bioeng* **17**:315-326 (1975).
50 Chen RH, Lin JH and Yang MH, *Carbohydr Polym* **24**:41-46 (1994).
51 Tsaih ML and Chen RH, *J Appl Polym Sci* **71**:1905-1913 (1999).
52 Lii CY, Chen CH, Yeh AI and Lai VMF, *Food Hydrocolloids* **13**:477-481 (1999).
53 Ohta K, Urano S and Kawahara K, *Kobunshi Ronbunshyu* **40**:417-423 (1983).

USAD process applied to β-chitin: influence of ultrasound irradiation on the resulting chitosan

Jorge A. de M. Delezuk, [1] Márcia B. Cardoso,[1] Alain Domard,[2] Sérgio P. Campana-Filho[1*]

[1] Laboratório de Físico-Química Orgânica, Instituto de Química de São Carlos, Universidade de São Paulo, São Carlos, Brasil.
[2] Ingénierie des Matériaux Polymères, Université Claude Bernard Lyon I, Lyon, France.
[*] Correspondence to: Sérgio P. Campana-Filho, Laboratório de Físico-Química Orgânica, Instituto de Química de São Carlos, Universidade de São Paulo, Av. Trab. São-Carlense, 400 CP 780, ZIP 13560-970, São Carlos, São Paulo, Brasil. E-mail: scampana@iqsc.usp.br

Abstract
This paper presents a new process, the ultrasound-assisted deacetylation process (USAD), which uses the high intensity ultrasound irradiation to promote the deacetylation of β–chitin to produce chitosan possessing high viscosity average molecular weights (100,000g/mol<Mv<750,000g/mol) and low average degree of acetylation (6.0%<DA<25.0%). Moreover, the proper adjustment of the USAD parameters allows the production of chitosan extensively deacetylated (DA≈6.0%) and possessing high viscosity average molecular weight (Mv≈720,000 g/mol) after a single step short time processing (<60min) carried out at a low temperature (60º-80ºC) as compared to the conventional processes employed to produce chitosan by the deacetytlation of chitin.

Keywords: Ultrasound; Deacetylation; β–Chitin; Chitosan; USAD process

INTRODUCTION

The most used route for the deacetylation of chitin is the treatment of the polymer with concentrated solutions of alkali – aqueous sodium and potassium hydroxide (30 – 50%) are the most used solutions – at relatively high temperatures (80°C-115°C) during variable time (1–6 h).[1,2] The more severe reaction conditions in terms of alkali concentration and temperature result in more deacetylated products but prolonging the reaction also provokes a severe depolymerization and the loss of some polymer properties.[3] Indeed, it is known that the deacetylation reaction is fast during the first 40 min, but the reaction rate reaches a plateau from then on while the depolymerization process via oxidative alkaline hydrolysis of glycosidic bonds continues to occur.[1] Therefore, different routes have been proposed to improve the deacetylation reaction while minimizing the undesirable depolymerization. Thus, the following measures have been proposed: i)the use of inert atmosphere[4]; ii)the dilution with solvent[5]; iii)changes in processing conditions with the use of reactive extrusion[6], steam explosion (process "flash")[7], irradiation of ultrasound[8] and microwave[9]; iv)the use of reducing agents[10]; v)the execution of successive deacetylation reactions[11]; vi)the use of the process known as "freeze - pump out – thaw" (FPT).[12]

It is known that the prolonged exposure of solutions containing macromolecules to the ultrasound irradiation decreases the viscosity of the solution as a result of the depolymerization process. The experimental evidence suggest that the polymer degradation is caused by: i)the hydrodynamic forces promoted by cavitation; ii)the shear stress at the interface of the bubble pulse, and iii)the thermal effect associated with both the chemical stable cavitation and the transient.[13] However, the high intensity ultrasound irradiation, also known as sonication, was early used as a pretreatment of chitin in aqueous suspension and it resulted in a more efficient deacetylation as compared to the reaction carried out with untreated chitin, which was attributed to the effect of ultrasound on the morphology of the

chitin particles. [8,14] Indeed, as a heterogeneous process, the efficiency of the deacetylation reaction of chitin depends on the accessibility to the reactive sites on the polymer chains. Thus, the action of ultrasound irradiation can improve the reaction efficiency by increasing the accessibility to reactive sites via the cavitation phenomenon which increases the particles' surface area as a consequence of the released energy and the impact of the violent collisions it provokes.

In this work, the ultrasound assisted deacetylation process (USAD process) is applied to β–chitin from *Loligo sp*. and the influence of the process parameters on the characteristics of the resulting chitosans is discussed. As it will be shown in the following, the USAD Process is more efficient than most of those processes already described in the literature[1,2]Also, it allows the production of chitosan with variable DA and Mv, these characteristics being determined by the proper adjustment of the process parameters.

MATERIALS AND METHODS

Extraction of β-Chitin

The squid pens from *Loligo sp*. were used as the raw material for the extraction of β–chitin. The method described by Chaussard[15] was used to remove proteins and the demineralization treatment was not carried out due to the low content of inorganic compounds.

Ultrasound assisted deacetylation process (USAD process)

β-Chitin was suspended in 14.1 M NaOH and the suspension was poured into a glass reactor coupled to a circulating thermostat to allow the control of the reaction temperature. The chitin suspension was submitted to the ultrasound irradiation by using a Branson Sonifier Model 450 (ν=20 kHz) coupled to a ½' stepped probe and the equipment was adjusted for intermittent irradiation to minimize the heat release due to the ultrasound irradiation. In the non-isothermal experiments (NI), the irradiation amplitude (A) was adjusted to low (L), medium (M) or high (H) while the irradiation duration was varied in the range 10-60 min, and the temperature was allowed to increase. In the isothermal experiments (I), the irradiation amplitude was the same as during the NI experiments, the irradiation duration was kept constant at 30 min. and the reaction temperature was adjusted to 50°, 60°, 70° or 80ºC.

Characterization of chitosans produced from USAD process

The average degree of acetylation (DA) of chitosan was determined by titrimetry and ^{1}H NMR spectroscopy as described elsewhere.[15] The intrinsic viscosities were determined at 25,00 ± 0,01ºC by viscosity measurements of the chitosan samples dissolved in 0.3 M acetic acid/0.2 M sodium acetate buffer (pH≈4.5) as described elsewhere.[16] The viscosity average molecular weights (Mv) were calculated by employing the values of K and a determined in the same solvent and temperature and according to the average degree of acetylation of the chitosan sample.[16] The thermal behavior, crystallinity and morphology of the samples were determined by thermogravimetric analysis (TGA), X-ray diffraction (XRD) and scanning electron microscopy (SEM), respectively.

RESULTS AND DISCUSSION

The SEM analyses showed that the surfaces of the particles of β–chitin are relatively smooth (Fig. 1a) as compared to those of sample NILS (Fig. 1b), a chitosan sample obtained by applying the USAD process, which are much more rough. Additionally, sample NILS is composed by smaller particles, the reduction in the particles' average size and the consequent increase in its surface being observed in all samples of chitosan produced by the USAD process.

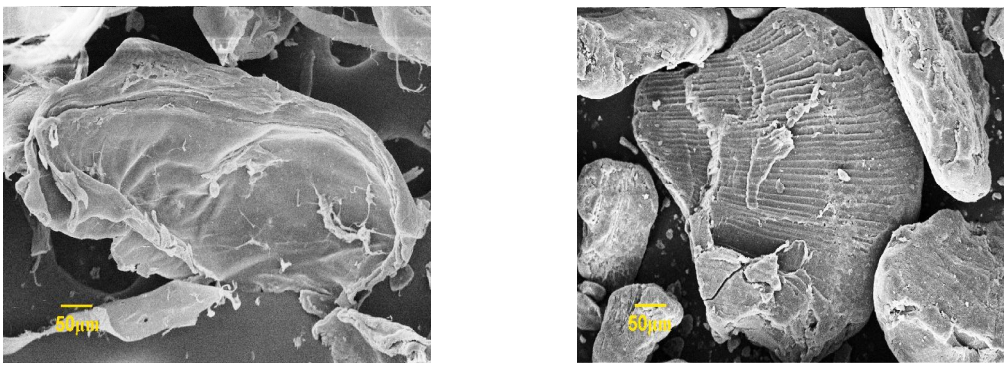

(a) (b)

Fig. 1 - Micrographs of β–chitin (a) and sample NILS (b), with 500x magnification. NILS identifies the USAD product resulting by applying non-isothermal (NI) conditions, low (L) irradiation amplitude and short (S) duration treatment.

The X ray spectrum of β–chitin exhibits two crystalline peaks at 2θ≈8º and 2θ≈20º, attributed to the plans (010) and (020, 110), respectively. In contrast, that one of sample ILS60 (Fig. 2) shows a single peak at 2θ≈20º which is much less intense and broader, indicating the loss of crystallinity provoked by the conversion of β–chitin to chitosan by applying the USAD process.

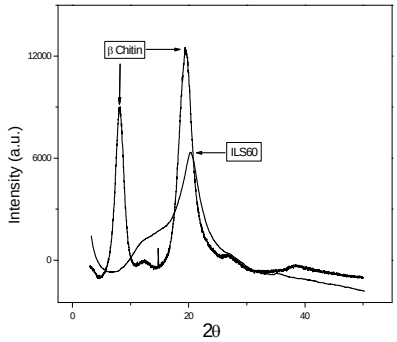

Fig. 2 – X ray diffraction of β–chitin and sample ILS60.

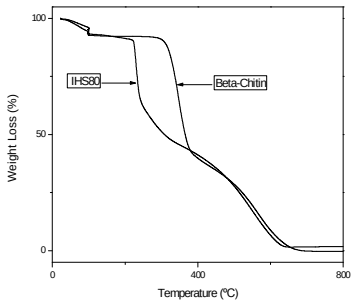

Fig. 3 - TGA curves of β–chitin and sample IHS80.

The TGA curves of β–chitin and the USAD products were acquired in synthetic air atmosphere at a heating rate of 10 °C/min and from them (Fig. 3) it was concluded that the chitosan produced by applying the USAD process are less thermally stable than the parent β–chitin, the lower crystallinity of chitosan samples being responsible for it.

Non-Isothermal USAD

The application of different irradiation amplitude and duration when carrying out non-isothermal reactions (NIUSAD process) resulted in chitosan samples with different characteristics (Fig. 4 and Fig. 5).

When low (L) amplitude irradiation was applied, the DA of the NIUSAD products was somewhat affected by the irradiation duration (Fig. 4), as it presented a decrease of approximately 17% as a result of applying long (L) irradiation duration. However, when medium (M) and high (H) amplitude irradiation were employed the decrease of DA was more important even if a short (S) duration irradiation was applied, as it corresponded to approximately 37% and 50%, respectively. The decrease of DA was yet more pronounced

when applying medium (M) irradiation duration but it leveled off for long irradiation duration (L), attaining approximately 70% regardless of the irradiation amplitude being medium (M) or high (H). Thus, these data revealed that NIUSAD process promoted the deacetylation of β–chitin in a relatively shorter reaction time and more efficiently than most of the processes carried out in similar conditions concerning the raw material, the concentration of aqueous sodium hydroxide and the temperature.

The effects of the irradiation amplitude and duration on Mv (Fig. 5) were qualitatively similar to those concerning the DA, however they were relatively more important. Indeed, Mv decreased steadily with increasing irradiation amplitude and duration but its decrease attained approximately 82% when high (H) irradiation amplitude and long (L) irradiation duration were employed. These data revealed the occurrence of severe chain depolymerization simultaneously to chitin deacetylation during NIUSAD process, the depolymerization rate being more important the higher the irradiation amplitude and the longer the irradiation duration.

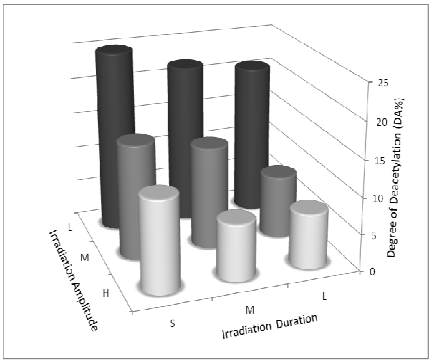

Fig. 4 - Effects of the irradiation amplitude and irradiation duration on DA of chitosan produced by applying NIUSAD process to β–chitin from *Loligo sp*.

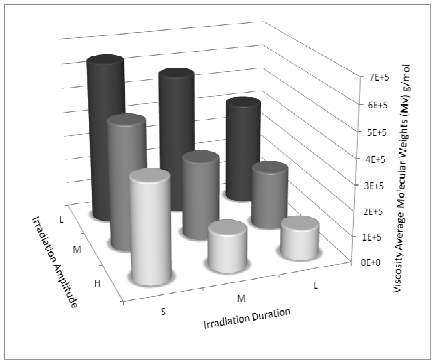

Fig. 5 - Effects of the irradiation amplitude and duration on Mv of the chitosan produced by applying NIUSAD process to β–chitin from *Loligo sp*.

Isothermal USAD

The data of DA and Mv of chitosan samples obtained by applying isothermal conditions (IUSAD process) showed that this is a better process as compared to NIUSAD process as the products of the former process present higher viscosity average molecular weight and lower average degree of acetylation.

The variation of the DA of the IUSAD products as a function of the irradiation amplitude and reaction temperature (Fig. 6) showed that when irradiation amplitude is kept constant the increase in temperature tends to favor the deacetylation of β–chitin, except in the case of medium amplitude (M). In the range of temperature 60º-80ºC a slight trend of increase of DA with increasing temperature was observed, except when medium amplitude (M) was applied. In contrast, the variation Mv as a function of the irradiation amplitude and reaction temperature (Fig. 7) indicated that there were no simple correlation between the reaction conditions and the characteristics of the IUSAD products. However, a trend of Mv decrease with increasing temperature was observed when medium and high irradiation amplitude were used. Considering the variation of both characteristics, DA and Mv, of the IUSAD products, it was concluded that a critical temperature (≥ 60ºC) must be achieved to favor the production of high viscosity average molecular weight chitosan.

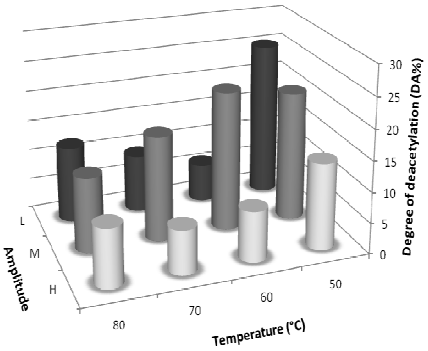

Fig. 6 - Variation of DA in function of the irradiation amplitude and reaction temperature.

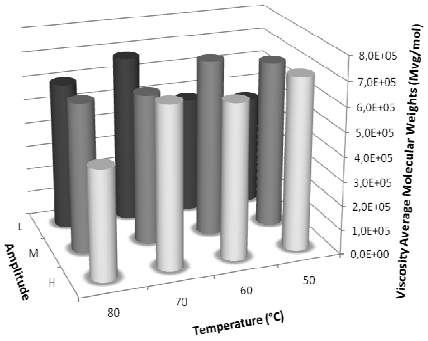

Fig. 7 - Variation of Mv in function of the irradiation amplitude and reaction temperature.

CONCLUSIONS

There is a strong compromise among the process parameters, the average degree of acetylation and the viscosity average molecular weight of chitosan produced when applying the USAD process. Thus, the deacetylation of β–chitin is favored the higher the irradiation amplitude and the longer the process duration, however the simultaneous depolymerization is also favored as a consequence of the temperature increase due to the high intensity ultrasound irradiation. The proper choice of the process parameters is very important to attain the desired result, the shorter processing times and the lower temperatures favoring the deacetylation of β–chitin while minimizing the occurrence of depolymerization.

ACKNOWLEDGEMENTS

The authors thank to the Brazilian agencies CAPES, CNPq and FAPESP for financial support and to Miami Pescados (SP-Brazil) for supplying the squid pens.

REFERENCES

1 Lamarque G, Viton C and Domard, A, *Biomacromolecules*, **5**:992 (2004).
2 Kurita K, *Prog Polym Sc* **26**:1921 (2001).
3 Rege PR and Block LH, *Carbohydr Res* **321**:235 (1999).
4 Campana Filho SP and Siginini R, *Polímeros* **11**:169 (2001).
5 Sannan T, Kurita K and Iwakura Y, *Die Makromolekulare Chemie* **176**:3589 (1975).
6 Rogovina SZ, Akopova TA and Vikhoreva GA, *J Appl Polym Sci* **70**:927 (1998).
7 Focher B, Beltrame PL, Naggi A and Torri G, *Carbohydr Polym* **12**:405 (1990).
8 Cardoso MB, Signini R and Campana Filho S P, *Polym Bull* **47**:183 (2001).
9 Sagheer FAA, Al-Sughayer MA, Muslim S and Elsabee MZ, *Carbohydr Polym* 77:410 (2009).
10 Campana Filho SP and Signini R, *Int J Polym Mater* **51**:701 (2002).
11 Roberts GA and Wood FA, In: Peter MG, Domard A and Muzzarelli RAA (Eds.). Advances in chitin science. Potsdam: Universitat Potsdam **4**:34 (2000).
12 Lamarque G, Cretenet M, Viton C and Domard A, *Biomacromelules* **6**:1380 (2005).
13 Price GJ, *Ultrason Sonochem* **3**:229 (1996).
14 Campana Filho SP, Signini R and Cardoso MB, *Int J Polym Mater* **51**:695 (2002).
15 Chaussard G and Domard A, *Biomacromolecules* **5**:559 (2004).
16 Rinaudo M, Milas M and Le Dung P, *Int J Biol Macromol* **15**:281 (1993).
17 Suslick KS, Hammerton DA and Cline Junior RE, *J Amer Chem Soc* **108**:5641 (1986).

Characterization of chitin isolated from legs, pincers and carapace of the crab *Aegla chol chol*

Patricio De Los Ríos[1], Adrián Hernández[2], Patricio Dantagnan[2], Ricardo Oliva[3], Edelio Taboada[3], Liliam Becherán[4], Patricia Bernabé[4], Manuel Gidekel[5], Gustavo Cabrera[5]*

[1] Escuela de Medioambiente, Universidad Católica de Temuco, Temuco, Chile,
[2] Escuela de Acuicultura, Universidad Católica de Temuco, Temuco, Chile.
[3] Escuela de Ingeniería Ambiental, Universidad Católica de Temuco, Temuco, Chile.
[4] Instituto de Ciencia y Tecnología de Materiales (IMRE), Universidad de La Habana, La Habana, Cuba.
[5] VentureLab, Escuela de Negocios, Universidad Adolfo Ibáñez, Santiago de Chile, Chile.
* E-mail: gustavo.cabrera@uai.cl

Abstract: Two kinds of materials: legs, pincers and carapace of *Aegla chol chol* crab and chitin isolated from them were characterized by TG/DTG, Fourier transform infrared spectroscopy (FTIR), scanning electron microscopy (SEM) and elemental composition. The later analysis proved the demineralizing process effectiveness and high levels of proteins, lipids and astaxanthin in raw material. Infrared spectra showed absorption bands at 1665 and 1630 cm^{-1}, characteristic of α-chitin. Two exothermic peaks exhibited TG/DTG curves of the exoskeleton, while only one peak was observed for isolated chitin. Changes in samples morphology were observed after acid and alkali treatment.

Keywords: *Aegla chol chol*, chitin, thermogravimetric analysis, scanning electron microscopy, proteins content

INTRODUCTION

Chitin is the second most abundant polysaccharide in nature next to cellulose. Chitin and its derivatives are widely used in medicine, pharmacy, agricultural and environmental fields. The main industrial sources of chitin are shellfish industry waste materials, such as crab, shrimp, lobster and krill.[1]. Knowing raw material and final product characteristics is fundamental in order to carry out further applications, since their properties may differ depending on the source. Therefore, several papers deal with chitin obtaining and characterization.[2, 3, 4].
Aegla chol chol is an endemic crab from the Chol Chol river, which is located on the Chilean southern region. In this study, various parts of the exoskeleton of *Aegla chol chol* (legs, pincers and carapace) were treated with hydrochloric acid and alkali for chitin isolation. Further characterization of both crab shell as well as chitin obtained was carried out in terms of their humidity, ash, metal, proteins and lipids content. Electronic microscopy, thermogravimetric analysis and infrared spectroscopy were used in order to know structural changes during chitin obtaining process.

MATERIALS AND METHODS

Exoskeletons from freshwater crab-like decapod crustacean *Aegla chol chol* were collected in the Chol Chol river in the southern rAraucania Region of South of Chile.
The parts of the exoskeleton (pincers, legs and carapace) were demineralized with 2 M HCl (solids to solvent ratio of 1:10 w/v) at room temperature for 1 h with constant stirring. The deproteinization procedure was carried out stirring the demineralized parts with 1 M NaOH (solids to solvent ratio of 1:20 w/v) at 100 ºC for 3 h. The isolated chitin was washed and dried at 60°C in a vacuum oven.
Humidity was determined gravimetrically. Each sample was placed in a porcelain crucible and

heated at 105°C in an oven to a constant weight. The dried sample was placed in an oven and heated at 900°C to a constant weight to determine the ash content.[6] Ashes were dissolved in nitric acid to analyze the metal content by atomic absorption with an Unicam series spectrophotometer (Spectronic Unicam, Cambridge, UK) with cathodic lamp. Phosphorus content was estimated by the molybdenum blue colorimetric method.[6] Nitrogen percentage was determined by the method of Kjeldahl[6] and the protein content was calculated by multiplying nitrogen percentage of the sample by 6.25. The content of chitin in the exoskeleton was estimated by the method of Black and Schwartz.[7] Total lipids were determined according to Bligh and Dyer[8] with the modifications described by Hardy and Keay.[9] Extraction and quantitative determination of astaxanthin were performed as explained by Schiedt and Liaaen-Jensen.[10]

Morphological analysis was performed with an ETEC autoscan Model U-1 scanning electron microscope (University of Massachusetts, Worcester, MA). The samples were fixed in a sample holder and covered with a gold layer for 3 min using an Edwards S150 sputter coater (BOC Edwards, São Paulo, Brazil). Fourier transform infrared (FTIR) spectra were recorded with a Nicolet Magna FTIR spectrophotometer (Nicolet Analytical Instruments, Madison, WI) connected to a PC with Omnic software (Thermo Electron Corp., Woburn, MA) for data processing. The samples were prepared in KBr pellets at a concentration of 2 % (w/w). Spectra were run at a resolution of 4 cm^{-1}. The thermogravimetric studies were performed with a Cahn-Ventarn 2000 differential scanning calorimeter with a microprocessor driven temperature control unit and a thermal analysis data station. The weight of the samples ranged between 3 and 5 mg. The sample pan was placed in the balance system equipment and the temperature was raised from 25 to 1000 °C at a heating rate of 5 $°C \cdot min^{-1}$ under a nitrogen dynamic flow of 50 $mL \cdot min^{-1}$. The mass of the sample pan was continuously recorded as a function of temperature.

RESULTS AND DISCUSSION

The chemical composition of different parts of the exoskeleton of *Aegla chol chol* was determined and the results are shown in Table 1. In general, the composition among the parts of the exoskeleton differs. The ash content varied between 42.6 % and 49.0 % of the dry weight. The inorganic elements in ash were quantified and the results are displayed in Table 2. The main elements were found to be calcium, phosphorus, sodium, potassium and magnesium. Likely, the main components of the mixtures of salts in the exoskeleton could be the phosphate and carbonate of calcium, as have been reported previously for other crustacean shells.[11, 12]

Our results showed contents of lipids ranging between 5.0 % and 12.5 % of the dry weight, depending of the part of the shell (Table 1). The highest percentage was found in legs and a detailed study of the composition of lipids revealed polyunsaturated fatty acids as the major components, mainly *cis*-5, 8, 11, 14, 17 eicosapentanoic acid (results not shown). Also relatively high content of protein were found in all the samples and the content of astaxanthin showed significant levels in comparison with other crustacean sources. This composition in terms of lipids, protein and pigments could make *Aegla chol chol* shells valuable for a variety of feed applications. The chitin content was in agreement with the compositions that can be found in other crustacean shells and the ash content in chitin isolated from the exoskeleton is significantly low, which is indicative of the effectiveness of the method used for demineralization of the shells.

Table 1. Chemical composition of the exoskeleton of *Aegla chol chol* and chitin.

	Humidity (w/w) (%)	Ash (w/w) (%)	Chitin (w/w) (%)	Protein (w/w) (%)	Lipid (w/w) (%)	Astaxanthin (ppm)
Exoskeleton						
Pincers	7.5	49.0	9.0	29.1	5.0	17047
Legs	5.9	45.1	10.4	25.3	12.5	9287
Carapace	5.2	42.6	9.3	34.8	7.6	25874
Chitin						
Pincers	8.2	0.21	-	-	-	-
Legs	8.9	0.18	-	-	-	-
Carapace	8.6	0.24	-	-	-	-

Table 2. Main inorganic elements in the exoskeleton of *Aegla chol chol.*

Element	Pincers	Legs	Carapace
Ca (g/kg)	158 ± 1	139 ± 2	1260 ± 75
P (g/kg)	9.5 ± 0.1	9.7 ± 0.1	102 ± 1
K (g/kg)	3.6 ± 0.1	3.3 ± 0.1	37.2 ± 0.4
Na (g/kg)	6.3 ± 0.1	6.2 ± 0.3	80 ± 8
Mg (g/kg)	2.8 ± 0.1	2.4 ± 0.1	22 ± 1
Mn (mg/kg)	125.3 ± 0.6	360 ± 4	1752 ± 42
Fe (mg/kg)	87.4 ± 0.2	169.4 ± 0.2	2327 ± 71
Zn (mg/kg)	62 ± 2	64.8 ± 0.4	355 ± 13
Cu (mg/kg)	40.4 ± 0.8	43.6 ± 0.7	849 ± 4

FTIR studies were performed for the characterization of chitins obtained from different parts of the exoskeleton of *Aegla chol chol*. Only the spectrum of the chitin isolated from carapace is shown (Figure 1) because all other spectra are quite similar. In Table 3 the signals and their assignments are summarized. In the region from 3600 to 3000 cm^{-1}, the shoulder at 3480 cm^{-1} is attributed to the intramolecular hydrogen bond involving the $CH_2OH\cdots O{=}C$ and the band that appears at 3446 cm^{-1} corresponds to the intramolecular hydrogen bond $OH\cdots O$ in the ring.[4] The bands at 3269 and 3108 cm^{-1} are assigned to the antisymmetric and symmetric NH stretching, respectively.

Table 3. Main signals in the FTIR spectra of chitin obtained from shells of *Aegla chol chol.*

ν (cm^{-1})	Assignment	ν (cm^{-1})	Assignment
3480, 3446	ν OH	1259	δNH
3269	ν^{as} NH	1155	ν^{as} C-O-C (ring)
3108	ν^{s} NH	1112	ν C-O
2964	ν^{as} CH_3	1074	ν C-O
2929	ν^{s} CH_2	1025	ν C-O
2883	ν^{as} CH_3	958	γ CH_3
1665, 1630	ν C=O (Amide I)	898	γ CH (C1 axial)
1560	ν C-N (C-N-H); δ NH (Amide II)	746	ρ CH_2
1423	δ CH_2	698	γ NH (Amide V)
1376	δ CH; δC-CH_3	604	γ C-O
1311	νC-N; δNH (Amide III)	567	γ C-C

The absorption bands at 1665 and 1630 cm^{-1} are distinctive for α-chitins and corresponds to the vibration modes of amide I. The signal at 1665 cm^{-1} is attributed to the hydrogen bonds between part of the carbonyl groups and the amino groups of the same chain, while the absorption band at 1630 cm^{-1} is related to the hydrogen bonds between the other fraction of carbonyl groups with the CH_2OH groups of the neighboring chains.[4] Also, the absorption band at 898 cm^{-1} (γ CH of the anomeric center) is characteristic of α-chitins, as has been stated before by several authors.[4, 13]

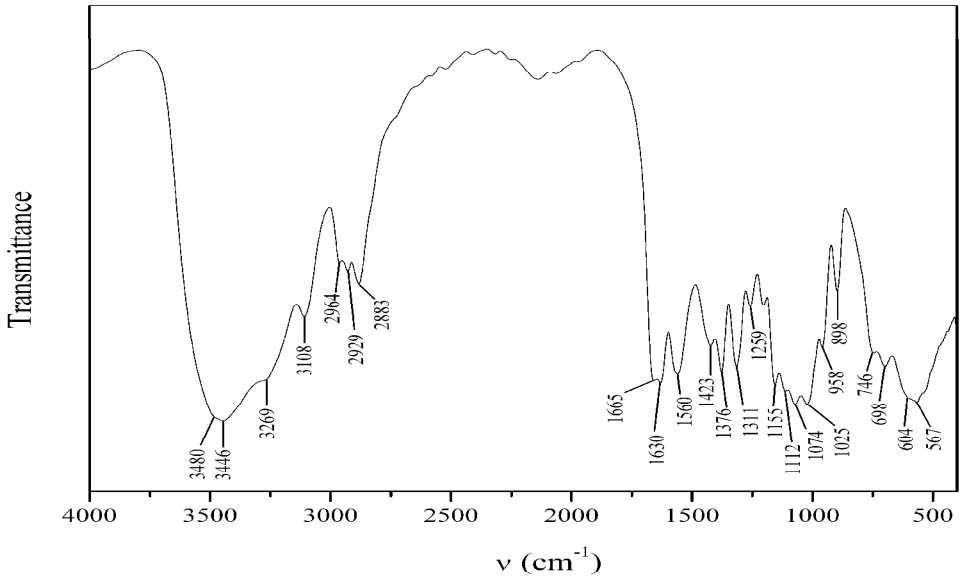

Figure 1. Infrared spectra of chitin isolated from *Aegla chol chol*.

In order to study the morphology of the different parts of the exoskeleton and the chitin isolated from them, several samples were observed by scanning electron microscopy (SEM). Figure 2 shows the SEM photographs of the exoskeleton before (Fig. 2a, 2c) and after (Fig. 2b, 2d) acid and alkali treatment to isolate chitin. It is observed that, as a result of the chitin isolation procedure, a rough surface without porosity is obtained and chitin shows a fibrous appearance. In other studies, this has been attributed to the high molecular packing of α-chitins, due to the presence of inter- and intramolecular hydrogen bonds in the structure.[4]

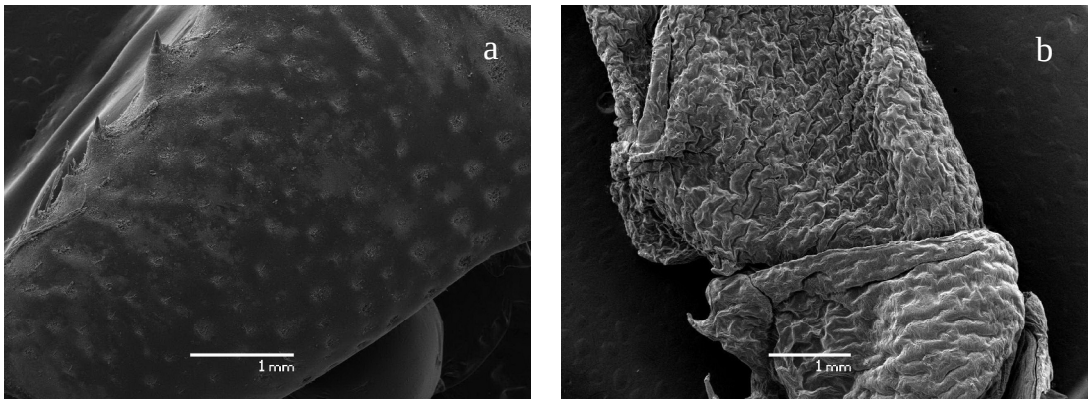

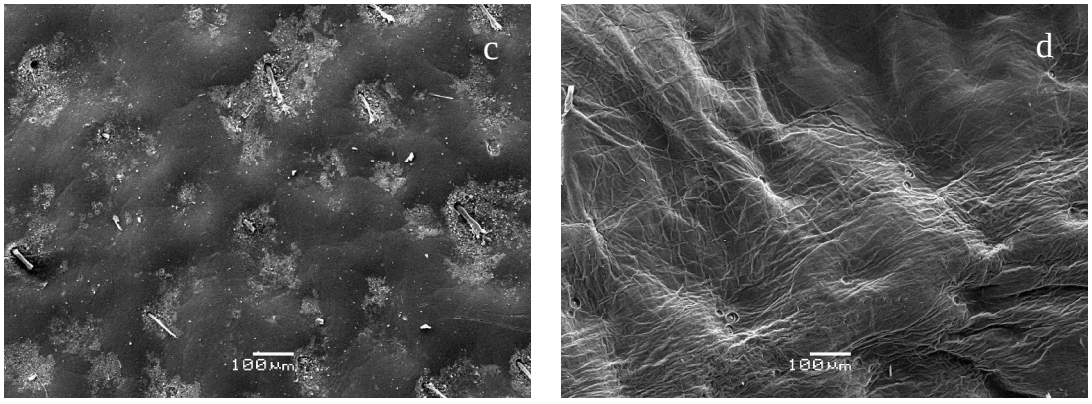

Figure 2. SEM microphotographs of *Aegla chol chol* exoskeleton: (a, c) before acid and alkali treatment and (b, d) after acid and alkali treatment (chitin)

Figure 3 shows thermogravimetric analysis curves (TG) and their derivatives (DTG) of the exoskeleton of *Aegla chol chol* (Fig. 3a) and chitin (Fig. 3b) and related data appears in Table 4. In both cases a thermal effect under 100 ºC was observed, which is assigned to loss of water associated to the macromolecules[13] (not shown). Thermogravimetric curves of the exoskeleton exhibit two thermal effects. The first one occurs around 340 ºC and may be related to the degradation of the saccharide structure of the chitin molecule, including the dehydration of saccharide rings and the decomposition of the N-acetylated units,[14, 15] whereas the second one (670-685 ºC) describes the inorganic salts decomposition and volatilization. Chitin-proteins, chitin-salts and chitin-pigments associations in the exoskeleton could be the reason in TG curves difference between the raw material and the isolated chitin[5]. The appearance of a unique transition in the TG curve of chitin revealed the good efficiency of the demineralizing process.

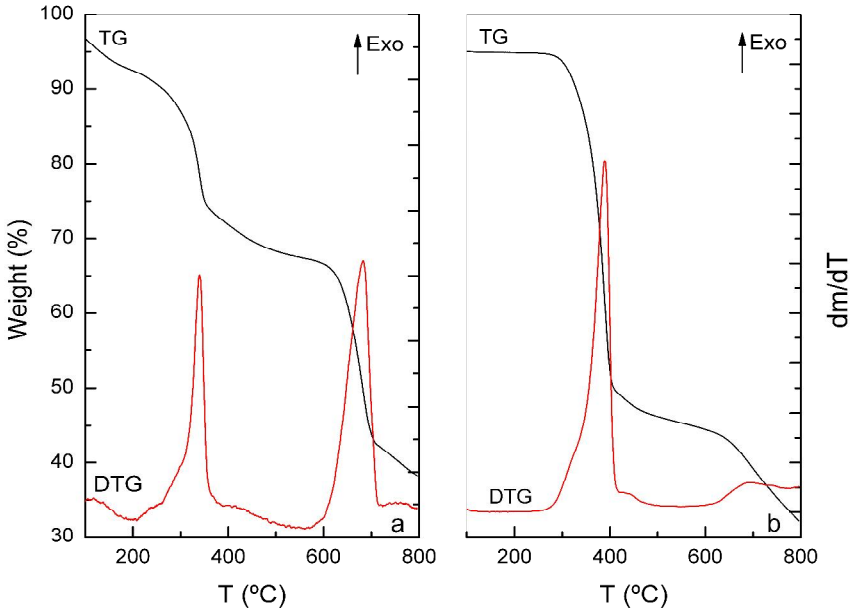

Figure 3. Thermogravimetric curves of (a) exoskeleton of *Aegla chol chol* and (b) chitin isolated from it.

Table 4. Temperatures of the thermal effects and variation in enthalpy of the decomposition process of the exoskeleton of *Aegla chol chol* and chitin extracted from it.

Sample	First stage		Second stage		ΔH dec. ($J.g^{-1}$)
	T (ºC)	Weight loss (%)	T (ºC)	Weight loss (%)	
Exoskeleton					
Pincers	339.16	14.64	683.01	22.77	-19.92
Legs	340.3	22.00	684.05	17.20	-35.17
Caparace	341.78	28,36	671.94	12,29	-37.92
Chitin					
Pincers	389.07	65.44	-	-	-62.37
Legs	372.6	64,04	-	-	-37.29
Caparace	397.01	81,72	-	-	-82.13

CONCLUSIONS

Chitin was isolated from legs, pincers and carapace of *Aegla chol chol* crab. The results of the chemical composition of the shells suggest their potential for feed applications. Chitin content was similar to that found in other crustacean shells and the good efficiency of the demineralizing process was confirmed. Hence, *Aegla Chol Chol* can be a valuable source for the production of α-chitin.

ACKNOWLEDGEMENTS

The authors would like to thank to Project Grant DGIUCT 2006-3-07.

REFERENCES

1 Simionato Guinesi L and Gomes Cavalheiro ET, *Termochim Acta* **444**:128 (2006).
2 García Alonso I, Peniche-Covas C and Nieto JM, *J Thermal Anal* **28**:189 (1983).
3 Shi B, Zhao S, Jia L and Wang L, *Carbohyd Polym* **67**:398 (2007).
4 Cárdenas G, Cabrera G, Taboada E and Miranda SP, *J Appl Polym Sci* **93**:1876 (2004).
5 Nieto JM, Peniche Covas C and Padrón G, *Thermochim Acta* **176**:63 (1991).
6 Vogel AI, *Química Analítica Cuantitativa*. Kapelusz, Buenos Aires (1974).
7 Black M and Schwartz H, *Analyst* **75**:185 (1950).
8 Bligh EG and Dyer WJ, *Canad J Biochem Physiol* **37**(8):911 (1959).
9 Hardy R and Keay JN, *Int J Food Sci Tech* **7**:125 (1972).
10 Schiedt K and Liaaen-Jensen S, *Carotenoids. Vol. IA: Isolation and Analysis,* ed by Britton G, Liaaen-Jensen S and Pfander H. Birkhiluser, Basel, p. 81 (1995).
11 Naczk M, Synowiecki J and Sikorski ZE, *Food Chem* **7**:175 (198l).
12 Boßelmann F, Romano P, Fabritius H, Raabe D and Epple M, *Thermochim Acta* **463**:65 (2007).
13 Al Sagheer FA, Al-Sughayer MA, Muslim S, Elsabee MZ, *Carbohyd Polym* **77**:410 (2009).
14 Kittur FS, Harish Prashanth KV, Udaya Sankar K and Tharanathan RN, *Carbohyd Polym* **49**:185 (2002).
15 Paulino AT, Simionato JI, García JC and Nozaki J, *Carbohyd Polym* **64**:98 (2006).

Characterization of chitosan arising of waste exoskeleton shrimp

Flavio Vinicius C Kock,* Eloi A Silva Filho, Eustáquio VR de Castro

Departamento de Química, Universidade Federal do Espírito Santo, Vitória, ES, 29060-910, Brazil
*E-mail: kock.flavio@gmail.com

Abstract: The characterization of chitosan was realized using the exoskeleton of shrimp collected in the coast of state of the Espirito Santo, the yield of the biopolymer processing by stages was 59% for demineralization and 36.5% in acetylation, showing a good agreement with the results of literature[1-4]. The characterization by potentiometric titration showed a deacetylation degree DD = 65.4%, other techniques such as in infrared spectroscopy confirmed the presence of functional groups characteristic of the molecule of chitosan. Thermal Analysis (TG and DSC) were performed to verify the loss of weight and glass transition (Tg) temperature of the biopolymer. The average molecular weight was determined by measures of viscosity and calculated by the Mark-Houwink equation, providing the value of 88.0 Kg/mol. The SEM microscopy confirmed that fibrous structure of the biopolymer.

Keywords: chitosan; chitin; shrimp; biopolymer; degree of deacetylation

INTRODUCTION

Chitin is a natural polymer found by Braconnot in 1881, but only after 1970 that began to arouse interest in many studies aimed at increasing knowledge about the potential of the polymer and its derivatives. The chitosan is a derivative of chitin with great application in cosmetic and food industries, and that more than 25 years is used as flocculation agent in the treatment of aqueous effluents[1]. Chitin and chitosan are also called natural biopolymers consisting of repeating units of the disaccharide N-acetyl-D-glucosamine and D-glucosamine linked by glycosidic bond in varying proportions, with the first unit of this type predominates in chitin and chitosan in the β-(1-4)-D-glucosamine, predominates as shown in Figure 1.

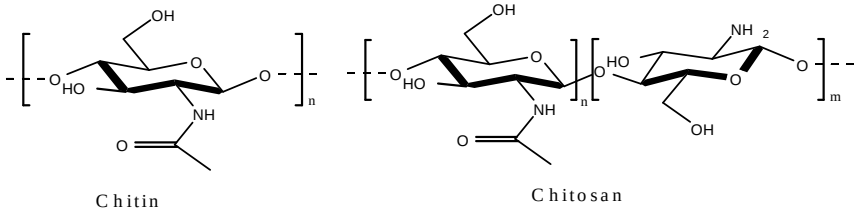

Figure 1. Molecular Structure of chitin and chitosan

The interesting part of these natural products is that chitin is the second most abundant polysaccharide in nature after cellulose, the main component of the exoskeletons of crustaceans and insects, its presence also occurs in nematodes and cell walls of fungi and yeasts[2]. Moreover, chitosan is obtained from chitin via deacetylation with alkali, can also be naturally present in some fungi, such as those belonging to the genera Mucor and zygomicetos. The objective of this work is the extraction and characterization of the biopolymer chitosan from shrimp arising from the coast of state of Espirito Santo.

MATERIALS AND METHODS

Materials

Hydrochloric acid (PA, Merck), sodium hydroxide (PA,Vetec), and sodium hypochlorite (PA, Vetec) were used without further purification. The chitosan was performed in four steps: demineralization, deproteinization, depigmentation (deodorizing) and deacetylation based on the following. Demineralization: a mass of 6.0 g was dissolved in 40 mL of hydrochloric acid 0.25 mol/L under continuous agitation for 6 hours at room temperature. Deproteinization: was done using the mass resulting from demineralization step and added to a round bottom flask with 20 mL of a solution of sodium hydroxide 1% (w/v). After kept the system under stirring for about 10 h a 50 ºC, and then the material was vacuum filtered and washed with distilled water until pH neutral and then dried in an oven for 12 hours at 40 °C. Depigmentation (deodorizing): the stage of deproteinization, the resulting material was added to 50 mL of sodium hypochlorite 1% (v/v) at 40°C stirring for 16 hours after placed in a desiccator for 24 h. Deacetylation of Chitin: The dry and colorless material was added to 200 mL of sodium hydroxide 50% (w/v). After kept under reflux and stirring for 5 hours at 100 °C material was washed with distilled water and ethanol to neutral pH and dried in a desiccator for 24 h. The characterization this biopolymer were realized by through the analysis of infrared spectroscopy, scanning electron microscopy (SEM), viscosimetry, thermal analysis (TG and DSC) and potentiometric titration. Thermogravimetry (TG) and differential scanning calorimetric (DSC) were made to the equipment SDT Q 600 of the TA instruments LabPetro-DQUI (UFES) using change in heat flow in the range of 25 °C to 700 °C with a heating rate of 20 °C/min under inert atmosphere of nitrogen.

RESULTS AND DISCUSSION

The result from the preparation of chitosan at each stage indicated that significant variations occur in securing this biopolymer by reason of being a natural material and as it is done the remaining steps of this initial yield of 59.03% deproteinization decreases to 36.50% in the deacetylation is the fundamental step to define the purity of chitosan and that is consistent with the literature data[3,4]. Others researchers, such as Campana and Signin[3] have studied the effect of additives in the deacetylation of chitin and also confirmed that regardless of the presence of additives and the use of inert gas flow,the reactins of desacetylation of chitin were reproductible experiments that have led,in all cases, the recorvery of 50 to 60% of mass of the starting material in the form of chitin. After obtaining the purified chitosan was made to measure the degree of deacetylation (%DD) using the method of potenciometric titration[4] in wich the graph by volume in mL of titrant sodium hydroxide (NaOH) as a function of voltage (mV) and the equation

$$\%DD = 16.1\left[\frac{C_{NaOH} \times (V2 - V1)}{m}\right]$$

where C_{NaOH} is the NaOH concentration in mol/L,V1 is the volume of the NaOH used for neutralization of HCL in excess, (V2-V1) is the volume the NaOH used for neutralization of acidic amino groups of chitosan, expressed in mL,and m is the mass of chitosan, resulted in the value of %DD = 65,4%. The average molecular weight of chitosan was calculated by the Mark-Houwink equation ($\eta = K(\overline{M})^a$), where the intrinsic viscosity obtained experimentally was 5.189 Pa.s and using the values of the constants $K=1.81x10^{-6}$ mL/g and a=0.93 described by Rinaudo[5] for the system acetic acid/sodium chloride 0.2 mol/L, resulted in the value of the average molecular weight of 88.00 Kg/mol. The infrared spectrum obtained in Figure 2-A, showed the highest intensity band in 3442 cm^{-1} due to stretching of the axial OH group of the aliphatic chain of the polymer, a band at 1563 cm^{-1} attributed to vibrational

modes and NH group stretching CH at 1418 cm^{-1}, the band at 1042 cm^{-1} are assigned to polysaccharides as described in the literature[4], represented in Figure 2-B. Although the spectra in the infrared region of chitin and chitosan have certain similarities, it is possible to observe some differences that are attributed to different rates of acetamide groups, especially in regions corresponding to the following ranges of wave number: 3700 to 3000 cm^{-1} and 1800 to 1500 cm^{-1}. Comparing the spectra of the chitosan from chitin, it appears that there were significant changes in the region of 1700 to 1300 cm^{-1}. For the sample of chitosan (Figure 2-A) is visible disappearance of the shoulder around 3480 cm^{-1} present in the spectrum of chitin Figure 2-C. The emergence of a new band at 1600 cm^{-1}, and the disappearance of the band at 1560 cm^{-1} is due to the NH_2 deformation dominates over the band in 1655 cm^{-1}, the latter band is associated with carbonyl (C = O) tends to decrease, as will increasing the degree deacetylation of chitosan. The disappearance of two bands between the regions 3200 and 3100 cm^{-1}, as already mentioned, is related to the deacetylation of the $NHCOCH_3$ group, transforming the primary amide to amine. However, there is the permanence of the bands in the regions around 3400 cm^{-1}, which is related to hydroxyl.

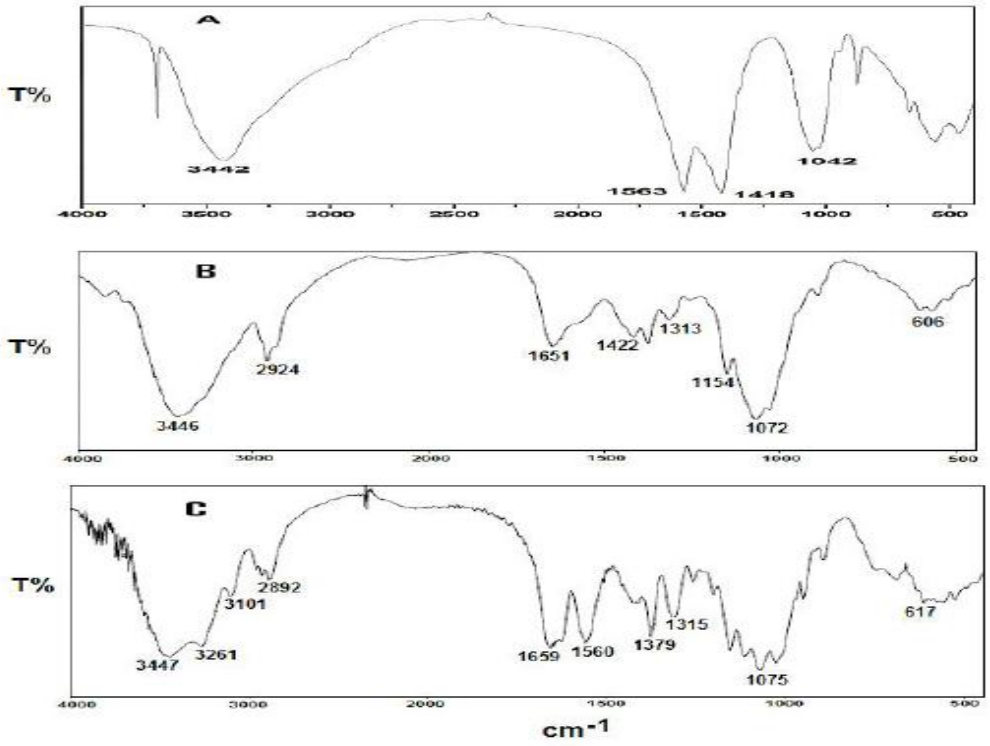

Figure 2. Spectrum Infrared of chitosan obtained (A), literature[4] (B) and (C) chitin[4] .

The results of thermal analysis by TG shown, showed that the first peak, on the evaporation of water, occurred at a temperature of 75.5 °C, with mass loss of 8.96%, whereas the second peak on the loss of organic material occurred at a temperature of 383.3 °C, with loss of 3.3%. The third event occurs decomposition, referring to the carbonized material, a peak temperature of 745.5 °C, with mass loss of 18.5%. These show that the degree acetylation directly influence the mass loss of chitosan, as observed in studies by Yen[6] . Regarding the effect on the thermal decomposition of the biopolymer was found that this presents a high peak temperature as described in the DSC curve. The value of enthalpy of the endothermic

process was ΔH = 590.4 J/g, with a peak temperature at 153 °C and a glass transition of 275.75 °C.

CONCLUSIONS

This study of the characterization of chitosan was interesting because it is a natural polymer obtained from exoskeleton of shrimp and rich in the presence of this biopolymer. The data obtained were compared with those of literature and all agree with those achieved in this research. We confirmed that for the pure chitosan to be a degree of deacetylation over 50% and obtained a value of 65.4%, a value which ensures the purity of the polymer obtained. Finally, with data from infrared spectroscopy obtained which confirmed the existence of characteristic functional groups, and thermal analysis (TG and DSC), which provided important data related to weight loss and glass transition temperature respectively, and the SEM showed that the fibrous aspect of this important biopolymer.

AKNOWLEDGEMENTS

To LabPetro and CCE/UFES for their support during the development of this research work.

REFERENCES

1 Silva HSR, Santos KSCR, Ferreira EI, Quitosana: Derivados hidrossolúveis, aplicações farmacêuticas e avanços. *Química Nova* **29**: 776-785 (2006).
2 Dias FS, Queiroz DC, Nascimento RF, Lima MB, Um sistema simples para preparação de microesfera de quitosana. *Química Nova* 31: 160-163 (2008).
3 Campana Filho SP, Signini R, Caracteristicas e propriedades de quitosanas purificadas nas formas neutra, acetato e cloridrato. *Polimeros: Ciência e Tecnologia* 11: 58-64 (2001).
4 Carvalho TV, Queiroz DC, Barros FCF, Cavalcante RM, Nascimento RF, Vasconcelos LCG, Produção e caracterização de esferas de quitosana modificada quimicamente. *Revista Iberoamericana de Polímeros* **7**: 1-15 (2006).
5 Rinaudo M, Chitin and chitosan: Properties and applications. *Prog. Polym. Sci*. **31**: 603-632 (2006).
6 Yen MT, Yang JH, Mau JL, Physicochemical characterization of chitin and chitosan from crab shells. *Carbohydrate Polymers* **75**: 15-21 (2009).

Structure and function of glycoside hydrolase family 19 chitinases

Wimal Ubhayasekera

MAX-lab, Lund University, Box 118, S-22100 Lund, Sweden and
Institute of Medicinal Chemistry, University of Copenhagen, Universitetsparken 2, DK-2100 Copenhagen Ø, Denmark.
E-mail:Wimal.Ubhayasekera@maxlab.lu.se; Phone +46-(0)709 320013

Abstract
Glycoside hydrolase family 19 chitinases are found in plants, bacteria and viruses playing various roles. Plant chitinases are important for defense and development where bacterial examples are useful for nutrition. The available structural studies show that family 19 enzymes are highly α-helical bi-lobed structures with a wide cleft lined by conserved residues. These inverting endochitinases demonstrate an opening-closing mechanism of the catalytic cleft during chitin hydrolysis due to loop movements. However, complex structures with inhibitor/substrate analogs are required for a deeper understanding of these enzymes.

Keywords: endochitinase, inverting mechanism, loop movements, opening-closing

INTRODUCTION

Chitin, an insoluble homopolymer of β-(1->4) linked N-acetylglucosamine units (GlcNAc), is one of the most abundant natural polymers. Chitinases (EC 3.2.1.14) are the nature's tool to breakdown chitin by hydrolyzing the glycosidic bonds between GlcNAc units, thus many organisms have retained chitinase genes during evolution. It is one of the major weapons for the defense against pathogens not only in higher plants and seaweeds but also in fish and mammals. Microorganisms digest the chitinous substrates for nutrients or hydrolyze their own chitinous cell walls for cell proliferation, while arthropods such as insects and crustaceans produce chitinase in order to degrade the exo-skeleton during ecdysis. These functional variations result in the difference in spatial and temporal localization, substrate specificity and structure of chitinases.

Classification

Chitinases are classified into two main glycoside hydrolase (GH) families, 18 and 19 based on the amino acid sequence identity of the catalytic module (CM).[1] These two groups are different in sequence, structure as well as in the catalytic mechanism. Several organisms such as bacteria, plants, fungi, arthropods, amphibians, fish and mammals including humans, produce GH family 18 chitinases having 8-stranded α/β barrel (TIM-barrel) fold whereas eight strands of parallel β-sheet are laid down with a helix as the "return stroke". The eight strands of the sheet bend into a barrel structure with the helices forming a ring around the outside.[2] There are two types of family 18 chitinases, viz. 'plant type' with endo-activity that generates products of varying length and a 'bacterial type' with exo-activity releasing chitobiose or chitotriose from the non-reducing end of chitin.[3] Family 19 consists of enzymes from plants, bacteria and viruses, which play different roles depending on the origin. Plant chitinases up-regulate as a result of pathogenic attacks (pathogenesis-related protein), variety of stress conditions (e.g. drought, salinity, wounding, heavy metals in their environment, endogenous and exogenous elicitor treatments and plant growth regulators),[4] phytohormones and during growth and development[5] where bacterial chitinases play a main role in nutrition. Pathogenesis-related proteins (PR) are defined as plant proteins that are induced in pathological or related situations. Out of 14 PR protein families, four are chitinases.[6]

Plant endochitinases, a diverse group of enzymes, with differences in primary structure, isoelectric point and cellular localization, have been classified into 6 different classes (I-VI) based on amino acid sequence similarities of the CM, and the presence and absence of an N-terminal cysteine rich domain.[7, 8] Most of the GH family 19 plant chitinases fall into classes I, II and IV. Class I and II are highly similar; the crucial difference is that the former has a chitin binding module (CtBM). These chitinases act on chitin in pathogen cell walls, bacterial peptidoglycan and lipochito-oligosaccharides (Nod factors) produced by nitrogen fixing bacteria. Although there are no information on endogenous substrates for plant chitinases, supporting evidence for the hydrolysis of arabinogalactan proteins and N-acetylglucosamine containing glycoproteins in cell walls has been reported.[4] Chitinase expression in plants has been observed in all organs and tissues in both the vacuole and the apoplast.[4]

STRUCTURAL STUDIES OF FAMILY 19 ENDOCHITINASE

Chitin binding module

Some family 19 chitinases possess CtBMs, which contain a common structural motif of 30-43 amino acid residues with several cysteines and glycines at conserved positions.[9,10] So far only class I chitinase from rice contain the crystal structure of the intact protein (PDB entry 2DKV). However the linker region between the two modules was not traceable in the structure. These binding modules may have affinity towards various complex glycoconjugates containing GlcNAc or N-acetyl-D-neuraminic acid (NeuNAc). CtBMs may be helpful to promote the activity of the enzyme by increasing the affinity for its substrate. Both the reported as well as unpublished observations suggest that the CtBMs of plant chitinases may help the CM to destroy the hyphae in fungal pathogenic attacks by placing the CM closer to the cell wall chitin.

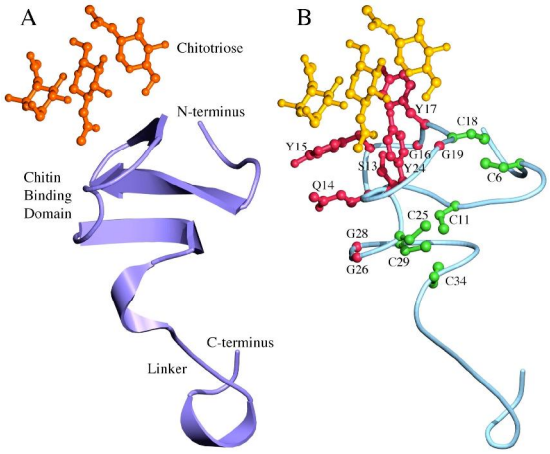

Figure 1. Homology model of the CtBM from Norway spruce chitinase. A. Ribbon representation showing the CtBM. B. CtBM is shown as a rattler. Conserved cysteines, chitin binding residues and chitin are shown in green, red and orange, respectively.

The CM and CtBM can function separately. However, it was obvious that when the two modules were linked together, activity toward the insoluble chitin polymer was enhanced (unpublished). Further, the CtBM plays a vital role for the effectiveness of antifungal activity but it is not necessary for the antifungal or catalytic activity.[11,12] Most of the CtBM found in family 19 chitinases belong to carbohydrate binding module (CBM) family 18. The rice chitinase structure as well as homology models of the CtBMs of chitinases from Norway

spruce (Fig.1) and mustard have shown the fold of the module is similar to that of wheat germ agglutinin isolectin structure, having a small globular shape with irregular β-sheet (Fig. 1A), at least containing three β-strands. The smallest CtBMs, which are in class IV chitinases, have at least three conserved disulfide bridges (Fig. 1B).[12] The highly conserved residues, including aromatic residues, clustered on one face of the protein are likely to be important for chitin binding. However, it is not clear whether the CtBM has any activity other than anchoring the protein on chitin. The class IV chitinase from Norway spruce is known to inhibit *Heterobasidion annosum* growth better when the CtBM is attached to the CM.[12]

Linker

CtBMs of enzymes are connected to CMs by linkers. There are no structures of the linkers alone or together with binding and CMs known for chitinases. It has been speculated for Norway spruce chitinase that binding module and CM can act independently and are functional separately, although the linking of the two modules clearly allows the CM to gain better access to substrate. Binding modules bind to the solid substrate giving the possibility for the CM to act nearby. The module-connecting linkers can be relatively short or long. The longer linkers are protected from proteolytic cleavage possibly by its glycosylation, which may also act facilitating protein secretion and stabilizing the enzyme. These linkers are Ser/Thr/Pro rich. By analogy to the linkers known for cellulases, chitinase linkers are long and flexible enough for allowing the modules to orientate in a way needed to gain the maximum efficiency.

Vacuolar targeting

There are reports indicating that at the C-terminus of several family 19 plant chitinases, an extension of amino acid sequence represents a vacuolar targeting signal; this signal could be cleaved off post-translationally.[10] The absence of such a C-terminal extension could be correlated with extracellular targeting; i.e. class II and class IV chitinases. Therefore, these extracellular (unlike intravacuolar) chitinases could be a defensive tactic against fungal pathogens. These chitinases also have a signaling function for releasing elicitors from either invading fungal hyphae or glycolipids present in the cell walls during development.[4] However, none of the available chitinase structures contain this particular C-terminal extension limiting the knowledge on it.

Catalytic module structure

There are 8 family 19 chitinase crystal structures, 6 from plants and 2 from bacteria, reported to date (Table 1). Family 19 enzymes have a highly α-helical bi-lobed structure with a wide cleft lined by conserved residues. The catalytically important residues and 3 disulfide bonds are conserved in family 19 plant enzymes (Fig. 2) where there are only two disulfide bridges in bacterial examples due to loop deletion. Considering *Brassica juncea* (mustard) chitinase as the reference structure (PDB code 2Z37)[13] (Fig. 2), Glu212 and Glu234 have been identified as the proton donor and the general base respectively. The mutational studies have shown that Arg361 and Glu349 can work together as a catalytic triad altering properties of Glu212 especially changing the pKa to activate it.[14] The distance between Glu212 and Glu234 is ~9Å showing a feature of inverting hydrolases. The residue His211 is also essential for the enzyme, although the reason for this is not yet clear. It may simply play a role in changing the properties of Glu212 supporting the function. The other guess is that it may be important for proton transfer during the reaction or in binding. The mutational studies have shown that Glu234 is not essential for the reaction.[14,15] These residues are highly conserved in this family. The catalytic triad is located in rather rigid region of the structure. Glu234 is located in the mobile loop III. The conserved motif 268-NYNYG is located closer to loop III.

Table 1: Comparison of mustard chitinase structure (PDB entry 2Z37)[13] with other family 19 chitinase structures.

Source	PDB entry	Number of Cα atoms matched	R.m.s. difference (Å)	Sequence identity to mustard chitinase (%)	Plant chitinase class	Loops
Carica papaya	3CQL	237	0.867	67	I or II[a]	I, II, III, IV, V
Streptomyces coelicolor A3(2)	2CJL	175	1.226	41		III, IV
Streptomyces griseus HUT 6037	1WVU	189	1.081	39		III, IV
Canavalia ensiformis	1DXJ	238	0.969	58	II	I, II, III, IV, V
Hordeum vulgare	1CNS	238	0.638	60	II	I, II, III, IV, V
Hordeum vulgare	2BAA	237	0.910	61	II	I, II, III, IV, V
Oryza sativa	2DKV	239	0.782	60	I	I, II, III, IV, V
Picea abies	3HBE	191	1.081	45	IV	I, III,

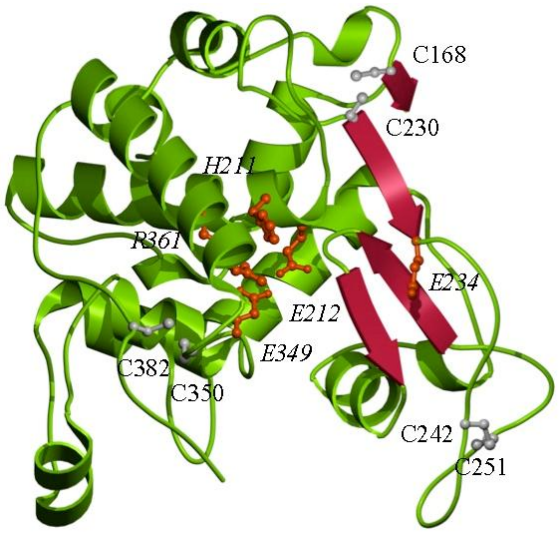

Figure 2. Ribbon representation of the mustard chitinase structure (PDB entry 2Z37) showing the catalytically important residues (orange-red) and conserved cysteines (gray). The irregular β-sheet is shown in crimson.

The structural alignment of mustard chitinase reveals that these enzymes have a fairly rigid core with structural plasticity of some loops border the wide catalytic cleft. The loop movements in segments 164-170, 217-222, 235-257, 308-311 and 325-332 (designated as loops I-V respectively) in mustard chitinase structures were well supported by electron density (Fig. 3).[13]

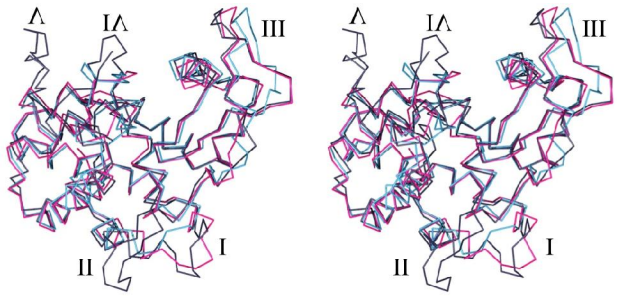

Figure 3. Stereo plot showing the comparison of chitinase structures from Norway spruce (Class IV) (PDB entry 3HBE), mustard (Class I-like) (PDB entry 2Z38) and *Streptomyces coelicolor* A3(2) (PDB entry 2CJL) in magenta, mid-night-blue and sky-blue respectively. The loops are marked I-V.

Class I/II structures possess these loops where class IV enzymes lack loops II, IV and V. Bacterial enzymes do not have loops I, II and V where loops III and IV have different conformations (Fig. 3). Flexibility of these loops was obvious among the molecules of the same structures as well as in different structures. It has been observed for mustard chitinase that loops move when different ligands are soaked.[13] Papaya chitinase bound to GlcNAc (PDB code 3CQL)[16] is more closed compared to other structures without bound ligands. It is not only loops but also the others parts move upon GlcNAc binding. Catalytic residue in class IV enzyme structure from Norway spruce (PDB code 3HBE)[12] shows conformational changes displaying that the side chain can move if necessary during the reaction keeping the interaction with Arg in the triad (Fig. 4).[12]

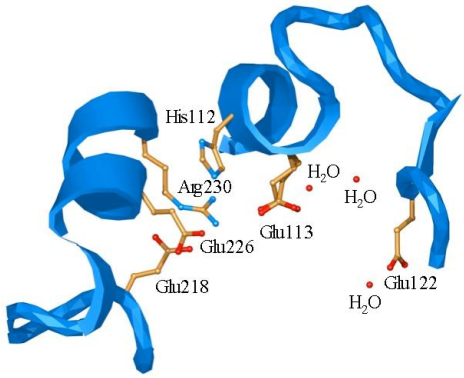

Figure 4. Active site of Norway spruce chitinase showing the conformational changes of the catalytic acid Glu113 (PDB entry 3HBE).

The catalytic clefts are varying in the length, probably accommodating 3 to 7 GlcNAc units depending on the enzyme. Modeling of chitin on class I-like mustard chitinase shows that the catalytic cleft can accommodate 7 GlcNAc units; 3 on the product side and 4 on the substrate binding side. Loop II deletion in bacterial enzymes shortens the product side by one sugar unit, whereas in class IV enzymes deletion of loops II and IV has left space in the cleft only for 3 sugar units. One prominent observation is that family 19 enzymes lack aromatic residues in the catalytic cleft compared to family 18 chitinases and cellulases. Therefore, chitin binding in these CMs is dominated by hydrogen bonding interactions.

The lack of effective inhibitors for family 19 enzymes has hampered obtaining complex

structures. This may be partly due to the wide catalytic cleft; that is suited for large insoluble molecular binding rather than small soluble compounds.

CATALYTIC MECHANISM

The observations so far suggest an opening-closing mechanism for family 19 chitinases during the activity. The catalysis takes place after binding an undistorted chair conformation of the chitin chain in the open cleft at the vicinity of the proton donor (Glu212).[13] Then, the movements both in the lobes and the loops tighten the grip on the substrate making it easier for the catalysis. The loop III has a significant role in placing the substrate in the catalytic cleft. First, Glu212 donates a proton to O1 of sugar activating it. Then, loop III moves bringing Glu234 closer to the substrate, where Glu234 abstract a proton from a water molecule and direct the attack on the anomeric carbon of the sugar inverting the anomeric configuration in the product. It is also suggested that the Glu234 has a role in stabilizing the oxocarbenium ion intermediate of the reaction. Mutational studies have shown the importance of the role of Glu212 rather than the Glu234 suggesting that it actives a water molecule in the bulk solvent, which can attack the sugar directly. The product must leave the enzyme freely since there is no product inhibition observed.

ACKNOWLEDGEMENT

Financial support from DANSCATT and Lundbeckfonden is acknowledged.

REFERENCES

1 Henrissat B and Bairoch A, *Biochem J* **293:**781-788 (1993).
2 Robertus JD and Monzingo AF, *Exs* **87:**125-135 (1999).
3 Andersen OA, Dixon MJ, Eggleston IM and van Aalten DM, *Nat Prod Rep* **22:**563-579 (2005).
4 Kasprzewska A, *Cell Mol Biol Lett* **8:**809-824 (2003).
5 Wiweger M, Farbos I, Ingouff M, Lagercrantz U and Von Arnold S, *J Exp Bot* **54:**2691-2699 (2003).
6 van Loon LC and van Strien EA, *Physiol Mol Plant P* **55:**85-97 (1999).
7 Meins F, Fritig B, Linthorst HJM, Mikkelsen JD, Neuhaus JM and Ryals J, *Plant Mol Biol Rep* **12:**S22-S28 (1994).
8 Neuhaus JM, Fritig B, Linthorst HJM, Meins F, Mikkelsen JD and Ryals J, *Plant Mol Biol Rep* **14:**102-104 (1996).
9 Raikhel NV, Lee HI and Broekaert WF, *Annu Rev Plant Phys* **44:**591-615 (1993).
10 Beintema JJ, *FEBS Lett* **350:**159-163 (1994).
11 Iseli B, Boller T and Neuhaus JM, *Plant Physiol* **103:**221-226 (1993).
12 Ubhayasekera W, Rawat R, Ho SW, Wiweger M, Von Arnold S, Chye ML and Mowbray SL, *Plant Mol Biol* **71:**277-289 (2009).
13 Ubhayasekera W, Tang CM, Ho SW, Berglund G, Bergfors T, Chye ML and Mowbray SL, *FEBS J* **274:**3695-3703 (2007).
14 Tang CM, Chye ML, Ramalingam S, Ouyang SW, Zhao KJ, Ubhayasekera W and Mowbray SL, *Plant Mol Biol* **56:**285-298 (2004).
15 Hoell IA, Dalhus B, Heggset EB, Aspmo SI and Eijsink VG, *FEBS J* **273:**4889-4900 (2006).
16 Huet J, Rucktooa P, Clantin B, Azarkan M, Looze Y, Villeret V and Wintjens R, *Biochemistry* **47:**8283-8291 (2008).

Evaluation of different protocols for isolation of chitin from the mushroom *Ganoderma lucidum*

Sandra P. Ospina[1], David A. Ramírez[1], Deisy N. Mesa[2], Diana M. Escobar[2], Claudia P. Ossa[2], Lucía Atehortúa[1] and Paola Zapata[1]

[1] Biotechnology Group, Institute of Biology, Universidad de Antioquia, Street 62 No 52-59, Laboratory 210, Medellín, Colombia
[2] Biomaterials, Faculty of Engineering, Universidad de Antioquia, Medellín, Colombia
*E-mail: sandritao@gmail.com

Abstract
Fungal chitin was prepared from mycelial biomass of *Ganoderma lucidum* by alkaline treatments and decolorization methods. The chitin was isolated from mycelium of submerged cultures of *Ganoderma lucidum* as potential source of chitin under biotechnological processes. The extraction of chitin was carried out by developing 5 different assays (A1, A2, A3, A4, A5) that involved mainly three phases, deproteinization of the mycelia with NaOH solution, extraction of chitosan with acetic acid, and a process of decolorization with potassium permanganate and oxalic acid. The chitin contents from 9-day mycelia of submerged culture were 413, 339, 87, 78, and 144.2 mg g^{-1} (milligrams of chitin/grams of dry biomass) for A1, A2, A3, A4 and A5, respectively. The chitin was characterized by X-Ray Diffraction to determine their crystallinity and Fourier Transform Infrared Spectroscopy to determine their molecular structure. The major crystalline peak for chitin was at 19º and characteristics bands at 2922, 1657, 1572, 985 and 3414 cm^{-1}. The advantage of the biotechnological processes was demonstrated and it has been shown that *Ganoderma lucidum* fungus may be used as a potential raw material for chitin production.

Keywords: Chitin, *Ganoderma lucidum*, Submerged Culture, Mycelial Biomass.

INTRODUCTION

Chitin is the second abundant biopolymer in the nature, found in the shell of crustacean, the cuticles of insects, and the cell walls of fungi. Chitin in cell walls of fungi such as mushrooms is a straight-chain polymer composed of *β*-1,4-*N*-acetylglucosamine and classified as *γ*-chitin[1,2,3,4]. Chitin and its derivative chitosan are natural aminopolysaccharides that have unique structures, multidimensional properties, highly sophisticated functions and wide ranging applications in biomedical and other industrial areas [1,5,6]. The most important characteristics of this biomaterial are: excellent biocompatibility and biodegradability with ecological safety and low toxicity. In addition, chitin and chitosan have versatile biological activities and low immunogenicity[5]. It has become of great interest not only as an under-utilized resource but also as a new functional biomaterial of high potential in various fields such as pharmaceutical, medical, cosmetic, food and agricultural industries [7,8,9,10].

The traditional and commercial source of chitin is from shells of crab, shrimp and krill that are wastes from the processing of marine food products. The annual worldwide crustacean shells production has been estimated to be 1.2×10^6 tons, and the recovery of chitin and protein from this waste is an additional source of revenue[11]. However, crustacean shell wastes can be limited and subject to seasonal supply. In recent years, chitin obtained by extraction from fungal mycelia is gaining importance. Fungal mycelia can be cultivated throughout the year by fermentation under submerged culture that is rapid, synchronized and can be performed in bioreactors with all automated and controlled conditions; therefore, mycelial biomass is homogeneous, both in quality and quantity produced in each batch [6,11,12].

In this study, we report five protocols for isolation of chitin from *Ganoderma lucidum* produced under submerged culture conditions, in a culture medium optimized for biomass production[12]. Chitin analysis was performed using x-ray diffraction; also the chitin content and crystallographic type of chitin extracted were determined.

MATERIALS AND METHODS

Materials

Sodium hydroxide, acetic acid, potassium permanganate, ethanol 96% pure and oxalic acid was obtained from Merck KGaA (Darmstadt, Germany).

Microorganism

Strain of *Ganoderma lucidum* was grown in the Universidad de Antioquia Plant Biotechnology Laboratory. The organisms were maintained by an occasional transfer on potato dextrose agar (PDA) medium at 4°C.

Cultivation

Actively growing mycelia were obtained from a newly prepared agar-plate culture after it was incubated for 9 days at 24°C. The pre-inolucums were prepared as follows. Around 1 cm × 1 cm of the mycelia was inoculated into a 250 ml erlenmeyer flasks that contained 50 ml of complex medium developed in the Biotechnology Laboratory, Universidad de Antioquia[12]: (50 g l^{-1} complex carbon source, 0.03 g l^{-1} K_2HPO_4, 0.08 g l^{-1} $NaNO_3$, 0.01 g l^{-1} KCl and 0.02 g l^{-1} $MgSO_4.7H_2O$). Flask cultivation was carried out at 100 rpm for 7 days.
Subsequently, a bioreactor (Bioflo 110 Reactor New Brunswick® of 7 liters, with 5 liters of work volume) was inoculated with an inoculum of 4% v/v, agitation rate of 200±2 rpm and aeration of 5 VVM. Sterilization was done in an autoclave at 121°C for 20 min. All cultures were carried out at temperature of 26±1°C in bioreactor and pH 6.0 for 14 days. The fungal biomass was dried by lyophilization (FDU-100 Liophilizer Eyela®) to obtain and measure the amount of mycelium formed. All conditions were monitored throughout the culture period. The experiment was performed in triplicate.

Chitin Isolation

Chitin was prepared from *Ganoderma lucidum* according to three modified protocols of Synowiecki & Al-Khateeb[13], Yen and Mau[6] and Su *et al.*[14]:

Assay 1 (A1): The dried fungal biomass was pulverized. Deproteinization was performed using alkaline treatment 1 M NaOH at ratio of 1:30 (w/v) at 40°C for 2 h. The absence of proteins was indicated by the absence of colour of the solution. The suspension was centrifuged and washed with deionized water to neutrality. Chitosan was extracted with acid treatment with acetic acid solution 5 and 10% at the ratio 1:30 (w/v) at 90°C for 3 h. The mixture was centrifuged and washed with deionized water, 95% ethanol and acetone and dried at 50°C to a constant weight.

Assay 2 (A2): The dried fungal biomass was pulverized. Deproteinization was performed using alkaline treatment with 1 and 2 M NaOH at the ratio of 1:30 (w/v) at 90°C for 2 h. The absence of proteins was indicated by the absence of colour of the solution. The suspension was centrifuged and washed with deionized water to neutrality. Chitosan was extracted with acid treatment with acetic acid solution 5 and 10 % s at the ratio 1:30 (w/v) at 90°C for 3 h. The mixture was centrifuged and washed with deionized water, 95% ethanol, and acetone and dried at 50°C to a constant weight.

Assay 3 (A3): The dried fungal biomass was pulverized. Deproteinization was performed using alkaline treatment with 2 and 4 M NaOH at the ratio of 1:30 (w/v) at 90°C for 2h and 100 °C during 2 h, respectively. The absence of proteins was indicated by the absence of colour of the solution. The suspension was centrifuged and washed with deionized water to neutrality. For decolorization, the crude chitin was treated with 10 g L^{-1} potassium permanganate for 1 h, and then reacted with 10 g L^{-1} oxalic acid for 1 h. The mixture was centrifuged and washed with deionized water to neutrality and dried at 30°C to a constant weight.

Assay 4 (A4): The dried fungal biomass was pulverized and a part of it was subjected to extraction twice with hot water for removing some unwanted polysaccharides. The residue was collected and dried in an oven at 40°C. Deproteinization was performed using alkaline treatment with 2, 4, 6 and 8 M NaOH at the ratio of 1:20 (w/v) at 100 °C for 3 h. The absence of proteins was indicated by the absence of colour of the solution. The suspension was centrifuged and washed with deionized water to neutrality. For decolorization, the crude chitin was treated with 10 g L^{-1} potassium permanganate for 1 h, and then reacted with 10 g L^{-1} oxalic acid for 1 h. The mixture was centrifuged and washed with deionized water to neutrality and dried at 50°C to a constant weight.

Assay 5 (A5): The dried fungal biomass was pulverized and mixed with deionized water and then, the mixture was subjected to a sonication process for 40 minutes. Biomass was washed with ethanol for 24 hours. Deproteinization was performed using alkaline treatment with 4 M NaOH at the ratio of 1:20 (w/v) at 100 °C for 2 h, this treatment was repeated three times. The absence of proteins was indicated by the absence of colour of the solution. The suspension was centrifuged and washed with deionized water to neutrality. For decolorization, one part of the crude chitin was treated with 10 g L^{-1} potassium permanganate for 1 h, and then reacted with 10 g L^{-1} oxalic acid for 1 h. The mixture was centrifuged and washed with deionized water to neutrality and dried at 50°C to a constant weight.
Finally, the amount of chitin produced by each protocol was determined by dry weight method.

X-Ray Diffraction
The X-ray diffraction (XRD) analysis was applied to detect the crystallinity of chitins prepared and their patterns were recorded using a X´Pert PRO MPD diffractometer from PANalytical with Cu Kalpha radiation of 1.5406 Å, power of 1.8 kW (40 mA and 45 kV). Data were collected at a scan rate of 0.057088°/s with the scan angle from 3 to 50.

FTIR Analysis
Fourier transform infrared spectroscopy (FT-IR) analysis was used to analyze the molecular structure of isolated chitin with Assay 5 and their spectra were recorded using a SpectrumOne Spectrophotometer with detector DTGS from Perkín Elmer®. The average number of scans taken per sample was 8 in the spectral region between 450 and 4000 cm^{-1}, with a resolution of 4 cm^{-1}. The samples were prepared in 0.25 mm thickness KBr pellets (5 mg in 100 mg of KBr) and stabilized under controlled relative humidity before obtaining the spectrum.

RESULTS
Cultivation
The fungal growth was monitored for 12 days through batch submerged culture. Biomass production under growing conditions was 21.87±2.2 g L^{-1}.

Chitin Isolation

Chitin was obtained from dried biomass of *Ganoderma lucidum* by mean of alkaline treatment, acid treatment and/or decolorization processes with potassium permanganate and oxalic acid. The average amount of chitin obtained is between 46.4 and 877 mg g^{-1} in the different assay (milligrams of chitin for grams of dry biomass). The percentages of the yields for chitin prepared from the mycelium of *G. lucidum* are shown in Table 1.

Table 1.
Yield percent of chitin prepared from the mycelial biomass of *Ganoderma lucidum*

Assay	Yield chitin (%)
A 1	41.3
A 2	33.9
A 3	8.7
A 4	7.8
A 5	14.42

Assays 1 and 2 were acid treatment to precipitate chitosan of the fungal biomass, however chitosan recovered was very low and therefore it could not be quantified and analyzed. Thus, assays 3, 4 and 5 are not performed this stage.

The best results of XRD analysis for each assay are shown in Figure 1. Diffractograms for firsts four assays exhibit two peaks of highest intensity, located approximately between 18-21° and another at 30°, both with variations at intensity and bandwidth according to the assay done. Assays 1, 2 and 3 show chitin diffractograms with peaks of low intensity and wide bandwidth at 21.1°, 20° and 22.1°, respectively. At once, diffractograms of assays 4 and 5 present a marked increase at the intensity of crystalline peaks. Chitin XRD pattern at assay 4 shows three crystalline peaks at 5.6°, 21.7° and 30.1°, the last one with low intensity, while chitin XRD pattern shows high intensity peaks at 5.7° and 19.6°.

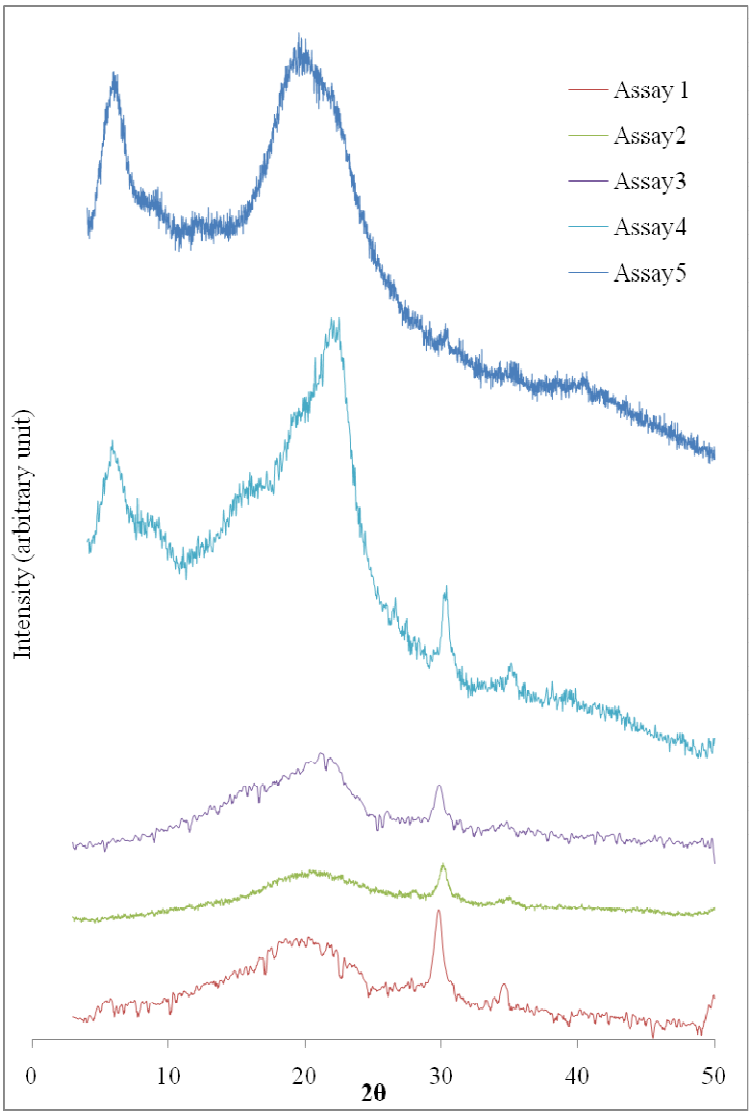

Figure 1. X-ray diffraction patterns of chitins Assay 1-5.

FTIR analysis was made for chitin from assay 5 and it is shown at Figure 2. The FTIR shows representative bands at 3414, 2922, 1657, 1381, 1160, 1078 and 985 cm^{-1}. Additionally, a correlation of 79.53% between the chitin obtained and a standard chitin (Chitin from crab shells, Sigma-Aldrich) was found.

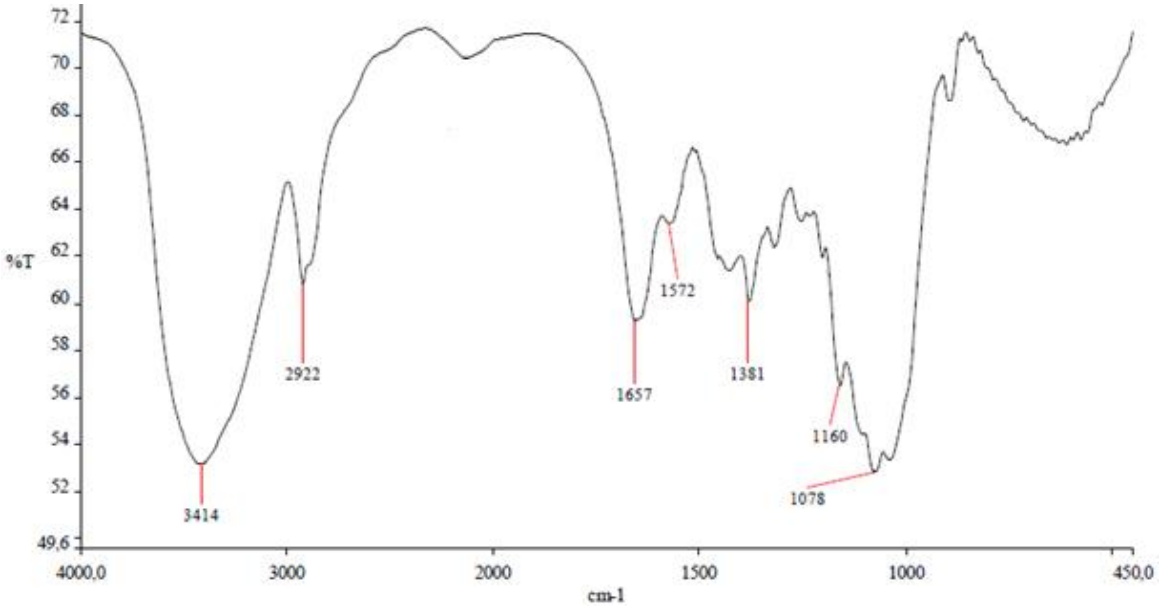

Figure 2. IR spectrum for chitin (Assay 5).

DISCUSSION

XRD patterns of assays 1, 2 and 3 were similar; however, the XRD pattern of the assay 2 had peaks with a lowest intensity. Apparently, concentrations of the alkaline solutions did not affect the crystallinity of chitin obtained, it was observed that the decolorization process increases the crystallinity and decreases the peak intensity located at 30°, which is not characteristic of chitin. Reviewing XRD patterns of the reagents used for extraction of chitin was observed that the peak located at 30° corresponds to a peak characteristic of NaOH, indicating that there was not a complete elimination of this compound and it still remained in small amounts in the analyzed samples. These results suggest the presence of chitin with one or more undesirable compounds which produce a broad peak near 19° and non-characteristic peaks of the interested biopolymer. Some authors have reported characteristic crystalline peaks of the different types of chitin. They are shown in Table 2.

Table 2. Characteristic peaks of α, β and γ chitin reported by some authors.

Author	Type of chitin	Characteristic peaks	Source
Jang *et al.*[15]	α-chitin	9.6°, 19.6°, 21.1° and 23.7°	Crab Shell
	β- chitin	9.1° and 20.3°	Squid pen
	γ- chitin	9.6° and 19.8°	*Lucainade*
Cardenas *et al.*[16]	α- chitin	19.18° and 19.26°	Shrimp, praw, king crabs and lobster
	β- chitin	18.78°	Squid
Kim *et al.*[17]	β- chitin	9.8° and 19.3°	Squid
Yen and Mau[18]		9.3° and 19°	Crabs
Yen and Mau[6]		5.4°-5.6°, 9.1° and 19.3°-19.6°	*Lentinula edodes*

The evidence seems to confirm that the chitin obtained in the five trials showed above have the characteristic peak of standard chitin about 19°. Furthermore, the chitin obtained at assays 4 and 5 showed the characteristic peak of standard chitin around 5.6 °.

FTIR analysis of chitin obtained in assay 5 showed a similar spectrum of standard chitin (not shown). Band located approximately at 2900 cm^{-1} is used in the literature as a representative band for chitin and chitosan[11]. Another band at 2922 cm^{-1} corresponds to the absorption band of C - C bonds (alkanes). Others chitin characteristic bands are also present at 1657 cm^{-1} for the amide I, 1572 cm^{-1} for the amide II and 985 cm^{-1} for the amide III. Band for carbonyl groups link through hydrogen bonds to the amino group can be seen at 1657 cm^{-1}. Vibration present at 3414 cm^{-1} corresponds to intramolecular hydrogen bond involving the OH (6)···O = C, also in this region are two modes of vibration due to the NH of the amide bonds, specifically because of the intramolecular hydrogen bonds C = O···H-N and NH groups linked intramolecularly with H .

Similarity of FTIR spectrum between chitin from *G. lucidum* for final assay and standard presented a correlation percentage of 79.53%, so it, XRD results for this assay show a pattern of peaks whose corresponds with standard chitin is presented at 5.6° and 19°. From previous results it is possible to say that chitin from this fungus may be a promising source to obtain this biomaterial.

CONCLUSIONS

The highest production of chitin was obtained in 1 assay (41.3% g/g), however, XRD and FTIR analysis showed that chitin obtained at assay 5 had the greatest similarity to the standard chitin at both, therefore, best result were obtained when the biomass was sonicated and washed with ethanol and then deproteinization with 1M NaOH at 100°C for 2h and subsequently bleaching using potassium permanganate and oxalic acid. Finally, it can conclude that the biomass from *Ganoderma lucidum* obtained by biotechnological culture, is a promising source of chitin and its derivatives.

ACKNOWLEDGEMENTS

THE AUTHORS ACKNOWLEDGE FINANCIAL SUPPORT FROM CODI (UNIVERSIDAD DE ANTIOQUIA) AND BIOTECHNOLOGY GROUP OF INSTITUTE OF BIOLOGY AND BIOMATERIALS GROUP OF FACULTY OF ENGINEERING, UNIVERSITY OF ANTIOQUIA (MEDELLÍN, COLOMBIA).

REFERENCES

1 Brunner E, Ehrlich H, Schupp P, Hedrich R, Hunoldt S, Kammer M, Machill S, Paasch S, Bazhenov VV, Kurek DV, Arnold T, Brockmann S, Ruhnow M and Born R, *Journal of Structural Biology* **168**:539 (2009).
2 Campana-Filho SP, de Britto D, Curti E, Abreu F, Cardoso M, Battisti M, Sim P, Goy R, Signini R and Lavall R, *Química Nova* **30**:644 (2007).
3 Muzzarelli RAA and Jeuniaux C, *Pergamon Press* (1976).
4 Knorr D, *Food Technology* **38**:85 (1984).
5 Pillai CKS, PaulW and Sharma CP, *Progress in Polymer Science* **34**:641 (2009).
6 Yen MT and Mau JL, *LWT* **40**:558 (2007).
7 Khor E and Lim LY, *Biomaterials* **24**:2339 (2003).

8 Khor E. Chitin: a biomaterial in waiting. *Current Opinion in Solid State & Materials Science* **6**:313(2002).
9 Prashanth KVH and Tharanathan RN, *Trends in Food Science & Technology* **18**:117 (2007).
10 Rudrapatnam NT and Farooqahmed SK, *Critical Reviews in Food Science and Nutrition* **43**:6 (2003).
11 Teng WL, Khor E, Tan TK, Lim LY and Tan SC, *Carbohydrate Research* **332**:305 (2001).
12 Zapata PA, Rojas DF, Ramírez DA, Fernández C and Atehortúa L, *International Journal of Medicinal Mushrooms* **11**:93 (2009).
13 Synowiecki J and Al-Khateeb NAAQ. *Food Chemistry* **60**:60 (1997).
14 Su CH, Sun CS, Juan SW, Hu CH, Ket WT and Sheut MT, *Biomaterials* **16**:1169 (1997).
15 Jang MK, Kong BG, Jeong YI, Lee CH and Nah JW, *Journal of Polymer Science Part A: Polymer Chemistry* **42**:3423 (2004).
16 Cardenas G, Cabrera G, Taboada E and Miranda SP, *Journal of Applied Polymer Science* **93**:1876 (2004).
17 Kim SS, Kim SH and Lee YM, *Journal of Polymer Science Part B: Polymer Physics* **34**:2367 (1998).
18 Yen MT and Mau JL, *Annual of Tainan Woman's College of Arts and Technology* **23**:229 (2004).

Production and activity of chitinases and hydrophobins obtained from solid and liquid cultures of *Lecanicillium lecanii*

Zaizy Rocha-Pino and Keiko Shirai*

Universidad Autonoma Metropolitana, Biotechnology Department, Laboratory of Biopolymers, Av. San Rafael Atlixco No. 186. Col. Vicentina, C.P. 09340, Mexico City, Mexico
*Email: smk@xanum.uam.mx

Abstract
The aim of this study was to evaluate the effect of culture type and carbon source on production and activity of chitinases and hydrophobins produced by *Lecanicillium lecanii*. The microorganism was grown on solid state culture using polyurethane as support (SSC) in submerged culture (SmC). Fructose (F), fructose with chitin (ChF), sucrose with chitin (SCh) and chitin (Ch) were tested as carbon sources in mineral media. The presence of endochitinases, exochitinases, chitobiases and *N*-acetylhexosaminidases were determined by electrophoresis using chitooligomers, with molecular weights (M_w) from 9 to 112 kDa. The SSC increased the production of chitinases and hydrophobins compared with SmC. The hydrophobins isolated from SSC with chitin reduced *ca.* 50% the hydrophobicity of teflon and showed a band with M_w of 7 kDa. This paper contributes to the understanding of how the media composition affects the production of both chitinases and hydrophobins, which can be related to the pathogenesis of these fungi.

Keywords: chitinases, hydrophobins, *Lecanicillium lecanii*, solid, colloidal chitin

INTRODUCTION

The development of infective processes of entomopathogenic fungi displays the formation of aerial hyphae, which occurs by the secretion of surfactant molecules that reduce the surface tension of aqueous environments. These surfactant molecules enable the mycelia to grow in air and mediate the adhesion of the hyphae on the surface of the host (i.e. insect cuticle). These are proteins known as hydrophobins and its production is related to growth and early stages of the pathogenesis.[1,2] Later on, the fungi excrete enzymes that degrade polymeric substrates (i.e. chitin, protein) to simpler compounds that serve as nutrients; such enzymes may be chitinases and proteases, which are required during penetration of the fungus to the host cuticle. Chitinases are regulated by degradation products of chitin and they are classified as endochitinases (EC 3.2.1.1.4), which randomly break down internal links of the chain; exochitinases (EC 3.2.1.14) that release diacetylchitobiose; chitobiases (EC 3.2.1.30) that split dimer of *N*-acetylglucosamine (chitobiose) and *N*-β-acetylhexosaminidase (EC 3.2.1.52) responsible for hydrolyze chitobiose, chitotriose or chitotetraose[3].
The study of both, hydrophobins and chitinases, are of great interest for their role in antagonistic mechanisms and also for biotechnology applications.[1-4] Despite of the numerous reports, there is a lack of research on the detection of hydrophobins of *Lecanicillium lecanii* in SSC related to chitinases production. The study aimed to evaluate the effect of the carbon source and culture type on the production and activity of chitinases and hydrophobins of *L. lecanii*.

MATERIALS AND METHODS

Culture conditions. *L. lecanii* 2149 was grown in mineral medium with yeast extract[4], the carbon sources tested were (g L^{-1}): Ch- colloidal chitin (30); F-fructose (22), ChF-fructose

(10) with Ch (10) and SCh-sucrose (10) with Ch (10). SSC was carried out in glass columns packed with polyurethane with support: nutrient ratio of 1:15 (w/v) an aeration rate of 1.4 ml air/min/g of moist material. SmC was performed in flasks and incubated in rotary shaker at 180 rpm. Both systems were inoculated with $5X10^7$ spores g^{-1} substrate and incubated at 25 °C for 7 days[4].

Chitinolytic activity on SDS-PAGE. Crude enzyme obtained at 144h was subjected to electrophoresis, using 12% SDS-PAGE[5] with added 0.01% (w/v) of 4-methylumbelliferyl *N*-acetyl-β-D-glucosamine oligosaccharides ($Mu(GlcNAc)_n$ with n = 2, 3, 4 or 5). The gel was incubated in 0.1 M phosphate buffer, pH 6 and 1% (v/v) Triton X100 for 24 h at 37 °C and stained with white calcofluor[6,7]. The bands were analyzed with the ImageJ program (version 2.1 for Windows).

Extraction and analysis of hydrophobins and their surface activity. The hydrophobins class I were extracted from mycelia obtained at 144 h of cultivation with formic acid[8]. Protein was determined by method of Bradford[9]. The surface activity was determined by contact angle[10]. The proteins extracted was subject to electrophoresis, utilizing 17% SDS-PAGE[5], stained with silver and analyzed with the ImageJ program. The analysis by reversed phase high performance liquid (RP-HPLC) was performed with a 5µm Supelcosil column LC 304. The mobile phase was with a gradient of trifluoroacetic acid (TFA) at 0.1 w/v% in water and TFA 0.1 w/v% in acetonitrile. The detection was carried out at 280 nm.

RESULTS

Chitinolytic activity on SDS-PAGE. The SSC with colloidal chitin showed endochitinases with bands between 15 and 21 kDa with activity on chitopentaose $(GlcNAc)_5$; the activity of *N*-acetylhexosaminidase (Nhase) was evidenced by bands between 111 and 113 kDa, activity on chitotetraose $(GlcNAc)_4$ and Mu(GlcNAc), and bands of 60, 80 and 96 kDa with activity on Mu(GlcNAc). SmC cultivation with Ch, showed two bands with endochitinase activity of 10 and 21 kDa, acted on $Mu(GlcNAc)_3$, and Nhase with bands of 60, 90 and 107 kDa in the gel with Mu(GlcNAc). SmC with FCh showed exochitinase activity on gels with chitotrioside bands of 17, 21 and 27 kDa and chitobiases activity of 19 kDa which acts on the $Mu(GlcNAc)_2$. SmC cultivation with SCh showed activity of 105 kDa endochitinase acting on the Mu $(GlcNAc)_3$ and Nhase activity, with bands of 9 and 15 kDa, with activity in Mu(GlcNAc) (Figure 1).

Hydrophobins production and activity on surface. The hydrophobins produced in SSC (620 µg protein mL^{-1}) were 10 times higher than in SmC (57 µg protein mL^{-1}). SSC with added Ch or F showed a band of 7.6 kDa (Figure 2). However, in the RP-HPLC chromatogram of proteins extracted from SSC with added Ch was also determined several peaks (Figure 2).

The proteins extracted displayed surface activity on hydrophobic solid (Teflon) since it was able to reduce *ca.*50% of the contact angle; whereas SSCF did not show activity (Table 1).

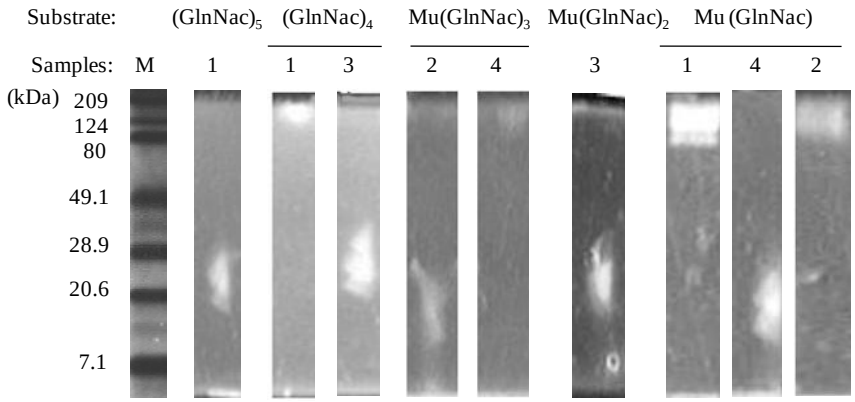

Figure 1. Chitinolytic activity of crude enzyme of *L. lecanii* on SDS-PAGE with oligosaccharides as substrate. Lanes: M- protein standard, 1- SSCCh, 2- SmCCh, 3- SmCFCh, 4- SmCSCh.

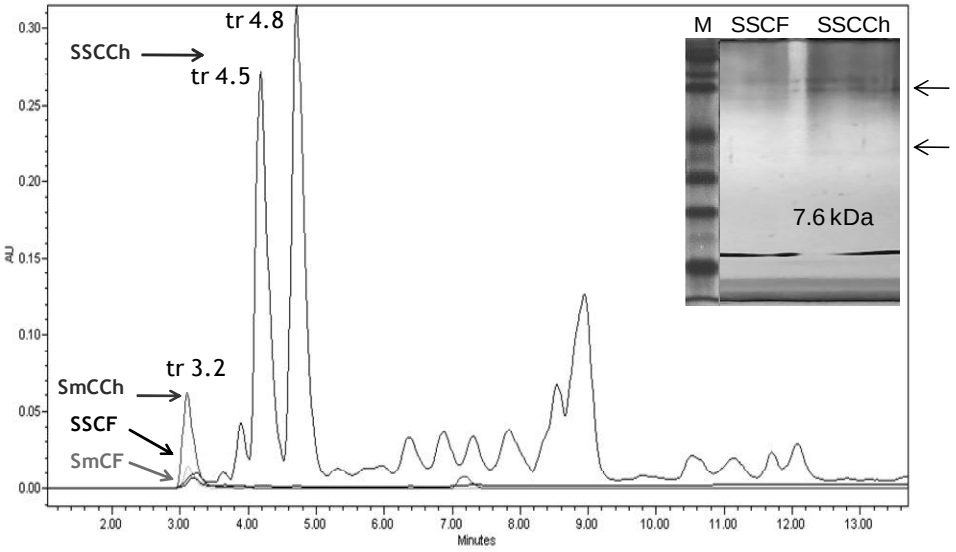

Figure 2. Chromatogram and SDS PAGE of hydrophobins of *L. lecanii* in SSC and SmC with fructose or chitin.

Table 1. Surface activity of hydrophobins of *L. lecanii* produced in SSC with fructose or chitin on hydrophobic solid (Teflon). Teflon (200 µL) was added, with a concentration of 50 µL/mL of protein. The data are the mean of 6 independent observations (± standard errors).

Sample	Contact angle
Distilled water (control)	124.60 ± 3.57^{b}
Solid-Fructose (SSCF)	114.61 ± 1.67^{b}
Solid-Chitin (SSCCh)	63.11 ± 3.09^{c}

*Different letters in the same column are significantly different ($\alpha \leq 0.05$) according to Tukey's multiple comparison test.

DISCUSSION

SSC produced more chitinolytic enzymes than SmC, which might be due to the enhanced aeration, thus affecting the fungal metabolism on insoluble substrates i.e. chitin.[4] The carbon source, fructose, showed catabolic repressive effects evidenced by the decrease in the number

of bands and the type of chitinases produced. SmC with fructose and chitin presented a band with chitobiase activity, which was not observed in any other treatment. The presence of sucrose and chitin triggered the production of *N*-acetylhexosaminidases with different M_w to that observed in cultures with only chitin (Figure 1). This might be due to the process of induction and repression exerted by each carbon source.

Culture type also affected the production of chitinases and hydrophobins, which was evidenced by the yield of protein obtained in each case. The hydrophobins produced by *L. lecanii* in SSC using chitin and fructose have the same M_w (*ca.* 7.6 kDa), a value that is within those reported for other hydrophobin sources, such as *Verticillium fungicola*[11]. However, the presence of several bands was detected in the chromatogram from SSC with chitin (Figure 2). This evidenced the production of more than one hydrophobin, which would contribute to the surface activity since only hydrophobins extracted from SSC with chitin showed activity (Table 1).

CONCLUSIONS

The hydrophobins of *L. lecanii* were produced at high levels under favorable conditions for the induction of chitinases (SSC and addition of chitin to the culture media). These results are relevant since both proteins hydrophobins and chitinases plays a key role on fungal pathogenesis.

ACKNOWLEDGMENTS.

The authors gratefully acknowledged to CONACYT for the research funding (Project Number 105628) and for PhD scholarship grant to Z.R.

REFERENCES

1 St. Leger RJ, Joshi I and Roberts D, *Appl Environ Microbiol* **64(2):** 709-713 (1998).

2 Linder M, Szilvay G, Nakari-Setälä T, Penttila M, *FEMS Microbiol Rev* **29:** 877–896 (2005).

3 Duo-Chuan L, *Mycopathologia* **161:** 345-360 (2006).

4 Marin-Cervantes MC, Matsumoto Y, Ramírez-Coutino L, Rocha-Pino Z, Viniegra G, and Shirai K, *Proc Biochem* **43:** 24-32 (2008).

5 Laemmli UK, *Nature* **227:** 680-685 (1970).

6 Trudel J and Asselin A, *Anal Biochem* **178:** 362-366 (1989).

7 Liau CY and Lin CS, *J Biosci Bioeng* **106(1):** 111-113 (2008).

8 Vigueras G, Shirai K, Martins D, Franco TT, Fleuri LF and Revah S, *Appl Microbiol Biotechnol* **80:** 147- 154 (2008).

9 Bradford MM, *Anal Biochem* **72:** 248-254 (1976).

10 Van der Mei HC, de Vries J and Busscher HJ *Appl Environ Microbiol* **59:** 4305-4312 (1993).

11 Calonje M, Bernardo D, Novaes-L M and García M *Can J Microbiol* **48:**1030-1034 (2002).

Evaluation of antifungal activity of chitosan coating on cut apples by image analysis technique

Odilio B.G. Assis, Douglas de Britto

Embrapa Instrumentação Agropecuária, Rua XV de Novembro, 1452.
13560-970 São Carlos, SP, Brazil, odilio@cnpdia.embrapa.br

Abstract
Image analysis techniques have often been chosen as a fundamental tool for evaluating the surface and/or structure of organic and inorganic materials over a broad range of magnification. In this work, a simple image capture system comprising a commercial desktop scanner combined with free image analysis software was used to evaluate the efficiency of antifungal activity of commercial medium molecular weight chitosan as edible coating on the evolution of fruit decay by fungi infestation (predominantly *Penicillinum* sp. and *Alternaria* sp.) on cut apple surfaces. The images were acquired twice daily and binary transformed for quantitative analysis. The inhibitory effect of chitosan coating in the mycelial fungi growth in on apple cut surface was confirmed.
Keywords: Chitosan, Edible coating, Antifungal activity, Minimally processed fruit.

INTRODUCTION

Protective treatment of minimally processed and post harvest products entails a variety of different techniques, including controlled cold room environment, ozone washing, biocidal action by irradiation and additional protective procedures such as packaging and coatings. Recent emerging technology provides the ability to apply biobased materials on freshly cut surfaces, offering an alternative method of controlling and extending the quality and shelf life during storage. Chitosan has been suggested as a potential material for edible coatings processing, mainly concerning its non-toxic nature, biocidal activity and gas barrier properties. It is widely known that chitosan has excellent antimicrobial activity against bacteria, viruses and fungi and have the ability to induce the expression of a variety of genes involved in plant defense responses.[1] The antifungal property of chitosan has been observed for a broad range of concentrations upon several spoilage yeasts.[2] Chitosan, as edible coatings have been evaluated, for example, on carrots, on mangos, on strawberries and on apples.[3] When deposited on fruit cut surfaces, chitosan forms a high transparent film, allowing a statistical and comparative quantification of fungi spreading against time storage. In this study, image analysis technique was used in order to follow the fungi area evolution on coated and non-coated processed fruits.

MATERIALS AND METHODS

Chitosan coating and sample contamination

Commercial medium molecular weight chitosan of shrimp (60% or more deacetylated units, from Sigma) was dissolved in 1% acetic acid in deionized water with constant stirring for 2 hours. Solutions of 2.0 g/L chitosan were prepared at a pH approximately 4.0. Supermarket apples, cv. Gala (*Malus domestica*) were first sliced into two halves and then displayed separately in two groups of 20 samples each. The first group underwent chitosan coating by direct dipped into the solution. Excess gel was allowed to drain off and the coating was then formed by drying at room temperature.

Groups of 20 coated and 20 non-coated apple slices were put into a controlled temperature chamber (25 ± 0.5^{o}C) where petri dishes containing non-classified cultures of fungi (predominantly *Penicillium* sp. and *Alternaria* sp.) were equidistantly allocated amongst the samples, so as to allow spontaneous inoculation of the fruit slices by ambient contamination.

The fungus was originally isolated from a decayed apple and the cultures prepared by growing on potato dextrose agar (PDA) at pH 5.5, according to Zhang & Han.[4]

Image capture and analysis

Qualitative and quantitative analysis were performed using a commercial scanner (HP ScanJet 4C) for image capture. All cut surfaces were individually scanned twice a day. Images were 250% enlarged from original and 512 by 512 pixels, each with a grayness (brightness) level ranging from 0 to 255. Images were recorded to allow monitoring of the samples, providing a visual history and track alterations on the surface by assessing the percentage of blackness due to the fungus spreading. The acquired images were directly imported into the image processing software and a threshold applied, i.e., binary transformed to remove debris and quantification was performed considering a two dimensional growth. We adopted the grayness level of 130 for all captured images. The infected area was then isolated and automatically estimated by pixel counting and numerically compared to each precedent data. The analysis program used was the free software Image Tool v.3 from UTHSCSA.[5]

RESULT AND DISCUSSION

Fungal evaluation

Figure 1 illustrates the two dimensional digital image analysis procedure of a non-coated sample surface after 6 days exposure. Setting a threshold enables a selection of ranges of pixel values in grayscale images that distinguish the objects under consideration from the background, thus allowing assessment of the infected area.

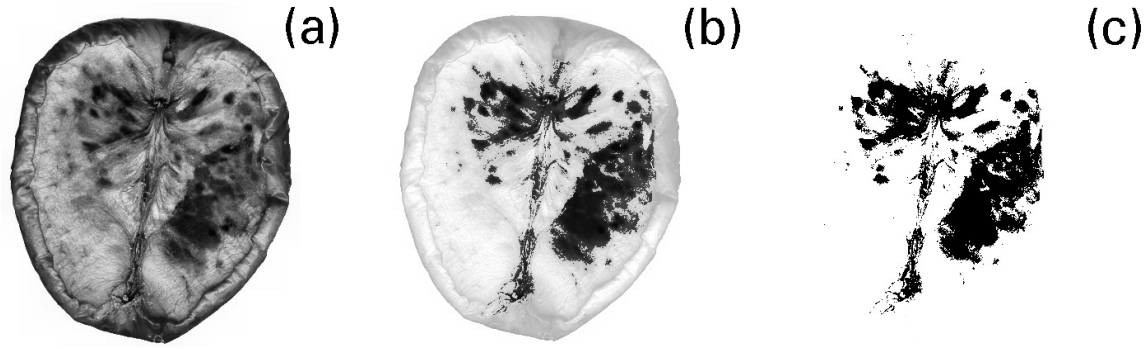

Figure 1. An example of image processing and infected area measurement. The image of a fungi-contaminated non-coated sample is digitally recorded (a), and the fungal pattern proliferation identified (b), and the correspondent area (c), after a threshold is removed for percentage fraction measurement (27.25 % of the area infected).

Fungi are filamentous microorganisms that grow as tubular cells extended by a vesicle based process of apical growth. The typical colonies are characterized by pellet morphology which is highly entangled, dense masses of hyphae. According to Cox et al.,[6] the general structure of fungal pellets is a dense core showing gradual steps to a hairy external region. Such morphology allows an easy visual approach of microbial progressive spreading.

Numerically, as expected, the non-protected faces entail higher marked fungal growth and proliferation with time, as can be seen when comparing the evolution data as plotted in Figure 2. Infected samples were considered as those having at least 10% of the total scanned area identified as covered by fungus pattern. After 10 days of image acquisition, it was apparent that 90% non-protected samples and 40% chitosan-coated fruits slices were infected.

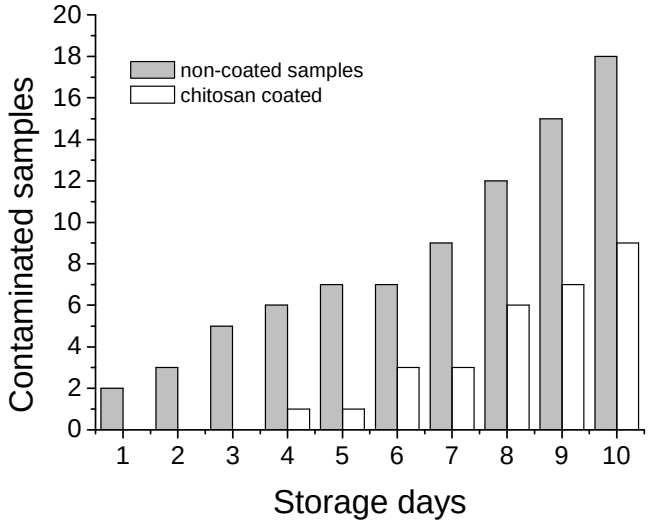

Figure 2. Evolution of the number of infected samples during 10 days of storage, over a total of 20 samples (chitosan coated and non-coated), according to the analysis of scanned surfaces.

The software was used to count pixels in the acquired images corresponding to the isolated area. A simple comparison of the evolution area in the same set of samples over a period reveals the kinetic tendency of the fungal growth. Figure 3 summarizes the percentage of infected area. The dissemination is, as expected faster for non-protected surfaces, with a reduced rate of proliferation on chitosan-coated surfaces, mainly in the first 1-4 days of exposure to fungi.
The profile of the curves clearly approach to typical standard growth kinetics found in fungi, i.e., comprising lag, exponential, and stationary phases in accordance with the literature (see for comparison the kinetics presented by Viniegra-Gonzalez, *et al*.[7] and Olsson,[8] and the numerically not far different from those reported with conventional chemical analysis.[9]

Antifungal chitosan activity
Similarly to bacteria, the chitosan activity against fungus is assumed to be fungistatic (hinders the growth of fungus but does not imply whether or not fungi are killed), rather than fungicidal (kills the live fungus or some fraction therein) with a potential to communicate regulatory changes in both the host and fungus.

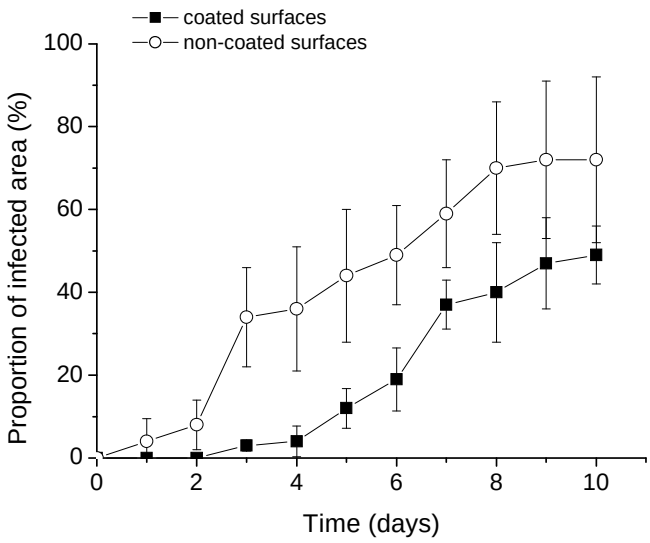

Figure 3. Proportion of infected area for sliced surfaces versus exposure time, as measured by image analysis. The error bar represents the standard deviation on 20 image acquisitions in each condition.

Generally chitosan has been reported as being very effective in inhibiting spore germination, germ tube elongation and radical growth.[10] The antifungic mechanism of chitosan involves cell wall morphogenesis with chitosan molecules interfering directly with fungal growth, similarly to the effects observed in bacteria cells.[11] The most accepted model for explaining antimicrobial activity is related to the polycationic nature of the polysaccharide that can interact with anionic sites in proteins. Such interaction is mediated by the electrostatic forces between the protonated NH_2 groups in chitosan and the negative residues at cell surfaces. Such interaction interferes with fungal cell wall membranes causing alterations in the permeability, promoting internal osmotic imbalances.[12] Microscopic observation reported that chitosan oligomers diffuse inside hyphae interfering on the enzymes activity responsible for the fungus growth. The intensity of degradation action of chitosan on fungal cell walls is also dependant upon the concentration, degree of acetylation and local pH[11].

CONCLUSIONS

From the results of the present work, the chitosan was confirmed a successful material in protecting sliced apples against fungus contamination. When directed applied on cut surfaces (with no additives) chitosan has the potential to form invisible coatings with inhibitory activity on fungi development. Such activity can be easily traced by means of image observation. Adequate application, however, requires additional knowledge of the factors that determine chitosan performance including the effects of pH, temperature, concentration, strain-specificity, etc. Anyway, chitosan may be considered as a good source for preservation of cut fruits in substitution to conventional antifungal agents. Evidently, the storage life of coated samples may be much prolonged by the conjugated use of refrigeration.

ACKNOWLEDGEMENTS

The authors would like to thank the Embrapa (Rede AgroNano), CNPq and FAPESP for financial support.

REFERENCES

1 No HK, Parj NY, Lee SH and Meyers SP, *Intern J Food Microbiol* **74**:65-72(2002).
2 Jeihanipour A, Karimi K and Taherzadeh MJ, *Res J Biol Sc* **23**:239-243(2007).
3 Assis OBG and Pessoa JDC, *Braz J Food Techn* **7**:17-22 (2004).
4 Zhang M and Han T, *J Bioactive Comp Polym* **18**:391-401(2003).
5 available at http://ddsdx.uthscsa.edu/dig/itdesc.html.
6 Cox PW, Paul GC and Thomas CR, *Microbiology* **144**:817–827(1998).
7 Viniegra-Gonzalez G, Saucedo-Castañeda G, López-Isunza F and Favela-Torres E, *Biotechn Bioeng* **42**:1-10(1993).
8 Olsson S, Colonial Growth of Fungi. In: Howard RJ and Gow NAR (Eds). *The Mycota: A Comprehensive Treatise on Fungi as Experimental Systems for Basic and Applied Research.* 1st ed, New York: Springer, v. 3, pp. 125-144, 2002.
9 McKellar R and Lu X, (eds). *Modeling microbial Response in Foods*. Oxford: CRC Press, UK. 360 p., 2003.
10 Sashai AS and Manocha MS, *FEMS Microbiol Rev* **11:**317-338(1993).
11 Goy RC, Britto D and Assis OBG, *Polímeros: Ciênc Tecnol* **19**: 241-247(2009).
12 Tsai G-J and Su W-H, *J Food Prot* **62**:239–243(1999).

Chitosan production by S*yncephalastrum racemosum* using low cost media

Anabelle C. L. Batista[1,2], Marlene Lopes[3], Valdemir A. Santos[4], Clarissa D. C. Albuquerque[2], Rosa Valéria S. Amorim[5], Galba M. Campos-Takaki[2*]

[1] RENORBIO, UNICAP, Boa Vista 50 050-590 Recife, PE, Brazil
[2] Nucleus of Research in Environmental Sciences (NPCIAMB), UNICAP, Boa Vista 50 050-590 Recife, PE, Brazil
[3] IBB-Center for Biological Engineering, UMINHO
4 Department of Chemical/UNICAP
5 Histology and Morphology Department, UFPE
*E-mail: gmctakaki@pq.cnpq.br ; Phone: +55 21194017; Fax: +55 21194043

ABSTRACT
This study investigated the influence of the independent variables related to the growing conditions for the production of chitosan by *Syncephalastrum racemosum* (WFCC 0148), according to the Factorial Design. The results showed that the serum milk and the cassava wastewater influenced negatively in the chitosan production, while CSL has positively influenced with incomes of up to 6.24 % (DD = 88.14 %, ICR = 59.63 %). Due to the low cost of production and high deacetylation degree, the CS produced by *S. racemosum* cultivated in CSL has a great potential for for future up-scaling and biotechnological application.

Keywords: Chitosan, *Syncephalastrum racemosum,* Corn steep liquor, Serum milk, Cassava wastewater

INTRODUCTION

Nowadays, the natural synthesis of biopolymers by microorganisms have been related to the selected strain, to the phase of lifecycle of the microorganism, to the carbon and nitrogen sources of the midst of culture, to the pH and to the incubation temperature. All these factors can cause an increase and improvement of the physical-chemical characteristics of the biopolymers.[1-6] Among the many polymer, there are the chitosan (CS), a biopolymer made up of glycoside residues β-(1-4)-2-amino-2-deoxy-D-glucopyranose which is naturally found as constituent of the cell wall of fungi, especially of those belonging to the Zygomycetes class [7,8], or it is obtained by the chemical deacetylation of chitin residues. Among the Zygomycetes, the specie *Syncephalastrum racemosum* has presented a great potential for CS production when it is grown in simple medium and, furthermore, it is not of high cost.[1]
The present research evaluates different concentrations of sources of carbon and nitrogen, temperature, pH and size of the inoculum as factors which influence in the CS production by *Syncephalastrum racemosum*.

MATERIALS AND METHODS

Microorganism and Culture media

Sub-cultures of *S. racemosum* (WFCC – 0148) grown in the PDA medium (Potato Dextrose Agar, Oxoid) 120 h / 28 ºC was used during all experiments. The industrial residues of serum milk, cassava wastewater and corn steep liquor (CSL) were kindly provided by local industries of milk processing, cassava and corn wet-milling, respectively. *S. racemosum* was grown in an shaker condition (150 rpm / 120 h), according to the conditions proposed in Table 1. The CS was extracted according to Hu et al. method.[9]

Table 1 Factorial design, 2^4 with 3 central values. Independent variables: A = concentration of industrial residue (%), B = initial pH, C = Temperature (ºC), D = size of inoculum (spores ml^{-1}); Dependent Variable: R = yield of chitosan (mg g^{-1}).

Run n°	***Independent Variables***				***Response Variable***
	A (x_1)	***B(x_2)***	***C(x_3)***	***D(x_4)***	***R[b]***
1	2.0 (-1)	4.0 (-1)	25 (-1)	10^2 (-1)	11.37
2	10.0 (+1)	4.0 (-1)	25 (-1)	10^2 (-1)	23.10
3	2.0 (-1)	8.0 (+1)	25 (-1)	10^2 (-1)	62.44
4	10.0 (+1)	8.0 (+1)	25 (-1)	10^2 (-1)	47.84
5	2.0 (-1)	4.0 (-1)	37 (+1)	10^2 (-1)	20.33
6	10.0 (+1)	4.0 (-1)	37 (+1)	10^2 (-1)	7.84
7	2.0 (-1)	8.0 (+1)	37 (+1)	10^2 (-1)	7.43
8	10.0 (+1)	8.0 (+1)	37 (+1)	10^2 (-1)	11.15
9	2.0 (-1)	4.0 (-1)	25 (-1)	10^6 (+1)	0.30
10	10.0 (+1)	4.0 (-1)	25 (-1)	10^6 (+1)	17.14
11	2.0 (-1)	8.0 (+1)	25 (-1)	10^6 (+1)	0.78
12	10.0 (+1)	8.0 (+1)	25 (-1)	10^6 (+1)	38.87
13	2.0 (-1)	4.0 (-1)	37 (+1)	10^6 (+1)	0.87
14	10.0 (+1)	4.0 (-1)	37 (+1)	10^6 (+1)	9.66
15	2.0 (-1)	8.0 (+1)	37 (+1)	10^6 (+1)	0.66
16	10.0 (+1)	8.0 (+1)	37 (+1)	10^6 (+1)	7.30
17[a]	6.0 (0)	6.0 (0)	31 (0)	$5x10^5$ (0)	15.13
18[a]	6.0 (0)	6.0 (0)	31 (0)	$5x10^5$ (0)	15.19
19[a]	6.0 (0)	6.0 (0)	31 (0)	$5x10^5$ (0)	14.09

[a]Central values. [b]Means of duplicate

Physical chemical characterization of chitosan

The principal parameters that can be used for the characterization of CS for biotechnological application are the degree of deacetylation (DD) and the crystallinity.[10] The DD was detemined by Fourier Transform Infrared Spectroscopy (FTIR) according to Roberts [11] and crystallinity index I_{CR}(%) was calculated according to Focher et al.[12]

Factorial Design and Statistical analysis

Differences between data sets were analyzed by analysis of variance (ANOVA) and multiple t tests. $p < 0.05$ was considered to be statistically significant. All data analyses and graphs were made with the Statistica 7.0 software package.[13]

RESULTS AND DISCUSSION

Screening of low cost media

At the present moment, the CS commercialized in a large scale is from the chemical alkaline processing of shrimp chitin, with cost of, approximately, U$10.00/g (Sigma Chemical Co., USA). In the microbiological CS production, there is a very high cost of production due to its low yielding. However, for its competitive commercialization, industrial residues have been used as alternative media for fungi grown in batch. These media are readily available and are of low cost resulting in 38 – 73 % saving of the total cost of the bioproduct production.[1,14]

The obtained results showed that among the industrial residues used in the work, serum milk and the cassava wastewater influenced negatively in the CS production by *S. racemosum*, excluding these results of the statistical analysis. In the literature, it was observed a low production of fungi biomass when fungus was grown in the presence of lactose as the only source of carbon.[15] The presence of high concentration of cyanide in cassava wastewater is supposed for inhibition of S. racemosum growth.[16]

In this experiment, the CSL used as the only source of carbon and nitrogen influenced positively the CS production. This fact may have been influenced by high concentrations of nitrogen (17.57 %) and total carbohydrates (13.03 %) of CSL used in the present research. Different authors confirmed the CSL as a good carbon and nitrogen sources for the biopolymer production as due to its nitrogen high concentration.[14,17] Divergences among the values of the nutritional compositions for CSL may occur due to the corn origin or to the way as the CSL was acquired.

Physical chemical characterization of chitosan

FTIR estimated the amount of free amine group present in the CS molecule obtained from *S. racemosum*, DD = 88.14 % (Fig. 1). Such result is compatible with the CS which is attained from shrimp and, at the moment, it is commercialized reaching DD about 90 % (Sigma Chemical Co., USA). The fermentation processes for bioproduct production can facilitate the chitosan constant production presenting a higher deacetylation degree.

In figure 1 the commercial CS (A) and microbiological CS (B) are characterized by the bands about 1650 cm^{-1} (peak 1), about 1590 cm^{-1} (peak 2) and about 3440 cm^{-1} (peak 3).[2] The presence of characteristic peaks of the bioproduct in both CS corroborates the production value of the microbiological CS by alternative sources of carbon and nitrogen. In figure 2, CS characteristic peaks in both samples are observed[18]. The higher crystallinity (I_{CR} = 55.96 %) of microbiological CS suggests a larger amount of structural intermolecular connections among the amine groups of residues [19], and a high molecular weight [2] when compared to the commercial CS.

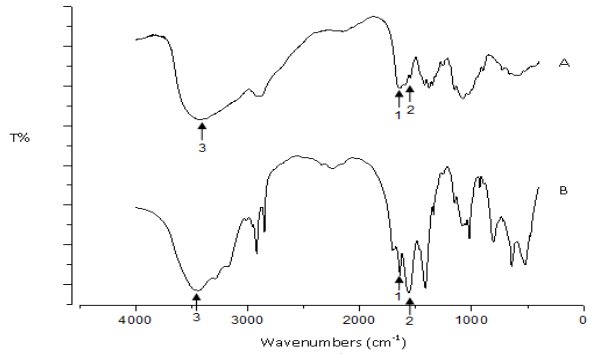

Figure 1. Comparative FTIR spectra of commercial CS (A) and microbiologic CS (B).

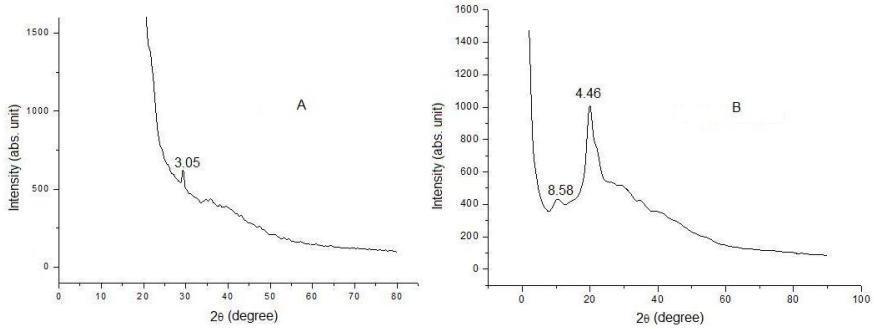

Figure 2. Comparative X-ray patterns of commercial CS (A) and microbiologic CS (B).

Statistical analysis

In the analysis of variance (ANOVA data not show) for the results of Factorial Design, the low *p* value ($p < 0.05$) indicates a significant effect of interference of independent variables in the production of CS, especially for factors 2 * 3 * 4 (Fig. 3). The low experimental error when compared with the lack of fit suggests a security of the extraction technique and production of microbiological CS.

The factorial design used demonstrated that the optimal conditions for CS production occurred when the only carbon and nitrogen source was 2 % of CSL (-1) with initial pH 8.0 (+1), temperature 25 ºC (-1) and size of inoculum 10^2 (-1). The goodness of the model was checked by the determination coefficient R^2 (0.9212), which explain 92.12 % of the variability of the response.

Under these optimal conditions there was a production of up to 8 g / kg substrate, surpassing the results of Wang et al., which used *Absidia coerulea* grown in CSL supplemented with molasses.[2] The influences of different growing conditions and strain to produce a bioproduct were previously described by several authors[1,14,20,2,21-23].

In figure 4 are set values of influence of independent variables through Pareto chart, where the level -1 for the effect of size of inoculum and +1 for the effect of pH corroborate [15,23], suggesting do not need high concentrations of inoculum and the need of pH adjustment for the production of microbiological CS. The temperature has been described as a regulator factor of morphogenesis, with range of about 33 – 39 ºC determined yeastlike development; at lower temperatures, a filamentous growth developed.[15] The temperature of 25 °C was associated with filamentous growth, when *S. racemosum* accumulated higher amount of CS in cell walls.[24]

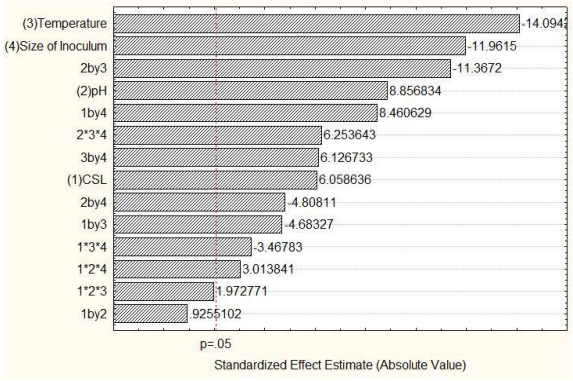

Figure 3. Model of 3-way interactions with Pure Error = 11.74, R^2 = 0.92 and Adj = 0.87. Pareto chart of standardized effects of independent variables for CS production by *S. racemosum* in CSL.

CONCLUSION

The results obtained in this study suggest a great potential for for future up-scaling for CS production by Syncephalastrum racemosum in low cost medium and with higher degree of deacetylation.

ACKNOWLEDGMENTS

The authors are grateful to CAPES for PhD fellowship and the financial support of FINEP, CNPq and UNICAP.

REFERENCES

1 Amorim RSV, Ledingham WM, Kennedy JF and Campos-Takaki GM, *Food Biotechnol* **20**:43 (2006).

2 Wang W, Dua Y, Qiu Y, Wang X, Hub Y, Yang J, *et al*, *Carbohydr Polym* **74**:127 (2008).
3 Hursta KM and Lewis RS, *Biochem Eng J* **48**:159 (2010).
4 Kanda M, Yamamoto E, Hayashi A, Yabutani T, Yamashita M and Honda H, *J Biosci Bioeng* **109**:138 (2010).
5 Kannan M, Nesakumari M, Rajarathinam K and Singh AJAR, *Adv Biol Res* **4**:10 (2010).
6 Leee K-M, Jeya M, Joo A-R, Singh R, Kim I-W and Lee J-K, *Enzyme Microb Technol* **46**:206 (2010).
7 Bartniki-Garcia S, *Annu Rev Microbiol* **22**:87 (1968).
8 Campos-Takaki GM, The fungal versatility on the co-polymers, in *Chitin and chitosan: Opportunities & Challenges*, ed. by Dutta PK. Midnapore: Contai, pp. 69-94 (2005).
9 Hu KJ, Yeung KW, Ho KP and Hu JL, *J Food Biochem* **23:**187 (1999).
10 Kittur A, Kulkarni S, Aralaguppi M and Kariduraganavar M, *J Memb Sci* **247**:75 (2005).
11 Roberts GAF, Chitin Chemistry, ed. by Roberts GAE. Macmillan Press, Ltd.: London, pp. 85-91 (1992).
12 Focher B, Beltrame PL, Naggi A and Torri G, *Carbohyd Polym* **12**:405 (1990).
13 StatSoft, Inc.: 2004, STATISTICA (data analysis software system), version 7. http://www.statsoft.com.
14 Hamano PS and Kilikian BV, *Braz J Chem Eng* **23**:443 (2006).
15 Bartnicki-Garcia S and Nickerson WJ, *J Bacteriol* **84**:841 (1962).
16 Gonzaga AD, Garcia MVB, Sousa SGA, PY-Daniel V, Correa RS and Ribeiro JD, *Acta Amazonica* **38**:101 (2008).
17 Téllez-Luiz SJ, Moldes AB, Vázquez M and Alonso JL, *Trans IChemE* **81**:250 (2003).
18 Jaworska M, Sakurai K, Gaudon P and Guibal E, *Polym Int*, **52**:198 (2003).
19 Guibal E, *Separation and Purification Technology* **38**:43 (2004).
20 Rufino RD, Sarubbo L, Neto BB and Campos-Takaki GM, *J Ind Microbiol Biotechnol* **35**:907 (2008).
21 Kammoun R, Naili B and Bejar S, *Bioresour Technol* **99**:5602 (2008).
22 Rai KS and Mukherjee AK, *Biochem Eng J* **48:**173 (2010).
23 Feng Y-L, Li W-Q, Wu X-Q, Cheng J-W and Ma S-Y, *Biochem Eng J* **49**:104 (2010).
24 Baker LG, Specht CA, Donlin MJ, and Lodge JK, Eukaryot Cell 6:855 (2007).

Antifungal effect of chitosan on the growth of *Aspergillus parasiticus* and production of aflatoxin B1

O. Cota-Arriola,[1] M.O. Cortez-Rocha,[1] Y.L. López-Franco,[2] A. Burgos-Hernández,[1] E.C. Rosas-Burgos,[1] M. Plascencia-Jatomea[1]

[1] Department of Food Research and Graduate, University of Sonora, Mexico
[2] CIAD A.C., Hermosillo, Sonora, México
E-mail: tavo_baviacota@hotmail.com

ABSTRACT
Contamination of agricultural products by toxigenic fungi and the presence of mycotoxins cause serious economic damage and toxic effects to man and animals. In this study we evaluated the effect of chitosan (CQ_{50}) as a natural alternative for the control of the fungus *Aspergillus parasiticus*. The chitosan inhibited radial growth on 122 h and germination of spores in less than 50% before 8 h. Also increased ($P \leq 0.05$) the average diameter of the spores and hyphae, reduces the septation process and increase the number of mitotic divisions during germination. However, chitosan does not inhibit the production of aflatoxin in corn grain.

Keywords: Chitosan, Aflatoxins B1, *Aspergillus parasiticus.*

INTRODUCTION

In vitro analysis demonstrated that chitosan has fungistatic activity against filamentous fungi such as *Aspergillus* and *Fusarium*, causing damage to the microbial cell membrane and increasing the production of defense molecules in plant cells [1]. Some fungi produce mycotoxins contaminants during storage of agricultural products, causing great economic losses in addition to being harmful to humans and animals, being aflatoxin B1 (AFB1), the most important because of its high toxicity. It has been reported that chitosan inhibits the production of aflatoxin (AF) produced in vitro by *A. parasiticus* [2], representing an important alternative of control in Mexico, where corn grain is the food base and is a susceptible to aflatoxin contamination, unavailable for human consumption. The aim of this study was to evaluate the effect of chitosan on *in vitro* growth of *A. parasiticus* (ATCC16992), and AFB1 production in corn grain.

MATERIALS AND METHODS

Obtention of chitosan. Chitin was obtained from the head of shrimp (*Litopenaeus vanameii*) by chemical method by deproteinization with NaOH (2%) and demineralization with 1.2 M HCl at 25 ° C for 2 h. and by biological method, adding sucrose, *Lactobacillus* and lactic acid (10%) at 37 ° C for 2 days. Chitosan was then obtained from the chitin biological and chemical methods (Q1 and Q2, respectively), by homogeneous deacetylation with NaOH (60%) at 37 ° C with stirring for 6 days.

Characterization of chitosan. Protein content was determined by micro Kjeldahl method and ash by method 938.08 of AOAC (1999). The molecular weight (MW) was calculated from intrinsic viscosity by the formula of Mark-Houwink-Sakurada $[\eta] = KM_V^{\alpha}$ [3]. The degree of deacetylation (DD) was determined by infrared spectroscopy using the formula: $\%DD = 97.67 - [26.486 \times (A_{1655}/A_{3450})]$ [4]**.**

Bioassays. We determined the half inhibitory concentration (CQ_{50}) of chitosans from radial growth of *A. parasiticus* (ATCC16992) by Probit analysis (NCSS Inc., USA). Solutions of chitosan (CQ_{50}) acetic acid (pH 5.6) were used for bioassays, using controls pH 5.6 acetic acid (CAc), water (CH_20), potassium sorbate 0.4% pH 6.5 (CSor) and commercial low viscosity chitosan at pH 5.6 (Q3).

Radial growth and spore germination. Petri dishes with Czapeck medium supplemented with chitosan (CQ_{50}) in proportion 3:7 (v / v) chitosan: culture medium, pH 5.6, were inoculated with $1x10^4$ spores / mL of *A. parasiticus* by the technique of pit and planting grass to radial growth and germination of spores, respectively, incubated at 28 ° C [5].
Epifluorescence microscopy. The effect of chitosan CQ_{50} on the process of mitotic division of nuclei by staining with Hoechst 33258 solution (100 ng/mL) and the formation of septa using Calcofluor white staining (10 µL/m). Czapeck liquid medium inoculated with $1x10^5$ spores / mL of *A. parasiticus* was used [5].
Morphometric parameters. The average diameter of spores and hyphae of *A. parasiticus* in the presence of the chitosans CQ_{50} was measured by image analysis (Image Pro-Plus Version 6.3. Media Cybernetics, USA) [5].
Production of aflatoxins. Three portions of 50 g of hydrated corn, to 40% humidity and sterilized, 10 mL of CQ50 estimated for each of the chitosans and inoculated $1x10^5$ spores / mL of *A. parasiticus* were added, incubating at 28 ° C for 8 to 16 days. Removal of AF was performed with 100 mL of methanol: water (80:20) and 5 g of NaCl. The mixtures were purified through an immunoaffinity column (Vicam) and the aflatoxins were eluted with methanol. The quantification of total aflatoxins (B1, B2, G1, G2) was determined by fluorometry using the method AflaTest (Vicam) using a fluorometer Series 4 (Vicam model 1107-103606). Quantitation of AFB1 was performed by HPLC (Varian Pump model 9012) using a reverse phase column (C18) (Vydac of 250 x 4.5 mm) and a fluorescence detector (Varian Prostar, model 363) [6].
Statistical analysis. An analysis of variance with factorial design to determine significant difference between treatments, comparing each with the multiple range test of Tukey at a range level of 95% using the statistical package Infostat.

RESULTS AND DISCUSSION

Yields for Q1 and Q2 obtained from shrimp head were 5.74 and 6.20, respectively. Q2 had lower ($P \leq 0.05$) and protein content of residual ash (Table 1). The chitosans were low (Q1 and Q3) and medium (Q2) PM, with% DD> 80.9.

Table 1. Physicochemical characterization of chitosans.

Treatment	Protein (%)	Ash (%)	MW (Kda)	DD (%)
Q1	0.67 ± 0.01^b	0.57 ± 0.04^b	168.4^a	82.6^a
Q2	0.48 ± 0.06^a	0.44 ± 0.02^a	306.3^b	80.9^b
Q3	0.67 ± 0.01^b	0.78 ± 0.06^c	171.1^a	89.7^a

Different superscripts indicate statistical difference. Tukey test $p < 0.05$ (Infostat).

The CQ_{50} found at 122 h for Q1, Q2 and Q3 were 6.71 ± 0.81, 6.24 ± 0.27 and 6.28 ± 0.72 g / L, respectively. At this concentration the three chitosans significantly ($P \leq 0.05$) the radius of the colony of *A. parasiticus* with respect to controls (Figure 1), Q2 and Q3 showing greater inhibitory effect, which may be due to higher% DD of Q3 and MW of Q2 . The least effect was of Q1, which is why it was not considered in subsequent bioassays. With regard to the germination of spores (Figure 1), it was found that chitosans delayed germination in the first 8 h, while in the CSor a higher delay was found, which is associated with increased stress.

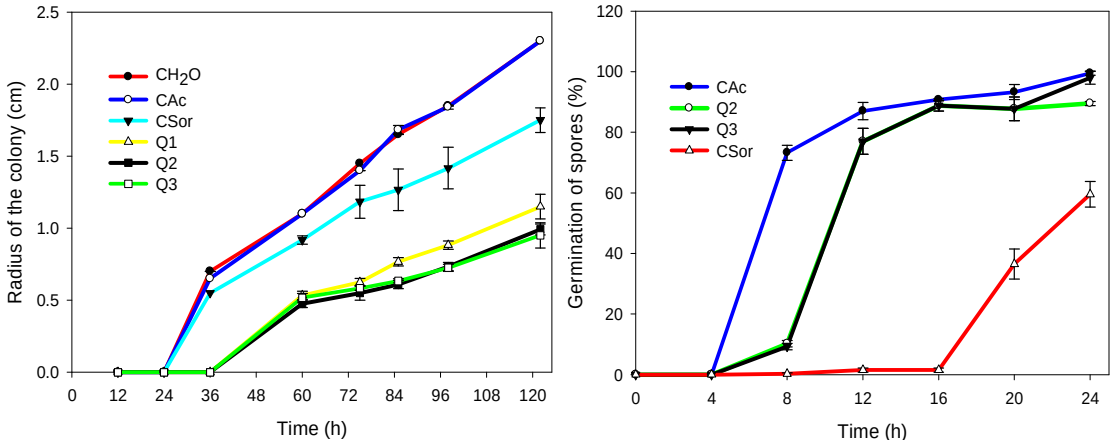

Figure 1. Radial growth and spore germination of *A. parasiticus.*

The morphology of spores and hyphae of the fungus in the presence of chitosan is affected, increasing its diameter (P <0.05) compared to controls (Table 2). This may be due to changes in cell wall structure or the adaptation of the fungus to the presence of chitosan forcing him to synthesize defense compounds, causing swelling of the spore, also may be due to disruption of normal chitin synthase enzyme to produce chitin, which is responsible for providing rigidity to the cell wall [7].

Table 2. Diameter of spores and hyphae of *A. parasiticus* in solid medium Czapeck.

	Spores diameter (µm)		Hypha diameter (µm)	
Treatment	**8 hours**	**16 hours**	**8 hours**	**16 hours**
CAc	8.36 ± 0.795^{a}	9.24 ± 0.549^{a}	4.05 ± 0.319^{a}	4.23 ± 0.883^{a}
CSor	7.53 ± 0.794^{a}	8.94 ± 0.716^{a}	----------	5.47 ± 0.860^{a}
Q3	10.08 ± 0.804^{b}	10.54 ± 0.504^{b}	4.75 ± 0.219^{b}	5.78 ± 0.640^{b}
Q2	10.03 ± 0.850^{b}	10.32 ± 0.493^{b}	4.96 ± 0.492^{b}	6.09 ± 0.807^{b}

Different superscripts indicate statistical difference. Tukey test p <0.05 (Infostat).

This also affects septation in *A. parasiticus*, and minor septa were observed in the hyphae in the presence of chitosan, in addition, the number of mitotic divisions grew in the presence of chitosan (Figure 2), possibly as a defense mechanism to the stress induced.

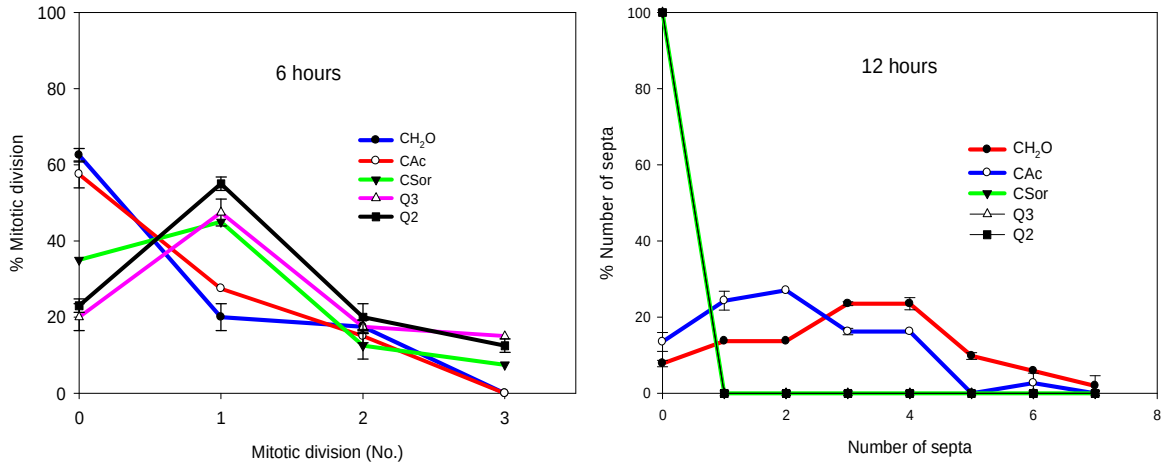

Table 3. Effect of chitosan on the production of aflatoxins by *Aspergillus parasiticus.*

Treatment	Total Aflatoxins (µg/kg)		Aflatoxin B1 (µg/kg)	
	8 days	16 days	8 days	16 days
CH_2O	690 ± 7.07^{d}	530 ± 14.14^{a}	54.34 ± 11.39^{a}	90.51 ± 23.08^{a}
CAc	560 ± 7.07^{b}	680 ± 7.07^{c}	260.73 ± 2.05^{b}	134.93 ± 6.22^{a}
CSor	470 ± 7.07^{a}	590 ± 7.07^{b}	73.61 ± 13.04^{a}	131.14 ± 25.07^{a}
Q3	660 ± 7.07^{c}	750 ± 14.14^{d}	95.00 ± 12.47^{a}	110.51 ± 25.39^{a}
Q2	650 ± 7.07^{c}	700 ± 7.07^{c}	107.60 ± 15.33^{a}	120.71 ± 32.42^{a}

Different superscripts indicate statistical difference. Tukey test $p < 0.05$ (Infostat).

It was observed that acetic acid increased the production of aflatoxins, because the fungus probably used as a nutrient source via the Glyoxylate [8]. By contrast, production of AFB1 decreased ($P < 0.05$) within 8 days in the presence of chitosan with respect to CAc (Table 3), and possibly after 16 days fungus incresead, once adapted to chitosan, which can be used as nutrient.

.

CONCLUSIONS

The low MW chitosan affected the growth, development and morphology of *A. parasiticus in vitro*, however, it increased total production of AF in corn and AFB1 decreased within 8 days. It has been reported that chitosan inhibits the production of aflatoxins in solid medium[2], due to its ability to chelate compounds required for aflatoxin production. However, the grain of maize not presented the same effect due to the chitosan was not subjected to internal components of the grain, limiting its chelating capacity, being important further studies for possible applications in food grains.

ACKNOWLEDGEMENTS

To CONACyT for funding provided through key projects and No. 58249 y No. 53493 J1, and scholarship for postgraduate studies.

REFERENCES

1 Hernandez-Lazaurdo AN, Bautista-Baños S, Velásquez-Del Valle MG, Mendez-Montalvo MG, Sánchez-Rivera MM, and Bello-Perez LA, *Vuill. Carbohyd. Polym* **73**(4):541-547 (2008).

2 Fang S., Li C.F., y Shih C, *J. Food. Prot* **56**:136-140 (1994).

3 Rinaudo M, Milas M, Le Dung P, *Int J Biol Macromol* **15**:281-285 (1993).

4 Khan, T.A., Peh, K.K., and Chang, *J. Pharm. Pharmaceut. Sci* **5**(3): 205-212 (2002).

5 Plascencia-Jatomea M., Viniera G., Olayo R., Castillo-Ortega M. M., and Shirai K, *Macromol.Biosci* **3**(10):582-586 (2003).

6 Norma Oficial Mexicana NOM-188-SSA1-2002.

7 McIntyre M, Muller C, Dynesen J, and Nielsen J, *Advances in Biochemical Engineering/ Biotechnology*, **73**:150-190 (2001).

8 Deacon JW, Introducción a la Micología Moderna. Ed Limusa, Noriega editores. Segunda reimpresión. México (1993).

Solid state fermentation for chitosan hydrolysing enzymes producing bioactive chitosan oligomers

Talita L. Honorato[1], Flávia Granuso[1], Sueli Rodrigues[2], Bruno M. Moerschbacher[3], Telma T. Franco[1*]

[1] School of Chemical Engineering, University of Campinas, Av. Albert Einstein 500, Campinas 13083-852, SP, Brazil
[2] Departamento de Tecnologia de Alimentos – Universidade Federal do Ceará/Brazil
[3] Institute of Plant Biochemistry and Biotechnology – University of Muenster/Germany
*E-mail: franco@feq.unicamp.br

Abstract
The goal of this work is to obtain the enzymes chitosanases by solid state fermentation by *Trichoderma polysporum* of shrimp shells. The crude enzyme extracts obtained were then employed in the hydrolysis of chitosan for the production of potentially bio-active oligomers. The chitosanolytic enzymes produced by *T. polysporum* under different fermentation conditions and their hydrolizate products were analyzed by electrophoresis followed by activity staining and by thin layer chromatography (TLC). Enzyme activities of ß-N-acetylglucosaminidase, chitobiosidase and a small amount of exo-chitinase and endo-chitinase were observed, which were able to produce different oligomeric products when hydrolyzing chitosan with degrees of acetylation (DA) 15%, 27% and 56%.

Keywords: amino-oligosaccharides; *Trichoderma polysporum*; chitosanases; shrimp shells

INTRODUCTION

Chitin is an abundant polysaccharide with an annual production of 10^{10} to 10^{11} tons[1]. Chitin and chitosan are commercially obtained from shrimp and crab shells, which are considered a waste from the seafood industry. Chitosan, a D-glucosamine polymer, is a totally or partially deacetylated obtained by deacetylation of chitin with an alkali[1]. Studies on chitin and chitosan have drawn interest for their conversion into oligosaccharides, which are water-soluble and present attractive biological activity[1,2]. Traditionally, chitosan derived oligosaccharides are obtained by chemical methods, which, when out of rigorous control, produce a large amount of very short-chain oligosaccharides, achieve low yields, are not very selective and generate a broad spectrum of products, requiring high cost separation. Chitosanase hydrolysis became more popular in recent years due to lower cost, low environmental impact and highly reproducibility of results [3,4,5]. Amongst several biological activities of chitooligosaccharides described by current literature, they can induce the expression of pathogenesis-related proteins in higher plants, even act as immunopotentiating effectors[6] and inducing apoptosis of tumor cells[7]. San-Lang[8] reported antioxidant activity and inhibitory effects on *Fusarium oxysporum*. The utilization of GlcNAc and N-acetyl chitooligosaccharides would be particularly promising as elicitors for phytopathogens control and to promote growth in sustainable agricultural systems[9]. Besides of this use, chitooligosaccharides, prepared by large scale enzymatic hydrolysis of chitin/chitosan with chitinase/chitosanase, have several potential applications in food, agriculture and pharmaceutical industries. Biotechnology tools have allowed the identification and development of microbial strains with high productivity offering a wide variety of enzymes of industrial interest. Among them, the filamentous fungi are the most frequently used in industrial processes[10-13] being *Trichoderma* species the most studied biocontrol agent commercially available as biopesticides and biofertilizers[14-17]. The enthomopatogenicity of *Trichoderma* species is closely related to their ability to synthesize

hydrolytic enzymes and several studies on the production of its chitinase have been published[18-24]. Most studies are related to *T. harzianum* and according the our searches, there are no reports on the production of enzymes by *T. polysporum*. Solid-state fermentation is a useful technology for developing new bioprocesses and products, where the crude fermented extract may be directly used as enzyme source. In addition to the conventional applications in food and fermentation industries, microbial enzymes have attained significant roles in biotransformation involving organic solvent media, mainly for bioactive compounds. Herein, the chitosanases and amino-oligosaccharides (AGO's) obtained by solid state fermentation of shrimp shells were studied.

EXPERIMENTAL

Microorganisms and inoculum preparation. *T. polysporum* was obtained from the Embrapa Semi-Arido (Petrolina - PE, Brazil) and was isolated as a biocontrol agent. The spore's culture of *T. polysporum* was maintained in wheat bran at 4ºC after growing it for 7 days at 27ºC. Sterile 0.01% (v/v) Tween 80 solution (30 mL) was added to the erlenmeyer containing the spore culture. The spores were counted in a haemocytometer. Each flask containing the medium to fermentation was inoculated with an amount initially containing 10^7 spores/mL.

Solid substrate preparation. Shrimp shell waste from captivity of Ceará's state, Brazil was used as the substrate. Prior to storage, the shells were washed with water and then dried for 24 h at 60°C. Wheat bran was purchased from the local market (Mercado São Sebastião, Fortaleza- CE, Brazil). Solid substrate contained wheat bran (2.0 g), shrimp shell (1.0 g), and 2.5 mL of a saline solution containing (g/L): $NaNO_3$, 1.0; $(NH_4)_2HPO_4$, 1.0; $MgSO_4.7H_2O$, 1.0; NaCl, 1.0 g/L. The pH of the saline solution was adjusted to 5.5 (this was the best pH for growth in CDA plates). *T. polysporum* under different fermentation conditions were investigated and the crude enzyme extracts were compared and analyzed. Liquid media for submerged fermentation were produced in *Trichoderma* complete medium (TCM)[25] which contained (g/L): bactopeptone, 1.0; urea, 0.3; KH_2PO_4, 2.0; $(NH_4)_2SO_4$, 1.4; $MgSO_4.7H_2O$, 0.3; $CaCl_2.6H_2O$, 0.3; $FeSO_4.7H_2O$, 0.005; $MnSO_4$, 0.002; $ZnSO_4$, 0.002; $CoCl_2$, 0.002 with glucose 0.3% (w/v). The medium was adjusted to pH 5.5 and supplemented with 0.5% (w/v) of shrimp shells, colloidal chitin or chitosan (Table 1).

The medium was sterilized and inoculated with 1 mL of spore inoculum. The contents were then mixed thoroughly and incubated at 27 ºC for 72h, statically for SSF and at 120 RPM for submerged fermentation. Samples were withdrawn after 72 hours of fermentation. Assays were carried out in 250 mL Erlenmeyer's flasks capped with cotton plugs.

Table 1. Medium and type of fermentation for chitosanase production.

Medium	Condition of fermentation	Name
TCM[25]	Submerged	S1
TCM[25] + 0.5% (w/v) of shrimp shell	Submerged	S2
TCM[25] + 0.5 (w/v) of colloidal chitin	Submerged	S3
Wheat bran and shrimp shell (2:1, w/w) in saline solution	Solid state	S4

Trichoderma complete medium (TCM) contained (g/L): bactopeptone, 1.0; urea, 0.3; KH_2PO_4, 2.0; $(NH_4)_2SO_4$, 1.4; $MgSO_4.7H_2O$, 0.3; $CaCl_2.6H_2O$, 0.3; $FeSO_4.7H_2O$, 0.005; $MnSO_4$, 0.002; $ZnSO_4$, 0.002; $CoCl_2$, 0.002 with glucose 0.3% (w/v). Solid substrate medium contained wheat bran (2.0 g), shrimp shell (1.0 g), and 2.5 mL of a saline solution containing (g/L): NaNO3, 1.0; (NH4)2HPO4, 1.0; MgSO4.7H2O, 1.0; NaCl, 1.0 g/L.

Preparation of enzyme extracts. Enzymes were extracted from the fermented solid substrate by adding 20 mL of acetate buffer (200 mM, pH 5.5) to the flask and shaking at 27°C, 150 RPM, for 6 min. The crude enzyme extract was then separated by filtration through analytical filter paper (70 mm) and then through 0.2-µm pore size Filtropur S (Sarstedt, Nümbrecht, Germany) syringe filters. The filtrate (enzymatic extract) was concentrated in Vivaspin20 10,000 MWCO (Sartorius, Goettingen, Germany), desalted on prepacked Sephadex G-25 columns (PD-10, Amersham Bioscience), equilibrated with amonium acetate buffer 50 mM, pH 5.5, eluted with the same buffer and stored in vials at 4^{o}C.

Detection of extracellular chitinase activity. SDS-PAGE of the enzyme extract proteins were performed according to Laemmli[26]. Proteins showing chitosanolytic activity were detected according to the method described by Trudel and Asselin[27] using poly-acrylamide gels containing 0.01% (w/v) chitosan DA 11% and chitosan DA 56%. After incubation in 50mM amonnium acetate buffer (pH 5.2) overnight at 37 °C, overlay gels were incubated for 10 min in solution containing 0.01% (w/v) calcofluor M2R (Sigma) in 500 mM Tris-HCl (pH 8.9). After 10 min, the calcofluor solution was removed and the overlay gel was rinsed overnight in distilled water. Lytic zones were visualized by fluorescence under UV light.

Three chromogenic derivatives p-nitrophenyl-N-acetyl-β-D-glucosaminide (pNP-GlcNAc), p-nitrophenyl-β-D-N,N'-diacetylchitobiose [pNP-$(GlcNAc)_2$] and p-nitrophenyl-β-D-N,N',N''-triacetylchitotriose [pNP-$(GlcNAc)_3$] (Sigma) were used as substrates for determination of chitinolytic activity[28]. The release of the chromophore p-nitrophenol from the substrates was determined by measuring the absorbance at 410. One unit of enzyme activity was defined as the amount that released one micromole of p-nitrophenol per minute under the specified conditions.

Enzymatic hydrolysis assays. The enzymatic extract was incubated overnight at 37^{o}C with polymeric chitosans (2 g/L) with three different degrees of acetylation (DA), 15%, 27% and 56% in acetate buffer 50 mM, pH 5.5). The hydrolizate was mixed with a solution of ethanol/ammonia (7:3, v/v) in the proportion 1:3 (v/v), respectively. The precipitated fraction was discarded and the supernatant was freeze-dried and resuspended in distilled water. Aliquots of the 3 different hydrolysis were applied on silica gel thin-layer chromatography (TLC) plates 60 (Merck Co., Berlin, Germany) using *n*-butanol–methanol–25% ammonia solution–water (5:4:2:1, v/v/v/v) as solvent system. The plates were sprayed with aniline-diphenylamine reagent (4 ml of aniline, 4 g of diphenylamine, 200 ml of acetone and 30 ml of 85% phosphoric acid) to visualize the oligomers and the spots developed by heating at 180°C for 3 min. The retention factor of the samples were compared with N-acetylglucosamine (degree of polymerization, DP, 1,3,4,5,6) and D-glucosamine (DP 1 to 6) standards.

RESULTS AND DISCUSSION

The enzyme extracts produced by *T. polysporum* using different inducing substrates (Table 1) differed in terms of quantity and quality of iso-enzymes produced (Figures 1, 2 and 3) and consequently, different oligomeric products were obtained when the crude enzyme mixtures were incubated with chitosan polymers (data not shown).

The analyze the enzymatic extracts protein by SDS– PAGE (Figure 1) showed that *T. polysporum* produces a large number of proteins when grown on media supplemented with chitin or shrimp shell. An approximately 50 kDa protein was induced independent of the individual (S1) or combined (S2 to S4) source used, except for the chitosanase standard (CTN). Caroline et al[29] reported a 30-kDa protein by SDS-PAGE from purification of the secreted during *Metarhizium anisopliae* growth on chitin as carbon/nitrogen sources. The chitosanolytic activity gel (Figure 2 and 3) shows differences qualities in the production of iso-enzymes for the different fermentations. Two protein bands to S4 and three proteins bands to S2 were showed a similar behavior when shrimp shell is used as carbone/nitrogen source.

The activities was stronger in chitosan DA 56%, hydrolising more easily acetylated products. The differences between the extracts can be indicated the production of oligomeric products with some particularities as bioactivity. Esteban et al[30] reported three bands of the enzyme extract crude protein samples producing by *Lecanicillium lecanii* after 48h of solid state fermentation utilizing shrimp shell. Carolina et al[31] reported a 42kDa protein with endochitinase activity in *T. harzianum.*

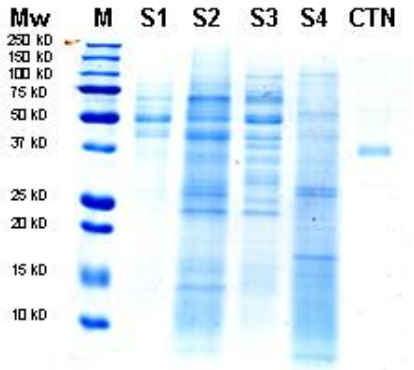

Figure 1. SDS-PAGE analysis of the enzymatic extracts. M – Molecular marker; S1 – Extract of submerged fermentation (SmF) from *Trichoderma* Complete Medium (TCM); S2 – Extract of SmF (TCM+shrimp shell); S3 – Extract of SmF (TCM+colloidal chitin)**;** S4 – Extract of SSF (filtration in paper filter and centrifugation); S5 – Extract SSF**;** CTN – Chitosanase (standard).

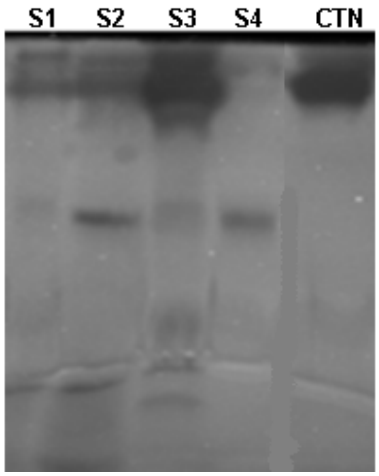

Figure 2. Evaluation of chitosanolytic enzyme production during SSF and SmF in overlay gel containing 0.01% (w/v) chitosan DA 11%. Legend: S1 – Extract of Submerged Fermentation (SmF) from *Trichoderma* Complete Medium (TCM); S2 – Extract of SmF (TCM+shrimp shell); S3 – Extract of SmF (TCM+colloiddal chitin); S4 – Extract of SSF; CTN – Chitosanase (standard).

The ability of enzymatic extract S4 to hydrolyze the oligomers of *p*-NP-GlcNAc (DP1 to3) were also investigated. The strongest enzyme activity was found with the substrate *p*-NP-GlcNAc and the weakest for the dimeric substrate *p*-NP-$GlcNAc_2$, however an intermediate enzyme activity was found for the trimer substrate, *p*-NP-$(GlcNAc)_3$ (Table 2). The use these substrates are to differentiate the enzymes on the basis of the type of activity: ß-N-

acetylglucosaminidase (active on three substrates), chitobiosidase (active on pNP-GlcNAc), exo-chitinase (active on pNP-$GlcNAc_2$) or endo-chitinase (typically active on pNP-$GlcNAc_3$ and possibly also on pNP-$GlcNAc_2$)[28].

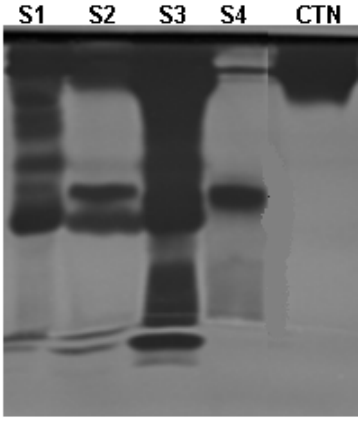

Figure 3. Evaluation of chitosanolytic enzyme production during SSF and SmF in overlay gel containing 0.01% (w/v) chitosan DA 56%. S1 – Extract of Submerged Fermentation (SmF) from *Trichoderma* Complete Medium (TCM); S2 – Extract of SmF (TCM+shrimp shell); S3 – Extract of SmF (TCM+colloiddal chitin); S4 – Extract of SSF; CTN – Chitosanase (standard).

Table 2. Hydrolytic activity of enzyme extract by solid state fermentation (S4) of *T. polysporum* on *p*-NP-$(GlcNAc)_{1–3}$.

Substrate	***Type of enzyme***	***Enzyme activity (µmol/min. L)***
p-nitrophenyl-N-acetyl-β-D-glucosaminide [*p*-NP-GlcNAc]	ß-N-acetylglucosaminidase or chitobiosidase	14
p-nitrophenyl-β-D-N-N'-diacetylchitobiose [p-NP-$(GlcNAc)_2$]	ß-N-acetylglucosaminidase, exo-chitinase	1
p-nitrophenyl-β-D-N-N'-N''-triacetylchitotriose [*p*-NP-$(GlcNAc)_3$]	ß-N-acetylglucosaminidase or endo-chitinase	3

Probably the enzyme extract S4 presented mainly ß-N-acetylglucosaminidase and chitobiosidase against a small amount of exo-chitinase and endo-chitinase. Figure 4 shows the TLC separation of the oligomeric products obtained when the enzyme extract S4 was incubated with polymeric chitosans with three different degrees of acetylation (DA).

According to the literature, crude enzyme preparations by *Trichoderma viride* and *Acremonium cellulolyticus* were used to produce GlcNAc from chitin32. The multi-chitinolytic enzyme complex produced by *Paenibacillus illinoisensis* KJA-424 was reported as effective in the production of GlcNAc and N-acetyl chitooligosaccharides, facilitating its potential use in industrial applications6. The chitosanase of *Bacillus cereus* NTU-FC-4 catalyzed a reaction to produce octamer from a mixture containing dimer to heptamer, possibly the transglycosylation [33]. Jo et al[34] concluded that higher concentrations of chitosan

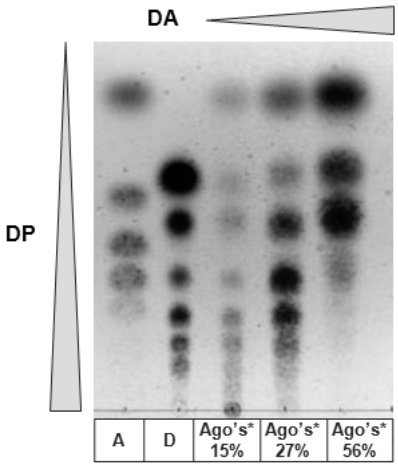

Figure 4. Chitosan oligomer profiling. A: N-acetylglucosamine (DP 1,3,4,5,6); D: glucosamine (DP 1,2,3,4,5,6); *Ago's: Chitosan oligomers.

produced high degree of polymerized chitooligosaccharides. They compared the endochitosanolytic enzymes by *Bacillus cereus* P16 with some commercial chitosanase preparations and the microorganism was indeed found to be a valuable enzyme source for industrial production of chitooligosaccharides. André et al[35] reported the application of chitosan oligomers produced by chemical hydrolysis induced an oxidative burst and the elicitor activity increased with increasing DA. Chitin oligosaccharides (DP2, DP3, DP4, DP5 and DP7) were investigated for their effects on epithelial cells and tissue[36]. Oliveira Jr et al[37] reported the inhibition of the growth rate of *Alternaria alternata*, *Rhizopus stolonifer*, *Penicillium expansum* and *Botrytis cinerea* by a mixture contained oligosaccharides of DP2–DP10. Here, our work with the enzymatic extract produced by solid state fermentation of *T. polysporum* and different inducing substrates showed differences in the production of iso-enzymes. This extract is estimated to act most efficiently in the release of *N*-acetyl-chitooligosaccharides, produced mainly ß-N-acetylglucosaminidase and chitobiosidase. In our case, higher DP oligosaccharide products were obtained when low DA substrate was hydrolyzed, indicating the presence chitinase activity.

Therefore, the oligosaccharides produced from chitosan using the crude enzyme extract from solid state fermentation by *T. polysporum* with shrimp shell to the fermentation is currently used to analyze the induction of an oxidative burst in plant cells, the induction of disease resistance in intact plants, the induction of an inflammatory response in human macrophages, and the antimicrobial activities. The novel aspect of this work is the description of the effect of the shrimp shell, a waste from the captivity, to the production of chito-enzymes by solid state fermentation of the *T. polysporum* and the utilization of the crude enzyme to produced chitooligosaccharides bioactives.

CONCLUSIONS

The enzyme cocktail produced by *T. polysporum* using different inducing substrates (colloidal chitin, chitosan and shrimp shells) differed in terms of quantity and quality of iso-enzymes produced. The enzymatic extract hydrolyzed most efficiently the substrate *p*-NP-GlcNAc. It's possible that the enzyme extract presented mainly ß-N-acetylglucosaminidase and chitobiosidase. The products obtained when different chitosan substrated were incubated with the crude enzyme extract differed in their degree of polymerisation (DP): the lower the DA of the substrate, the higher the DP of the products, clearly indicating the presence of chitinase rather than chitosanase activity.

ACKNOWLEDGEMENTS

This research was supported by São Paulo Research Foundation – FAPESP, The National Council for Scientific and Technological Development (CNPq), Coordination for the Improvement of Higher Level Personnel (Capes) – German Academic Exchange Service (DAAD) and European Union (EU).

REFERENCES

1. Wang SL, Lin TY, Yen YH, Liao HF, Chen YJ, *Carbohydr. Res.* **341**: 2507–2515 (2006).
2. Suzuki K, Mikami T, Okawa Y, Tokoro A, Suzuki S, Suzuki M, *Carbohydr. Res.* **151**: 403–408 (1986).
3. Wang J, Zhou W, Yan H, Wang Y, *Carbohydr. Res.* **343**:2583-2588 (2008).
4. Su C, Wang D, Yao L, Yu ZJ, *J. Agric. Food Chem.* **54**: 4208–4214 (2006).
5. Lee YS, Yoo JS, Chung SY, Lee YC, Cho YS, Choi YL, *Appl. Microbiol. Biotechnol.* **73**: 113–121 (2006).
6. Jung WJ, Souleimanov A, Park RD, Smith DL, *Carbohydrate Polymers* **67**: 256–259 (2007).
7. Liang TW, Chen YJ, Yen YH, Wang SL, *Process Biochem* **42:** 527–534 (2007).
8. dos Santos, AL, El Gueddari NE, Moerschbacher BM, *Biomacromolecules* **9**: 3411-3415 (2008).
9. Archer DB, Wood DA *In: Gow NAR, Gadd GM (eds) The growing fungus. Chapman & Hall* 137–162 (1995).
10. Punt PJ, van Biezen N, Conesa A, Albers A, Mangnus J, van den Hondel C, *Trends Biotechnol* **20**(5): 200–206 (2002).
11. Grim LH, Kelly S, Krull R, Hempel DC, *ApplMicrobiol Biot* **69**: 375–384 (2005).
12. Nedwin GE, Schaefer T, Falholt P, *Chem Eng Progress* **101**(10): 48–55 (2005).
13. Izume M, Ohtakara A, *Agric Bio. Chem* **51**:1189–1191 (1987).
14. Yalpani M, Pantaleone D, *Carbohydr Res* **256**:159–175 (1994).
15. Harman GE, Howell, CR, Viterbo A, Chet I, Lorito, M, *Nat Rev Microbiol* **2**: 43–56 (2004).
16. Vinale F, Sivasithamparamb K, Ghisalbertic EL, Marra R, Woo SL, Lorito M, *Soil Biol Biochem* **40**: 1–10 (2008).
17. Harman GE, *Plant Disease* **84**: 377–393 (2000).
18. Parameswaran B, Chandran S, Pradeep S, George S, Ashok P, *Biores Technol* **14**: 2742-2748 (2007).
19. Donzelli BGG, Siebert KJ, Harman GE, *Enz Microbial Technol* **37**: 82-92 (2005).
20. Nampoothiri KM, Baiju TV, Sandhya C, Sabu A, Szakacs, G, Pandey A, *Process Biochem* **39**:1583-1593 (2004).
21. Felse PA, Panda T, *Biochem Eng J* **4**: 115-120 (2000).
22. Deane EE, Whipps JM, Lynch JM, Peberdy JF, *Enz Microbial Technol* **24**:419-424 (1999).
23. Felse P, Panda T, *Process Biochem* **37**: 563-566 (1999).
24. Eddie ED, John MW, James ML, John FP, *Biochim Biophys Acta* **1383**: 101-110 (1998).
25. Laemmli UK, *Nature* **227**: 680-685 (1970).
26. Trudel J, Asselin A, *Anal Biochem* **178**: 362-366 (1989).
27. Nawani NN, Kapadnis BP, *J Appl Microbiol* **90**: 803-808 (2001).
28. Moraes CK, Schrank, A, Vainstein, MH, *Curr Microbiol* **46**: 205-210 (2003).
29. Florido EB, Camilo PB, Reyes LM, Cervantes RG, Cruz PM, Azaola A, *Interciencia* **34**: 356-360 (2009).
30. Carsolio C, Gutiérrez A, Jimenez B, Montagu MV, Estrella AH, *Proc. Natd. Acad. Sci.* **91**: 10903-10907 (1994).

31. Hitoshi S, Shizu F, Naoko Y, Norioki K, Atsuyoshi N, Einosuke M, Mongkol S, Rath P and Sei-ichi A, *Carbohydr Polym* **51:** 391–395 (2003).
32. Hsiao YC, Lin YW, Su CK, Chiang BH, *Process Biochemistry* **43**: 76-82 (2008).
33. Young JY, Jong JK, Lan JY, Jin JW, Hee KJ, Yong KK, Hwan KT, Dong PR, *Journal of Microbiology and Biotechnology* **13**: 960-968 (2003).
34. Deters A, Petereit F, Schidgall J, Hensel A, *Journal of Pharmacy and Pharmacology* **60**: 1-8 (2008).
35. Oliveira Jr EN, El Guedari NE, Moerschbacher BM, Peter MG, Franco TT, *Mycopathologia* **166**: 163–174 (2008).

Formulation of fermentation medium for aquatic species residues for the production of xanthan gum

Elisiane C.A. Reis[1,2], Yzila L.F. Maia-Araujo[1], Cezar B.Z. Oliveira[1,2], Jamile L. Rodrigues[1,2], Juliana C. Cardoso[1,2], Janice I. Druzian[3], Francine F. Padilha[1,2*]

[1]Institute of Technology and Research, Laboratory of Biomaterials, Aracaju, SE, Brazil
[2] University Tiradentes, Aracaju, SE, Brazil
3 University Federal of Bahia, Salvador, Brazil
* E-mail: fpadilha@yahoo.com; ylmaia@yahoo.com.br.

Summary

Xanthan gum, a polymer synthesized by *Xanthomonas* sp has high commercial interest, mainly for the food industry, pharmaceuticals and oil, due to its physical and chemical properties. The aim of this study was to evaluate the production of xanthan gum obtained starting waste oyster (*Crassostrea brasiliana*), lambreta (*Lucina pectinata*), crab (*Ucides cordatus*) and massunim (*Anomalocardia brasiliana*) and characterize the aqueous solutions of 3% on the apparent viscosity. The inoculum was prepared with the YM (yeast malt) and *Xanthomonas campestris* IBSBF 629, urea (0.1 gL^{-1}) and phosphate (1.0 gL^{-1}), incubated at 28 ° C, 250 rpm for 96 h. For analysis of the apparent viscosity of aqueous solutions were used gum to 3%. You can obtain xanthan gum with high viscosity and yield from waste crustacean and bivalve supplemented with urea and phosphate.

Keywords: Fermentation, rheology, crustacean, bivalve.

INTRODUCTION

Chitin is found in nature as a structural component in the exoskeleton of arthropods or cell wall of fungi and yeasts. The main commercial source of chitin is found in crabs, shrimp shells and other crustaceans. Chitin has proteins in its composition, some pigments and calcium carbonate, which is produced annually in large scale, making it the second most abundant polymer after celulose.[1]

Several investigations have been carried out with the waste, but none of them related to its use for the production of xanthan gum. The exoskeletons of crustaceans are commonly used for extraction of carotenoids because there is a great demand in the pharmaceutical, food or even to manufacture of food.[2]

Xanthan gum, a polymer synthesized by *Xanthomonas* sp has high commercial interest, mainly for the food industry, pharmaceuticals and oil, due to its physical and chemical properties that allow its application in industrial processes or products in a wide pH range and temperature.[3] Sucrose is the carbon source used industrially, but due to various environmental problems related to excess waste released daily and cost, there are numerous studies evaluating different carbon sources such as corn syrup, dextrose, whey, waste fruit, molasses, among others. The residues of crustaceans and molluscs are a source of macronutrients and micronutrients such as calcium carbonate and chitin, which is an excellent carbon source for many processos.[4]

The aim of this study was to evaluate the production of xanthan gum obtained starting waste oyster (*Crassostrea brasiliana*), lambreta (*Lucina pectinata*), crab (*Ucides cordatus*) and massunim (*Anomalocardia brasiliana*) and characterize the aqueous solutions of 3% on the apparent viscosity.

MATERIALS AND METHODS

The residues were obtained starting from specimens collected along the coast of Sergipe, Brazil. These were cleaned in hypochlorite solution containing 2% during 3 hours, rinsed in water and allowed to dry at 45 ° C for 8 h. All material was ground in a knife mill until obtaining a fine powder.

The inoculum was prepared with the YM (yeast malt) and *Xanthomonas campestris* IBSBF 629, incubated at 28 °C, 180 rpm, 24h, then transferred to fermentation medium containing 2% waste, urea (0.1 gL^{-1}) and phosphate (1.0 gL^{-1}), incubated at 28 °C, 250 rpm for 96 h. Sucrose was used as positive control. The broth was centrifuged at 10 000 x *g* for 15 minutes. The supernatant was precipitated with ethyl alcohol (92.8 ° GL) (1:4 v / v). The polymer was recovered and dried at 40 ° C for 48 h.

For analysis of the apparent viscosity of aqueous solutions were used gum to 3%. Was used rheometer Anton Paar model Physio 301 with plate-plate geometry 25mm. The parameters were observed: shear rate applied between 0.1s^{-1} to 300s^{-1}, Gap 1 mm and 30 seconds per point at 25 °C. The temperature of the samples were adjusted and maintained in the same test conditions for 10 minutes to ensure thermal homogeneity of the sample. The tests were performed in triplicate.

RESULTS AND DISCUSSION

There was production of xanthan gum obtained starting residues of crustaceans and bivalves used in the tests. Table 1 shows that the higher productivity of xanthan gum was obtained it from a medium containing residue of oyster (4.70 ± 0.07 gL^{-1}). Despite the large difference in composition, waste lambreta (3.00 ± 0.10) and crab (3.15 ± 0.16) showed no significant difference in the production of xanthan gum ($p < 0.05$), while the lowest production was observed starting from the residue bivalve massunim (2.50 ± 0.06).

Table 1. Production of Xanthan Gum with the strain of *Xanthomonas campestris* 629.

Residues	***Production (g × L^{-1})****
Crab	3.15± 0.16 [b]
Oyster	4.70± 0.07 [a]
Lambreta	3.00± 0.10 [b]
Massunim	2.50± 0.06 [c]
Sucrose*	1.32± 0.04 [d]

* Equal letters in the same column represent statistically identical values ($p < 0.05$).

All values found with residues massunim, lambreta, crab or oysters were superior to the control of sucrose used in this study that showed a value of 1.32 gL^{-1}.

There are only few studies with residues of crustaceans and molluscs to obtain xanthan gum. One of the few studies using shrimp waste presented a production of 1.39 to 2.65 gL^{-1} using the same bacterial strain that study.[5] Although these values are lower than those obtained in the present study, the production values of xanthan gum obtained from the residues evaluated are smaller than most of the results found in literature involving other residues. However, it should be noted that the positive control (sucrose) in this study showed lower values than those obtained with all residues.

Production between 14.2 and 33.5 gL^{-1} from alternative means containing cane juice was obtained by Brandão[6] while Faria[7] obtained with the same alternative means production of 15.1 gL^{-1}. In other studies using agro-industrial residues, the values ranged from 7 gL^{-1}, using waste water from olive oil [8], 14.5 gL^{-1} using citricos residues [9] and 17 gL^{-1} using alfarroba extract.[10]

This variation in production is due to several variables that affect the final result as the type of strain used in the test, temperature, rotation, and the composition of the nutrient medium. It is important to note that in the context in which values the cost of the fermentation process, the greater the production of xanthan gum becomes more interesting use of this residue. Moreover, it is important to highlight another aspect of the use of residue of aquaculture species, which is the contribution to the reduction of environmental impacts caused by the amount of waste released into nature.

In the Northeast region of Brazil is the common large consumption of crustaceans in pubs, homes and industry, which generates huge amount of waste released daily. Considering its low cost, these residues can be seen as a promising alternative for reducing the cost of the final product when used in place of current media such as glucose or sucrose.

As for the data of rheology, it can be seen from Figure 1 that the gum obtained with strain 629 from crab waste, obtained viscosity values higher than that obtained with sucrose, which is the default font currently used in industry. The gums showed pseudoplastic behavior is characteristic of these polymers, where the viscosity decreases with increasing shear rate, similar result was observed by Padilha.[11]

According to Brandão[6] the apparent viscosity of xanthan gum produced from sugar cane residue was 99.36 mPa.s (2.0% solution and 25 s^{-1}) higher than that found in this study for oyster supplemented, which showed a value of 50.6 mPa.s (3.0% solution and 29 s^{-1}).

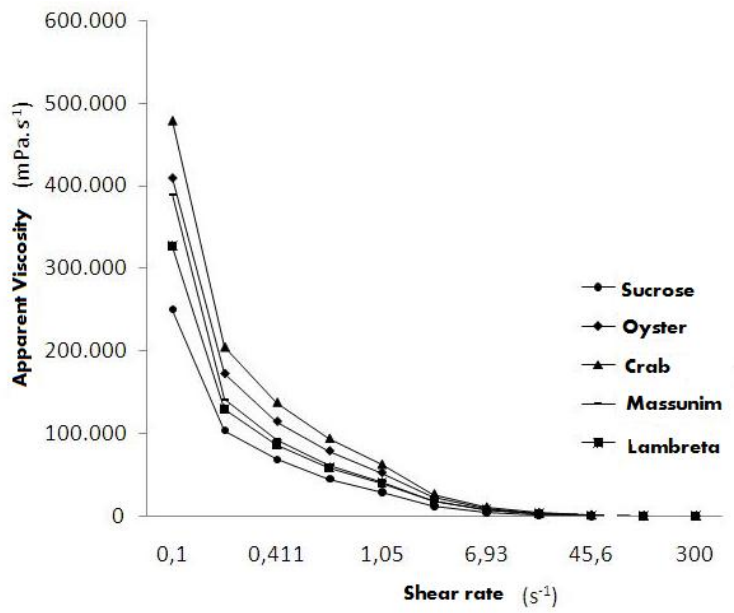

Fig 1. Apparent viscosity of xanthan gum obtained from aquaculture waste and sucrose

CONCLUSIONS

The results indicate that it is possible to obtain xanthan gum with high viscosity and yield from waste crustacean and bivalve supplemented with urea and phosphate. The maximum yield of xanthan gum was 4.70 g L^{-1} containing residue oyster. The xanthan gums produced behaved as pseudoplastic fluids.

ACKNOWLEDGEMENTS

The authors thank CAPES-PROCAD/NF, CNPq, FAPITEC UNIT and the financial support and scholarships to aid the search.

REFERENCES

1 Craveiro, A. A.; Craveiro, A. C.; Queiroz, D. C. *Parque de Desenvolvimento Tecnologico – PADETEC*. (1999).
2 Sringate & Nickell. *Roche Vitamins Ltd.* (2000).
3 Garcia-Ochoa, F., V.E. Santos, J.A. Casas and E. Gomez. *Xanthan Biotechnol***. 18**, 549–579. (2000).
4 Andriguetto, J. M., Perly, L., Minaroi L, Gemael, A., Flemming, J. S., Souza, G. A., Bona Filho, A. *Nobel*, **I**, 395. (1981).
5 Costa, LAS, Campos, MI, Silva, SM, Druzian, JI. *Anais VII Sinaferm* (2009).
6 Brandao LV, Nery TBR, Esperidiao MCA, Druzian JI. *Ciencia e tecnologia de alimentos*, **28**, 217-222. (2008).
7 Faria, S. Dissertação. Universidade Federal de Uberlândia, 119 f. (2005).
8 Lopez, M. J., Moreno, J., & Ramos-Cormenzana, A. *Water Research*, **35,** 1828–1830. (2001).
9 Green, M., Shelef, G., & Bilanovic, D. *Chemical Engineering Journal*, **56**, 37–41. (1994).
10 Roseiro, J. C., Costa, D. C., & Collaco, M. T. A. *Food Science and Technology*, **25**, 289–293. (1992).
11 Padilha, F.F. Tese de doutorado. Universidade Estadual de Campinas. (2003).

Biotechnological process for the production of chitin from the fungus *Ganoderma lucidum*

Sandra P. Ospina[1], David A. Ramírez [1], Erika J. Obando [1], Claudia P. Ossa [2], Lucía Atehortúa [1] and Paola Zapata[1]

[1] Biotechnology Group, Institute of Biology, Universidad de Antioquia, Street 62 No 52-59, Laboratory 210, Medellín, Colombia
[2] Biomaterials, Faculty of Engineering, Universidad de Antioquia, Medellín, Colombia
*E-mail: sandritao@gmail.com

Abstract
Submerged cultures of basidiomycete mushroom *Ganoderma lucidum* has been used to obtain mycelial biomass and different bioactive metabolites, such as exopolysaccharides, endopolysaccharides, and ganoderic acid; however this fungus also becomes a promising source for the production of chitin, a component of its cell wall. In this paper was assessed and proposed a biotechnological process for the production of chitin from this mushroom. Mycelial biomass production of medicinal mushroom *G. lucidum* obtained in a stirred bioreactor under submerged culture conditions was 21.87±2.2 g L^{-1} and chitin production was 14.42 mg g^{-1} (milligrams of chitin/grams of dry biomass).

Keywords: Biotechnological Process, Chitin, *Ganoderma lucidum*, Fungal Source.

INTRODUCTION

The fermentative abilities of microorganisms in various forms have been used for many centuries and nowadays more than 200 types of fermented food product are available in the market. There are several biological processes actively used in the industry, with high-quality products such as synthesis of proteins and amino acids, lipids and fatty acids, simple sugar and polysaccharides such as xanthan gum, glycerol, many more fine chemicals and alcohols are produced by bioprocesses with suitable industrial applications[1]. These processes have also been applied for fermentation of different types of fungi, between them basidiomycetes, because of lots of compounds which may be obtained by their fermentation, some of them are: *Lentinus edodes*[2], *Grifola frondosa*[3], *Agaricus bisporus*[4], *Ganoderma lucidum*[5], among others. The interest about generation of biomass and compounds from these fungi have generated the development of protocols to grow them efficiently, in special *Ganoderma lucidum*[6], whose compounds have many applications, especially in medicine, for the treatment of lots diseases[7,8,9,10]. The importance of this fungus and its compounds let that the Biotechnology Group from Universidad de Antioquia, Medellin (Colombia) worked during several years in a protocol for the biotechnology production of this fungus, generating a protocol for its production[11] and at the same time the group seeks different by-products, which can be obtained from it, one of them may be chitin.

Chitin is a straight-chain polymer composed of β-1,4-N-acetylglucosamine and classified into α-, β- and γ-chitin[12] and it is needed as a precursor of chitosan, which is obtained by partial N-deacetylation of chitin, and it is also a straight-chain polymer of glucosamine and N-acetylglucosamine[13]. Because chitin and chitosan possess many beneficially properties such us antioxidant[13], antimicrobial activity[14], biocompability and biodegradability[15], in general potential and usual applications of chitin, chitosan and their derivatives are estimated to be more than 200[16]. Exosceletons of crustaceans are the key source of chitin. Limitations of utilization are high costs for purification done by chemical processes, which include alternating acid and alkali treatments, resulting in large amounts of liquid waste of harsh

chemicals[17].
A biotechnological process obtaining chitin from fungus *Ganoderma lucidum* represents an alternative source for this material. Such process included *Ganoderma lucidum* culture in bioreactor, freeze drying and sonication of biomass, ethanol washing, deproteinization, decolorization and chitin oven-drying. Biotechnological process proved to be an economical mean for obtaining chitin from the fungus *Ganoderma lucidum*, and it is also environmentally friendly.

MATERIALS AND METHODS

Materials

Potassium chloride, magnesium sulphate, potassium dihydrogen phosphate, sodium nitrate, sodium hydroxide, ethanol (96% pure), potassium permanganate, and oxalic acid were obtained from Merck KGaA (Darmstadt, Germany). Chitin from crab shells was obtained from Sigma-Aldrich.

Microorganism

Strain of *Ganoderma lucidum* was grown in the Universidad de Antioquia Plant Biotechnology Laboratory. The organism was maintained by an occasional transfer on potato dextrose agar (PDA) medium at 4 °C.

Cultivation

Actively growing mycelia was obtained from a newly prepared agar-plate culture after it was incubated for 9 days at 24°C. The pre-inolucums were prepared as follows. Around 1 cm × 1 cm of the mycelia was inoculated into a 250 ml erlenmeyer flask that contained 50 ml of complex medium developed in the Biotechnology Laboratory, Universidad de Antioquia[11]: (50 g l^{-1} complex carbon source, 0,03 g l^{-1} K_2HPO_4, 0,08 g l^{-1} $NaNO_3$, 0,01 g l^{-1} KCl and 0,02 g l^{-1} $MgSO_4.7H_2O$). Flask cultivation was carried out at 100 rpm for 7 days.
Subsequently, a bioreactor (Bioflo 110 Reactor New Brunswick® of 7 liters, with 5 liters of work volume) was inoculated with an inoculum of 4% v/v, agitation rate of 200±2 rpm and aeration of 5 VVM. Sterilization was done in an autoclave at 121°C for 20 min. All cultures were carried out at temperature of 26±1°C in bioreactor and pH 6.0 for 14 days.

Biomass and substrate quantification from *Ganoderma lucidum* cultures

To follow kinetic growth of *Ganoderma lucidum* during the time of culture, 100ml of sample was taken out every day during time culture from the bioreactor culture. The sample was filtered through a mesh US standard number 35 screen sieve, washed twice with DDI water. Fungal biomass was dried by lyophilization (FDU-100 Liophilizer Eyela®) to obtain and measure the amount of mycelium formed and precipitate was filtered through a tared GFC paper to quantify residual substrate. All conditions were monitored throughout the culture period. The experiment was performed in triplicate.

Chitin Isolation

Chitin was prepared from *Ganoderma lucidum* according to the modified protocol of Su *et al.*[18].

The dried fungal biomass was pulverized and mixed with deionized water and then, the mixture was subjected to a sonication process for 40 minutes, using a Sonicator S-4000-010 from Misonix®. Biomass was washed with ethanol for 24 hours. Deproteinization was performed using alkaline treatment with 4 M NaOH at the ratio of 1:20 (w/v) at 100 °C for 2 h, this treatment was repeated three times. The absence of proteins was indicated by the

absence of colour of the solution. The suspension was centrifuged and washed with deionized water to neutrality. For decolorization, the crude chitin was treated with 10 g L^{-1} potassium permanganate solution for 1 h, and then reacted with 10 g L^{-1} oxalic acid solution for 1 h. The mixture was centrifuged and washed with deionized water to neutrality and dried at 50°C to a constant weight. Finally, the amount of chitin produced by each protocol was determined by dry weight method.

X-Ray Diffraction

The X-ray diffraction (XRD) analysis was applied to detect the crystallinity of chitins prepared and their patterns were recorded using a X´Pert PRO MPD diffractometer from PANalytical with Cu Kalpha radiation of 1.5406 A, power of 1.8 kW (40 mA and 45 kV). Data were collected at a scan rate of 0.057088°/s with the scan angle from 3 to 50.

FTIR Analysis

Fourier transform infrared spectroscopy (FT-IR) analysis was used to analyze the molecular structure of isolated chitin with Assay 5 and their spectra were recorded using a SpectrumOne Spectrophotometer with detector DTGS from Perkín Elmer®. The average number of scans taken per sample was 8 in the spectral region between 450 and 4000 cm^{-1}, with a resolution of 4 cm^{-1}. The samples were prepared in 0.25 mm thickness KBr pellets (5 mg in 100 mg of KBr) and stabilized under controlled relative humidity before obtaining the spectrum.

RESULTS

Cultivation

The fungal growth of *Ganoderma lucidum* using the medium developed in the Biotechnology Laboratory of Universidad de Antioquia[11] were performed in a lab-scale reactor with a nominal volume of 7 L, this process was monitored for 14 days and was obtained 21.87±2.2 g L^{-1} as a maximum biomass production at 8-day.

Biomass and substrate quantification from *Ganoderma lucidum* cultures

Figure 1 shows a growth kinetic for biomass production and substrate uptake for 14-days of culture.

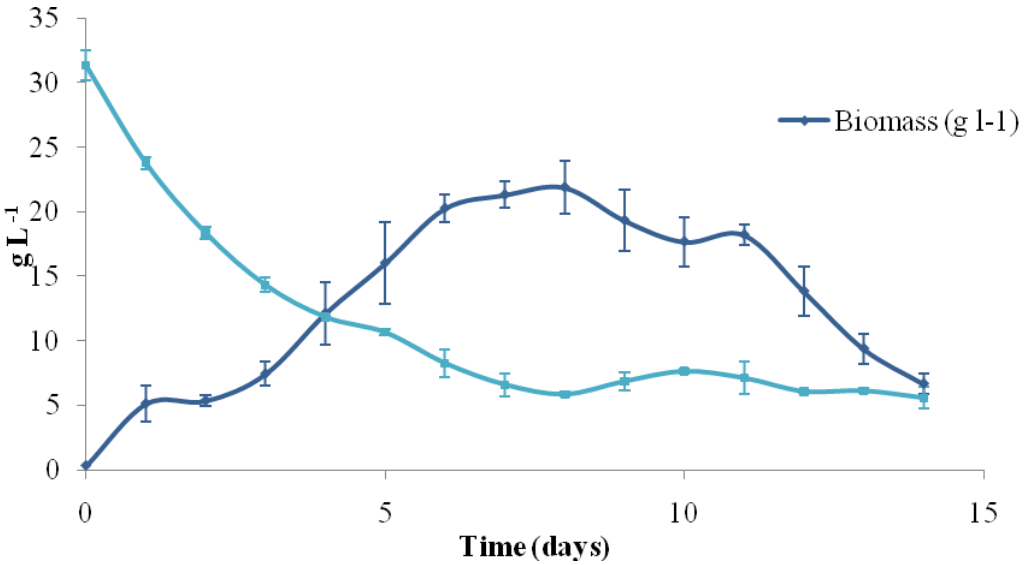

Figure 1. Biomass production and substrate uptake kinetic of *Ganoderma lucidum* growing in liquid culture in a Bioflo 110 Reactor New Brunswick® of 7 Liters.

From the figure above is totally clear the different phases of growth during the culture, such as (day 0-2) lag phase, (day 2-6) log phase, (day 2-8) stationary phase and (day 8-14) death phase. Maximum biomass production was identified at 8-day with a production of 21.87±2.2 g L^{-1}. Likewise substrate uptake kinetic was identified for 14-day of culture, substrate decreased during days of culture until a minimum of 5.57±0.85 g L^{-1}. For the last curve maximum substrate uptake was registered for the 6 first days, after that decreasing was constant until the last day of culture.

Chitin Isolation

Chitin was obtained from dried biomass of *Ganoderma lucidum* by mean of alkaline treatment, acid treatment and/or decolorization processes with potassium permanganate and oxalic acid. The amount of crude chitin was 14.42 mg g^{-1} (milligrams of chitin/grams of dry biomass).

The result of XRD analysis for chitin is shown in Figure 2. The XRD pattern of the chitin show two high intensity crystalline peaks at 5.7° y 19.6°.

Fourier transform infrared spectroscopy (FT-IR) analysis performed to chitin is also illustrated in Fig. 3. The FTIR shows representative bands at 3414, 2922, 1657, 1381, 1160, 1078 and 985 cm^{-1}. Additionally, a correlation of 79.53% between the chitin obtained and a standard chitin (Chitin from crab shells, Sigma-Aldrich) was found.

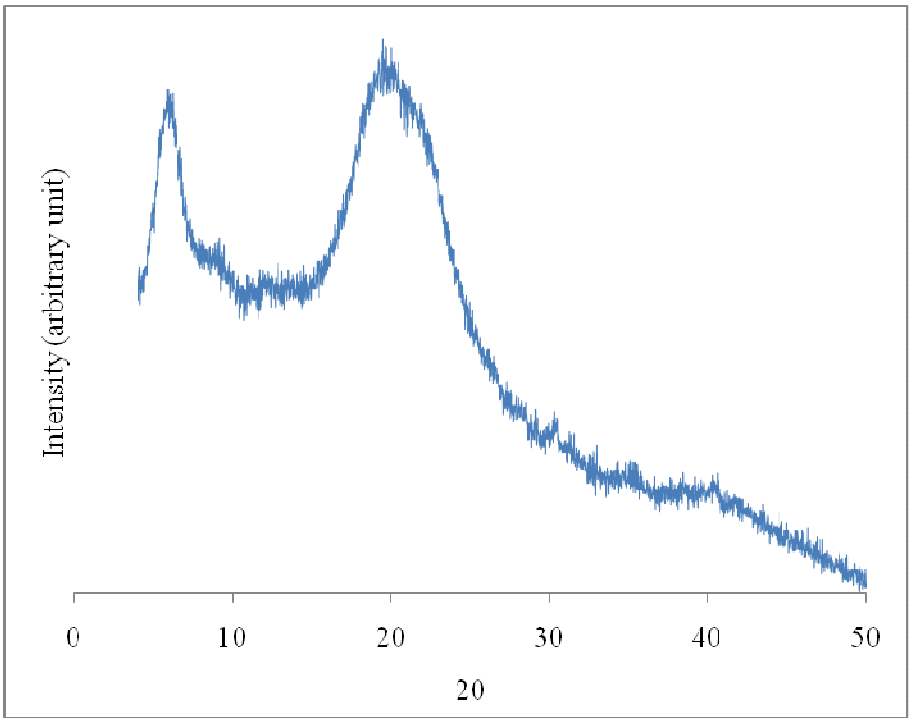

Figure 2. X-ray diffraction patterns of chitin.

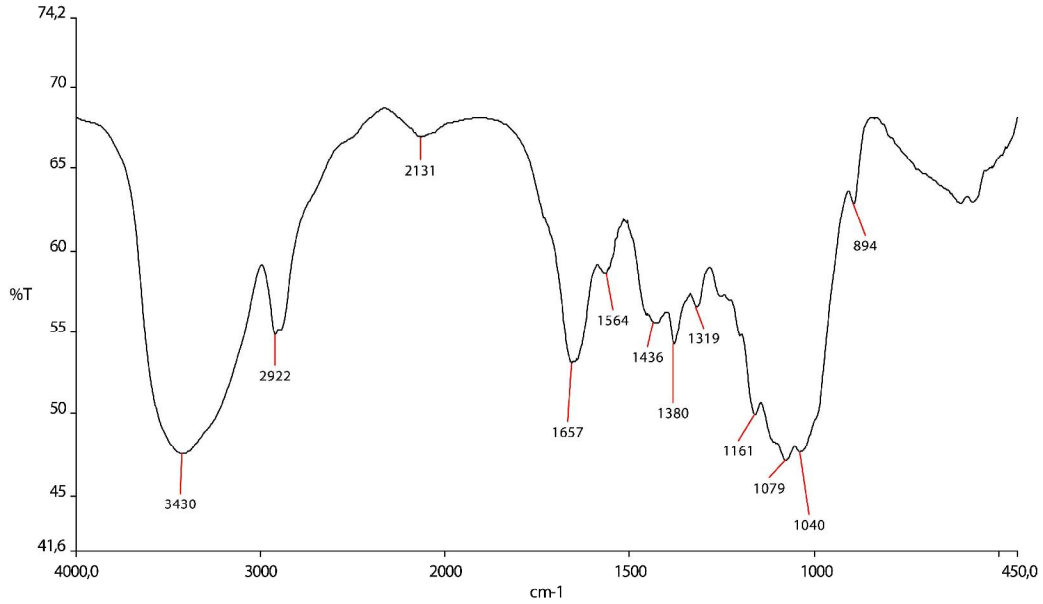

Figure 3. FTIR spectrum of chitin.

DISCUSSION

High biomass yield achieved was 21.87±2.2 g L^{-1}. This biomass yield was highest than those obtained by Berovic *et al.*[19] and Tang *et al.*[20], who used carbon sources such as glucose and lactose, respectively; also these authors used stirred tank reactor of 10 L and 5.5 L (working volume), respectively. However, the biomass yield was similar to the biomass obtained for Tang and Zhong[21], although they used a stirred bioreactor 2L (working volumen). Also the cost of the culture medium used by Tang and Zhong[21] is greater than the cost of the culture medium reported in this paper as reported by Zapata *et al.*[11]

About X-ray diffraction patterns of chitin, some authors have reported characteristic crystalline picks for different types of chitin. Jang *et al.*[22] found that crystalline peaks were 9.6°, 19.6°, 21.1° and 23.7° for α-chitin, 9.11° and 20.31° for β-chitin, and 9.61° and 19.81° for γ-chitin. Similarly, Cardenas *et al.*[23] reported that XRD patterns of α-chitin and β-chitin showed their major characteristic peak at 19.18°–19.26° and 18.78°, respectively. β-chitin from squid pen exhibited crystalline peaks at 9.8° and 19.3°[24]. Yen and Mau[25] found that crude chitin prepared from crabs exhibited two sharp peaks at 9.3° and 19°. Also, these authors isolated chitin from *Lentinula edodes*, a basidiomycete mushroom, and they obtained characteristic crystalline peaks at 5.4°-5.6°, 9.1° and 19.3°-19.6°. It is showed that the chitin had a consistent major peak at 19° in their crystallinity structure.

The evidence seems to confirm that the chitin obtained has two characteristic peaks similarly to standard chitin, a higher intensity at 19.6 ° and a lower intensity at 5.7°.

FTIR analysis of chitin obtained in assay 5 showed a similar spectrum of standard chitin (not shown). Band located approximately at 2900 cm^{-1} is used in the literature as a representative band for chitin and chitosan[26]. Another band at 2922 cm^{-1} corresponds to the absorption band of C - C bonds (alkanes). Others chitin characteristic bands are also present at 1657 cm^{-1} for the amide I, 1572 cm^{-1} for the amide II and 985 cm^{-1} for the amide III. Band for carbonyl groups link through hydrogen bonds to the amino group can be seen at 1657 cm^{-1}. Vibration present at 3414 cm^{-1} corresponds to intramolecular hydrogen bond involving the OH (6)···O =

C, also in this region are two modes of vibration due to the NH of the amide bonds, specifically because of the intramolecular hydrogen bonds C = O···H-N and NH groups linked intramolecularly with H .

Similarity of FTIR spectrum between chitin from *G. lucidum* for final assay and standard presented a correlation percentage of 79.53%, so it, XRD results for this assay show a pattern of peaks whose corresponds with standard chitin is presented at 5.6° and 19°. From previous results it is possible to say that chitin from this fungus may be a promising source to obtain this biomaterial.

CONCLUSIONS

Biotechnological process for biomass production of *Ganoderma lucidum* fungus is an appropriate source for chitin production. Facility to produce this kind of biomass with chitin yield of 14.42 mg g^{-1} (milligrams of chitin/grams of dry biomass) allows having a raw material with excellent conditions for the extraction of this kind of biomaterial.

The XRD analysis show that the highest crystalline peaks were in the 5 assay, with peaks in 5.6° and 19.4°. The five XRD patterns were similar and presented the crystalline peak around of 19°.

It is finally concluded that the biomass of *Ganoderma lucidum* obtained by biotechnological culture, is a promising source for chitin and its derivatives.

ACKNOWLEDGEMENTS

THE AUTHORS ACKNOWLEDGE FINANCIAL SUPPORT FROM CODI (UNIVERSIDAD DE ANTIOQUIA) AND BIOTECHNOLOGY GROUP OF INSTITUTE OF BIOLOGY AND BIOMATERIALS GROUP OF FACULTY OF ENGINEERING, UNIVERSITY OF ANTIOQUIA (MEDELLÍN, COLOMBIA).

REFERENCES

1. Najafpour GD, *Elsevier* 2 (2007).
2. Feng YL, Li WQ, Wu XQ, Cheng JW and Ma SY, *Biochem Eng J* **49**:104 (2010).
3. Shih IL, Chou BW, Chen CC, Wu JY and Hsieh C, *Bioresour Technol* **99**:785 (2008)
4. Kurbanoglu EB, Zulkadir A and Algur OF, *Industrial crops and products* **19**:225 (2004).
5. Zhu LW, Zhong JJ and Tang YJ, *Process Biochemistry* In Press, Corrected Proof.
6. Ko HH, Hung CF, Wang JP and Lin CN, *Phytochemistry* **69**:234 (2008).
7. Wagner R, Mitchell DA, Sassaki GL and Amazonas MALA, *Journal of Biotechnology* **114**:153 (2004).
8. Lu H, Kyo E, Uesakea T, Katoh O and Watanabe H, *Int J Mol Med* **9**:113 (2002).
9. Zhang GL, Wang YH, Ni W, Teng HL and Lin ZB, *World J Gastroenterol* **8**:728 (2002).
10. Zhe J, Tang Q, Zhang J, Yang Y, Jia W and Pan Y, *J Ethnopharmacolog* **112**:445 (2007).
11. Zapata PA, Rojas DF, Ramírez DA, Fernández C and Atehortúa L, *International Journal of Medicinal Mushrooms* **11**:93 (2009).
12. Cabib E, Bowers B, Sburlati A and Silverman SJ, *Microbiological Sciences* **5**:370 (1988).
13. Yen MT, Yang JH and Mau JL. *Carbohydr Polym* **74**:840 (2008).
14. Fujimura M, Ideguchi M, Minami Y, Watanabe K and Tadera K, *Biosci Biotechnol Biochem* **69**:642 (2005).

15. Zia KM, Zuber M, Bhatti IA, Barikani M and Sheikh MA, *International Journal of Biological Macromolecules* **44**:18 (2009).
16. Abdou ES, Nagy KSA and Elsabee MZ, *Bioresour Technol* **99**:1359 (2008).
17. Daum G, Stöber H, Veltrup K, Meinhardt F and Bisping B, *Journal of Biotechnology* **131**:S188 (2007).
18. Su CH, Sun CS, Juan SW, Hu CH, Ket WT and Sheut MT, *Biomaterials* **16**:1169 (1997).
19. Berovic M, Habijanic J, Zore I, Wraber B, Hodzar D, Boh B and Pohleven F, *Journal of Biotechnology* **103**:77.
20. Tang YJ and Zhong JJ, *Enzyme and Microbial Technology* **31**:20 (2002).
21. Tang YJ, Zhang W and Zhong JJ, *Bioresource Technology* **100**:1852 (2009).
22. , Jang MK, Kong BG, Jeong YI, Lee CH and Nah JW, *Journal of Polymer Science Part A: Polymer Chemistry* **42**:3423 (2004).
23. Cardenas G, Cabrera G, Taboada E and Miranda SP, *Journal of Applied Polymer Science* **93**:1876 (2004).
24. Kim SS, Kim SH and Lee YM, *Journal of Polymer Science Part B: Polymer Physics* **34**:2367 (1998).
25. Yen MT and Mau JL, *Annual of Tainan Woman's College of Arts and Technology* **23**:229 (2004).
26. Teng WL, Khor E, Tan TK, Lim LY and Tana SC, *Carbohydrate Research* **332**:305 (2001).

Analysis of a polyelectrolyte complex formed with jicama pectin and water soluble chitosan

A.M. Ramos-de-la Peña[1], Adriana M. Rangel-Rodrigeuz[2,3], Nagami Balagurusamy[4], A. Carillo-Castillo[1] and J.C. Contreras-Esquivel[1,2*]

[1] School of Chemistry, Universidad Autonoma de Coahuila, Saltillo City, Coahuila State, Mexico.
[2] Research and Development Center, Coyotefoods Biopolymer and Biotechnology Co., Simon Bolivar 851-A, Saltillo City 25000, Coahuila State, Mexico.
[3] Center of Investigation for Advanced Materials (CIMAV), S.C, Apodaca City 66600, Nuevo Leon State, Mexico.
[4] School of Biological Sciences, Universidad Autonoma de Coahuila, Torreon City 27000, Coahuila State, Mexico.
*E-mail: ramos.mayela@gmail.com

Abstract
BACKGROUND: Polyelectrolyte complexes were formed through the reaction between water soluble chitosan (WSCh, 0.5, 1.0 and 2.0 g/L) and jicama pectin (1 g/L).
RESULTS: The yield and infrared spectroscopic analysis of the polyelectrolyte complexes was evaluated. The formation of polyelectrolyte complexes between biopolymers depends upon the WSCh ratio employed. The yields of the polyelectrolyte pellets were of 13.3% ± 0.0, 26.7% ± 9.4 and 18.3% ± 2.3 for WSCh 0.5, 1.0 and 2 g/L, respectively. According to FITR finger print, both biopolymers was mainly composed of the absorption band finger print corresponding to polysaccharides. Thermogravimetric analysis showed complex formation between WSCh with jicama polysaccharides.
CONCLUSION: The WSCh is a promising polycation able to react with low methoxylated pectins from jicama to produce polyelectrolyte complexes with application in food technology and medicine.

Keywords: *Pachyrhizus erosus;* pomace; pectic substances; starch

INTRODUCTION

Mixing counter-charged biopolymers leads to formation of compound coacervates and polyion (polyelectrolyte) complexes, supermolecular structures that may precipitate or gel under specific conditions of ionic strength, biopolymer ratio, and pH. The specific nature of the biopolymers critically influences the properties attainable from the complexes.[1]
WSCh (a mucoadhesive cationic polyelectrolyte) is a natural linear copolymer of D-glucosamine and N-acetyl-D-glucosamine, derived from the partial depolymerization of chitosan. The amino group WSCh has a pKa value of 6.2 to 7.0, which makes chitosan a polyelectrolyte at low pH values.[2]
WSCh perform a variety of biological activities, such as inhibiting the growth of bacteria and fungi exerting antitumor activity, acting as immunopotentiating effectors, and eliciting pathogenesis-related proteins in higher plants. Chain length and deacetylation degree are considered the most important factors influencing the biological activities of this biopolymer.[3]
Pectin is a heterogeneous complex polysaccharide present in plant cell walls, having important roles in the plant physiology. The major constituents are the linear sequences of 1-4-linked D-galacturonic acid with some carboxyl groups methyl-esterified with methanol. [4]
Low-methoxyl pectins are linear polyanions (polycarboxylates) of about 300-1000 saccharide units, with polymer molecular weights ranging from 50 to 150 kDa and with a pKa of 3.0 to

4.5.[1]

Jicama (*Pachyrhizus erosus* L.) is a tropical legume originally from Mexico and Central America and cultivated by Precolombian cultures. It is currently produced in Mexico (source of most jicama in U.S. markets), Brazil, United States, China, Indonesia, Philippines and Nigeria. The root consists of a light or dark brown periderm, and a white, crisp, succulent and sweet-starchy pulp.[5-6] Its pectin residues obtained after starch extraction is a very promising source of low methoxylated pectin.[7] The aim of this work was evaluate the formation of a polyelectrolyte complex between pectin extracted from jicama and WSCh.

MATERIALS AND METHODS

Enzymatically de-starched jicama pomace, WSCh (molecular weight of 20 kDa) and isopropyl alcohol were procured from Coyotefoods Biopolymer and Biotechnology Co. (Saltillo City, Coahuila State, Mexico). All other chemicals were analytical grade.

Pectin extraction by autoclaving-assisted technology

Jicama pectin was extracted according to a simplified modifications of the method of Contreras-Esquivel *et al*.[4] Enzymatically de-starched jicama pomace (11.3 g) was mixed with 1% w/v sodium hexamethaphosphate solution (140 mL) and placed in glass vessel covered with aluminum foil. Then the slurry fiber was autoclaved for 10 min at 121 °C (2 atm) and the final volume was registered. The pectic substances from filtrate were precipitated by adding two volumes of isopropanol to extract. The precipitate was recovered by centrifugation and dried until constant weight at 40ºC, stored in microtubes and kept at room temperature until its use. Treatments were carried out in duplicate.

Polyelectrolyte formation

Jicama pectin was dissolved (1 g/L) in 20 mM sodium acetate buffer (pH 5.00). The pectin was added slowly to avoid the conglomerates formation. WSCh was dissolved in distilled water at 0.5, 1.0 and 2.0 g/L. Later 20 mL of jicama solution were mixed with 20 mL of each WSCh solution in a conical tube. The tubes were settled by 30 min at room temperature and after that, were centrifuged at 8000 rpm by 20 min at room temperature. The supernatant was discarded and the pellet was washed with isopropanol (3×) and centrifuged again at 8000 rpm by 20 min. Finally, the complex was dried at 60ºC until constant weight and its weight was registered. All experiment was carried out by duplicate.

Infrared spectroscopy

The polyelectrolyte complex was investigated by FTIR attenuated total reflectance (FTIR/ATR) spectroscopy, which was performed by Perkin Elmer (Waltham, MA, USA) equipment operating at 4 cm^{-1} resolution. The mirror velocity was 0.08 cm^{-1} and 35 interferograms were co-added before Fourier transformation. Spectra were collected from 4000 to 650 cm^{-1} and normalized that the absorption band at ca. 1008 cm^{-1} equaled 1. Normalization did not alter the proportion of signals in the origin spectra.

Thermogravimetric analysis

Thermogravimetric (TGA) analysis was carried out in air using thermogravimetric (TGA-50, Shimadzu Corporation, Kyoto, Japan) analyzer connected to the PC computer. Before loading of powder samples, the instruments were calibrated with aluminum and zinc standards. Dried polyelectrolyte complexes were analyzed with a linear heating rate of 10°C/min using 3-5 mg samples in an aluminum container.

RESULTS AND DISCUSSION

Polyelectrolyte complexes yield of WSCh and jicama pectin

The polyelectrolyte complex was obtained between jicama pectin and WSCh. Fig. 1 shows the appearance of the pellets obtained after centrifugation of polyelectrolyte complexes

formed by means of opposite charges of biopolymers. The pellet of greatest size was observed when WSCh 2 g/L was used and the smallest size pellet was produced when WSCh 0.5 g/L was occupied. When WSCh 1 g/L was used, the formation of an intermediate size pellet was registered. The pellet size was according to the WSCh ratio utilized, and it suggests the quantity of polyelectrolyte formed. When the pellets were dried, the registered yields were of 13.3% ± 0.0, 26.7% ± 9.4 and 18.3% ± 2.3 for WSCh 0.5, 1.0 and 2 g/L, respectively. As a result of polyelectrolyte complexes by increasing the concentration of WSCh of 0.5 to 1.0 g/L increased the quantity of dried precipitated. However, no difference was observed when tested concentration of 1.0 and 2.0 g/L. These results confirm previous reports which show the polyelectrolyte capacity of both biopolymers to form complexes.[1] It is possible to obtain a polyelectrolyte complex when pectin from jicama and a 20 kDa WSCh are combined. The yield in dry basis depends upon the oligosaccharide ratio employed.

Figure 1. Photographs of wet polyelectrolyte complexes formed after mixing jicama pectin with WSCh (a: 0.5; b: 1.0; and c: 2.0 g/L).

Characterization of polyelectrolyte complex by FTIR

Polysaccharides and polyelectrolyte complexes formed were analyzed by FTIR in the region 4,000-650 cm^{-1} to determine whether IR spectroscopy could differentiate the chemical structure and composition of the materials (Fig 2a-b). In Fig. 2a, the jicama pectin show major peaks around 3,400 (O-H stretching), 2,920 (C-H stretching and C-C ring stretching), 1,640 (C=O stretching and C-C ring stretching), 1,413 (C-H bending), 1,239 (C-O-H bendings) and 1,000 cm^{-1} (C-O-C bendings). Small ester groups could be evidenced because peaks were found at 1,730 cm^{-1} which indicates the presence of endogenous low methoxyl pectins.[4] The major peaks detected in WSCh (Fig 2b) can observed around 3265 cm^{-1} (N-H stretching) and 3100 cm^{-1} (O-H stretching), 2920 cm^{-1} (C-H stretching), 1665 cm^{-1} (N-H stretching), 1594 cm^{-1} (C-C ring stretching), 1466 cm^{-1} (C-H bending), 1234 cm^{-1} (C-O-H bending), and 1008 cm^{-1} (C-O-C stretching).[8]

Accord to FITR finger print, both biopolymers was mainly composed of the absorption band finger print corresponding to polysaccharides. Meanwhile, Fig 2c, showed IR spectra of the polyelectrolyte complexes formed by using 0.5, 1.0 and 2 g/L of WSCh. The higher the ratio of WSCh used the higher interaction to form the complex.

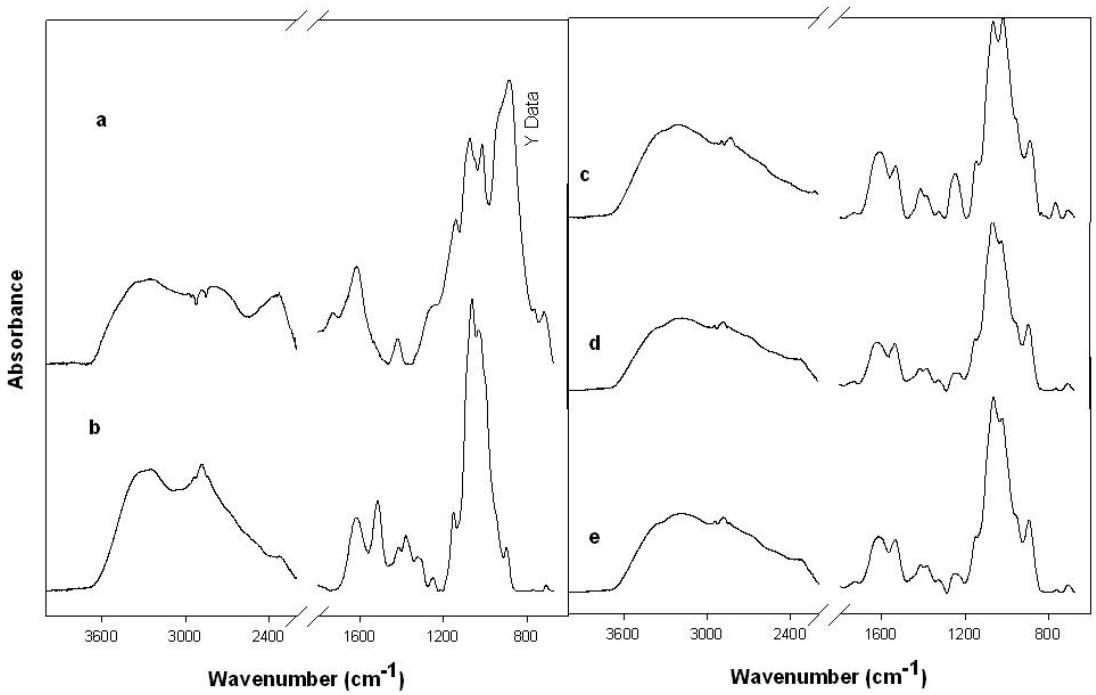

Figure 2. IR spectra of destarched jicama pectin (a), WSCh (b), polyelectrolyte complex jicama pectin-WSCh 0.5 g/L (c), polyelectrolyte complex jicama pectin WSCh 1.0 g/L (d) and 2.0 g/L (e).

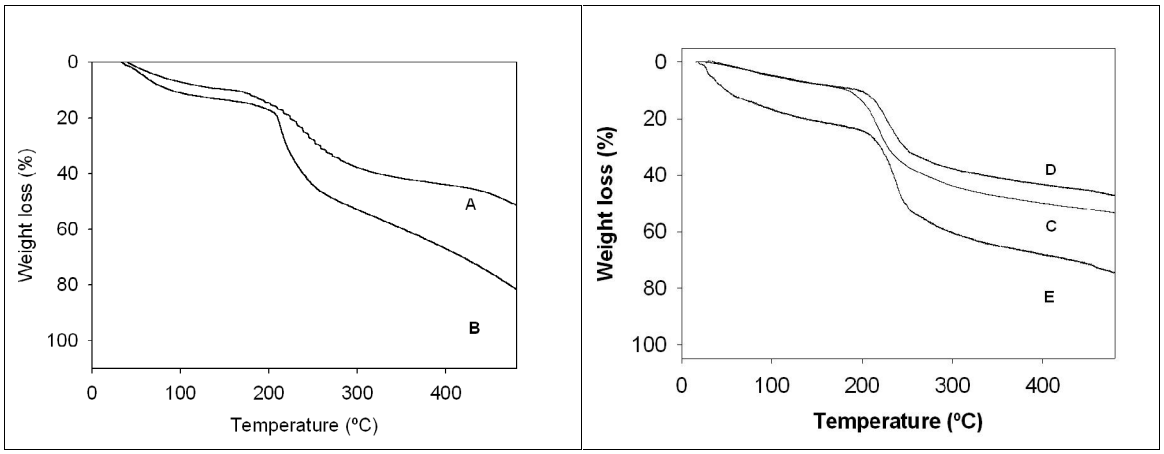

Figure 3. Thermal analysis of destarched jicama pectin (A), water soluble chitosan (B) and polyelectrolyte complexes of water soluble chitosan with jicama pectin. Pectin concentration (g/L) and codes: C: 0.5, D: 1.0, and E: 2.0.

Thermal properties

Thermograms of chitosan, jicama pectin and polyelectrolyte complexes of water soluble chitosan with jicama pectin are showed in Figure 3. Jicama pectin and 20 kDa chitosan degraded around 170 and 200 ºC, respectively. The main decomposition of pectin sample starts above 170 ºC and shows similar weight loss (50%) pattern until 400 ºC. [9] The degradation of polyelectrolyte complexes showed one event around 200 ºC, than can be considered a proof of the complex formation.

CONCLUSIONS

A polyelectrolyte complex was formed as a result of reaction between when pectin from jicama and 20 kDa WSCh. The yield on dry basis was dependent on the ratio of WSCh used and the formation of this polyelectrolyte complex was confirmed by FTIR and TGA characterization. The polyions formed have wide applications in medicine as tailor-made tissue scaffolds or as sponges in food industry.

ACKNOWLEDGMENTS

This work (project number: 2005-12532) was partially supported by the National Council of Science and Technology (CONACYT, Mexico) and The Ministry of Agriculture, Livestock, Rural Development, Fisheries and Food (SAGARPA, Mexico). A.M. Ramos-de-la-Peña was supported by a graduate student scholarship from CONACYT.

REFERENCES

1 Farris S, Schaich K, Lui L, Piergiovanni L, Yam K, Trends in Food Science and Technology, **20**, 316 (2009).

2 De Vasconcelos C L, Bezerril P M, Dos Santos D E S, Dantas T N C, Pereira M R, Fonseca J L C, Biomacromolecules, **7**, 1245 (2006).

3 Yeon J C, Eun J K, Zhe P, Young C Y, Yong C S, Appl. Environ. Microbiol., **70**, 4522 (2004).

4 Contreras-Esquivel J C, Espinoza-Pérez J D, Montañez J C, Charles-Rodríguez A V, Renovato J, Aguilar C N, Rodríguez-Herrera R, Wicker L, ACS Symposium Series, **935**, 215 (2006).

5 Aquino-Bolaños E N, Cantwell M I, Peiser G, Mercardo-Silva E J, Food Sci., **65**, 1238 (2000).

6 Mélo Z L, Bueno C R, Acta Amazónica, **29**, 173 (1999).

7 McClements J, J. Agric. Food. Chem., **48**, 5604 (2000).

8 Seo S B, Kajiuchi T. Macromol. Res., **10**, 103 (2002).

9 Contreras-Esquivel J C, Aguilar C N, Montanez J C, Brandelli A, Espinoza-Perez J, Renard C M G C J, Food Sci., **15**, 57-66 (2010).

Microbial treatment of shrimp waste for recovery of chitin and astaxanthin

Paola Islas-Enríquez,[1] Miquel Gimeno,[2] E. Rodríguez-Huezo,[3] Keiko Shirai[1]*

[1] Universidad Autónoma Metropolitana. Departamento de Biotecnología. Laboratorio de Biopolímeros. México D.F., México.
[2] Universidad Nacional Autónoma de México. Facultad de Química. Departamento de Alimentos y Biotecnología. México D.F., México.
[3] Instituto Tecnológico de Ecatepec. Estado de México, México.
*E mail: smk@xanum.uam.mx

ABSTRACT
Shrimp waste fermentations using lactic acid bacteria were carried out using molasses as sole carbon source. Lactic acid fermentations were initially conducted in batch with several molasses concentrations 20, 30, 40 and 50 (w/w%). The highest acidification of batch reactors was observed using 20 w/w% of molasses with a total titratable acidity of 0.52 mmol/g. This condition was used for fermentation in column reactors with stirring and without stirring, as well as in a rotating drum reactor. The column reactor with stirring and the rotating drum had the lowest pH, as well as the highest acidification and deproteinisation. Astaxanthin was recovered from the wet raw chitin after LAF, with a concentration up to 254 μg/g.

Keywords: chitin, shrimp waste, fermentation, lactic acid bacteria.

INTRODUCTION

The annual world production of shrimp in 2005 was 6,091,869 Tons.[1] However, only 50-60 w/w% of the shrimp is edible and the remainder is discarded. Approximately, 40% of this waste is chitin, which is associated with calcium carbonate, pigments (astaxanthin), proteins and lipids.[2]
The commercial value of chitin or its deacetylated derivative chitosan and astaxanthin have increased due to their applications in several areas.[3-6] Purification of chitin has been reported from crustacean wastes by lactic acid fermentation (LAF) using refined carbon sources (e.g. glucose, lactose, sucrose). However, molasses represents a promising economical alternative due to its high sugar content and low cost. Herein, we aim at reporting further advances on the LAF of shrimp wastes using molasses in column (CR and SCR) and rotating drum (RDR) reactors for recovery of added value products.

MATERIALS AND METHODS

Materials. Cephalothoraxes and exoskeleton of *Litopenaeus vanamei* was minced and frozen. Sugarcane molasses was used as carbon source.[7] *Lactobacillus* spp. B2 was employed as starter (10^8 CFU/mL).
Batch flask fermentations. The molasses were added at concentrations of 20, 30, 40 or 50 (w/w %) with 5 v/w % of inoculum and incubated at 30 °C in flasks. Samples were withdrawn for pH and TTA determinations. Water activity (a_w) was determined at the beginning and at end of each fermentation batch.
Batch reactors. The following stainless steel batch reactors were used with a 20 w/w% of molasses concentration at 30°C: column reactors (CR) and with stirring (SCR), as well as rotating drum reactor (RDR). 2 kg loads of shrimp waste were placed in each reactor. Agitation was performed in RDR and SCR. Samples were taken from the liquid fraction of the three reactors. Another set of samples were taken from the solid fractions at the beginning and end of fermentation.

Recovery of astaxanthin and HPLC determinations. Astaxanthin extraction in acetone was carried out from raw chitin obtained at the end of CR fermentation (120 h). HPLC determinations were carried out by the method reported elsewhere.[6]

Determination of pH, Total Titratable Acidity (TTA) and water activity (a_w)

pH were determined using a potentiometer. TTA was determined by titration with 0.1 N NaOH and expressed as lactic acid (LA). The determination of a_w was carried out in an Aqualab CX-2 (US).[5]

Deproteinisation. Total nitrogen and chitin nitrogen[8] were measured by Elemental Analysis. The protein content was calculated considering the total nitrogen and chitin nitrogen. The percentage of DP was calculated on the basis of the initial amount of protein and that obtained in the reactor after 120 h of fermentation.

Data analyses. Determinations were performed in duplicate. Data analyses were conducted using ANOVA and Tukey multiple comparisons test using NCSS. Kinetic parameters of acidification were estimated by the Gompertz model for each level of molasses.[5]

RESULTS

Batch flask fermentations

As can be observed in Table 1 the highest acidification and fastest pH decrease was achieved using 20% molasses (0.52 mmol/g of LA) ($\alpha < 0.05$). The a_w was significantly different at the beginning and end of fermentation ($\alpha < 0.05$).

Table 1. Kinetic parameters of acidification of the LAF of shrimp waste estimated by the Gompertz model and a_w using different levels of molasses.

Molasses level (w/w)	P_{max} (mmol/g)	k (h^{-1})	V_{max} (mmol/g h)	pH 120 h	TTA (mmol/g) 120 h	a_w 0 h	120 h
20%	**0.5487**	0.02081	**0.00420**	4.765	0.526	0.959[a]	0.946[c]
30%	0.4007	0.02034	0.00300	5.065	0.385	0.953[b]	0.948[c]
40%	0.3925	0.02026	0.00292	5.09	0.376	0.9465[c]	0.937[e]
50%	0.3527	0.02056	0.00266	5.155	0.338	0.943[d]	0.94[e]

$R \geq 0.98$. Different superscript letters in a column are significantly different ($\alpha < 0.05$).

Stainless steel reactors

Figure 1 shows the TTA measured in the liquid fractions of LAFs conducted in SCR, RDR and CR. CR displayed a faster acidification than SCR and RDR, however, the highest TTA was recorded in the RDR (ca. 0.35mmol/g). TTA and pH of the solid fractions at the end of fermentation showed significant differences between reactors (Figure 2). CR displayed the highest acidification, followed by RDR and CR . On the other hand, the DP in CR and RDR were 70 and 60%, respectively, whereas CR presented the lowest ca. 40% (Figure 3).

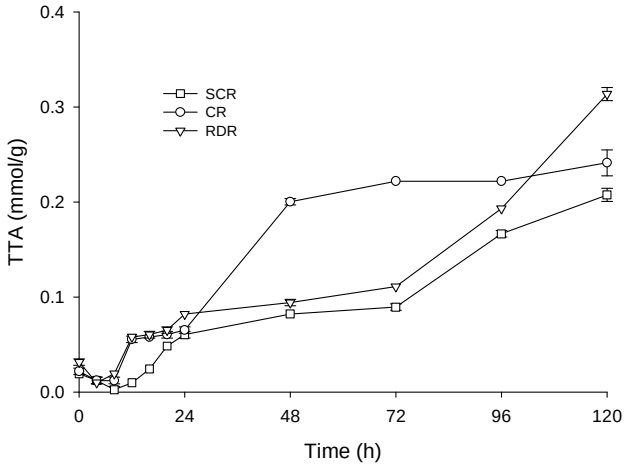

Figure 1. Time course of acidity (TTA) of the liquid fractions from LAF obtained with molasses 20 w/w% in SCR, RDR and CR.

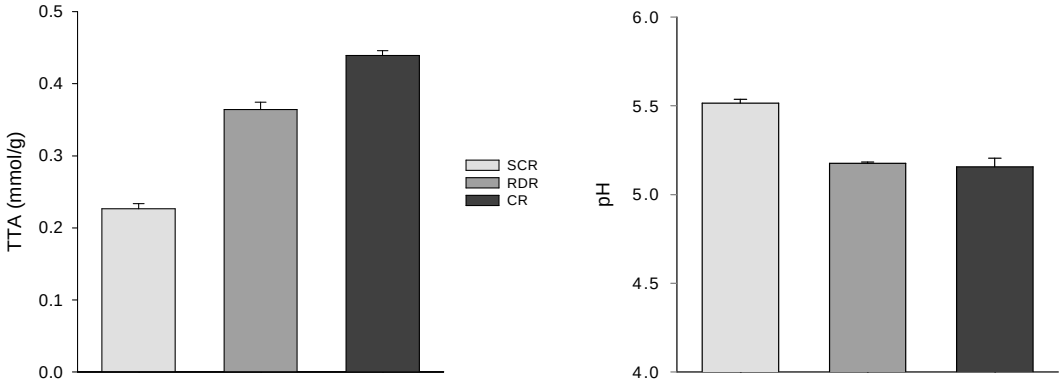

Figure 2. TTA and pH of solid fractions (120 h) determined in LAF with molasses 20 w/w% in SCR, RDR and CR.

Table 2 shows the proximate composition of the shrimp and the molasses used in this work as well as the raw chitin obtained from fermentation in CR.

Table 2. Proximate composition of raw chitin obtained with CR and sugar cane molasses.[7]

Component	% Moisture	% Protein	% Chitin	% Ash	Astaxanthin (µg/g)
Raw Chitin	66.18±0.74	9.21±1.57	56.71±2.71	24.93±0.65	254±17.2
Molasses*	27.15±0.23	4.25±0.17	ND	13.03±0.13	ND

*Content of total sugars 57 w/w%. ND Non determined.

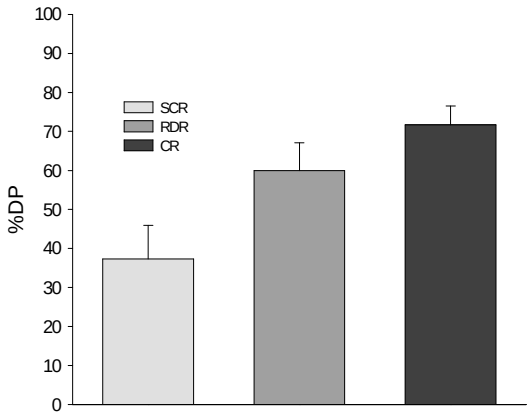

Figure 3. DP of solid fractions of 120 h determined in SCR, RDR and CR LAFs.

DISCUSSION

The experimental data pointed out that V_{max} decreased when level of molasses increased, which was also associated to remarkable a_w decrease (Table 1). The variations in the measured a_w at the beginning and at end of fermentation might be explained by the breakdown of molecules such as proteins into smaller molecules that are added to the system as solutes.[9]

The difference in acidification among stainless steel reactors (Figures 1 and 2) might be due to the agitation, which favors the inclusion of oxygen. This might enhance the growth of other microorganisms that could consume the organic acids produced and compete for the carbon source with the starter, thus affecting their growth. On the other hand, the packing of the fermented shrimp waste in the solid fraction of CR might explain the highest acidification observed which is responsible to retain the acid in the upper phase longer than in RDR. Higher pH than those obtained in previous reports using column reactors acidifications using 10 w/w % of sugar cane. [5,10] This might be explained by the high amount of ash contained in the sugar cane molasses (Table 2), which increases the buffering capacity of the substrate. The astaxanthin recovery was 254 µg/g (Table 2), which is in the range of the amount reported by Pacheco and co-workers[10] in LAF of shrimp wastes with sucrose. The highest DP was obtained also in the CR system (70%).

CONCLUSIONS

This paper presents the alternative of using an economic source of carbon for biotechnological obtaining of chitin from shrimp wastes. It was concluded that the level of addition of this source plays an important role in the production of LA. The stirring was an important factor in maintaining homogeneous conditions inside the reactor; however, the inclusion of oxygen affected the production of LA.

ACKNOWLEDGMENTS

The authors would like to thank CONACyT (No. 105628) for funding and scholarship (PI).

REFERENCES

1. Synowiecki J, Al-Khateeb N. Critical Reviews in Food Science and Nutrition, 43(2):145–171 (2003).
2. Xu Y, Gallert C, Winter J. Appl Microbiol Biotechnol 79: 687–697 (2008).
3. Alonso D, Gimeno M, Olayo R, Vázquez H, Sepúlveda J, Shirai K. Carbohydrate

Polymers 77: 536–543 (2009).
4. Martinez G, Shirai K, Pelayo C, Perez L, Sepulveda J. Food Microbiology 26: 444–449 (2009).
5. Cira L, Huerta S, Hall G, Shirai K. Process Biochemistry 37: 1359–1366 (2002).
6. Gimeno M, Ramírez-Hernández J, Mártinez-Ibarra C, Pacheco N, García-Arrazola R, Bárzana E, Shirai K. J. Agric. Food Chem. 55: 10345–10350 (2007).
7. A.O.A.C. 1990. Methods of analysis (15th ed.). Association of Official Analytical Chemists. Washington, DC.
8. Black M, Schwartz A. Analyst 75: 185–189 (1950).
9. Shirai K, Guerrero I, Huerta S, Saucedo G, Gonzalez R, Castillo A, Hall G. Enzyme Microbial Technology, 28:446–452 (2001).
10. Pacheco N, Garnica M, Ramírez Y, Flores B, Gimeno M, Bárzana E, Shirai K. Bioresour.Technol. 100: 2849–2854 (2009).

Potential of chitosan from *Mucor circinelloides* as alternative natural compound to inhibit *Aspergillus*

Sergio Roberto Cabral de Alcântara[a]; Thayza Christina Montenegro Stamford[a,b,c]*; Alberto Kioharu Nishida[a]; Newton Pereira Stamford[d]; Luciana de Oliveira Franco[d]; Marta Cristina da Silva[c]; Galba Maria Campos-Takaki[c,e]

[a] University Federal of Paraiba, Cidade Universirária, João Pessoa-PB, Brazil CEP: 58059-900
[b] Nucleus of Health Research, Integrated College of Patos-PB, Brazil;
[c] Nucleus of Environmental Science, University Catholic of Pernambuco, Brazil.
[d] University Federal Rural of Pernambuco, Brazil
[e] University Catholic of Pernambuco, Brazil
*E-mail: thayza.stamford@pq.cnpq.br

Abstract
Chitosan has been proven to control numerous pre and postharvest diseases on various horticultural commodities. The aim of this study was to investigate the antifungal activity, in vitro, of chitosan, from *Mucor circinelloides* UCP 050, against pathogens *Aspergillus* species. Chitosan was extracted from *M. circinelloides* biomass by alkali-acid treatment. Chemical characterization was effected by infrared spectroscopy (Deacetilation degree) and viscosity (Molecular weight). The effectiveness of chitosan, at concentrations ranging from 10.0 to 0.025 mg/mL, in inhibiting the growth of five *Aspergillus* species was evaluated. The antifungal activity was assessed by determining the minimum inhibitory and fungicidal concentration using broth dilution method in Sabouraud medium. The chitosan showed the degree of deacetylation and the viscosimetric molecular weight respectively of 85% and 2.72 $\times$ 10^4 g $\times$ mol^{-1}. Chitosan showed a lower minimum inhibitory concentration against *A. fumigates, A. ochraceus* and *A. parasiticus* than *A. flavus* and *A. niger,* which was 2.5 mg/mL and 5.0 mg/mL, respectively, and identical minimum fungicide concentration for all *Aspergillus* assayed (5.0 mg/mL). The results obtained in this study demonstrate the antifungal potential of microbiological chitosan against *Aspergillus* species, food pathogens.

Keywords: chitosan; fungal pathogen; antifungal property; food preservative.

INTRODUCTION

The presence and growth of fungi in food may cause spoilage and result in a reduction in quality and quantity. Some *Aspergillus* species are responsible for many cases of food and feed contamination[1]. Mold fungi growth is commonly controlled using synthetic antimicrobials, however, natural antimicrobials have also demonstrated important antifungal properties[2].

Chitosan is a natural, biodegradable, polycationic aminopolysaccharide, essentially composed of β-1,4 D-glucosamine (GlcNAc) linked to *N*-acetyl-D-glucosamine residues[3,4], and is a common constituent of fungal cell walls[5]. Antifungal activity is one of the most important bioactivities of chitosan, and earlier studies have reported that chitosan can reduce the growth of phytopathogenic fungi, which are harmful to field crops, fruit, and vegetables[6,7].

The aim of this study was to investigate the antifungal activity, in vitro, of chitosan, from *Mucor circinelloides* UCP 050, against five pathogens *Aspergillus* species.

MATERIALS AND METHODS

Microorganism and spore suspension preparation

Aspergillus ochraceus, *Aspergillus fumigates, Aspergillus parasiticus, Aspergillus flavus* and *Aspergillus niger,* for antifungal assay, were isolated from horticultural commodities. Stock cultures were kept on Potato Dextrose Agar (PDA) slants at 4ºC[2].

Chitosan from *Mucor circinelloides* Extraction

The process of extraction involved deproteination with 2% w/v sodium hydroxide solution (30:1 v/w, 90ºC, 2 h), the separation of the alkali-insoluble fraction (AIF) by centrifugation (4000 rpm, 15 min.), the extraction of chitosan from AIF under reflux (10% v/v acetic acid 40:1 v/w, 60ºC, 6 hr), the separation of crude chitin by centrifugation (4000 xg, 15 min.) and the precipitation of chitosan from the extract at pH 9.0, adjusted with a 4 M NaOH solution. Crude chitin and chitosan were washed on a coarse sintered-glass funnel with distilled water and air-dried at 20ºC[5].

Characterization of chitosan

Infrared spectroscopy (Deacetylation degree - DD%). The degree of deacetylation for fungal chitosan was determined using infrared spectroscopy in accordance with Roberts[8], using the absorbance ratio A1655/A3450, and were calculated as per the following equation: A (%) = (A1655/A3450) x 100 / 1.33.

Molecular weight. The molecular weights of fungal chitosan was determined by viscosity, using the procedure described by Santos et al[3]. Using the Mark-Houwink equation, the average viscosimetric molecular weight is expressed in g/mol.

Chitosan preparation

Chitosan obtained from biomass of *M. circinelloides* UCP 050 grown in yam bean medium in accordance with the procedure described by Stamford et al[5]. Chitosan solutions at concentrations ranging from 10.0 to 0.025 mg/mL prepared in acetic acid 1% (v/v), in accordance with Shigemasa; Minami[9], were assayed in pH 5.5, which were adjusted using HCl and NaOH.

Determination of antifungal activity

Minimum inhibitory concentration (MIC) and minimum fungicidal concentration (MFC) of chitosan on the assayed fungi were carried out using the broth dilution method as described by Peng et al[10]. MIC was defined as the lowest chitosan concentration providing no visible growth and the MFC was the lowest chitosan concentration able to cause a 99.9 % kill rate of the initial spore suspension. For positive control, chitosan was replaced with sterile distilled water (control 1) and 1% acetic acid (control 2). The assays were made in triplicate and the results expressed as average values.

RESULTS AND DISCUSSION

Figure 1 shows the IR spectra to determine the degree of deacetylation of chitosan from fungi. Chitosan obtained from *M. circinelloides* present 85% DD. Authors report the deacetylation degree of chitosan from fungi between 80 to 90% DD[5]. Deacetylation degree (%DD) is an important parameter associated with the physical-chemical properties of chitosan, because it is linked directly to chitosan's cationic properties[10].

The average viscosimetric molecular weights (MW) of chitosan from *M. circinelloides* obtained in this study was 2.72×10^4 g/mol. The result is in agreement with the literature which reports molecular weights between 1.0×10^4 to 9.0×10^5 g/mol[3,5,10].

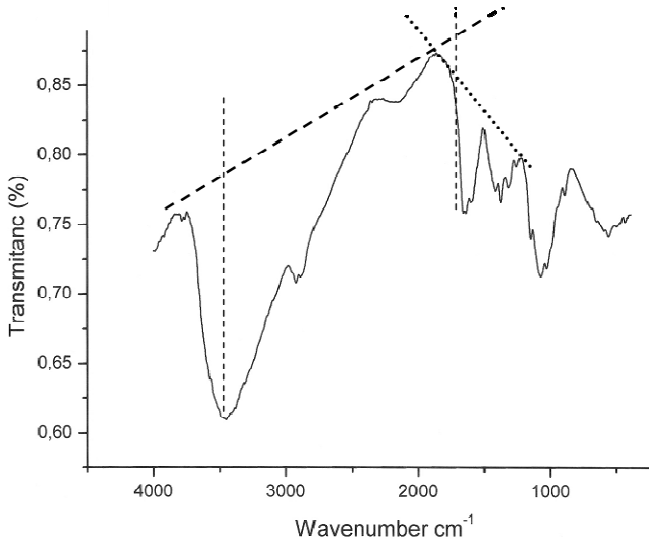

Figure 1. Infrared spectrum of chitosan from *Mucor circinelloides* UCP 050. Degree of acetylation (DD) was determined according to Roberts (1992).

The effectiveness of chitosan from *M. circinelloides* in inhibiting the growth of *Aspergillus* species by determining the minimum inhibitory concentration and minimum fungicidal concentration was shown in Tables 1.

As demonstrated in Table 1, fungal chitosan showed a lower minimum inhibitory concentration against *A. fumigates, A. ochraceus* and *A. parasiticus* than *A. flavus* and *A. niger*, which was 2.5 mg/mL and 5.0 mg/mL, respectively, and identical minimum fungicide concentration for all *Aspergillus* assayed (5.0 mg/mL). These results are in disagreement with those reported by Roller and Covill[11] which reported that *A. flavus* were resistant to chitosan, until concentration of 10 mg/mL.

Table 1. Antimicrobial activity of fungic chitosan solution on acetic acid 1% against *Aspergillus* species.

Fungi sample	Minimum inhibitory concentration (MIC)	Minimum fungicidal concentration (MFC)
A. ochraceus	2.5 mg/mL	5.0 mg/mL
A. niger	5.0 mg/mL	5.0 mg/mL
A. flavus	5.0 mg/mL	5.0 mg/mL
A. parasiticus	2.5 mg/mL	5.0 mg/mL
A. fumigatus	2.5 mg/mL	5.0 mg/mL

The antimicrobial activity of chitosan is well documented against a number of food spoilage and pathogenic fungus with MIC varying from 0.01% to 1% and the MFC varying from 5% to 14% [6,11]. However, it is important to emphasize that comparing antifungal values from different chitosan studies is difficult, because of possible differences in the chemical and structural properties of the chitosan used in these studies, the experimental circumstances, the chitosan solvent, the definition of MIC genera, species, strains and even the same strains under different environmental conditions[4,10].

Several authors have proposed that the antimicrobial action of chitosan against filamentous fungi could be explained by a disturbance of membrane function. An additional explanation includes marked morphological changes, structural alterations and molecular disorganization

of the fungal cells induced by chitosan[6,7].

CONCLUSIONS

The results obtained in this study demonstrate the antifungal potential of microbial chitosan against *Aspergillus* species. More research is required to provide a focus for the effective use of chitosan as a novel food preservative.

ACKNOWLEDGEMENTS

The authors are grateful to Conselho Nacional de Desenvolvimento Científico e Tecnológico (CNPq) for financial support and Universidade Católica de Pernambuco (UNICAP).

REFERENCES

1. Omidbeygi M, Barzegar M, Hamidi Z, Naghdibadi H. *Food Control* **18**:1518 (2007).
2. Lopez-Malo A, Alzamora SM, Palou E. *International Journal of Food Microbiology* **99:** 119 (2005).
3. Santos JE, Soares JP, Dockal ER, Campana Filho SP, Cavalheiro ETG. *Polímero: Ciência e Tecnologia*, **13**(4):242 (2003).
4. ikhonov VE, Stepnova EA, Babak VG, Yamskov IA, Palma-Guerrero J, Jansson HB, Lopez-Llorca LV, Salinas J, Gerasimenko DV, Avdienko ID, Varlamov VP. *Carbohydrate Polymers* **64**: 66 (2006).
5. Stamford TCM, Stamford TLM, Stamford NP, Neto BB, Campos-Takaki GM. *Electronic Journal of Biotechnology* **10**(1) (2007)
6. Guo Z, Chen R, Xing R, Liu S, Yu H, Wang P, Li C, Li P. *Carbohydrate Research* **341**: 351 (2006).
7. Bautista-Baños S, Hernandez-Lauzardo NA, Velázquez-Delo-Valle G, Hernandez-Lopez M, Barka EA, Bosquez-Molina E, Wilson CL. *Crop Protection* **25**:108 (2006).
8. Roberts GAF. *Chitin Chemistry*. London: The Macmillan Press. (1992)
9. Shigemasa Y, Minami S. *Biotechnology & Genetic Engineering Reviews* **17**: 383 (1996).
10. Peng G, Wan B, Liu W, Xu, X. *Carbohydrate Research* **340**:1846 (2005).
11. Roller S, Covill N. *International Journal of Food Microbiolog*, **47**: 67 (1999).

Characterization by FT-IR of chitosan oligomers produced by enzymatic sequential treatments

Eduardo M. Del Aguila[1*], Laidson P. Gomes[1], Carlos I.R. de Oliveira[2], Márcia C. Silva[2], Cristina T. Andrade[2], Joab T. Silva[1], Vânia M.F. Paschoalin[1]

[1] Instituto de Química. Univ. Federal do Rio de Janeiro. UFRJ. Brazil
[2] Instituto de Macromoléculas Heloisa Mano. Univ. Federal do Rio de Janeiro. Brazil
*E-mail: emda@iq.ufrj.br

Abstract
Chitosan has a unique chemical structure with high charge density, reactive hydroxyl and amino groups, and extensive hydrogen bonding. The broad use of chitosan is directly related to the molecular masses and degree of deacetylation of the polymers, which depend on the conditions of chitin hydrolysis. The aim was to characterize the chito-oligosaccharides obtained by sequential enzymatic treatments. Chito-oligosaccharides were prepared using purified chitinase from *Vitis vinifera* and recombinant chitin deacetylase from *Saccharomyces cerevisiae*. Chito-oligosaccharides obtained from crystalline shrimp chitin showed an acetylation degree of 30%, whereas those obtained from previously deacetylated chitosans were completely deacetylated when analyzed by FT-IR.

Keywords: Chitin, chitinase, chitosans, chitin deacetylase, deacetylation, FT-IR spectrum.

INTRODUCTION

Chitosan is a biopolymer with unique properties favorable for a wide variety of industrial applications, and is usually obtained from deacetylation of chitin.[1] Presently, chitosan is produced by the thermochemical alkaline deacetylation of chitin. However, the process is environmentally unsafe and not easily controlled, leading to a broad and heterogeneous range of products.[2] To develop an alternative, controlled, nondegradative, and well-defined process for chitosan production, studies of fungal chitin deacetylase have been initiated.[3]

The applications of chitosan and its derivatives depend on their chemical structures. Several studies have shown that the molecular weight and degree of deacetylation (DD) of the polysaccharide affect its properties, with many special functions appearing when its molecular weight and DD are reduced to some extent.[4] The development of viable processes for the controlled hydrolysis of chitosan is attracting interest because of the emergence of new biomedical and food applications for chito-oligosaccharides. Enzymatic processes are preferable to chemical processes, since the course of hydrolysis and product distribution are easier to control.

We report the characterization of chito-oligosaccharides prepared from crystalline shrimp chitin, and from chitosan prepared by the alkaline method, using a sequential enzymatic treatment consisting of chitinase hydrolysis followed by chitin deacetylase treatment. Both enzymes were used in their purified form; chitinase was prepared from *Vitis vinifera* L. cv. Red Globe, and chitin deacetylase from *Saccharomyces cerevisiae*.

MATERIAL AND METHODS

Chitinase purification.

Frozen Red Globe grapes (200 g) free from seeds were mixed with 800 ml of 50 mM sodium buffer, pH 5.0, and homogenized in a household blender for 2 min at maximum speed. Peels and other unwanted materials were separated by sieving. The extract was centrifuged twice at 1700 g for 10 min at 4 °C, and the resulting supernatant containing the crude enzyme extract

was stored at -20 °C. Proteins in the crude enzyme extract from grapes were precipitated with 80% $(NH_4)_2SO_4$ (final concentration expressed as percent of saturation), according to Coelho, 1993.[5] After overnight incubation at 4 °C, insoluble proteins were collected by centrifugation at 1700 g for 20 min at 4°C. The pellet was resuspended in 8 ml of 50 mM sodium acetate buffer, pH 5.0, and excess salt was removed by dialysis (membrane molecular weight cut-off 10 kDa) against distilled water for 24 h. The dialyzed sample was filtered through a 0.22 µm Millex GS membrane (Millipore). Protein concentration was determined using the QuBit fluorometer and the Quant-iT Protein Assay Kit (Invitrogen).

Sequential Enzymatic Treatment

Chitinase activity

Chitinase activity was assayed using crystalline shrimp chitin or chitosan prepared by chemical hydrolysis with degree acetylation (DA) of 60.2% and Mw 759.217 as a substrate. The reaction was performed adding 0.6 U of purified chitinase, 1 mg of each substrate, and 50 mM sodium acetate buffer at pH 3.0 or 6.0 at 42 °C for 50 min. The reaction was stopped with 200 µL of 4M HCl, the tubes were kept in ice for 20 min, centrifuged (9000 g for 5 min), and the pellet was submitted to the deacetylation treatment.

Chitin deacetylase treatment

Chitin deacetylase (CD) treatment was carried out in 1 mg of the previously centrifuged pellet, 5 µg of yeast recombinant chitin deacetylase,[6] 0.15 mg of BSA and 25 mM Tris.HCl buffer, pH 8.0, in a final volume of 150 µL. Reactions were run for 1 h at 50°C and stopped by heating at 100 °C for 10 min in sealed tubes.

FTIR spectroscopy.

Fourier Transform Infrared (FTIR) spectra were recorded in a Perkin-Elmer spectrometer, model 1720 (Salem, MA, USA), with an accumulation of 20 scans, and a resolution of 2 cm^{-1}. KBr, permanently maintained in an oven at 50 ºC, was used to prepare transparent disks. The sample of crystalline shrimp chitin and the resultant products from the enzymatic treatments were thoroughly dried and carefully weighed (2 mg) before grinding with KBr.

RESULTS AND DISCUSSION

Chitinases (CHases) from *Vitis vinifera* L. cv. Red Globe were purified by ammonium sulfate precipitation. Purified recombinant chitin deacetylase from *S. cerevisiae* in *Pichia pastoris* was used for deacetylation reactions.[7] Chitinase showed activity against crystalline shrimp chitin and chitosan obtained by chemical hydrolysis at pH 3.0 or 6.0 at 42 °C for 50 minutes of incubation. Chito-oligosaccharides obtained by chitinase hydrolysis were subsequently used as substrates for deacetylation treatment with the purified chitin deacetylase. The chito-oligosaccharides produced were better substrates for chitin deacetylase than intact crystalline chitin. The fragmentation of the chitin polymers probably breaks up the crystalline structure of chitin and makes the acetamide groups more accessible to deacetylation.

Fourier Transform Infrared (FT-IR) was used to estimate the degree of acetylation (DA) from the transmittance ratio at 1320 cm^{-1} and 1420 cm^{-1} (characteristic and reference bands, respectively) (Table 1) and the regression curve (A1320/A1420 = 0.3822 + 0.03133 x DA).[8] The amide II band at 1550 cm^{-1} (attributed to the C-N bond stretching and to C-N-H bonds bending) is characteristic of secondary amides. Crystalline shrimp chitin treated with chitinase at pH 3.0 or pH 6.0 prior to deacetylation with chitin deacetylase (CD) produced chito-oligosaccharides with DA of 29.3 and 32.5%, respectively (Table 1 and Figure 1). Using chitosan obtained by alkaline hydrolysis with DA of 60.2% and Mw 759.217 as the substrate, the enzymatic reaction produced completely deacetylated chitosans (Table 1 and Figure 2). The sequential enzymatic treatment using chitinase and chitin deacetylase is able to produce chitosans with DA of 30% from crystalline shrimp chitin, and completely deacetylated chito-oligosaccharides from chemically produced chitosans with DA of 60.2%.

Table 1. FT-IR parameters (transmittance at 1320 cm^{-1} and 1420 cm^{-1}) and the resultant DA obtained with chitin and chitosan samples

Sample	A1320	A1420	A1320/A1420	DA
Crystalline shrimp chitin (1a)*	0.124	0.0353	3.52	100.0%
Chitin + CHase (pH 3.0) +CD (1b)	0.017	0.013	1.30	29.3%
Chitin + CHase (pH 6.0)+CD (1c)	0.021	0.015	1.40	32.5%
Chitosan (2c)	0.023	0.046	0.50	3.8%
Chitosan (2b)	0.123	0.054	2.27	60.2%
Chitosan + CHase (pH 6.0) + CD (2a)	0.012	0.038	0.32	≅ 0.0%

The numbers in parentheses correspond to the FT-IR curves in Figures 1 and 2. One milligram of crystalline shrimp chitin and chitosan produced by chemical hydrolysis was submitted to deacetylation by purified chitin deacetylase (CD), with or without previous treatment with purified chitinase (CHase).

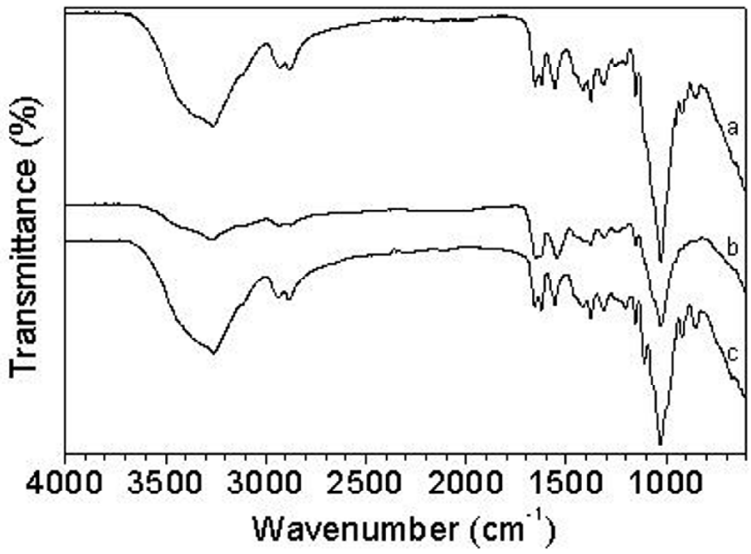

Fig. 1. FT-IR spectra of crystalline shrimp chitin and chitosan products before and after the sequential enzymatic treatment. (**a**) pure chitin, (**b**) chitosan treated with CHase, pH 3.0 and CD; (**c**) chitosan treated with CHase pH 6.0 and CD.

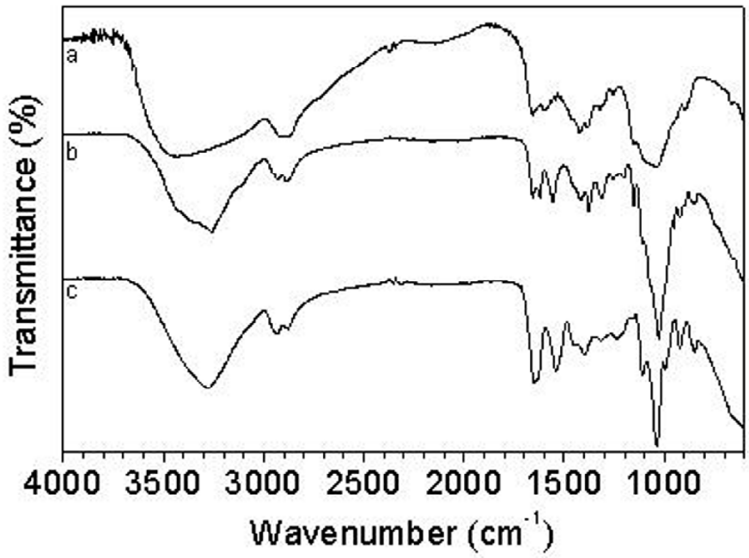

Fig. 2. FT-IR spectra of chitosans 60.2%. (a) chitosan treated with CHase pH 6.0 and CD; (b) chemically produced chitosan with DA of 60.2%,(c) control chitosan with DA of 3.8%.

CONCLUSIONS

The treatment with two purified enzymes added sequentially under mild conditions increased the degree of acetylation in different substrates leading to a product with more homogeneous characteristics. Nowadays, the deacetylation of chitin to chitosan is usually achieved using strong alkali at high temperatures for extended periods of time, an environmentally unsuitable and difficult-to-control process that frequently leads to a broad and heterogeneous range of products. By using the double enzymatic treatments, chitosans with 30% DA were obtained from crystalline shrimp chitin. If previously deacetylated chitosans were used as substrates for the enzymatic treatment, the DA was increased by approximately 40%.

ACKNOWLEDGEMENTS

FAPERJ, CNPq and CAPES for financial support.

REFERENCES

1 Shin WS, Kil JC and Park GM. *J. Microbiol. Biotechnol*. **16**: 1984 (2006).
2 Chang KL, Tsai G, Lee J and Fu WR. *Carbohydr. Res*. **303**: 327(1997).
3 Nahar P, Ghormade V and Deshpande V. *J. Invertebr. Pathol*. **85**: 80 (2004).
4 Illanes A, Ruiz A, Zúñiga ME, Aguirre C, O'Reilly S, and Curotto E. *Bioprocess and Biosystems Engineering*, **5**, 257 (1990).
5 Coelho MAZ (1993). *Dissertação de Mestrado*. Universidade Federal do Rio de Janeiro. Brasil.
6 Del Aguila EM. Doctoral Thesis (2006).
7 Martinou A, Koutsioulis D. and Bouriotis V. *Enzyme and Microbial Tech* **32** 757 (2003).
8 Brugnerotto J, Lizardi J, Goycoolea FM, Arguelles-Monal W, Desbrieres J and Rinaudo M. *Polymer* **42**, 3569 (2001).

Physico-chemical characterization of chitosan from *Absidia corymbifera*

Marta C. F. da Silva[1*], Thayza C. M. Stamford[1,2,3], Lucia R. R. Berger[4], Thatiana Montenegro Stamford[5], Sergio R.C. de Alcântara[2], Galba Campos-Takaki[1,5]

[1] Nucleus of Environmental Science, Catholic University of Pernambuco, Brazil
[2] University Federal of Paraiba, Cidade Universitaria, João Pessoa, PB, Brazil
[3] Nucleus of Health Research, Integrated College of Patos-PB, Belo Horizonte, Patos-PB, Brazil
[4] University Federal Rural of Pernambuco, Rua Dom Manuel de Medeiros, Recife, PE, Brazil
[5] University Federal of Pernambuco, PE, Brazil.
*E-mail: martacfs@yahoo.com.br

Abstract
Absidia corymbifera (UCP 134) growth in Corn Steep 6% medium. Physical and chemistry properties of chitosan. were analyzed. The polysaccharide was extracted from fungi biomass by alkali-acid treatment and characterized by infrared spectroscopy (Degree Deacetilation), viscosity, thermal analysis (DSC) and X-ray Diffractometry. Chitosan from *A. corymbifera* showed degree of deacetilation and viscosimetric, molecular weight up to 87% DD and 3.25 x 10^4 g/mol, respectively. In X-ray diffraction chitosan showed a Strong Bragg refractions at an angle 20.0- 2θ (d = 4.5341 Å). From the DSC curve, two peaks are observed. The first registered thermal event was a wide endothermic peak between 26 and 182ºC. The second thermal event registered, related to the polymer decomposition, was an endothermic peak. These results suggest the application of chitosan from *A. corymbifera* in different biotechnological fields.

Keywords: biopolymers; crystallographic properties; deacetylation; thermal analysis

INTRODUCTION

Chitosan is a polysaccharide found in a wide range of natural sources, such as crustaceans, insects, molluscs, coelenterates and is a common constituent of fungal cell walls fungal cell walls, particularly the class of Zygomycetes (3, 17, 18). It is produced by the chemical or spontaneous deacetylation of chitin. This is achieved by careful manipulation of the growth parameters such as pH and composition during the fermentation process. These manipulations result in chitosan of a varying molecular weight and degree of deacetylation, which influence various properties, the application and the biological response of the polymer (19).
This paper sets out to investigate chitosan production using Mucoralen fungi *Absidia corymbifera* (UCP 0134), grown by submerse fermentation in economic culture medium, Corn Steep, as substrate, and to describe the physical-chemical properties of chitosan.

MATERIALS AND METHODS

Absidia corymbifera UCP 0134 (Culture Collection of Catholic University of Pernambuco, Recife, Brazil) isolated from mangrove sediment from the Rio Formoso, PE, Brazil. The strain was maintained at 4°C on Potato Dextrose Agar (PDA) slants.
A. corymbifera was grown, for chitin and chitosan production, in Corn Steep medium a 6%. The spores were incubated at 28ºC during 96 hours. The mycelia were harvested, washed and were submitted to lyophylization process.

The process of extraction involved an acid-alkali treatment (20). The degree of deacetylation for microbial chitin and chitosan were determined by means of infrared spectroscopy with a Bruker 66 Spectrometer, using a 100mg KBr disk for reference in accordance with (2, 5, 6, 7). The molecular weights of chitin and chitosan were determined by viscosity, using the procedure described by Silva et al. (17, 18).
Differential Scanning Calorimetry (DSC) was carried out using the thermal analysis instruments. An accurately weighed (10mg) chitosan sample was placed in an aluminum cup and sealed. The X-ray diffraction patterns were determined using a wide-angle X-ray SIEMENS D5000 diffractometer and Ka, Cu radiation, with $\lambda = 1.5406$ Aº. The voltage was 40kV and the intensity 40mA. The 2θ angle was scanned between 3° and 80°, and the count time was 1sec at each angle (0.02°) (4).
The data were analyzed for significance using the STATISTICA program. All experiments were carried out in triplicate and the results are expressed as mean ± S.D.

RESULTS AND DISCUSSION
Deacetylation degree (%DD) is an important parameter associated with the physical-chemical properties of chitosan, because it is linked directly to the chitosan cationic properties (12). In the present study chitosan obtained from *A. corymbifera* grown on corn steep 6% medium presents 87% DD. That result is in accordance with (8, 12). The author reported the deacetylation degree of chitosan from fungi occurred between 80 to 90% DD (Fig. 1).

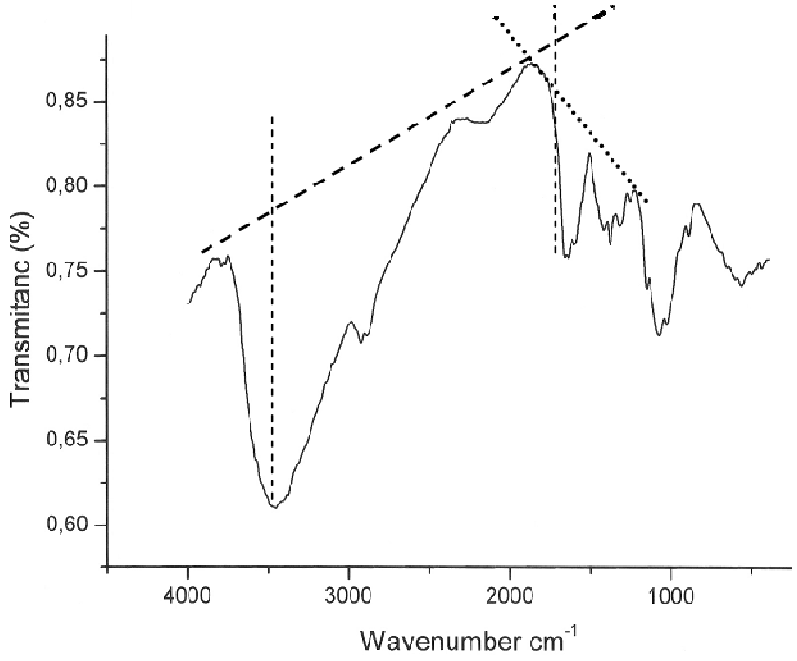

Figure 1. Infrared of chitosan from *A. corymbifera*

The average viscosimetric molecular weight (M_V) of chitosan from *A. corymbifera* obtained in this study is 3.25×10^4 g/mol. The result is in agreement with the literature, which reports molar weights ranging between $1,0 \times 10^4$ to $9,0 \times 10^5$ g/mol.. Chitosan with a low molecular weight was reported to reduce the tensile strength and elongation of the chitosan membrane but to increase its permeability (9, 12).
X-ray diffraction is commonly used to determine the polymorphic forms of a compound having different crystalline structures for which distinct powered X-ray diffraction patterns

are obtained. These patterns are indicative of different spacing of the crystal planes, which provide strong evidence for polymorphic differences and reported that chitosan crystallinity is related to the deacetylation degree function (Fig. 2) (10, 11, 13, 14).

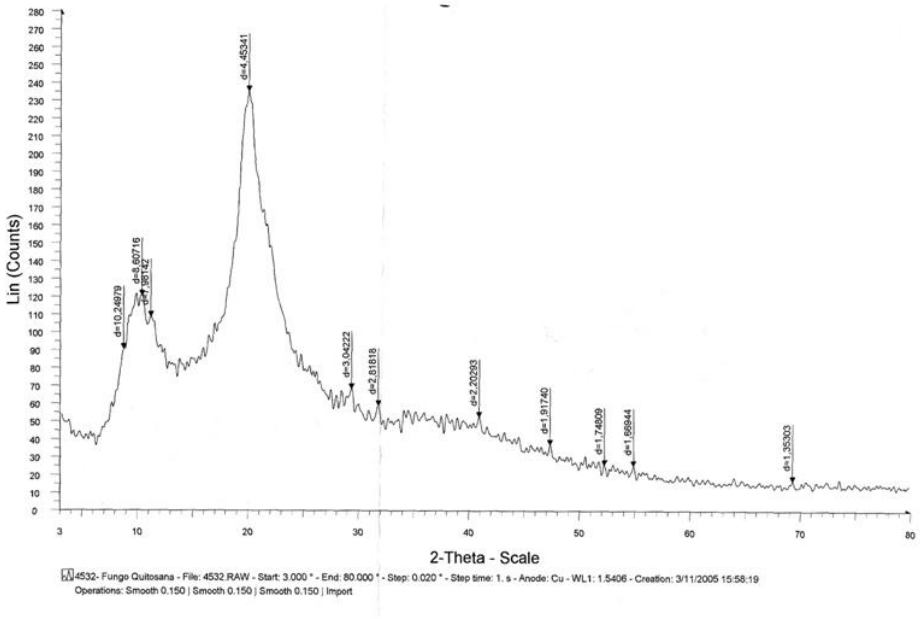

Figure 2. X-ray diffraction of chitosan from *A. corymbifera*

Figure 3 shows the DSC curve of microbiological chitosan under N_2 atmosphere between 25 - 400ºC. The first registered thermal event was a wide endothermic peak between 26 and 160ºC. According to (14, 15, 16, 21), the endothermic peak, related to the evaporation of water, is expected to reflect physical and molecular changes during *N*-deacetylation and carboxymethylation.

CONCLUSION

These results suggest the application of chitosan from *Absidia corymbifera* in different biotechnological fields.

ACKNOWLEDGEMENTS

The authors are grateful for financial support obtained from CNPq, CAPES, FINEP, and FACEPE.

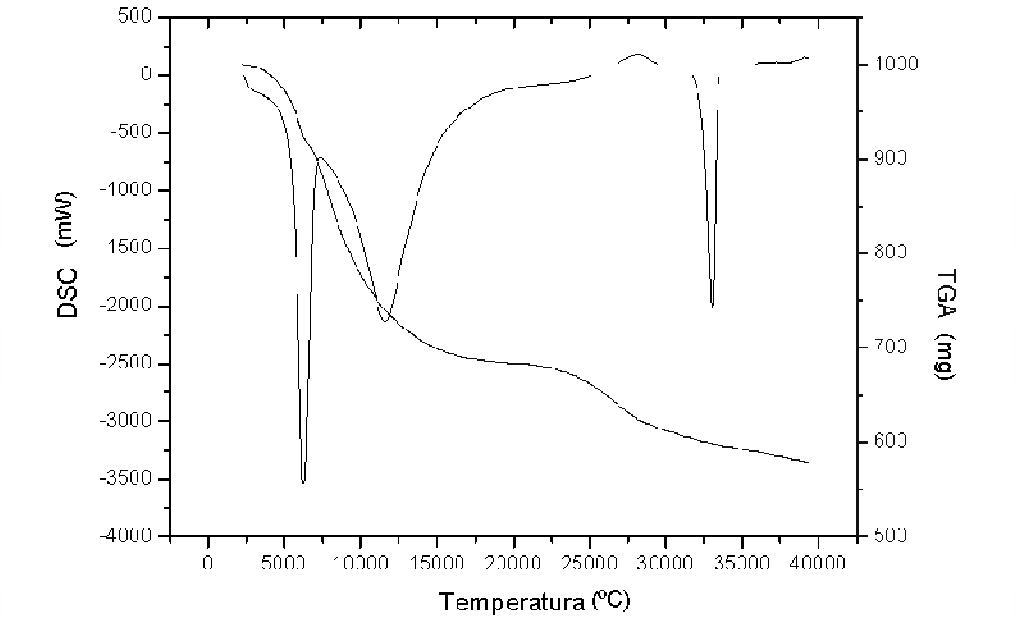

Figure 3. DSC and TGA curve of chitosan from *A. corymbifera*

REFERENCES

1. Amorim RVS, Ledingham WM, Fukushima EK and Takaki GMC. *Journal of Industrial Microbiology & Biotechnology* **31**: 19 (2005).
2. Amorim RVS, Pedrosa RP, Kazutaka F, Martinez CR, Ledingham WM. and Takaki GMC. *Food Technology Biotechnology* **44**: 519 (2006).
3. Campos-Takaki GM. *Dutta, P.K. editor. India: International Publication.* (2005).
4. Chatterjee S, Adhya M, Guah AK and Chatterjee BP. *Process Biochemistry* **40**: 395 (2005).
5. Francis SJK and Matthew HWT. *Biomaterials* **21**: 2589 (2000).
6. Franco LO, Maia RCG, Porto ALF, Messias AS, Fukushima K and Takaki GMC *Brazilian Journal of Microbiology* **35**: 243 (2004).
7. Franco LO, Stamford TCM, Stamford NP and and Takaki GMC *Revista Analytica* **14**: 40 (2005).
8. Inácio RGS, Freitas Silva MC, Okada K and Takaki GMC. *Asian Chitin Journal* **5**: 11 (2009).
9. Kittur FS, Prashanth KVH, Sankar KV and Tharanathan RN. *Carbohydrate Polymer* **49**: 185 (2002).
10. Liu H, Du Y, Yang J and Zhu H. *Carbohydrate Polymers* **55**: 291 (2004).
11. Nadarajah K, Kader J, Mohd M. and Paul DC. *Journal of Biological Sciences* **4** (3): 263 (2001).
12. Pochanavanich P and Suntornsuk W. *Letters in Applied Microbiology,* **35:** 17 (2002).
13. Qin CQ, Xiao Q, Li HR, Fang M, LiuY, Chen, X and Li Q. *International Journal of Biological Macromolecules*, **34:** 121 (2004).
14. Rinaldo M. *Progress in Polymer Science,* **31:** 603 (2006).
15. Santos JE, Soares JP, Dockal ER, Campana Filho, SP and Cavalheiro ETG. *Polímero: Ciência e Tecnologia*, **13(**4): 242 (2003).

16. Silva AM, Santos ER, Silva NSRL, Freitas Silva, MC, Albuquerque CD and Takaki GMC. *Asian Chitin Journal* **5**:93 (2009).
17. Silva MCF, Barros Neto B, Stamford TCM, and Takaki GMC *Asian Chitin Journal*, **3:** 15 (2007).
18. Silva MCF, Stamford TCM, Franco LO and Takaki GMC *Asian Chitin Journal*, **2**: 29. (2006).
19. Stamford TCM, Stamford TLM, Stamford NP, Neto BB. and Takaki GMC *Elect. J. Biotechn*. at: < http://www.ejbiotechnology.info/content/vol10/issue1/full/1/>. (2007).
20. Synowiecki J and Al-Khatteb NAA. *Critical Reviews in Food Science and Nutrition*, 43(2): 144. (2003).
21. Synowiecki J, Al-Khatteb NAAQ. *Food Chemistry*, **60**(4): 605 (1997).

Effects of starch gelatinization and oxidation on the rheological behavior of chitosan/starch blends

Marilia M. Horn, Virginia C. A. Martins, Ana M. G. Plepis*

Instituto de Química de São Carlos, Universidade de São Paulo – USP – Brasil
*E-mail: amplepis@iqsc.usp.br

Abstract
This paper reports on the effects of starch gelatinization and oxidation on the rheological behavior of chitosan/starch blends. The modifications in the starch structure cause changes in G´ and G´´ modulus as a function of frequency. For chitosan/starch, G´´ is higher than G´, showing a viscous behavior. However, for chitosan/gelatinized starch and chitosan/oxidized starch an increase in the angular frequency promotes a modulus crossover at $\omega = 0.02$ rad s^{-1} and 0.04 rad s^{-1}, respectively. The viscosity curves as a function of shear rate show that both modifications cause an increase in viscosity and all blends show a non-Newtonian behavior.

Keywords: Chitosan, starch, rheology, oxidation.

INTRODUCTION

Starch is a biodegradable polymer with excellent biocompatibility and non-toxicity and has been used due to properties, such as film-forming ability suitable for food industry[1] and biomedical applications[2]. Chitosan is obtained from N-deacetylation of chitin and both polysaccharides are copolymers of β (1→4) linked N-acetyl-D-glucosamine and D-glucosamine units[3]. Chitosan shows excellent biological properties, such as biocompatibility, biodegradability and lack of toxicity, being favorable to a large variety of industrial and biomedical applications[4].

Starch, which is a basic food product, can also be widely used in adhesives, packaging and pharmaceutical industry when functionally modified. In order to withstand modern processing and storage conditions as well as to provide special functionality to the end product, native starch can be chemically modified[5]. When starch powders are mixed with water and heated at or above the gelatinization temperature, the granules absorb large quantities of water and form a viscous paste[6]. Starch dialdehyde (DAS), which has considerable further industrial potential[5], is a polymeric aldehyde obtained by the reaction of native starch with periodic acid[7]. Dialdehyde starch (Figure 1) not only is biocompatible and biodegradable as starch, but also has more chemical activity, as it can react with amine groups of chitosan. The blends resulting of chitosan/starch are widely used in medicine field[8-10].

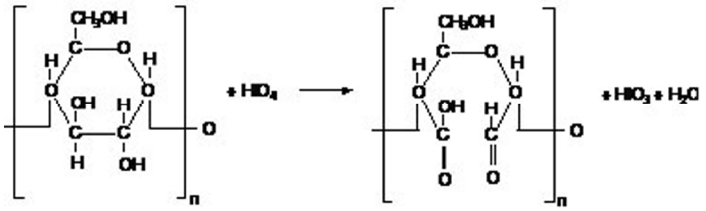

Figure 1. Dialdehyde starch oxidation.

The rheological behavior of chitosan/starch blends can be changed by a chemical modification in the starch structure. In this study two experiments were performed to analyze these modifications: i) the effect of starch gelatinization, which is characterized by the disorganization of crystalline granule arrangement; ii) oxidation with the formation of dialdehyde starch.

MATERIALS AND METHODS

Materials

Chitosan (16% degree of acetylation) was obtained in our laboratory as previously described[11] based on Kurita et al. (1993)[12] method. A 1% chitosan solution was prepared by dissolution in 1% acetic acid (HAc).

Starch powder (Sigma-Aldrich – 73% amylopectin/23% amylose) and 50 mL of deionized water were mixed with mechanical stirring and gelatinized at 90ºC for 30 min, and then cooled at room temperature, forming a homogeneous solution[13]. An aqueous solution of 2% (w/w) of corn starch was used in the blends preparation.

Starch (1 g in 30 mL water) was oxidized with a 5 wt% periodic acid (H_5IO_6) solution for 24 h at room temperature under stirring. The resulting products were dialyzed against distilled water for 72 h to remove the low molecular weight products[7], and then lyophilized. Structural analysis of oxidized starch was carried out with an FTIR spectrophotometer and the FTIR spectrum shows an additional band at 1735 cm^{-1}, confirming that dialdehyde starch is prepared successfully[7].

Blends preparation

Chitosan/starch blends were prepared by adding chitosan (1%) to starch (2%) in the 1:2 ratio under stirring for 30 min at 25ºC. The blends were denominated as chitosan/starch (CS), chitosan/gelatinized starch (CSGE) and chitosan/oxidized starch (CSOX). At the end of the preparation, the blends were immediately transferred to the rheometer plate for the measurements of rheological properties.

Rheological characterization

The rheological properties of the blends solution were investigated using a stress-controlled Rheometer (AR-1000N TA Instruments), fitted with a stainless steel cone/plate geometry (30' angle, 60 mm cone diameter) with the gap 15 μm. The viscoelastic region was measured by stress sweep between 0.01 and 100 Pa with constant frequency (1.0 Hz) and temperature (25 ºC) to obtain the modulus of storage (G') and loss (G'') as a function of deformation. Frequency sweeps were performed from 0.1 to 200 rad s^{-1} at 25 ºC and a constant strain of 10%. Dynamic temperature sweep tests were conducted after equilibration at the initial temperature and heated from 25 to 75 ºC at a rate of 5 ºC min^{-1} with constant frequency (1.0 Hz) and strain (10%).

RESULTS AND DISCUSSION

Preliminary amplitude sweeps (strain sweeps) were carried out for all the samples. A 10% strain, which was within the linear viscoelastic region, was used in the subsequent experiments for all the blends. The angular frequency (ω) dependence of the viscoelastic properties of blends as a function of G' and G'' is showed in Figure 2. An increase in ω causes a significant increase in G' and G'' modulus. For CS blend, G'' was higher than G', indicating it is predominantly non-elastic and its rheological behavior is typical of a "weak-gel". For CSGE and CSOX blends a crossover occurs at ω = 0.02 rad s^{-1} and 0.04 rad s^{-1}, respectively, suggesting the sol-gel process.

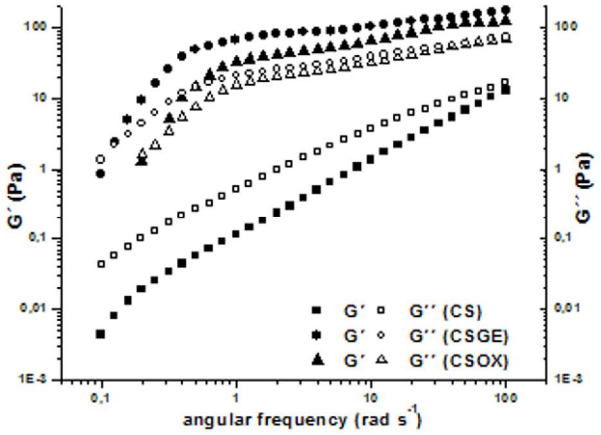

Figure 2: Modulus G' and G'' as function ω for corn starch/chitosan blends at 25°C.

Figure 3 shows complex viscosity (η*) data dependence of strain (%). The variation of η* according to the starch chemical modification can be explained by the fact that for CSGE and CSOX the interaction between chitosan and starch is stronger due the increase in interconnected network extension. In all the cases, η∗ decreased with increasing strain, indicating a shear-thinning behavior.

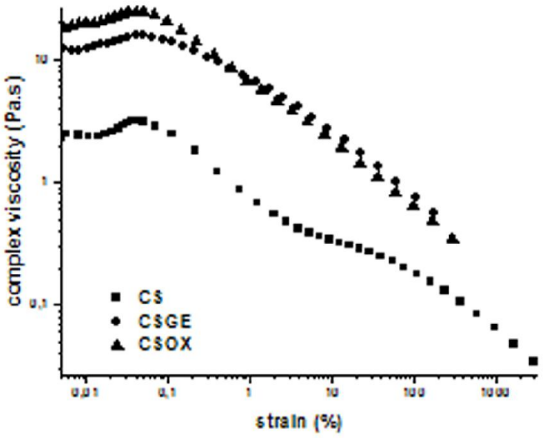

Figure 3. Strain (%) as function η* for corn starch/chitosan blends at 25°C.

Figure 4 show the temperature dependence of the G' and G'' for all blends. For CS blend, the curve show that with an increase of temperature, occurs the crossover of the modulus (66.7°C) and G' becomes higher than G'' indicating that an elastic gel network has been formed. For CSGE and CSOX blends the sol-gel transformation does not occurs with an increase of temperature.

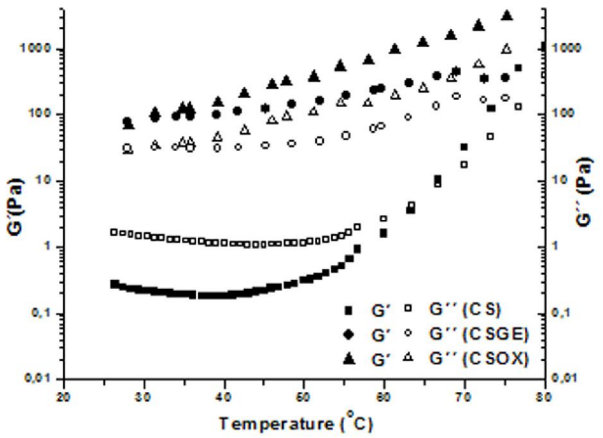

Figure 4: Modulus G' and G'' as function temperature for corn starch/chitosan blends.

The effect of temperature on apparent viscosity at a specified shear rate can be describes by the Arrhenius relationship (Equation 1):

$$\eta = A\, e^{Ea/RT} \quad (1)$$

where Ea is the activation energy for viscous flow and A is a constant. The Ea values for the viscous behavior of corn starch/chitosan blends were studied by the slope of ln η x 1/T curve (Figure 5).

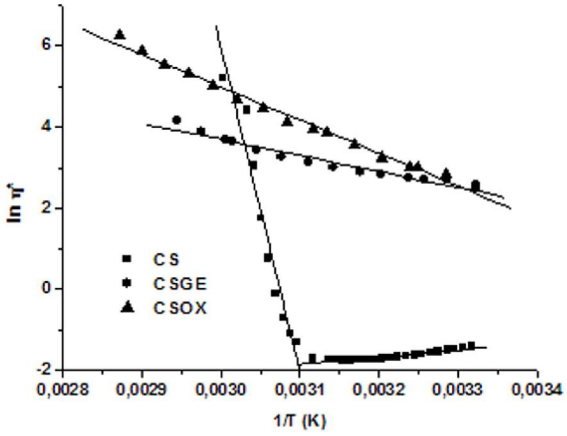

Figure 5. Viscosity dependence as temperature for corn starch/chitosan blends.

In the range between 25 and 75°C, for CSGE and CSOX blends, the Ea values are -0.47 and -0.97 KJ mol^{-1}, respectively, showing that for CSGE the Ea value is twice that for CSOX. For CS blend the curve show a quite different behavior, with two distinct inclinations and with calculated Ea values of: -9.63 KJ mol^{-1} (25-50°C) and 0.20 KJ mol^{-1} (50-75°C).

CONCLUSIONS

The results suggest that a three-dimensional network is obtained by the changes in starch molecule caused by gelatinization and oxidation treatments. Both modifications probably promote an increase in starch/chitosan interactions as well as increase in the solvation. Differently, the CS blend shows a sol-gel transition at 66.7ºC, and its rheological behavior is

typical of a "weak-gel". The calculated activation energy values show that for CSGE the Ea value is twice that for CSOX suggesting that interactions are higher when gelatinized starch is used.

ACKNOWLEDGMENTS
M.M.H. gratefully acknowledges the financial support of Conselho Nacional de Pesquisa (CNPq).

REFERENCES

1 Arvanitoyannis I, Nakayama A and Aiba A, *Carbohyd. Polym.* **36**:105 (1998).
2 Wang Q, Zhang N, Hu X, Yang J and Du Y, *Eur. J. Pharm. Biopharm.* **66**:398 (2007).
3 Rinaudo, M. *Polym. Int.* **57**:397 (2008).
4 Moura MJ, Figueiredo MM and Gil MH, *Biomacromolecules* **8**:3823 (2007).
5 Tomasik P and Schilling C H, Ad. Carbohydr. *Chem. Biochem.* **59**:175 (2004).
6 Wilhelm HM, Sierakowski MR, Reicher F, Wypych F, Souza GP, *Polym. Int.* **54**:814 (2005).
7 Hoffmann B, Volkmer E, Kokott A, Weber M, Hamisch S, Schieker M, Mutschler W and Ziegler G, *J. Mater. Chem.* **17**: 4028 (2007).
8 Para A and Karolczyk-Kostuch S, *Carbohyd. Polym.* **50**:151 (2002).
9 Tang R, Du Y and Fan L, *J. Polym. Sci. Pol. Phys.* **41**:993 (2003).
10 Yu D, Xiao S, Tong C, Chen L and LIU X, *Chin. Sci. Bull.* **52**:2913 (2007).
11 Horn MM, Martins VCA and Plepis AMG, *Carbohyd. Polym.* **77:**239 (2009).
12 Kurita K, Tomita K, Tada T, Ishii S, Nishimura S and Shimoda K, *J. Polym. Sci: Polym. Chem.* **31:**485 (1993).
13 Liu F, Qin B, He L and Song R, *Carbohyd. Polym.* **78**:146 (2009).

Addition of chitosan to apple juice: a sanitising treatment before pasteurization.

Fernando A. Greco [1, *], María A. Cubitto [2], María S. Rodríguez [1]

[1] INQUISUR UNS - CONICET. Av. Alem 1253, 8000 Bahía Blanca, Buenos Aires, Argentina.
[2] Departamento de Biología, Bioquímica y Farmacia. Universidad Nacional del Sur. San Juan 670, 8000 Bahía Blanca, Buenos Aires, Argentina.
* E-mail: fagreco@uns.edu.ar, Tel.: (+54) 291-4595100, ext 3565.

Abstract
A chitosan obtained from our laboratory was evaluated against *Kluyveromyces marxianus*, as a sanitising treatment before apple juice pasteurization. The chitosan concentration tested, 0.015% in 0.03% acetic acid, was determined in previous studies of minimum inhibitory concentration. Three treatments were assessed: (Ch) pre incubation with chitosan 3h at room temperature, (T) thermal treatment and (ChT) pre incubation with chitosan 3h at room temperature + thermal treatment. The thermal treatment was carried out in test tubes submerged in a thermostatic bath at 54 ºC for 5 minutes. The pre incubation with chitosan diminished *K. marxianus* in 3.71 log cycles while thermal treatment in 3.15 log cycles. However the combine action of pre incubation with chitosan plus temperature reduced the microbial population in 4.48 log cycles.

Keywords: Chitosan, Sanitizing Procedure, Apple Juice, *K. marxianus*.

INTRODUCTION

Several authors have studied the antimicrobial properties of chitosan and proposed it as a natural food preservative [1, 2, 3, 4]. The objective of this research was to determine the efficacy of additing chitosan in a step before fruit juice pasteurization. The assessed yeast was *Kluyveromyces marxianus*, apple juice spoilage yeast known due to its thermal tolerance [5]

MATERIALS AND METHODS

Chitosan

Chitin was obtained from shrimp shells of the estuary of Bahía Blanca, Bs. As., Argentina, provided by a local seafood processing plant. Chitosan (10 % AD, 100 kDa) was obtained from chitin by heterogeneous deacetylation at 136°C with 50% (w/w) NaOH for 5 h.

Yeast

In a preceding study in our laboratory, *Kluyveromyces marxianus* was isolated from an apple juice processing plant [6] The strain was stored in Yeast extract Glucose broth (YG) which consists of 5 g Yeast extract and 20 g Glucose in 1000 mL of distilled water, pH 5 ± 0.1, supplemented with 20 % v/v of glycerol at –70ºC.

Other microbiological medium employed in this study was YGA (5 g Yeast extract, 20 g Glucose and 12 g pure agar in 1000 mL of distilled water, pH 5 ± 0.1)

Apple juice pasteurization

A commercial apple juice (12º Brix clarified apple juice) containing no added chemical preservatives was purchased from a local retailer. The juice was sterilised by filtration through a 0.45 µm pore size cellulose acetate membrane filters (Metricel_Grid, 280 Gelman Sciences, MI, USA) and divided into sterile test tubes of 15 mm of diameter. *K. marxianus* was cultured in shake flasks containing 30 mL of sterile apple juice at 26ºC, 100 RPM for 48 h. Then, the inoculum was adjusted to A_{550} 1.25, which corresponds to 5 x 107 CFU/mL. The final cell

density in each test tube was approximately 106 CFU/mL. The chitosan concentration evaluated was 0.015 % m/v in 0.03 % v/v acetic acid, which was determined in previous studies of minimum inhibitory concentration.
Different treatments were assayed: (T) Thermal treatment at 54ºC, 5 min., (Ch) Pre-incubation with chitosan 3 h at room temperature, (ChT) Pre-incubation with chitosan 3 h at room temperature + thermal treatment at 54ºC, 5 min. The final volume in each test tube was 5 mL, which consists of apple juice + inoculum (T) or apple juice + inoculum + chitosan (Ch and ChT) The thermal treatment was carried out in a thermostatic bath. Once the thermal treatment finished, the test tubes were cooled to 5 ºC in an iced water bath. After each treatment the samples were taken and spread on YGA for counting. Samples, if necessary, were diluted in peptone water 0.1% (m/v). Each condition was evaluated in triplicate.
A treatment with acetic acid 0.03 % was not evaluated due to did not demonstrate any antimicrobial effect on *K. marxianus* in preceding studies.

RESULTS AND DISCUSSION

Figure 1 shows the $\log_{10}$ CFU/mL of *K. marxianus* after different treatments. After 3 h of pre incubation with chitosan it can be seen a diminution of viable and cultivable cell of 3.71 log cycles. Although thermal treatment diminished 3.15 log cycles, the combine action of pre incubation with chitosan and temperature allowed us to achieve a 4.48 log cycles reduction; heating the apple juice just at 54 ºC. Consequently pre incubation with chitosan permits a more efficient thermal treatment.

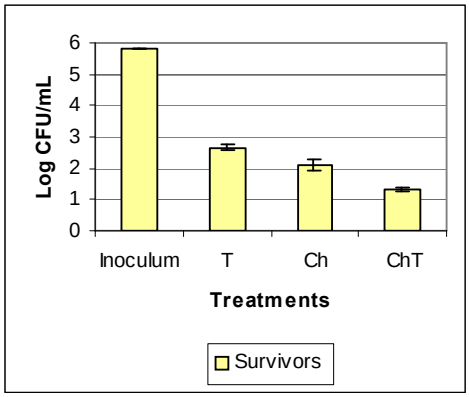

Figure 1. *K. marxianus* survivors after different treatments.

Diminishing the initial microbial load the apple juice industry would perform thermal treatments less intense, with the consequent preservation of the food characteristics. Other microorganisms and treatment conditions will be studied considering chitosan addition in a step before fruit juice pasteurization.

ACKNOWLEDGEMENT

The authors thank to Secretaría de Ciencia y Técnica of the Universidad Nacional del Sur for founding

REFERENCES

1. Roller S.and Covill N. *Int. J. Food Microbiol.*, **47:** 67 (1999)
2. Y. C. Chung, Y. P. Su, C. C. Chen, G. Jia, H. L. Wang, J. C. G. Wu, J. G. Lin. *Acta Pharmacol. Sin* **25 (7)**: 932 (2004)
3. Tikhonov V. E, Stepnova E. A, Babak V. G, Yamskov I. A, Palma-Guerrero J, Jansson

H. B, Lopez-Llorca L. V, Salinas J., Gerasimenko D. V., Avdienko I. D. and Varlamov. V. P. *Carbohydrate Polymers*, **64:** 66 (2006)
4. Chien P. J, Sheu F and. Lin H. R. *Food Chem.*, **100:** 1160 (2007)
5. Tomás-Pejó E., Oliva J.M, González A, Ballesteros I and Ballesteros M, *Fuel* **88**: 2142 (2009)
6. Brugnoni, L.I, Lozano, J.E and Cubitto M.A. *Food Res. Int.*, **40**: 332 (2007)

Optimization of the *N,N,N*-trimethyl chitosan (TMC) synthesis by factorial design

Douglas de Britto[1*], Fernando R. Frederico[2], Odilio B.G. de Assis[1]

[1] Embrapa - CNPDIA, R. XV de Novembro, 1452, CP 741, 13560-970, São Carlos, SP – Brazil
[2] Faculdade de Engenharia Química, UNICAMP, Campinas, SP – Brazil
*E-mail: britto@cnpdia.embrapa.br; odilio@cnpdia.embrapa.br, Tel: + 55 (16) 2107-2800, Fax + 55 (16) 2107-2902.

Abstract
The factorial design was applied to optimizes the synthesis of the N,N,N-trimethyl chitosan via dimethylsulfate synthetic route. The responses analyzed were weight yield, solubility and degree of quaternization. It was verified that the temperature was the most important variable, causing the main variation in the response, as X(T) = -54.52; -9.50 and -7.25 respectively for weight yield, solubility and degree of quaternization. Further analyses, including viscosimetry, contact angle and gel permeation chromatography gave additional information for some representative samples.

Keywords: optimization, factorial design, *N,N,N*-trimethyl chitosan, GPC, molecular weight

INTRODUCTION

Talking about chemical processes, words as chemiometry and optimization methods have become very common nowadays owing to the usefulness of the statistical tools in planning experiments.[1] One of these methods is the Factorial Design Analysis (FDA) largely used in synthesis processes optimization. For chitosan, FDA has been applied to study models of cupper ions-polymer adsorption,[2] to optimize film's mechanical properties[3] and in deacetylation processes.[4] Surprisingly, applications of factorial design on the synthesis of chitosan derivatives were found to be absent from published works.

To optimizes chitosan derivatives, as polysaccharides derivatives in general, is a challenger task due the complexity of the reaction as well as the many roles of the reagents. But it is indispensable mainly for new synthetic routes, as that the synthesis of the N,N,N-trimethyl chitosan (TMC) by means of dimethylsulfate (DMF) as methylant agent.[5]

Such chitosan quaternary salts are a special class of polyelectrolyte with permanent positive charges[6-9] and enhanced hydro solubility in a wide pH range. These derivatives have found several applications nowadays as gene delivery tool;[10,11] absorption enhancer for hydrophilic drugs across intestinal epithelia;[12,13] improved antibacterial activity[14,15] and nanoparticles for vaccine;[16] and controlled drug release.[17] Furthermore, properties such as biodegrability, non toxicity, bactericidal and fungicidal activities[18,19] and easy film forming ability[20] make these derivatives potential materials for uses on natural products.[21] Considering its potential applications, this work applies the FDA in an attempt to optimize the synthesis of the TMC via DMF.

EXPERIMENTAL

The reaction sequence comprised[5,7,21,22] a suspension of 1.0 g of chitosan in 16 mL of DMF and 4 mL of deionized water. Following, 1.2 g of NaOH and NaCl were added and the solution mixed over the desired times under magnetic stirrer. The factorial design was arranged for α=3 (temperature, time and NaCl addition) and b=2 (25/50^{o}C; 3/6 hours and 0/0.44g), resulting in 2^3 = 8 independent experiments, each done in duplicate. Finally, the

TMC was submitted to dialysis in a cellophane membrane (cut-off ~13000 g/mol), precipitated with acetone and dried. The three analyzed responses were weight yield, solubility and degree of substitution (DQ) with help of the software FATORIAL®, developed by Barros Neto *et al.*[1,23] Representative samples were further characterized by viscosimetric, contact angle and Gel Permeation Chromatography (GPC) techniques, as following:

i) **Solubility** was estimated by static method from an aqueous solution at 2.0 mg/mL at 25°C. After the dissolution for 24 h, it was centrifuged (10000 rpm) and supernatant aliquots were taken dried and weighted. From the difference between the initial and final weights the percentage of soluble was calculated. The experiment was realized in triplicate.

ii) **Viscosity** and **hydrophilic character** measurements were carried as described before.[5,24]

iii) The **GPC** analysis was carried out by using dextran and poly(ethylene oxide) standards from American Polymer Standard Corp.® for calibration and check the detectors. The system was composed by pump model 515 from Waters®, degasser Viscotek model VE7510, injector Rheodyne model 7715i and detectors (refractometer, viscosimeter, light scattering 90° and 7°) ViscoteK model TDA302. It was used two columns (Ultrahydrogel Linear, 7.8 x 300 mm from Waters®, the gel is a cross-linked hydroxylated polymer and contains some residual carboxyl functionality) set at 40°C and eluent flow rate of 0.8 mL/min. Eluent and solvent for solutions preparation (1 mg/mL) was a buffer acetic acid-sodium acetate solution (pH=4,5). Analyses were conducted in duplicate and the data handled through the software Viscotek OmniSEC v. 4.1.0.224.

RESULTS AND DISCUSSION

Based on suitable statistical equations[25] and imputing the averages response, the FATORIAL® software returned the values summarized in Table 1. The FDA showed that synthesis realized at high temperature, extensive reaction time and in the presence of NaCl resulted in samples with the lowest weight yield, taking in account the negative value for the global average (Table 1). Indeed, the temperature was the most critical factor to weight yield once X(T) showed high magnitude value compared with the other main effects (Table 1). The negative sign indicates that the weight yield decreases as the reaction temperature increases.

Table 1. Calculated effects for the factorial design for weight yield, solubility and $\overline{DQ}$ responses.

Responses	**Weight yield**	**Solubility**	$\overline{DQ}$
Global Aver.	-21.05	71	29.38
Main effects:			
X(T)	-54.52	-9.5	-7.25
X(t)	-9.84	2.0	4.75
X(S)	4.07	1.0	-1.75
2nd effects:			
X(Tt)	-13.46	-12.5	1.75
X(tS)	11.72	-4.0	-0.75
X(TS)	-6.23	-20.5	1.25
3rd effect:			
X(TtS)	7.79	11.5	9.25

Following, FDA showed that the reaction time, X(t), has also a negative influence on the weight yield (extensive reaction time decreases the weight yield) but not so intensively as that

seen for temperature factor. However, this feature must be analyzed taking in account the strong correlation between the variables, especially X(Tt). The value found for this correlation is expressive (second effects, in Table 1) and its negative sign can be due the highly negative influence of the X(T). This conclusion is supported by the fact that X(TS) has also a negative sign but X(tS), in with the temperature is absent, has a positive sign. The cause of the high reaction temperatures give samples with low weight yields in the quaternization synthesis is due to the formation of H^+ as byproduct in the reaction medium.[5] The acid medium provokes the chitosan chain depolymerization that becomes more expressive at high temperature. Finally, the fraction of small chains is inevitable washed out during the dialysis process. The salt addition does not influence so much in the weight yield, according to X(S) that is not high in magnitude.

The Fig. 1 shows the normal probability plot for the estimative effects. In such a plot, the low magnitude effects or not significant, must show normal distribution data close to zero and a constant variance. This behavior is followed for all effects, where the points fit a nearly linear scattering, excepting the X(T). On the other hand, significant effect presents normal distribution far from zero and is seen to be distant from that linear pattern, as the case of X(T). In fact, the temperature is a very significant factor X(T) for the weight yielding of the quaternization reaction.

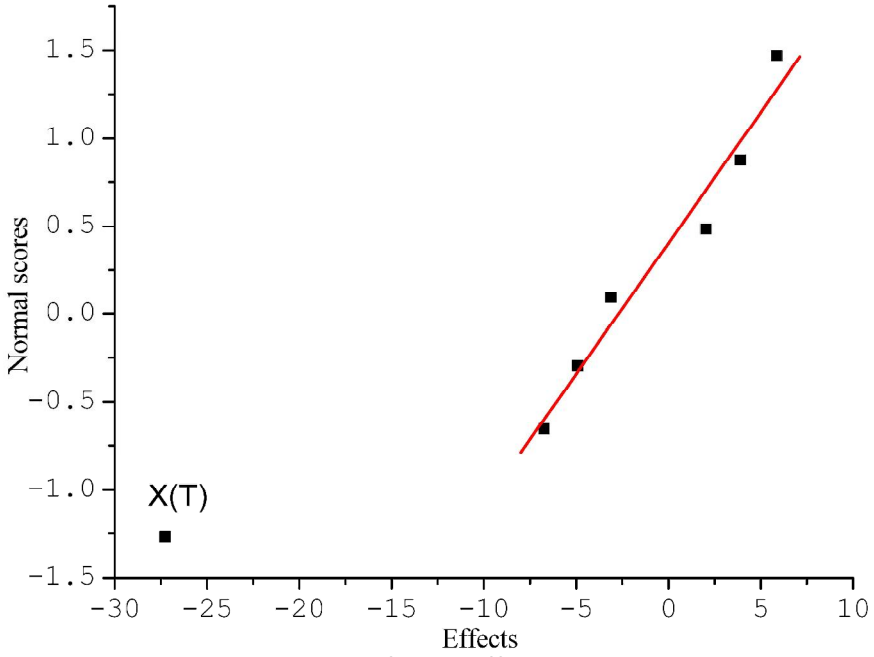

Fig. 1. Normal probability plot for the effects estimative concerning the reaction weight yield.

A very similar result is attained for the influence of these three factors on the solubility and $\overline{DQ}$ (Table 1). The main effects followed the same trend as found above, showing, however, lower magnitude values in comparison with that one. The $\overline{DQ}$ is the main concern in working with polysaccharide derivatives once its small variation may cause great changes in the derivative property. Considering this, if a high substituted TMC is desired the time must be increased, keeping the temperature near the lower level.

Further characteristics of the TMC

Degradations which took place during the reaction can be assessed by measuring the intrinsic viscosity that is related to the average molar mass by the Mark-Houwink equation, [η] =

K $\overline{M_v}$ [a]. The samples $TMCy_3$ and $TMCy_7$ presented [η] reduction[24] in comparison with the parent chitosan (Table 2). However, for the sample $TMCy_7$, reacted at high temperature, the [η] reduction was more expressive then for $TMCy_3$, reacted at low temperature. From the Mark-Houwink equation and the empiric values for *K* and *a* for chitosan reported in the literature,[5] was calculated $\overline{M_v} \cong 154$ kg/mol.

Table 2. Values of the intrinsic viscosity according to Huggins, $[\eta]_{Hug}$, and Kraemer, $[\eta]_{Kra}$, for chitosan and TMC in buffer aqueous solution (0.3/0.2 M CH_3COOH/CH_3COONa).

Samples	$[\eta]_{Hug}$	r	$[\eta]_{Kra}$	r
Chitosan	637	0.9978	646	-0.9819
TMC y_3	160	0.9773	162	-
TMC y_7	50	0.9980	50	0.9962

Contact Angle is a useful tool to evaluate the hydrophilic character expressing it in terms of wettability. For TMC a sharp decrease in the contact angle values was found when compared with the parent sample (Fig. 2), mainly for $TMCy_3$. As matter of fact, the introduction of permanent positive charges into the chitosan chains must increase its hydrophilic character. On the other hand, the methyl group is apolar and contributes to decrease of the hydrophilic character. Consequently the hydrophilic character will depend on a balance of these phenomena.[5] For $TMCy_7$ sample, the huge methylation imparts a very apolar characteristic, overtaking any hydrophilic feature. Evidently, this condition is not good for a desirable aqueous soluble derivative.

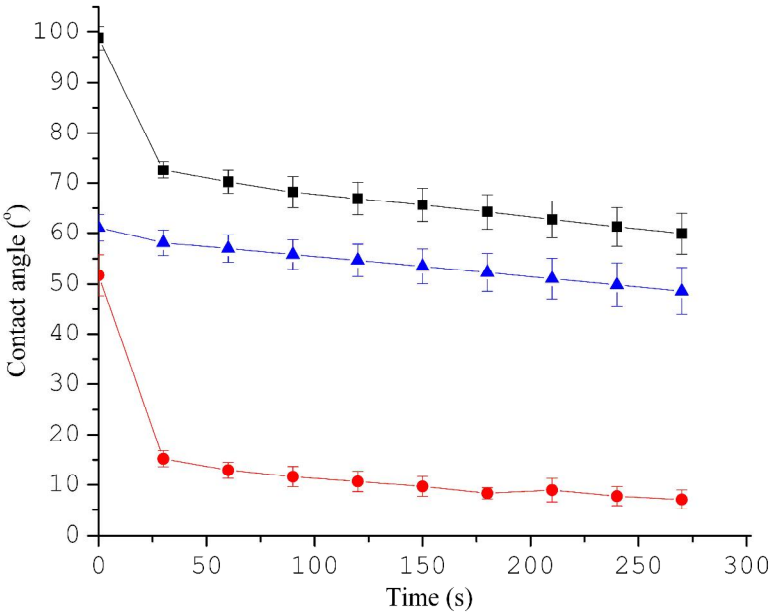

Fig. 2. Water contact angles variation with time measured on polymeric film surface for chitosan and TMC, in which: (■) chitosan; (●)TMC y_3 and (▲)TMC y_7.

The GPC data confirms the molecular weight of chitosan is altered after the quaternization reaction (Table 3). The weight-average molecular weight $\overline{M_w}$ and the number-average

molecular weight $\overline{M_n}$ decrease for the derivatives.[26] In confirmation, the sample $TMCy_7$ was the most degradated one with lowest $\overline{M_w}$ and $\overline{M_n}$. For the experiment conducted at room temperature ($TMCy_3$), the preservation of the polymeric chain is notable great. Other important feature is that the TMC salts show low polydispersity ($\overline{M_w}/\overline{M_n}$), what can be attributed to the purification dialyzes process that washes out small chain. This fact trends to become more accentuated as the degradation increases, as experienced for $TMCy_7$. For chitosan, the viscosimetric Mark-Houwink constant **a**, given by GPC analysis (Table 3) is in agreement with the literature,[27] while log **K** differ considerably. However, these parameters are empiric and dependent on the conditions, *e.g.*, temperature and solvent, and adopted methodology.

Table 3. Molecular weight and viscosimetric constants by GPC.

Sample	$\overline{M_n}$	$\overline{M_w}$	$\overline{M_w}/\overline{M_n}$	**a**	**log K**
Chitosan	60,146	218,718	3.636	0.583	-2.061
TMC y_3	56,779	116,813	2.059	0.744	-3.137
TMC y_7	12,593	19,364	1.538	0.836	-3.433

CONCLUSIONS

The use of FDA for evaluating the quaternization process of chitosan allowed concluding that the temperature is the most critical factor influencing the weight yield, solubility and degree of substitution of the derivative. Also, according to Contact Angle measurements, viscosimetric and GPC analyses, effective chain preservation is attained at room temperature and by extensive reaction time. The addition of NaCl did not show any positive influence on the response and can be definitely suppressed from the reaction.

ACKNOWLEDGMENTS

The authors are grateful to EMBRAPA, FAPESP and CNPq for financial support. Also to: Prof. Dr. José Fabian Schneider (IFSC-USP) and Prof. Dr. Antonio Gilberto Ferreira (DQ-UFSCar), solid state NMR; Prof. Dr. Paulo Sérgio Campana Filho (IQSC-USP), viscosimetry; and Prof. Dra. Telma Teixeira Franco (FEQ-UNICAMP), GPC; that kindly made available their equipments to data acquiring.

REFERENCES

1. Barros-Neto B, Scarmínio IS and Bruns RE, *Planejamento e otimização de experimentos*. Editora da Unicamp, Campinas (1995).
2. Lima IS and Airoldi C, *Colloids Surf A* **229:** 129-136 (2003).
3. Tao YG, Pan J, Yan SL, Tang B and Zhu LB, *Mater Sci Eng B* **138:** 84-89 (2007).
4. Weska RF, Moura JM, Batista LM, Rizzi J and Pinto LAA, *J Food Eng* **80:** 749-753 (2007).
5. de Britto D and Assis OBG, *Carbohydr Polym* **69:** 305-310 (2007).
6. de Britto D and Campana-Filho SP, *Polym Degrad Stab* **84:** 353-361 (2004).
7. Curti E, de Britto D and Campana-Filho SP, *Macromol Biosci* **3:** 571-376 (2003).
8. Dung P, Milas M, Rinaudo M and Desbrières J, *Carbohydr Polym* **24:** 209-214 (1994).
9. Sieval AB, Tahanou M, Kotzé AF, Verhoef JC, Brusse J and Junginger HE, *Carbohydr Polym* **36:** 157-165 (1998).
10. Germershaus O, Mao SR, Sitterberg J, Bakowsky U and Kissel T, *J. Controlled Release* **125:** 145-154 (2008).

11. Sajomsang W, Ruktanonchai U, Gonil P, Mayen V and Opanasopit P, *Carbohydr Polym* **78:** 743-752 (2009).
12. Mourya VK and Inamdar NN, *J Mater Sci: Mater Med* **20:** 1057-1079 (2009).
13. Sahni JK, Chopra S, Ahmad FJ and Khar RK, *J Pharm Pharmacol* **60:** 1111-1119 (2008).
14. Kim CH, Choi JW, Chun HJ and Choi KS, *Polym Bull* **38:** 387-393 (1997).
15. Jia Z, Shen D, Xu W, *Carbohydr Res* **333:** 1-6 (2001).
16. Amidi M, Romeijn SG, Verhoef JC, Junginger HE, Bungener L, Huckriede A, Crommelin DJA and Jiskoot W, *Vaccine* **25:** 144-153 (2007).
17. Cafaggi S, Russo E, Stefani R, Leardi R, Caviglioli G, Parodi B, Bignardi G, De Totero D, Aiello C and Viale M, *J. Controlled Release* **121:** 110-123 (2007).
18. Bautista-Baños S, Hernández-Lauzardo AN, Velázquez-del Valle MG, Hernández-López M, Barka EA, Bosquez-Molina E and Wilson CL, *Crop Protection* **25:** 108-118 (2006).
19. Rabea EI, Badawy MET, Stevens, CV, Smagghe, G and Steurbaut W, *Biomacromolecules* **4:** 1457-1465 (2003).
20. Hsu SH, Whu SW, Tsai CL, Wu YH, Chen HW and Hsieh KH, *J. Polym Res* **11:** 141-7 (2004).
21. de Britto D and Assis OBG, *Int J Biol Macromol* **41:** 198-203 (2007).
22. de Britto D, Forato LA and Assis OBG, *Carbohydr Polym* **74:** 86-91 (2008).
23. http://www.chemkeys.com (accessed February 2010).
24. Curti E and Campana Filho SP, *J Macromol Sci, Part A: Pure Appl Chem* **43:** 555-572 (2006).
25. Box GPG, Hunter WG and Hunter JS, *Statistics for Experimenter: An Introduction to Design, Data Analysis and Model Building*. John Wiley & Sons, New York (1978).
26. Jayakumar R, Reis RL and Mano JF, *J Macromol Sci, Part A: Pure Appl Chem* **44:** 271-5 (2007).
27. Yomota C, Miyazaki T and Okada S, *Colloid Polym Sci* **271:** 76-82 (1993).

Jumbo squid collagen-chitosan composites

Josafat M. Ezquerra-Brauer[1*], Joe L. Arias-Moscoso[1], Maribel Plascencia-Jatomea[1], Herlinda Soto-Valdez[2], Reyna Luz Vidal-Quintanar[1], Ofelia Rouzaud-Sández[1]

[1]Departamento de Investigación y Posgrado en Alimentos. Universidad de Sonora.Mexico
[2]Centro de Investigación en Alimentación y Desarrollo, A.C. Mexico
*E-mail: ezquerra@guayacan.uson.mx

Abstract
Film blends of chitosan with acid-soluble collagen (ASC) isolated from jumbo squid by-products were prepared by solution mixing and film casting. The goal of this study was to evaluate the potential application of ASC as a plasticizer agent in the preparation of biofilms in composites with commercial chitosan (85% deacetylated, viscosity >400 mPa·s, molecular weight 570.3 kDa). The ASC improved the percentage of elongation at break of chitosan film. The water barriers properties and the solubility of chitosan films increased with the addition of ASC. The *Tg* of chitosan film was 170°C and shifts to 160°C for the ASC:chitosan films containing 80 and 50% of ASC.

Keywords: by-products; collagen; chitosan; jumbo squid; films.

INTRODUCTION

Collagen, as well as chitosan, has a great potential, in the field of biomaterials. Collagen, the major protein of the connective tissues, was detected in a concentration about 9-18 % in jumbo squid (1). Jumbo squid is a renewable natural resource that is mainly harvested in the Sea of Cortez. After filleting, the waste from the squid fishery accounts for as much as 75% of the total catch weight in form of fins, heads, and guts (2). This waste is an excellent raw material to obtain important by-products with high commercial value, such as collagen. Collagen fibers have been used as an ingredient in a variety of meat products due to its water and fat binding abilities, but their physical-chemical properties and its potential use in biodegradable film for food packaging is still under exploration (3). Chitin is a naturally occurring macromolecule present in the exoskeleton of invertebrates and represents the second most abundant polysaccharide resource after cellulose. Chitosan is a polysaccharide that is produced by deacetylation of naturally occurring chitin. Chitosan has a great potential for a wide range of applications (4). Nonetheless, pure chitosan, as a film material, does not form films with adequate mechanical properties due to its low percentage of elongation. This suggests that chitosan blends may be accomplished by the addition of biodegradable plasticizers (5). Furthermore, since collagen in acid solution exhibited positively charged groups, it has a molecular interaction with chitosan with high potential to produce biocomposites with novel properties (4) such as a possible plasticizer agent (2). The aim of this study was to improve the percentage of elongation at break of chitosan film by blending it with acid soluble collagen (ASC) from jumbo squid by-products.

MATERIALS AND METHODS

Acid–soluble collagen (ASC) fraction from 100g of jumbo squid by-product sample was prepared as described by Uriarte and col. (2), which involves a preliminary extraction with 6M Urea in sodium acetate (pH 6.8) solution and neutral buffer (0.05M Tris + 1M NaCl, pH 7.2) to remove non collagenous proteins. Commercial chitosan with high viscosity (>400 mPa·s) and high molecular weight (570.3 kDa) was used. Chitosan (2% by weight) and ASC (2% by weight) were dissolved in 0.5 M acetic acid. The two solutions were blended until

homogenous solutions were obtained. The blend films were obtained by casting and evaporating at room temperature. The final composition (chitosan:ASC) were 0:100, 20:80, 50:50, and 80:20 (w/w). The ASTM-D882-91 method was used to measure tensile strength (TS) and percentage elongation at break (EL). The ASTM-96-80 method was used to measure water vapor transmission rates (WVR) of the films. The solubility of the films was evaluated by drying-rehydrated process (6). The thermal behavior was measured using a 1020 Series DSC7 thermal analysis system. All experiments were replicated three times. The data was analyzed using the SAS program 6.08 for PCS.

RESULTS

The 20: 80 and 50:50 (chitosan:ASC) blends showed the highest percentage of elongation at break however produced a brittle films with low tensile strength in comparison to 80:20 and 0:100 (chitosan:ASC) films (Table 1). The chitosan:ASC films showed a higher WVR than control film (Table 2). The addition of ASC increasing the solubility of the chitosan films (Table 2). Table 3 showed the glass transition temperature (*Tg*) values of chitosan:ASC films. The lower *Tg* was detected in 20:80 and 50:50 (chitosan:ASC) films.

Table 1. Mechanical properties of tensile strength (TS) and percentage elongation at break (EL) of chitosan:acid soluble collagen from jumbo squid films (CH:ASC)*.

CH:ASC	***TS (mPa)***	***EL (%)***
80%-20%	$1.5^{d} \pm 0.1$	$29.1^{b} \pm 0.9$
50%-50%	$4.1^{c} \pm 1.2$	$39.8^{a} \pm 3.2$
20%-80%	$35.5^{b} \pm 4.4$	$12.3^{c} \pm 1.1$
Control	$50.1^{a} \pm 3.6$	$5.2^{d} \pm 0.3$

*Mean value ± standard deviation from five separate samples.
Means with different letters within rows indicate significant differences ($P<0.05$).

DISCUSSION

Chitosan when it is combined with plasticizer agents, such as collagen, it can improve its mechanical properties, specifically its elongation at break (7). It was observed that the addition of collagen increased the percentage of elongation at break (EL) from 5.2 in the pure chitosan film up to 39.8. This behavior is attributed to the hydrophilic properties of collagen which provides a certain increase in the hydration degree of the film, resulting in a higher EL, WVR, and solubility values. It is well known that the *Tg* is an important criteria for the miscibility of the components. In a completely miscible blend of two polymers, only one *Tg* will appear in DSC thermograms (7). In the present study the chitosan:ASC films showed one Tg, with lower value than chitosan film. These results are in agreement with the theory of plasticization, the *Tg* of plasticized film decreases, indicating that collagen:chitosan have good miscibility (7). Based on the above, the collagen may act as plasticizer in chitosan film structure.

Table 2. Water vapor rate (WAR) and solubility of chitosan:acid soluble collagen from jumbo squid films (CH:ASC).

CH:ASC	***WAR (gr/m^{2}day)****	***Solubility (%)*****
80%-20%	190[b]	44.2[b] ±1.9
50%-50%	170[b]	40.4[b] ±2.4
20%-80%	100[a]	29.9[a] ±1.4
Control	120[a]	0

* Mean value ± standard deviation from six separate samples.
** Mean value ± standard deviation from three separate samples
Means with different letters within rows indicate significant differences (P<0.05).

Table 3. Glass transition temperature (*Tg*) and specific heat (ΔCp) of chitosan:acid soluble collagen from jumbo squid films (CH:ASC) *.

CH:ASC	***Tg (°C)***	***ΔCp (kJ/mol)***
80%-20%	160.5[b] ±0.8	0.83[b] ±0.1
50%-50%	157.5[b] ±1.1	0.27[a] ±0.1
20%-80%	169.5[a] ±1.1	0.26[a] ±0.1
Control	170.3[a] ±0.9	0.30[a] ±0.03

* Mean value ± standard deviation from three separate samples.
Means with different letters within rows indicate significant differences (P<0.05).

CONCLUSION

A positive plasticizer effect of squid collagen over a chitosan film was detected, being hydrogen bonding the most abundant interaction forces between the polymers. The blending of acid soluble collagen from squid by-products and commercial chitosan gives the possibility of producing new materials with potential applications in the food or biomedical industries.

ACKNOWLEDGMENTS

This study was supported by CONACYT through grant 89879.

REFERENCES

1 Torres-Arreola W, Pacheco-Aguilar R, Sotelo-Mundo RR, Rouzaud-Sández, O, Ezquerra-Brauer JM, *Cienc. Tecnol. Alim* **6**: 101-116 (2008).
2 Uriarte-Montoya MH, Arias-Moscoso JL, Plascencia-Jatomea M, Sántacruz-Ortega H, Rouzaud-Sández O, Cárdenas-López JL, Marquez-Rios E, Ezquerra-Brauer JM, *Bioresource Tech.* DOI:10.1016/j.biotech.2010.01.008 (2010)**.**
3 Wolf KL, Sobral PJA, Telis VRN, *IUFoST World Congress. 13th World Congress of Food Science and Technology*. DOI: 10.1051/IUFoST:20060929: 801-802 (2006).
4 Lopez-Caballero ME, Gomez-Guillen MC, Perez-Mateos M, Montero PA, *Food Hydrocolloids*, **19**: 303-311 (2004).
5 Butler BL, Vergano P.R., Testin RF, Bunn JM, Wiles, J.L, *J. Food Sci*. **61**:953-955 (1996).
6 Krochta JM and De Mulder-Hohnston C,*American Chem. Soc*., 120-140 (1996).
7 Suyatama N.E, Tighzert L, Copinet A, *J. Agri. Food Chem*. **53**: 3950-3957 (2005).

New method for chitooligomers preparation by oxidative degradation

Liliana Albertengo, Adriana Debbaudt, Mirta Montero and María Susana Rodríguez*

INQUISUR (UNS–CONICET), Bahía Blanca, Buenos Aires, Argentina.
*E-mail: mrodri@uns.edu.ar

Keywords Chitosan, chitooligomers, water solubility, hydrogen peroxide, microwave irradiation

Abstract
Chitooligomers were prepared by oxidative degradation of chitosan with hydrogen peroxide under microwave irradiation. For the determination of the optimal conditions the effects of H_2O_2 concentration, ethanol volume and resting time for oligomers precipitation were studied. A mathematical model (Taguchi method with orthogonal array) between degradation conditions and recovery water soluble chitosan was used. The structure of the product was confirmed by FT-IR spectrum and X-ray diffraction analysis. The number average molecular weight was determined by end group analysis method. The experimental results show that better conditions are H_2O_2 12.5% and 150 mL of ethanol to chitooligomers precipitation. It is demonstrate that resting time have no influence in chitooligomers recovery. Solubility of derivatives is 98 % and the number of repeating units is 2.

INTRODUCTION

Chitosan, a natural linear biopolyaminosaccharide is obtained by alkaline deacetylation of chitin, which is the principal component of protective cuticles of crustaceans such as crabs, shrimps, prawns, lobsters and of some fungi cell walls. Chitosan is a weak base and is insoluble in water and organic solvent.
Chitosan is inexpensive, biodegradable, and nontoxic for mammals. These properties among others make it suitable for use as an additive in the food industry, as a hydrating agent in cosmetics, and as a pharmaceutical agent in biomedicine.
The very high molecular weight and therefore the very high viscosity of chitosan solutions limit its use in several biological applications. Being a polymer it can be subjected to depolymerization producing low-molecular-weight chitosans, oligosaccharide (chitooligomers) and monomers. Because of the excellent solubility of oligomers, their applications are numerous and varied. Several chemical, physical and enzymatic methods have been suggested for the preparation of chitosan oligomers.[1-3].
The objective of this work is to find the best of experimental conditions for obtaining water soluble chitosan by oxidative degradation and its characterization.

EXPERIMENTAL

Chitosan obtained in Laboratorio de Investigaciones Básicas y Aplicadas en Quitina (LIBAQ) (2.0 g) was placed in a Erlenmeyer flask with 50.0 mL H_2O_2 (10%,12.5%, 15%), then (20 min later) was placed on a microwave oven at 700 W for 4 min. After irradiation the product was allowed to cool to room temperature. The mixture was filtered through a Buchner filter under reduced pressure.
Then 98% ethanol (90.0, 150.0, 210.0 mL) was added to the filtrate and left to rest during 15 min, 30 min and 60 min to obtain a white precipitate. The precipitate was filtered off and then washed thoroughly with ethanol. The precipitate was dissolved in water, freeze-dried and weight . All the test were done five times.

Characterization studies

Determination of molecular weight: The number average molecular weight (Mn) was determined by the method of end group analysis [4].

X-ray diffraction spectrometry: data were collected using a Rigaku D-Máx. III C diffractometer (Cu *K*α) irradiated at 35 kv-15 ma.

IR spectroscopy: The spectrum was recorded on a Nicolet FT-IR instrument. The KBr discs were prepared by blending anhydrous KBr

Solubility test*:* Water *s*olubility of chitooligomers was evaluated. Solutions were prepared with 0.05 g of chitooligomer in 5 mL of water, after 5 h of stirring the solution were filtered through paper (0.45μm). The filters were dried and weigh to calculate percentage of solubility.

RESULTS AND DISCUSSION

Some preliminary studies demonstrated that chitosan size must be smaller than 100 mesh and must be immersed in H_2O_2 at least 20 min to make chitosan swelling and the obtained chitooligomers must be solubilized in water and freezer-dried immediately to avoid Maillard reaction in the final products. The best conditions for preparing chitooligomers were studied by the Taguchi method. The three controllable variables were H_2O_2 concentration (10%,12.5%, 15%), volume 98% ethanol (90.0, 150.0, 210.0 mL) used for chitooligomer precipitation and time left to rest (15 min, 30 min and 60 min). The only dependent variable was water chitooligomers recovery. The obtained results are shown in table 1.

Table 1: Model fitness analysis for the recovery of water-soluble chitosan and Mw

Assay	% H_2O_2	Ethanol (mL)	Resting time (min)	Chitooligomers (g)	Molecular weight
1	10	90	15	0.296 ± 0.130	269.4
2	12.5	150	15	0.820 ± 0.006	319.0
3	15	210	15	0.776 ± 0.060	278.0
4	12.5	90	30	0.523 ± 0.030	300.3
5	15	150	30	0.794 ± 0.038	258.6
6	10	210	30	0.422 ± 0.146	267.2
7	15	90	60	0.446 ± 0.123	280.1
8	10	150	60	0.426 ± 0.136	276.0
9	12.5	210	60	0.825 ± 0.100	271.5

As shown in Table 1 the controllable values, H_2O_2 concentration and 98% volume ethanol are significant to increase the mean response (chitooligomers yield) and to reduce process variability with $p<0.00001$ and $p<0.000001$ respectively. Thus the optimum reaction conditions are 12.5% H_2O_2 concentration, 150.0 mL 98% ethanol demonstrating that time of rest has no influence on the final chitooligomers yield.

Taking into account the number average molecular weight of chitooligomers presented in table 1 (280) and the molecular weight of glucosamine repeating units (160) it must be conclude that the average number of repeating units is 2. Meanwhile, we found no dependence of the number average molecular weight with reaction conditions (Table1).

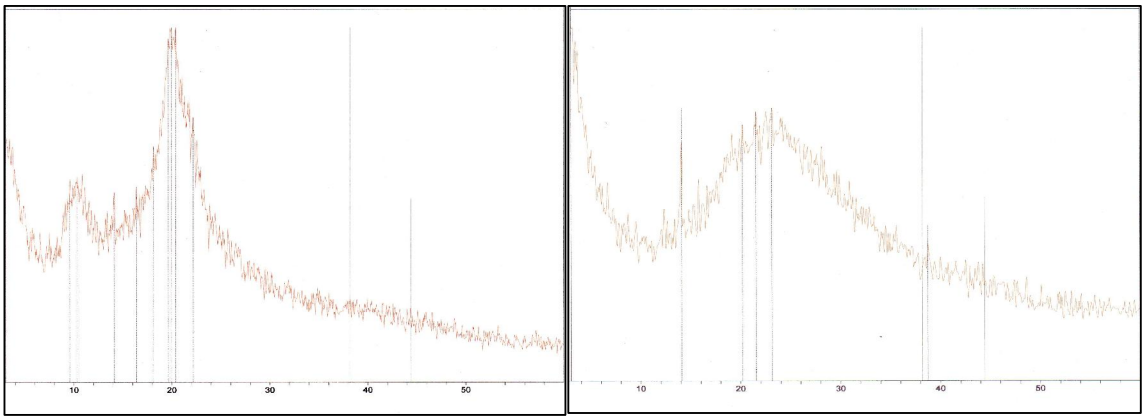

(a) (b)

Fig. 1. X-ray diffraction patternes (a) chitosan (b) chitooligomers

The X-ray patterns of the original chitosan and the chitooligomers are shown in Figure 1. For original chitosan, there were two characteristic peaks at 2θ = 10.09º and 2θ = 20.38º which corresponded to the pattern. Compared with the original chitosan, the main difference of the chitooligomers was the appearance of the peak at 2θ = 15.3 and the disappearance of the peak at 2θ = 10.09º. Moreover it can be seen that, the peaks at 2θ = 15.3, 21.1 and 2θ = 23.8º tend to be broad and weak, suggested that chitosan degradative process decreases not only molecular weight but the crystallinity of the chitooligomer too, transforming the biopolymer into an amorphous structure.

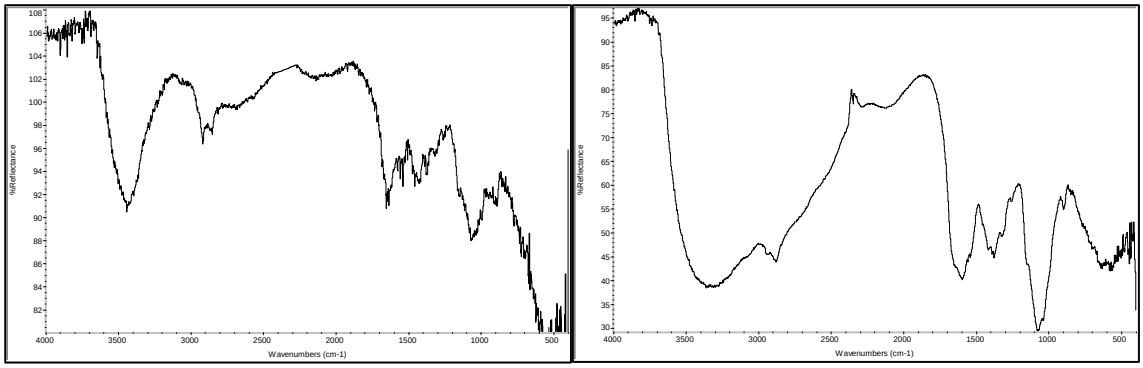

(a) (b)

Fig.2 FT-IR spectra of (a)chitosan (b) chitooligomers

The spectra of the chitooligomers, compared with the FT-IR spectrum of the original chitosan, exhibit most of the characteristic absorption bands of the original chitosan (Fig 2). However, some differences are as follows: the N–H and O–H stretching vibrations in the spectra of the chitooligomers are wider, which can be attributed to increased interaction between these groups due to the degradation of the biopolymer.
All chitooligomers samples show a very good solubility (94.3 -99.5%).

CONCLUSIONS

In this work the use of a mathematical model between assay conditions and chitooligomers yield allows to demonstrate the optimal experimental conditions to obtain water soluble chitosan. The chitooligomers obtained have excellent water solubility and small degree of polymerisation.

REFERENCES

1 Harish Prashanth KV and Tharanathan RN, *Trend in Food Science & Technology* **18:** 117-131 (2007)

2 Mourya VK and Inamdar NN, *Reactive & Functional Polymers* **68:**1013-1051 (2008)

3 Pillai CKS, Paul W and Sharma C P, *Progress in Polymer Science* **34:** 641-678 (2009).

4 Shao J, Yang Y, Zhong Q, *Polymer Degradation and Stability* **82:** 395-398 (2003).

Chitosan coated nanoparticles for heparin administration: development and evaluation for asthma treatment

Felipe A. Oyarzun-Ampuero*, Jose Brea, Maria I. Loza, Dolores Torres, Maria J. Alonso

Universidad de Santiago de Compostela, Campus sur s/n, Facultad de Farmacia 15782, Santiago de Compostela, España
*E-mail: foyarzuna1@gmail.com

Abstract: This work aimed to evaluate, by the first time, the potential of nanoparticles composed by chitosan (CS)-carboxymethyl-β-cyclodextrin (CMβCD) and CS-hyaluronic acid (HA) as vehicles for improving the delivery of heparin in mastocytes and, thus, for preventing mastocytes-degranulation. Physicochemical parameters of nanoparticles as size, polydispersity, and stability at physiological conditions were importantly influenced by the presence of CMβCD or HA. Studies performed in mastocytes showed that both systems were able to prevent histamine release in different extent depending on their composition. Importantly, nanoparticles consisting of CS-CMβCD were more effective in preventing histamine release than those of CS-CMβCD and that heparin alone.

Keywords: Chitosan; Carboxymethyl-β-cyclodextrin; Hyaluronic acid; Nanoparticles; Asthma; Mastocytes

INTRODUCTION

Heparin is a macromolecular drug that has shown important effects against asthma. These effects are mainly attributed to its capacity for preventing the mast cell degranulation and require the access of the drug into the cell[1]. Importantly, this antiasthmatic activity is independent of the anticoagulant activity of heparin and inversely proportional to its molecular weight[2]. Furthermore, several studies have demonstrated that the inhalation of high, medium and low molecular-weight-heparin is effective in preventing acute bronchoconstrictor responses and airway hyperresponsiveness[2].

Positively charged chitosan (CS) nanoparticles are known for their ability to interact favorably with negatively charged mucus and cellular membranes, thus improving the intracellular penetration[3]. Carboxymethyl-β-cyclodextrin (CMβCD) is an anionic, non-toxic and biodegradable oligosaccharide that has shown, among others beneficial characteristics, to acts as permeation enhancer for different macromolecular drugs and to inhibit the activity of certain enzymes[4]. Hyaluronic acid (HA) is a natural, non-toxic and biodegradable polysaccharide that has demonstrated interesting effects in airways as hypoproliferative activity on proliferating smooth muscle cells (typically founded in asthmatic patients) together with benefits on mucocilliary transport rate[5].

Taking the above information into account, this work aimed to combine the virtues of the above materials for the development of CS-CMβCD and CS-HA nanoparticles loaded with unfractioned heparin (UFH) or low-molecular-weight heparin (LMWH), intended for the pulmonary administration. The interaction among the nanosystems and mast cells will be investigated, and their potential for preventing the degranulation evaluated, to our knowledge, by the first time.

MATERIALS AND METHODS

Nanoparticles preparation: CS (125 kDa) and different ratios of CMβCD-tripolyphosphate (TPP) or HA (165 kDa)-TPP including UFH (18 kDa) or LMWH (4 kDa) were mixed to form nanoparticles following the ionotropic gelation method[6]. **Mast**

cell purification: Mast cells were obtained by lavage with Umbreit solution from pleural and peritoneal cavities of Sprague-Dawley female rats as described Lago et al.[7]. **Confocal microscopy studies:** Fluorescent CS was obtained following the procedure described by De Campos et al.[6]. Fluorescent nanoparticles were obtained by using the procedure described above (with fluorescent CS) and then nanoparticles were incubated 2 h with rat mast cells. **Measurement of histamine release in mast cells:** Rat mast cells ($1X10^5$ cells) were warmed in Umbreit containing the selected UFH or LMWH concentrations or the corresponding concentrations of nanoparticles loaded with UFH or LMWH, at 37 ºC for 10 min. Histamine release was initiated by incubating the cells with 100 µM of compound 48/80 for 20 min at 37 ºC following an analogue procedure to that described by Lago et al.[7].

RESULTS AND DISCUSSION

Resulting nanoparticles were in a nanometric range and showed a positive zeta potential as shown in table 1A and 1B. The positive zeta potential of the formulations indicates that the surface of all systems was composed mainly by CS.

Table 1: Physicochemical properties of the tested formulations comprising (A) CS-CMβCD and (B) CS-HA loaded with heparin (mean ± S.D., n≥3).

A

CS-CMβCD-TPP-heparin (mg)	Size (nm)	P.I.	ζ potential
6-1-0-1[a]	359±21	0.3–0.4	41±1
6-2-0-2[a]	729±54	0.8–1	33±1
6-2-0-2.1[a]	p.p.	---	---
6-0.85-0.34-1.6[a]	**375±69**	**0.3–0.5**	**37±2**
6-1-0.34-1.6[a]	473±24	0.6–0.9	35±1
6-1.15-0.34-1.6[a]	p.p.	---	---
6-1.3-0.34-1.6[a]	p.p.	---	---
6-0.85-0.34-1.6[b]	**221±26**	**0.2–0.3**	**37±1**

B

CS-HA-TPP-heparin (mg)	Size (nm)	P.I.	ζ potential
4-1.2-0.21-1[a]	201±24	0.2–0.4	32±2
4-1.2-0.21-1.2[a]	217±30	0.2–0.4	28±1
4-1.2-0.21-1.4[a]	p.p.	---	---
4-1.2-0.21-1.6[a]	p.p.	---	---
4-0.6-0.21-1.2[a]	162±17	0.1–0.3	35±1
4-0.6-0.21-1.4[a]	**193±32**	**0.2-0.5**	**33±2**
4-0.6-0.21-1.5[a]	p.p.	---	---
4-0.6-0.21-1.4[b]	**152±10**	**0.2-0.3**	**33±1**

[a]=UFH; [b]=LMWH; p.p.=precipitation or not resuspendable; P.I.=polydispersity index.

Following criteria of size and polydispersity among others, the formulations showed in red in table 1 were selected for next experiments. As you can appreciate in figure 1A and 1B, selected formulations of CS-CMβCD and CS-HA, showed spherical shape by transmission electron microscopy (TEM).

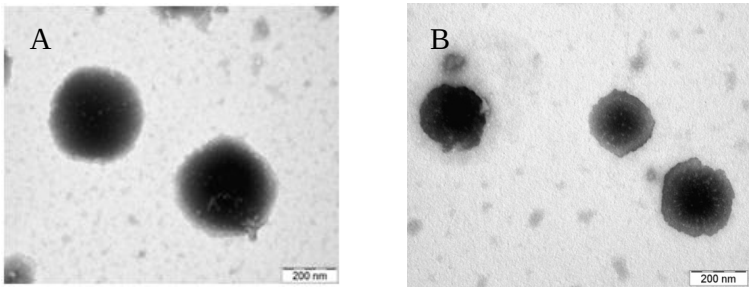

Figure 1: TEM micrographs of selected nanoparticle formulations of CS-CMβCD (A) and CS-HA (B) loaded with UFH.

All selected formulations presented drug association efficiencies of around 70%. Importantly, the stability profiles of selected formulations were very influenced by the composition of the nanocarriers because while the nanosystems of CS-CMβCD loaded with UFH or LMWH were similarly stable in Hanks' Balanced Salt Solution (HBSS, pH 6.4), those of CS-HA were stable in phosphate buffer solution (PBS, pH 7.4) (data not shown). The drug release profile from the formulations in HBSS or PBS seems to be very influenced by the molecular weight of heparin and requires more than 12 h for complete release (data not shown). Stability studies at storage conditions showed that all selected systems maintained their characteristics for more than 3 months (data not shown).

Experiments aimed to evaluate if selected formulations with fluorescent CS containing CMβCD or HA are able to be internalized into the mastocytes indicate a homogeneous distribution inside the cells independently of their composition; in figure 2 is showed the experiment carried out with CS-HA nanoparticles.

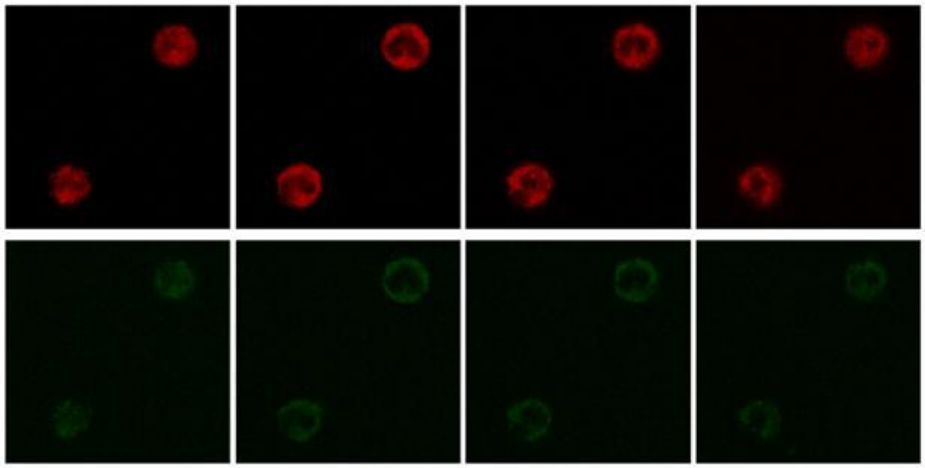

Figure 2: Confocal scanning microscopy images of fluorescent mastocytes and fluorescent UFH- loaded CS-HA nanoparticles. Slides of mastocytes taken every 1.5 μm in the "z" axis after 2 h of incubation with fluorescent nanoparticles. First line: signal of fluorescent mastocytes (red); second line: signal of fluorescent nanoparticles (green).

Experiments achieved with the selected formulations on the ability to prevent histamine release induced by compound 48/80 showed a dose-response behavior. Importantly, CS-CMβCD nanoparticles loaded with 0.2 mg/mL of UFH or LMWH significantly improved the effect obtained with the same dose of heparin solutions (in figure 3A and 3B are shown the experiments carried out with UFH and comprising CS-CMβCD and CS-HA nanoparticles).

Finally, the viability of mast cells was higher than 90% after the treatment with all tested doses of nanoparticles (data not shown), thus indicating the safety of the formulations.

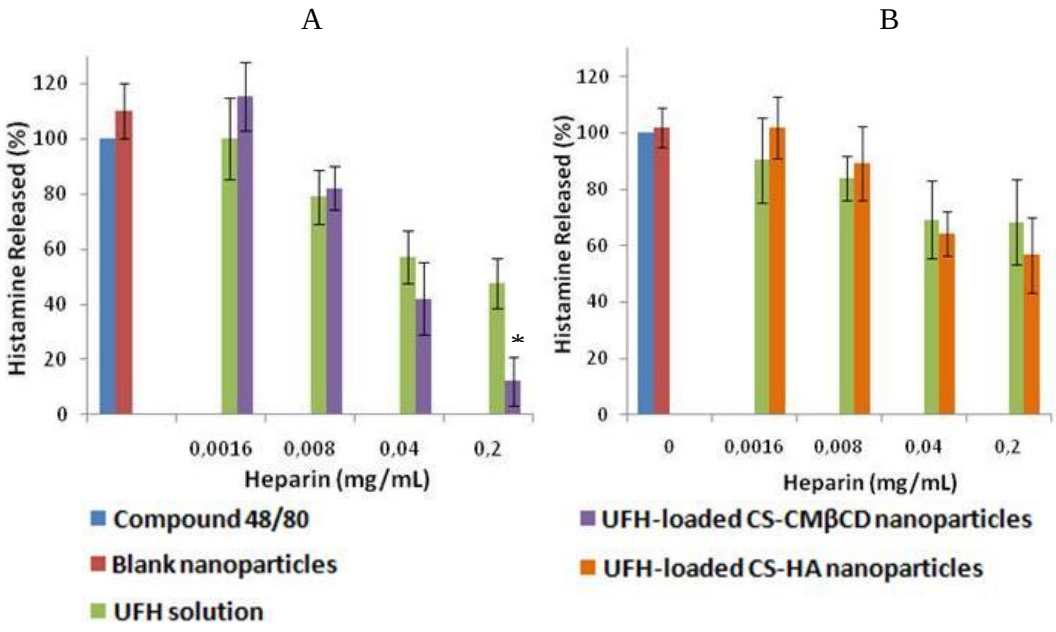

Figure 3: Effect of UFH solutions and UFH-loaded in (A) CS-CMβCD and (B) in CS-HA nanoparticles on histamine release induced by compound 48/80 in mast cells. ($p<0.05$).

CONCLUSIONS

In the present work we reported the development and characterization of nanoparticles comprising CS-CMβCD and CS-HA loaded with two different molecular weight heparins focused for the asthma treatment. Physicochemical parameters as size, polydispersity and stability at physiological conditions were importantly influenced by the presence of CMβCD or HA into the nanocarriers. Confocal studies indicate that all systems were uniformly internalized by mastocytes. Ex-vivo studies showed that both systems were able to prevent histamine release from mastocytes in different extent. Significantly lower values in histamine release were obtained with formulations consisting of CS-CMβCD compared with those of CS-HA or heparin solutions.

ACKNOWLEDGEMENTS

Authors acknowledge financial support of the Spanish Government (Consolider-Ingenio CSD 2006-00012), and of CONICYT for the scholarship of F.A. O.-A.

REFERENCES

1 Niven AS and Argyros G, *Chest* **123**:1254 (2003).
2 Campo C, Molinari JF, Ungo J and Ahmed T, *J Appl Physiol* **86**:549 (1999).
3 De la Fuente M, Csaba N, Garcia-Fuentes M and Alonso MJ, *Nanomedicine* **3**:845 (2008).
4 Matsubara M, Ando Y, Irie T and Uekama K, *Pharm Res* **14**:1401 (1997).
5 Lim ST, Martin GP, Berry DJ and Brown MB, *J Control Rel* **66**:281 (2000).
6 De Campos AM, Diebold Y, Carvalho EL, Sanchez A and Alonso MJ. *Pharm Res* **21:**803 (2004).
7 Lago J, Alfonso A, Vieytes MR and Botana LM, *Cell Signal* **13**:515 (2001).

Hydrogel beads based chitosan employed in protein delivery systems

R. Torelli-Souza[1], J. Lopes-Ferreira[1], T. Batista-Lins[1], L. Monteiro[1] and R. Amorim[2*]

[1] UFPB, Univ. Fed. da Paraíba, Campus I, 58059-900 João Pessoa – PB, Brazil.
[2] UFPE, Univ. Fed. de Pernambuco, 50670-901 Recife – PE, Brazil.
*E-mail: rosa.amorim@ufpe.br; amorim_rvs@hotmail.com

Abstract
Currently the goal of the pharmaceutical industry is the improvement of formulations of bioactive compounds of protein origin as insulin, hormones that can be employed for oral administration. The aim of this study was to develop hydrogel beads composed of chitosan (CS) and alginate (A) and their application in protein (BSA) delivery systems *in vitro*, as compared its stability in acid medium with CS beads, for the purpose of oral administration. The CS and A were used to form the hydrogels beads by coacervation methods and the beads characterization as morphology, bead size and the swelling ratio were studied in different physical states, FT-IR spectrum analysis also were performed. The hydrogel beads present good characteristics and stability and in general with size approximating 1000 μm. The release profile of BSA in different pHs in an orbital shaker 100rpm at 37° C, showed that the BSA delivery in hydrogel beads using 10mg/mL of BSA to loading the beads was sustained in the pH 7.3, but retained in acid pH and we can observe that in the acid medium the hydrogel beads are stable, can be employed in oral delivery systems of therapeutic peptides and proteins.

Keywords: Chitosan, hydrogel, delivery systems, BSA

INTRODUCTION

Natural polymers, as chitosan, have attracted attention for their use as vehicles in immobilization and controlled release systems for bioactive compounds in biomedical applications, due their biocompatibility and biodegradability, as well as their non toxicity to humans [1-3]. The delivery systems for drugs and vaccines acts in order to allow better efficiency and greater safety in therapy, since they are absorbed or encapsulated in carriers, mitigating the complications arising from treatment by conventional methods. Therapeutic peptides and proteins remain poorly bioavailability upon oral administration, one of the most comfortable ways for drug administration. Therefore, the oral route exhibits many inadequacies; the proteins are readily degraded, if taken orally, due to the harsh high acidity of stomach and the enzymatic attack in the upper small intestinal tract [4]. In the design of oral delivery of peptide or protein drugs, pH sensitive hydrogels have attracted increasing attention. Swelling of such hydrogels in the stomach is minimal and thus the protein release is also minimal. Due to increase in pH, the extent of swelling increases as the hydrogels pass down the intestinal tract. A variety of synthetic or natural polymers with acidic or basic pendant groups have been employed to fabricate pH sensitive hydrogels [1-5].
Chitosan (CS) has been widely used as base compound for the formation of these systems, acting as a carrier, through the formulation of films, beads and microparticulate systems [2]. The CS and A are cationic and anionic polymers, respectively, with physical and chemical properties favorable for the development of hydrogels that can be used to release therapeutic drugs, hormones or protein vaccines [2,5,6]. Bovine serum albumin (BSA) was used as a protein model for studies of *in vitro* release from CS beads and CS-A hydrogel beads, as potential carriers for oral delivery of protein drugs.

MATERIALS AND METHODS

Materials. Chitosan (CS)-Low Molecular Weight, alginate (A) and bovine serum albumin (BSA) were purchased from Sigma-Aldrich (St. Louis, MO, USA). All chemicals were analytic-grade and used directly without further purification.

Preparation of CS Beads and CS-A hydrogels beads and swelling studies. CS beads were prepared using a gel of 3% CS in 1% acetic acid which was streamed using an Insulin syringe 100 U (BD Ultra-Fine ^{TM}) in a solution of 2M NaOH (w/v). The CS-A hydrogel beads were obtained from the gel of 1.8% A, in which was streamed a solution of 0.2% CS in 1% acetic acid (v/v) and 6% $CaCl_2$ (w/v), under magnetic stirring, using an insulin syringe. The resulting beads were kept 24h in this medium to promote the stabilization of the polyelectrolyte complex, washed with distilled water, and frozen - 80°C and then freeze dryed (IP21 Liobrás). Swelling studies were conducted with dry beads in different buffers for 24 hours, according Abreu, et al., 2008[2].

BSA loading and encapsulation efficiency. For the loading of CS beads and CS-A hydrogel beads, 0.1 g of these were incubated with 10 mL of solution containing BSA (5 to 20mg/mL) in flask (25ml) and maintained in Shaker (G-25KC) 100 rpm at 37°C overnight. The drug encapsulation efficiency was determined using the following Equation established by Grenha et al. (2005) [7].

In vitro BSA release experiments. The in vitro release studies were performed in physiological saline solution (PBS) pH 7.3 (0.9%w/vNaCl) and KCl/HCl buffer pH 1.2 at 37±0.1 °C, using an orbital shaker 100 rpm. The 0.1 g of dried beads was placed in Erlenmeyer flasks (50 mL) containing 10 mL of the buffers. At a predetermined time, 1000 μL of samples were removed, the same quantities were replaced by fresh medium. These samples were assayed for BSA in a DU 640 Spectrophotometer at 595 nm by the Bradford method. The cumulative amount of the BSA released from the beads was quantified from the appropriate calibration curves.

RESULTS

Hydrogel beads characterization. The CS beads and CS-A hydrogel beads have mean sizes ±1000 μm after lyophilization. The morphological characterization of the beads, surface area and matrix performed by SEM, showed the CS beads (Fig. 1C) with porous matrix, featuring a sponge-type structure. Compared with CS beads, CS-A hydrogel beads displays the surfaces and matrix characteristically uniform, with lower porosity (Fig 1A and 1B).

FT-IR spectra of the A, CS and CS-A hydrogel were measured to evaluate the chemical interaction between CS and A. Analyzing the profile of the absorption spectrum of hydrogels, there have been changes in the modes of vibration of their peaks when compared to the spectrum of isolated polymers, characterizing the interaction between them (not shown). The appearance of the bands 1635 cm^{-1} and 1624 cm^{-1}, as well as the disappearance of the band 1596 cm^{-1} in hydrogel spectrum, characteristic of the amino group of CS, suggested the formation of polyelectrolyte complex between CS and A.

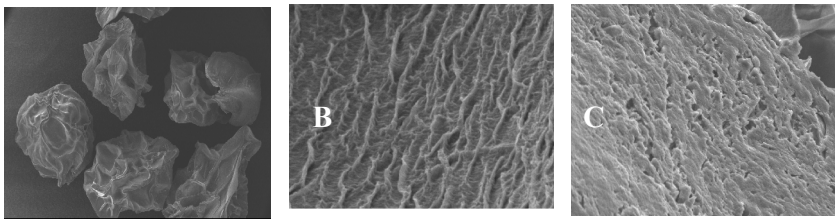

Figure 1. SEM images of (a) CS - A hydrogel beads; (b) surface details of CS – A hydrogel beads and (c) CS beads.

Drug release studies. BSA release from CS beads in PBS (pH 7.3) was determined over a time span of 48 hours (Fig. 2). All release profiles of the BSA using different BSA loading concentrations are similar, and exhibit a small burst release and then slow release at a constant but different rate. These CS beads loaded with BSA were not stable in release studies at pH 1.2. However, at this pH CS-A hydrogel beads remain unaffected, intact and displayed the release profiles of BSA in general with a low initial burst and retained output of BSA during the 48h of assay (Fig. 3a). In the release studies at pH 7.3 it could be seen that BSA release from these beads *in vitro* showed a very rapid initial burst, especially the higher the concentration of BSA for loading of the beads, however, no difference from the concentrations of 10 and 15 mg / mL was observed (Fig. 3b).

The degree of swelling of the sample CS-A hydrogel beads without drug, showed the highest swelling properties observed at pH 7.4 rather than at pH 1.2, in according with release ocuured in this pH. The BSA loading capacity of CS-A hydrogel beads was 87.0%.

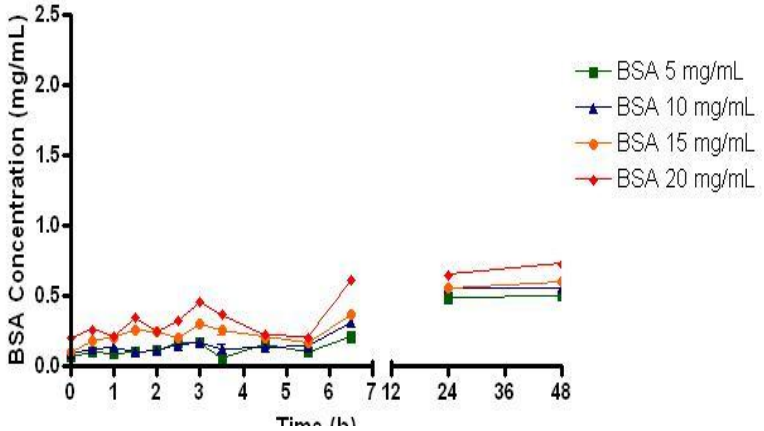

Figure 2. BSA release profile from CS beads at pH 7.3; BSA was loading in different concentration.

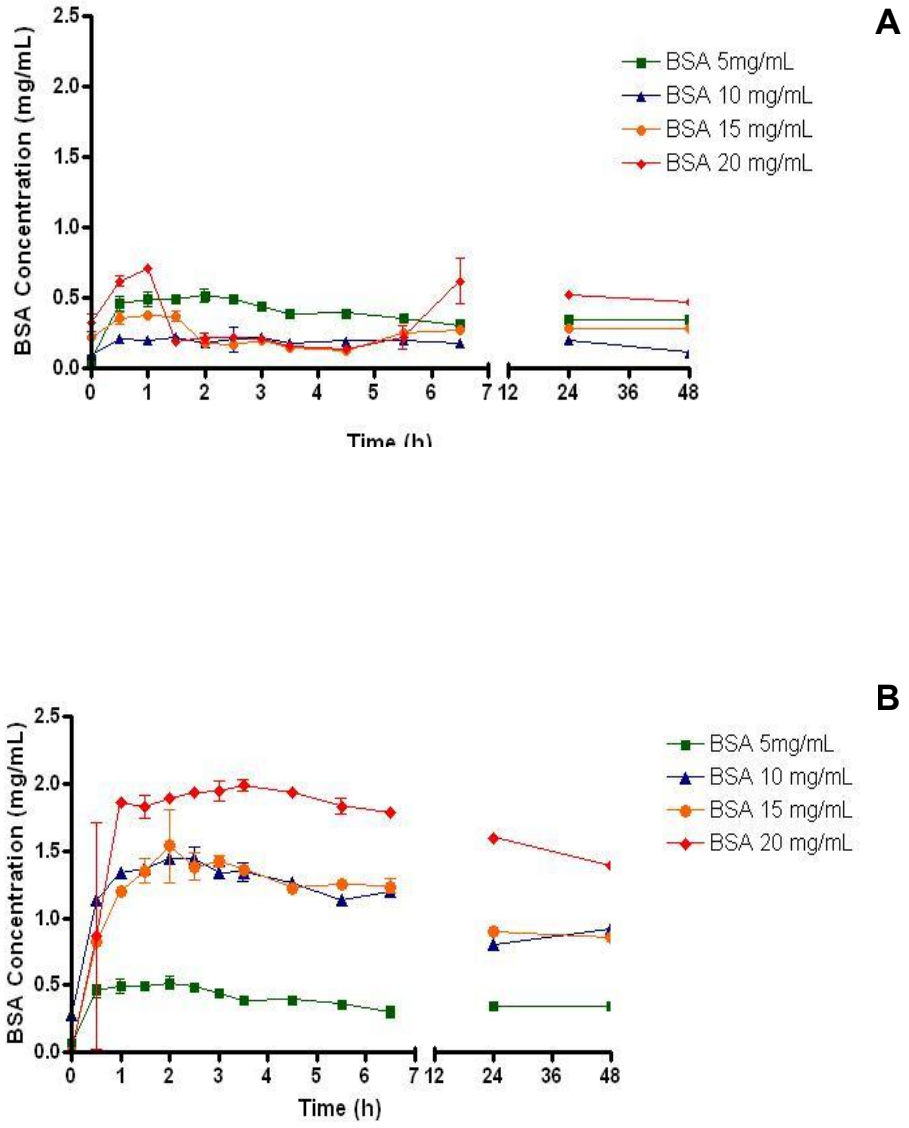

Figure 3. BSA release profile from CS-A hydrogel beads at pH 1.2 (a) and pH 7.3 (b); BSA was loading in different concentration.

DISCUSSION

The hydrogels have attracted considerable attention because of their potential in oral drug delivery systems [6]. The release of the drug from hydrogels is affected by the pH which can

influence the ionization of amino groups of CS and carboxyl groups of A. The complexation of A to CS makes these polymers stable in the face of changes in pH, reduces the porosity of the matrixes, reducing the spread of molecules seized and improved their stability in acidic media [1,9]. In relation to the BSA release studies, the CS-A hydrogel beads could be a good carrier to oral protein delivery systems, due to acidic conditions the protein remains on hold but when it is in an alkaline environment they swell thus releasing the substance contained in the beads. This fact probably is due to the higher concentration of the ionizable charges at pH 7.4, due to its dissociation constant (pKa) of 3.38 and 3.65 for the acid monomers manurônico and glucurônico respectively [3]. For the primary amino groups of CS pKa is between 6.0-6.5. Thus, at pH 1.2 most of their free amino groups are ionized, while with pH greater than pKa, the amino groups are less protonated, forming weaker electrostatic interactions [3, 10, 11].

CONCLUSIONS

The results indicate that the CS-A hydrogel beads could be a promising candidate biomaterial to oral protein delivery systems and the results of the BSA release reveal that there are possibilities to modulate the release of BSA by adjusting the concentration of the biopolymers and the protein concentration and . New assays are being performed to confirm the stability of BSA after released tests.

ACKNOWLEDGEMENTS

International Foundation for Science (IFS F/ 4095-5) Organisation for the Prohibition of Chemical Weapons-OPCW and CNPq 485316/2007-2.

REFERENCES

1. Yu, C.; Yin, B.; Zhang, W.; Cheng, S.; Zhang, X.; Zhuo, R. Sustained release of antineoplastic drugs from chitosan reinforced alginate microparticle drug delivery systems**.** *Colloids and Surfaces B: Biointerfaces* **68:** 245-249 (2009).
2. Abreu, F.O.M.S., Bianchini, C., Forte, M.M.C., Kist, T.B.L. Influence of the composition and preparation method on the morphology and swelling behavior of alginate-chitosan hydrogels. *Carbohydrate Polymers*. **74:** 283-289 (2008).
3. Saether, H. V.; Holme, H. K.; Maurstad, G.; Smidsrod, O.; Stokke, B. T. Polyelectrolyte complex formation using alginate and chitosan. *Carbohydrate Polymer*, **74.** 813-821 (2008).
4. Robert MS, Karlo P, Fanor B, Michael L, Tarek MF. The use of deoxycholic acid to enhance the oral bioavailability of biodegradable nanoparticles. *Biomaterials* **29**:703-708 (2008).
5. Cho, Y. I, Park, S., Jeong S. Y., Yoo, H. S. In vivo and in vitro anti-cancer activity of thermo-sensitive and photo-crosslink able doxorubicin hydrogels composed of chitosan–doxorubicin conjugates. *European Journal of Pharmaceutics and Biopharmaceutics* **73:** 59–65 (2009).
6. Min, K. H. , Park K., Yoo-Shin Kim , Bae S.M, Lee S., Jo H.G., Rang-Woon Park , In-San Kim et al. Hydrophobically modified glycol chitosan nanoparticles-encapsulated camptothecin enhance the drug stability and tumor targeting in cancer therapy. *Journal of Controlled Release* **127:** 208–218 (2008).
7. Grenha, A.; Seijo, B.; Lópes, C. R. Microencapsulated chitosan nanoparticles for long protein delivery. *European Journal of Pharmaceutical Sciences*. **25**: 427-437 (2005).
8. Chen, A., Hou, C. and Bao, J. Clinical study of gentamycin-loaded chitosan drug delivery system. *Chung Kuo Hsiu Chung Chien Wai Ko Tsa Chih*. **12**:355-8 (1998).
9. George, T. M., Abraham, E. Polyionic hydrocolloids for the intestinal delivery of protein drugs: Alginate and chitosan — a review. *Journal of Controlled Release* **114**: 1–14 (2006).
10. Kavimandan NJ, Losi E, Peppas N. Novel delivery system based on complexation hydrogels as delivery vehicles for insulin–transferrin conjugates. *Biomaterials* **27**:3846-

3854 (2006).
11. Haidar ZS, Hamdy RC, Tabrizian M. Protein release kinetics for core-shell hybrid nanoparticles based on the layer-by-layer assembly of alginate and chitosan on liposomes. *Biomaterials* **29**:1207–1215 (2008).

Antimicrobial analysis of gels and films from chitosan and *N,N,N*-trimethyl chitosan

Rejane C. Goy, Douglas de Britto, Odilio B. G. Assis*

Embrapa Instrumentação Agropecuária, Rua XV de Novembro, 1452, 13560-970 São Carlos, SP, Brazil
*E-mail: odilio@cnpdia.embrapa.br

Abstract
Chitosan and its derivatives have been explored as bactericidal and fungicidal agent in the inhibition against a large number of fungi and bacteria both gram-negative and gram-positive. Some antimicrobial mechanisms have been proposed being the most acceptable the presence of NH^{+3} and its interactions with the bacteria surface constituents. In this study the effectiveness of chitosan and water-soluble N,N,N-trimethyl chitosan against *Staphylococcus aureus* (gram-positive bacteria) and *Escherichia coli* (gram-negative bacteria) were evaluated in gel and cast film forms. The results show better activity against gram-negative microorganism, with influence of polymer concentration mainly for quaternized chitosan derivative.
Keywords: Antibacterial activity, Chitosan, Water-soluble chitosan; S. *aureus*; E. *coli.*

INTRODUCTION

Due the easily capacity to form gels and be transformed in films with good mechanical properties, chitosan has a potential for applications in several technological fields, such as in agriculture, food, medicine, biotechnology, textiles, polymers, and watertreatment. One important application area is its use as protective edible coating of natural products and foods. Chitosan coatings act against the development of microorganisms and also assists in the control of physiological, morphological and physicochemical changes.[1,2] Chitosan can be considered either bactericidal (killing the microorganisms) or bacteriostatic (preventing or inhibiting their growth), but hardly distinguished between the two mechanisms.

The N,N,N-trimethyl chitosan (TMC) is a partially quaternized derivative of chitosan synthesized to increase solubility in water at neutral or basic pH values, and thereby increasing the applications capability. TMC has several advantages upon the parent polymer where *in vivo* studies have shown that properties like absorption and biocompatibility are quite enhanced.[3]

In the TMC, the addition of permanent positive charges in the chains can be attained through the synthesis of quaternary chitosan salts - via the covalent addition of a substituent containing a quaternary ammonium group,[4] or by the quaternization of the amino groups in the parent polymer.[5] These quaternary salts have also shown to have greater bactericidal efficiency than the primary chitosan, since an increasing in amount of cationic sites will promote a better electrostatic interaction with microorganisms walls.[6,7] In function of their outer membrane composition, it has been demonstrated that hydrophilicity in gram-negative bacteria is significantly higher than in gram-positive bacteria, making them most sensitive to chitosan.[8] Additionally, the charge density on the bacteria cell surface also to play an important role in determining the amount of adsorbed chitosan. More adsorbed chitosan on hydrophilic surface would result in greater changes in the wall structure and consequently altering cell membrane permeability.[9] Such feature can explain, in part, why some gram-negative bacteria are most sensitive to chitosan.

In this study the effectiveness of chitosan and water-soluble N,N,N-trimethyl chitosan against gram-positive (*Staphylococcus aureus*) and gram-negative bacteria (*Escherichia coli*) were

assessed in function of the polymer concentration in gel and in film forms.

MATERIALS AND METHODS

The starting chitosan was medium molar weight purchased from Sigma-Aldrich (Brazil). For methylation reaction, the basic sequence consisted in an initial suspension of 1 g of chitosan (0.005 mol) in 16 cm^3 of dimethylsulfate (Synth, Brazil) and 4 cm^3 of deionized water. 1.2 g of NaOH (0.015 mol) and 0.88 g of NaCl (0.015 mol) were added and the solution mixed. The final product was obtained by precipitation with acetone. After rinsing, the derivative was filtered and vacuum dried. Methylation details and TMC characterization can be found elsewhere[5]. Gels were prepared by dissolving the commercial chitosan in 1% acetic acid in deionized water with constant stirring for 2 hours. Metlylated salt was directly dissolved in water. Concentrations of 0.5, 1.0, 2.0, 3.0 and 4.0 gL^{-1} were prepared for both materials. Films were then prepared by solution casting onto an acrylic plate. Solvents were allowed to evaporate at room temperature. After drying the films were peeled from the plate.

The antibacterial activity was evaluated according to the inhibitory halo area method. For that Petri dishes containing TSB (Tryptic Soy Broth) and agar medium were prepared and *E. coli* and S. *aureus* microorganisms inoculated after appropriated dilution. For gels testing parts of the medium were removed to form small holes where the gels were placed after the bacteria were inoculated. For films testing, pieces of them were cut and placed on the surface of culture medium previously inoculated with the microorganisms. The Petri dishes were left overnight inside a circulation oven for the bacteria to grow at 32-37 ^oC and inhibition zones measured on bases in the average diameter of the clear inhibition zone directly on the dishes.

RESULTS AND DISCUSSION

Figure 1 illustrates the antimicrobial activities by formation of inhibition zones for films of chitosan and TMC, both processed at a concentration of 2.0 $g \times L^{-1}$. Both materials present an effective antibacterial activity with larger zone to TMC in comparison to chitosan. For both type of bacteria tested inhibition zones around the films are visualized mainly for *S. aureus* growth whereas for *E. coli* no clear microbial inhibitions are evidenced. Similar results are obtained in gel form materials.

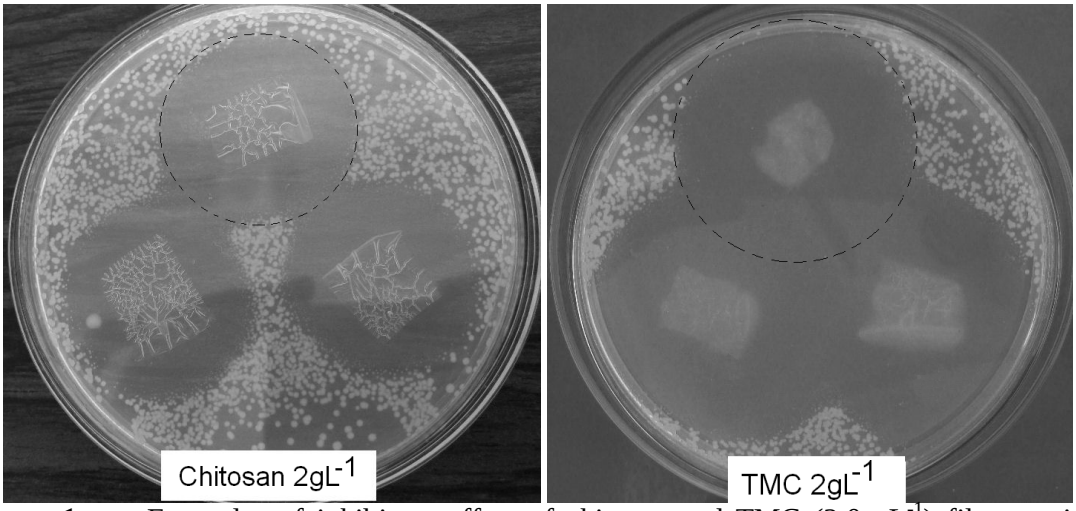

Figure 1. Examples of inhibitory effect of chitosan and TMC (2.0 gL^{-1}) films against gram-positive bacteria *S. aureus.*

These results in some way confirm a better antibacterial activity against gram-positive bacteria (*S. aureus*) is more effective than gram-negative (*E. coli*), which should be attributed to their different cell walls. In the gram-positive bacterium, the cell wall is fully composed of

peptide polyglycogen. According to Xie *et al.*[10] the peptidoglycan layer is composed of networks with plenty of pores, which allow foreign molecules to come into the cell without difficulty. But for *E. coli*, the cell wall is made up of a thin membrane of peptide polyglycogen and an outer membrane constituted of lipopolysaccharide, lipoprotein, and phospholipid. In such bilayer structure the outer membrane has high molecular weight and acts as a barrier against foreign molecules.

The film concentration also appears to play an important role in the antimicrobial activity, mainly for the TMC. For this derivative the measured inhibition zone increases exponentially with the concentration stabilizing up to 2 gL^{-1} (Figure 2). Further increases in the concentration of TMC result in no substantial improvement in the activity. Conversely, for commercial chitosan the antibacterial activity is confirmed to be inferior and reduces slightly as the concentration increases.

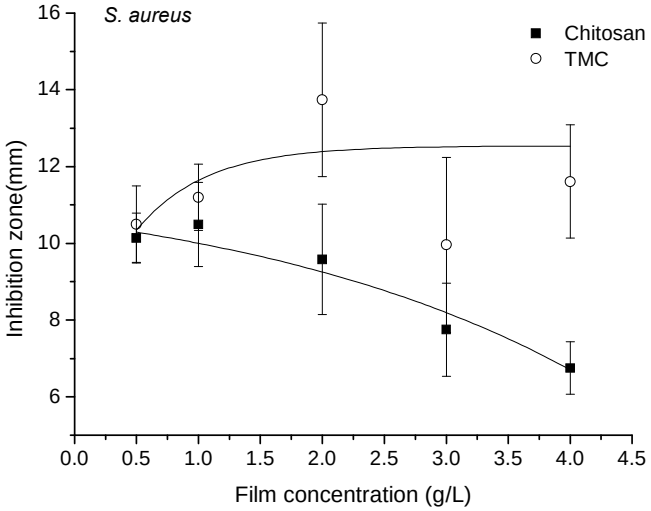

Figure 2. Inhibition zone in function of the film concentration, as measured against the bacteria *S. aureus.*

The inferior inhibitory effect observed to chitosan can be attributed to several factors though it is supposed that the relatively small number of charged amino groups in the molecules can be a determinant feature. In the quaternized salt positive charges are permanent in the polymer chains what results in better electrostatic interaction with the microorganisms walls and consequently a relatively higher antimicrobial activity. From the present tests it is not possible to determine an exact antimicrobial mechanism, anyway the effectiveness of water soluble chitosan (TMC) is evident.

CONCLUSIONS

The analyzed materials show effective antimicrobial activity against mainly gram-positive bacteria (*S. aureus*). The chitosan quaternary salt shown superior antimicrobial activity when compared with the chitosan and the material concentration in the films manufacture is important parameter, since increasing the film concentration also increases the inhibition zone formed but the same do no occurs with the chitosan, where the concentration is not so important, besides the inhibition is so effective too.

ACKNOWLEDGEMENTS

This work was supported by FAPESP and Embrapa (Rede AgroNano).

REFERENCES

1 Sharidi F, Arachchi JKV and Jeon Y-J. *Trends Food Sci Techn* **10**: 37-51(1999)

2 Britto D and Assis OBG. *Biol Macrom* **41**: 98-203 (2007).

3 Chen F, Zhang ZR, Yuan F, Qin X, Wang M and Huang Y. *Int J Pharm* **349**:226-33 (2008).

4 Curti E, Britto D and Campana-Filho SP. *Macromol Biosci* **3:**571-576(2003).

5 Britto D and Assis OBG. *Carbohyd Polym* **69:** 305-310(2007).

6 Simpson BK, Gagne N, Ashie INA and Noroozi E. *Food Biotechn* **11:** 25-44(1997).

7 Chung Y-C, Su Y-P, Chen C-C, Jia G, Wang H-L, Wu JCG and Lin J-G. *Acta Pharmacol Sinica* **25:**932-936 (2004).

8 Másson M, Holappa J, Hjálmarsdóttir M, Rúnarsson ÖV, Nevalainen T and Järvinen T. *Carbohyd Polym* **74:** 566–571(2008).

9 Goy RC, Britto D and Assis OBG. *Polímeros: Ciênc Tecnol*. 19:231-237(2009).

10 Xie W, Wang W and Liu Q. *Carbohyd Polym* **50:** 35-40(2002).

Chitosan blend biofilms: structural analysis, mechanical properties, thermic stability, and fungistatic acitivity against *Aspergillus niger*

A.P. Martinez-Camacho[1], M.O. Cortez-Rocha[1], J.M. Ezquerra-Brauer[1], A.Z. Graciano-Verdugo[2], E.I. Diaz-Rojas[1], M. Plascencia-Jatomea[1*]

[1] Departamento de Investigación y Posgrado en Alimentos. [2] Departamento de Ciencias Químico Biológicas. Universidad de Sonora, Hermosillo Sonora, México.
*E mail:apmartinezc@gmail.com

Abstract
Chitosan prepared from shrimp heads silage chitin had 100 kDa and 76.2% deacetilation degree. All chitosan films, made by casting, including those using sorbitol as plasticizer, shown a single glass transition temperature (168-174°C). An infrared spectroscopy analysis showed an increase on hydrogen bonds between sorbitol and chitosan amine groups which could results in the lower fungistatic effect on *A. niger* of the films.

Keywords: sorbitol, radial growth, spore diameter, glass transition temperature

INTRODUCTION

Chitosan, natural polymer derivate from chitin, has shown have antimicrobial activity on bacteria, yeast and some fungi[(1-4)]. It has been used to protect food products from microorganisms growth and also to preserve desirable characteristics [(2, 4-7)]. Chitosan is capable to form films when the solvent on the solution allows drying. Therefore, the films of pure chitosan have deficient mechanical properties but the addition of plasticizers improves it. Sorbitol, glycerol, polyethylenglicol, had been used as plasticizers on chitosan films[(8,9)]. The chitosan antimicrobial activity could be affected by these compounds and more studies are necessary to understand how this activity can be affected.

MATERIALS AND METHODOS.

Chitosan. QE chitosan was obtained through heterogeneous deacetylation of the chitin obtained from fermented silage made of shrimp heads[(11).] QM Chitosan was commercial grade (Fluka, Biochemika, Japan) obtained by chemically treating crab waste. The molecular weight (Mw) of chitosan was determined using the viscometric method [(12-13).] The deacetylation degree (%DD) was determined by FT-IR (Perkin Elmer FT-IR Spectrum GX) analysis[(14).]

Chitosan film elaboration. The chitosan films were elaborated by casting solutions of QE and QM 1% (w/v) in 0.1 M acetic acid and adding 20% (w/w) of sorbitol as a plasticizing agent. The physical properties of plasticized (pQES and pQMS) and non-plasticized (pQE and pQM) chitosan films were compared to those of commercial cellophane film (Control, C). The thickness of the chitosan films was obtained by a micrometer (PB-1 JIS.B.7502 Mitutoyo, USA). The strength and elongation were evaluated on an United equipment (SSTM 5KN model, USA) according to ASTM D882-94. The differential scanning calorimetry (DSC) was carried out heating from 26°C up until 300°C at 10 °C/min. An FT-IR analysis was made in a spectral range from 4000 to 400 cm^{-1}. Morphology images of the surface of films inoculated with *A. niger* were obtained by scanning electron microscopy (Jeol JSM 5410LV, Japan).

Fungistatic activity of chitosan against *Aspergillus niger*. A spore concentration of $1x10^5$ spores/mL on 0.1% (v/v) Tween 80 of *A. niger* (NRRL 3) was used. The chitosan concentration in the culture media was 2.82 g/L (w/v), with a final pH of 4.5[(3)]. Agar containing no chitosan with pH adjusted to 4.5 with 0.1 M of acetic acid was used as control.

The radial extension of the colony at 25°C was measured each 24 h until the control reached the plate border[15] and the fungistatic index was calculated[16]. All the measurements were carried out in triplicate.

Fungistatic activity of chitosan films. The prepared films were immersed in NaOH solution at 0.1% (w/v), cut into discs of 6 mm and sterilized by exposure to ultraviolet light before being inoculated. Radial growth of *A. niger* spores were determined[15]. The diameter of the spores was determined to a 40x objective by image analysis using Image-ProPlus version 6.3 software (Media Cybernetics Inc., USA), using an optical microscope (Olympus CX31, Japan) connected to an Infinity 1 camera.

RESULTS

The yields of chitin and chitosan obtained from fresh shrimp waste were of 2.38 and 1.59% respectively. The %DD (76.2) was similar to those from a commercial chitosan (78.03) meanwhile the QE Mw (100kDa) was lower than QM (480kDa). The chitosan films' thickness, mechanical properties and glass transition temperatures are shown in Table 1. The addition of sorbitol did not affect ($P \geq 0.05$) the films thickness but increased significantly the elongation of pQES films with respect to control (data not shown). It was found that the pQE and pQES films presented lower ($P \leq 0.05$) tensile strength (TS) values, whereas those of pQM and pQMS were similar to control. The presence of sorbitol in pQES film reduces the necessary effort for the deformation, as well as the deformation of the films before their rupture. A single value of Tg with not significant differences between treatments ($P \geq 0.05$), was observed in the films, so it can be assume that the sorbitol and chitosan were miscible and the degree of deacetylation of chitosan does not affect the Tg values of chitosan films. The plasticizer may have contributed to an ordering of polymer chains influenced by their degree of

Table 1. Physicochemical properties and fungistatic activity of the chitosan films prepared by the casting technique.

Treatment	Thickness (mm)	TS (mPa)	Tg (°C)	FI at 72h(%)	Spore diameter (μm)
QM	_	_	_	56.16[a]	_
QE	_	_	_	47.26[a]	_
pQM	0.04 ± 0.01[a]	54.42±10.51[b]	170.0a	33.47 ± 8.09[a]	4.05 ± 0.17a
pQMS	0.06 ± 0.02[a]	28.60±10.21[c]	172.2a	27.08 ± 3.56[a]	3.87 ± 0.11a
pQE	0.03 ± 0.01[a]	25.16±4.69[c]	170.9a	15.66 ± 1.78[a]	4.18 ± 0.23a
pQES	0.02 ± 0.01[a]	28.91±7.86[c]	169.2a	22.04 ± 6.22[a]	4.54 ± 0.22a
C	0.03 ± 0.00[a]	79.98±3.81[a]	163.9a	25.40 ± 6.56a	4.98 ± 0.33a

TS: tensile strength; Tg: Glass transition temperature; FI: Fungistatic index; QE: silage chitosan; QM: commercial chitosan (Fluka, BioChemika, Japón); pQE: silage chitosan film; pQES: silage chitosan+sorbitol film; pQM: commercial chitosan film; pQMS: commercial chitosan+sorbitol film; C: commercial cellophane film. Data, followed by their standard errors, are means of three experiments. Treatment means were separated using the Tukey test ($P \geq 0.05$).

polymerization favoring the interactions between it and increasing its crystalline character. FT-IR spectra of chitosan films show a broad peak between 3200 and 3570 cm^{-1}, attributed to stretching of OH bonds in the molecule and to the hydrogen bonds set in films with water and sorbitol.

In culture medium added with chitosan, QM and QE had higher ($P \leq 0.05$) inhibitory effect on the colony radius with respect to control at 96 h. Both chitosans have a similar %DD, which may explain having similar fungistatic activity, as the %DD shows the proportion of free amino groups that are directly related to the antimicrobial activity. The effect of chitosans was fungistatic but not fungicidal. It has been reported that chitosan and its derivatives are not able to inhibit 100% the growth of other fungi[3,15-17]. QE and QM presented inhibition in the germination stage. In the other hand, lower but no significant differences ($P \geq 0.05$) in fungistatic activity of all chitosan films were observed. Using the agar/fungi/film inoculation system the fungistatic activity of the films was moderately higher (data not shown) than the observed in chitosan on culture media, may be due to the synergistic effect of chitosan and low permeability of the films. The diameter of the spores (Table 1) of *A. niger* was not affected significantly ($P \geq 0.05$) by the films of chitosan, having also a small amount of visible spores. SEM images of the films showed a brittle structure and some porous (Figure 1).

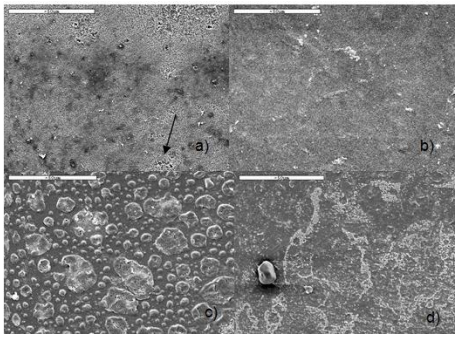

Figure 1. SEM images from chitosan films by casting: a) pQE; b) pQES; c) pQM; d) pQMS.

CONCLUSION

Chitosan films retain its antimicrobial activity before the preparation process and are more effective controlling the first stage of *A. niger* growth, and also had good mechanical properties that makes them suitable for its possible use as an fungistatic film to protect food from fungal contamination.

REFERENCES

1. Zivanovic S, Li J, Davidson M, Kit K. *Biomacromolecules.* 2007;8(5):1505-10.
2. Vargas M, Albor, A, Chiralt A, Gónzalez-Martinez, C. *Postharvest Biol Technol* 2006;41:164-171.
3. Martínez-Camacho, AP. Tesis de Licenciatura. Universidad de Sonora. Hermosillo, Sonora, México. 2006;126p.
4. Sebti I, Martial-Gros A, Carnet-Pantiez A, Grelier S, Coma V. *J Food Sci* 2005;70(2):M100-4.
5. Bhale S, No HK, Prinyawiwatkui W, Farr AJ, Nadarajah K, Meyers SP. *J Food Sci* 2003;68(7):2378-83.
6. Chien PJ, Sheu F, Yang FH. *J Food Process Eng* 2007;78:225-9.
7. Wu Y, Rhim JW, Weller CL, Hamouz F, Cuppett S, Schnepf M. *J Food Sci.* 2000;65(2):300-4.
8. Fernandez-Cervera M, Heinämäki J, Krogars K, Jörgensern AC, Karjalainen M, Iraizoz-Colarte A, Yliruusi J. *J Pharm Sci Technol* 2004;5(1):1-6.
9. Srinivasa PC, Ravi R, Tharanathan RN. *Food Hydrocolloids*. 2007; 21:1113-22.
10. Sebástien F, Stéphane G, Copinet A, Coma V. *Carbohydr Polym* 2006;65:185-193.

11. Jaime-Quijada EA. Tesis de Licenciatura. Universidad de Sonora. Hermosillo, Sonora. 2008. 76p.
12. Hwang KT, Jung ST, Lee GD, Chinnan MS, Park YS, Park HJ. *J Agric Food Chem* 2002;50(7):1876-82.
13. Rinaudo M, Milas M, Le Dang P. *Int J Biol Macromol* 1993;15:281-5.
14. Khan TA, Peh KK, Ch'ng, HS. *J Pharm Sci Technol* 2002;5(3):205-12.
15. Plascencia-Jatomea M, Viniegra G, Olayo R, Castillo-Ortega MM, Shirai K. *Macromol Biosci* 2003;3(10):582-6.
16. Guo Z, Chen R, Xing R, Liu S, Yu H, Wang P, Li C, Li P. *Carbohydr Res* 2006;341: 351-4.
17. Hernández-Lazaurdo AN, Bautista-Baños S, Velázquez-del Valle M G, Méndez-Montealvo MG, Sánchez-Rivera MM, Bello-Pérez LA. *Carbohydr Polym,* 2008;73(4):541-7.

Extruded chitosan/polyethylene composite films: physicochemical and fungistatic properties

A.P. Martínez-Camacho,[1] A.Z. Graciano-Verdugo,[2] J.M. Ezquerra-Brauer,[1] M.O. Cortez-Rocha,[1] M.M. Castillo-Ortega,[3] H.C. Santacruz-Ortega,[3] M. Plascencia-Jatomea[1]*

[1] DIPA
[2] DCQB
[3] DIPM, Universidad de Sonora. Hermosillo, Sonora, México.
*E-mail: apmartinezc@gmail.com

Abstract
Extrusion of composite blends of chitosan/low density polyethylene/ethylene acrylic acid constitutes an alternative to obtain novel and useful materials.

Keywords: chitosan blend films; extrusion; low density polyethylene; Primacor 1430

INTRODUCTION

Because of its similarities with macromolecular substances, immunogenic properties and biodegradability, chitosan has been employed as biomaterial with useful properties that can be achieved by blending chitosan and synthetic polymers. Little research has been conducted in melt blending of synthetic polymers and chitosan, however, extrusion offers advantages as it facilitates to obtain partial or completely biodegradable materials, besides improving the mechanical properties. The aim of this work was to obtain films by extrusion of composite blends of chitosan/low density polyethylene/Primacor 1430 (Dow), and to study the mechanical, structural and fungistatic properties against *Aspergillus niger*.

MATERIALS AND METHODS

Commercial-grade chitosan (Fluka, Biochemika, Japan) with low viscosity (<200 mPa·s), was used. For the extrusion, low density polyethylene (LDPE), LBA 253 (Muehlstein International-Latin America, Norwalk, Connecticut, USA), and ethylene acrylic acid copolymer (Primacor* 1430) (The Dow Chemical Co.) were used. The molecular weight (MW) of chitosan was determined by using the viscometric method[1,2] and the MW values were calculated using the Mark-Houwink-Sakurada equation.[3] The deacetylation degree (%DD) of chitosan was determined by Fourier Transform Infrared Spectroscopy (Perkin Elmer FT-IR Spectrum GX) analysis.[4]

Formulations of the composite blends (Table 1) were prepared by mixing the LDPE as a thermoplastic polymer, chitosan powder and Primacor 1430 as adhesive. The composite blends were firstly pelletized by extrusion on a monohusillo extruder machine (Beutelspacher, México, D.F.) and then were extruded in a LME Laboratory Mixing Extruder (ATLAS Polymer Evaluation Products, USA) (Figure 1).[5] The film thickness was determined by using a Mitutoyo micrometer (PB-1 JIS.B.7502, USA).

FT-IR analysis[6] and stress-strain mechanical properties (United equipment, SSTM 5KN model, USA) according to the conditions set by ASTM D-1708-96, were evaluated. Scanning electron microscopy (Jeol JSM 5410LV, Japan) observations of films were carried out.[7,8] The radial growth of *Aspergillus niger* was determined by using two inoculation systems, above (agar/film/inoculation) and below (agar/inoculation/film) the film, at 25°C. The diameter of the fungi spores and hyphae was determined by image analysis (Image-Pro Plus software, Media Cybernetics Inc., USA). Previous to being inoculated, the extruded films were sterilized by exposure to UV light on each side.

Table 1. Formulations of the composite blends of chitosan, low density polyethylene (LDPE) and ethylene acrylic acid copolymer (Primacor 1430, Dow) as adhesive.

Chitosan (%)	Chitosan:Adhesive:LDPE (%)*		
0	0:0:100	0:1:99	0:10:90
5	5:0:95	5:1:94	5:10:85

*100 g of composite blend were prepared.

RESULTS AND DISCUSSION

The extruded films containing chitosan were homogeneous, slightly transparent and brittle (Figure 1). Differences (P≤0.05) in the extruded film thickness were observed, finding higher thickness in the composed films of 10% Primacor and 90% LDPE.

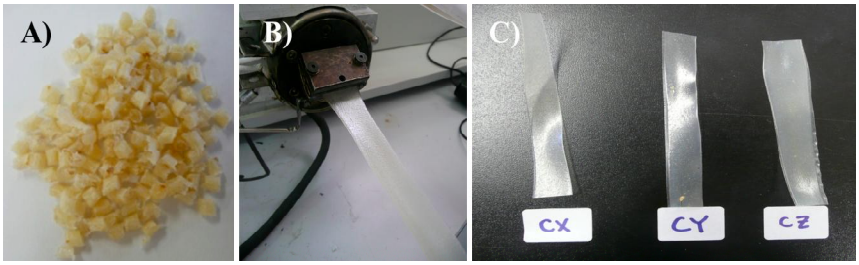

Figure 1. Extruded films containing chitosan, Primacor 1430 (Dow) and low density polyethylene (LDPE): A) pellets of chitosan/LDPE/adhesive composite blend; B) Extrusion of the chitosan composite blend pellets; C) Extruded films containing chitosan: CX: 95% LDPE + 5% chitosan; CY: 94% LDPE + 5% chitosan + 1% adhesive; CZ: 85% LDPE + 5% chitosan + 10% adhesive.

The FT-IR spectra of the 90% LDPE + 10% adhesive (Figure 2) and 85% LDPE + 5% chitosan + 10% adhesive films showed the appearance of a peak at 1704 cm^{-1}. These both types of films contain 10% adhesive and only the second one contains chitosan, therefore such peak can be attributed to intermolecular interactions between adhesive and LDPE. The characteristic of chitosan band at 1650 cm^{-1} was not observed, possibly due to an interaction of the group amino with the molecules of LDPE and adhesive.

Regardless of the concentration of adhesive, the addition of chitosan in to the mixtures did not increase (P>0.05) tensile strength of the films with respect to control of LDPE (Figure 3). The presence of chitosan decreased (P≤0.05) the percentage of elongation of the extruded films with respect to LDPE control, with and without adhesive, suggesting the presence of possible electrostatic interactions between molecules of adhesive and LDPE. However, with increasing concentration of adhesive (10%) in mixtures of chitosan (5%) + LDPE (85%), has significantly increased the elongation of the material with respect to the film of 95% LDPE + 5% chitosan.

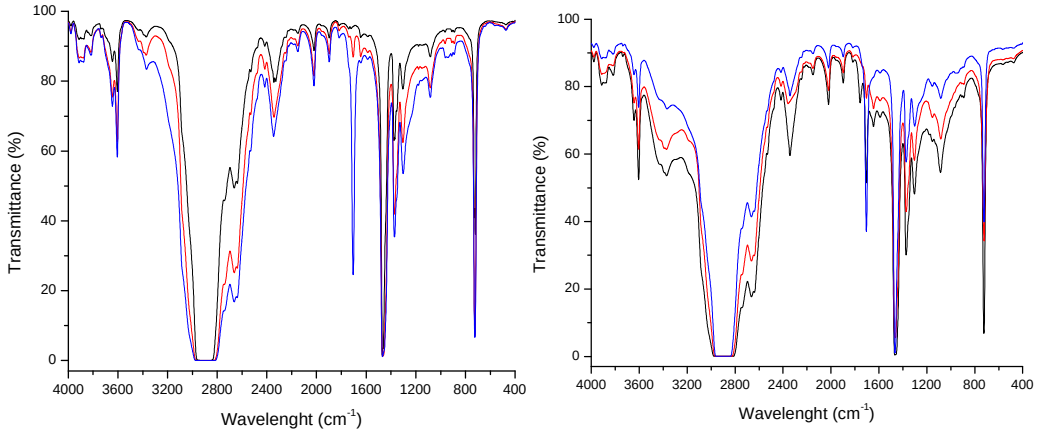

Figure 2. FT-IR spectra of the composite blend films. **(A)** Controls, without chitosan: (—) Low density polyethylene, LDPE; (—) 99% LDPE + 1% PRIMACOR 1430 (adhesive); (—) 90% LDPE + 10% adhesive. **(B)** Composite blends with chitosan: (—) 95% LDPE + 5% chitosan; (—) 94% LDPE + 5% chitosan + 1% adhesive; (—) 85% LDPE + 5% chitosan + 10% adhesive.

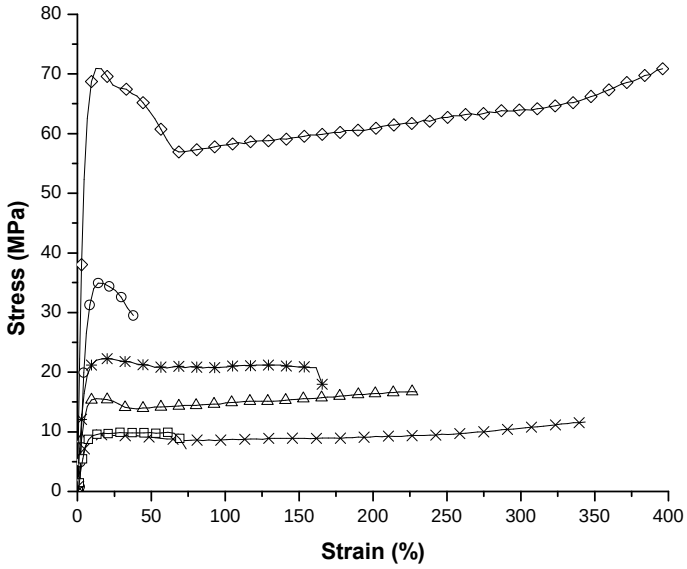

Figure 3. Stress-strain graph of the composite blend films. (×) Low density polyethylene, LDPE; (△) 99% LDPE + 1% PRIMACOR 1430 (adhesive); (◇) 90% LDPE + 10% adhesive; (○) 95% LDPE + 5% chitosan; (□) 94% LDPE + 5% chitosan + 1% adhesive; (∗) 85% LDPE + 5% chitosan + 10% adhesive.

Lack of adhesion led to the formation of pores due to the debonding of the fibers upon the application on stress in a particulate-filled material.[9] Thus, the mechanical performance of a filled polymer depends on the strength and modulus of the filler, which can explain the decrease in tensile strength.

Since chitosan particles did not melt, the morphology of the extruded films containing chitosan was slightly heterogeneous. Formation of cavities in the cross-section and polymer aggregates located mainly under the skin of the films were observed (Figure 4), which were reduced and dispersed by using higher adhesive concentration.

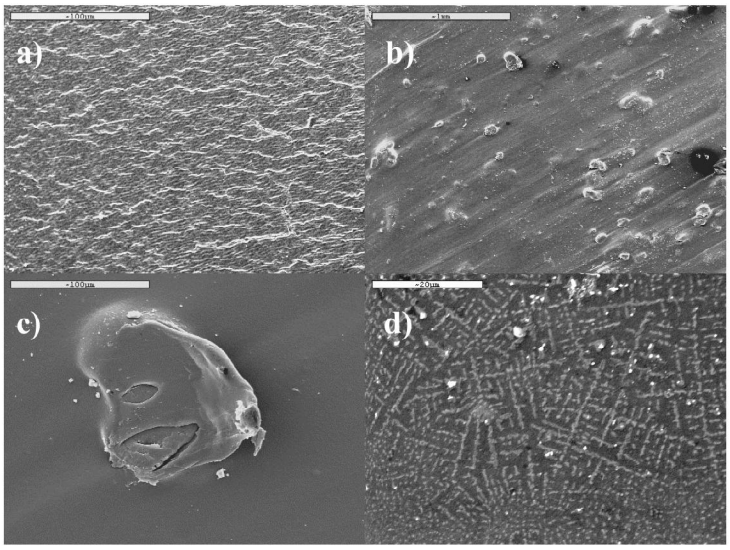

Figure 4 Scanning electron micrographs of the extruded chitosan films: a) 99% LDPE + 10% adhesive; b) and c) 94% LDPE + 5% chitosan + 1% adhesive; d) 85% LDPE + 5% chitosan + 10% adhesive.

Even though the diameter of the spores of *A. niger* was not affected ($P>0.05$) when in contact with the extruded films with chitosan, differences ($P\leq0.05$) were observed in the average diameter of hyphae with respect to the LDPE control, with and without adhesive (data not shown). In spite of the amount of adhesive, the inclusion of chitosan in the material caused a swelling of the hyphae.

CONCLUSIONS

Chitosan, an important biomaterial, can be melt blended with low density polyethylene and Primacor 1430 to produce materials with acceptable properties. Besides increasing the elongation of break of the extruded films containing chitosan, the Primacor addition reduced the size of the polymer aggregates located mainly under the skin of the films.

ACKNOWLEDGEMENTS

Financial support of the CONACyT (Project No. 53493 J1) is gratefully acknowledged.

REFERENCES

1 Mathew S, Brahmakumar M, and Abraham TE, *Biopolymers* **82**: 176-187 (2006).
2 Hwang KT, Jung ST, Lee GD, Chinnan MS, Park YS, and Park HJ, *Journal of Agricultural and Food Chemistry* **50**(7): 1876-1882 (2002).
3 Rinaudo M, Milas M, and Le Dang P, *International Journal of Biomacromolecules* **15**: 281-285 (1993).
4 Khan TA, Peh KK, and Ch'ng, *Journal of Pharmacy and Pharmaceutical Science*, **5**(3): 205-212 (2002).
5 Castillo-Ortega MM, Del Castillo-Castro T, Encinas JC, Perez-Tello M, De Paoli MA, and Olayo G, *Journal of Applied Polymer Science* **89**(1): 179-183 (2003).
6 Uriarte-Montoya MH, Arias-Moscoso JL, Plascencia-Jatomea M, Santacruz-Ortega H, Rouzaud-Sández O, Cardenas-Lopez JL, Marquez-Ríos E, and Ezquerra-Brauer JM,

Bioresource Technology **101**(11): 4212-4219 (2010)
7 Plascencia Jatomea M, Viniegra G, Olayo R, Castillo-Ortega MM, and Shirai K, *Macromolecular Bioscience* **3**(10): 582-586 (2003).
8 Echlin P, *Handbook of Sample Preparation for Scanning Electron Microscopy and X-Ray Microanalysis*. Ed. Springer, New York, USA. 330p. (2009).
9 Correlo VM, Boesel LF, Bhattacharya M, Mano JF, Neves NM, and Reis RL, *Materials Science and Engineering A* **403**: 57-68 (2005).

Microspheres of Chitosan conjugates covalently attached to steroids with potential biological activity as agrochemicals.

Javier Pérez[1]*, Richard Szopko[2], Claudia Schmidt[2], Carlos Peniche[3]

[1] Center of Natural Products, Faculty of Chemistry, University of Havana. Zapata S/N entre G y Carlitos Aguirre, Vedado, CP 10400, La Habana, Cuba. Tel: +53-7-8702102.
[2] Department of Chemistry, Faculty of Natural Sciences, University of Paderborn, Germany. Warburger Str. 100, D-33098 Paderborn, Germany.
[3] Center of Biomaterials, University of Havana. Ave. Universidad S/N entre G y Ronda, Vedado, CP 10400, La Habana, Cuba.
*Email: javierp@fq.uh.cu ; cybership01@fastmail.fm

Abstract
Chitosan microspheres (CS) linked to diosgenin and brassinosteroids monoesters with agrochemical activity were prepared by several methods. The steroid contents found by elemental analysis were between 15-57 wt-% and were dependent on the nature of the employed linker and the preparation method. Microspheres showed the CS and steroid FTIR characteristic peaks. Particle sizes ranged from 40 to 790 μm, with morphology dependent on selected method to obtain CS microspheres. Differential scanning calorimetry revealed the effect of the linked steroid. These compounds are released in acidic aqueous solution and release was extended up to 48 h.

Keywords: steroids; agrochemical; chitosan conjugates; drug delivery

INTRODUCTION

Chitosan is a biocompatible, biodegradable, nontoxic and mucoadhesive polymer, widely used as delivery matrix for the release of drugs in humans and animals, and non-steroidal agrochemicals in agriculture. [1-8] The antifungal and antibacterial activity of chitosan[9] and the reported ability to induce metabolic changes in plants allows it to increase the yield of crops, improving the germination of seeds and resistance against plagues.[10] The use of CS for controlled delivery of brassinosteroids (BS) will make possible to bring about the positive reported qualities of CS[11,12] with the beneficial effects of brassinosteroids on plants promoting the growth and resistance against several plagues. [13-17]
This article reports on linking of dicarboxylic diosgenin and brassinosteroid monoesters with biological activity to chitosan microspheres to achieve their controlled release. These novel delivery systems for agrochemicals base their action in hydrolysis and diffusion from the polymer matrix. Diosgenin derivatives to be released exhibit antiviral, antitumor and anticancer activity and the novel brassinosteroids studied are commercial agrochemicals.[13-21] Results are compared with those obtained by direct encapsulation of steroids without linking them to CS microspheres.

MATERIALS AND METHODS

Chitosan (deacetylation degree, DD = 85.2% determined by ^{1}H-NMR, Mv = 2.55×10^5) was obtained by extensive deacetylation of chitin isolated from shells of common lobster (*Panulirus argus*) at the Center of Biomaterials of the University of Havana, Cuba. Diosgenin and BS monoesters were synthesized as reported. [22] The solvents and reagents employed were purchased from Sigma-Aldrich and used without further purification.
The structures of diosgenin monoesters, monosuccinate of diosgenin (MSD), monoitaconate of diosgenin (MID), monomaleate of diosgenin (MMD) and BS monoesters (MSDI-31,

MIDI-31, MMDI-31, MSS-7, MIS-7 and MMS-7) are shown in Fig. 1.

Microspheres preparation

Chitosan microspheres (CS1) were obtained by simple coacervation-precipitation and cross-linking with sodium tripolyphosphate as reported. [23]

Chitosan microspheres (CS2) were also prepared by a water-in-oil emulsion-cross-linking with glutaraldehyde-evaporation as reported by Karewicz et al. [24]

Linking of the steroids to the CS microspheres

The CS microspheres were washed with an excess of N,N-dimethylacetamide (DMA) and stored 1 h on DMA at room temperature. 0.10 g (0.51 mmol) of these CS microspheres were filtered out and transferred into a 25 mL two-necked flask containing 10 mL of a 15% (w/v) solution of $LiNO_3$ in DMA. 0.13 g (1.03 mmol) of N,N'-diisopropylcarbodiimide, 10 mg (0.08 mmol, c.a. 5 wt-% Vs. steroidal monoester) of 4-(N,N'-dimethylamine)pyridine and 0.20 g (c.a. 0.4 mmol) of steroidal monoester were added in this sequence. The suspension was left bubbling with argon and stirring at 100 rpm overnight at 40 ^{o}C. Afterwards the microspheres were filtered out and washed several times with water, methanol and diethyl ether, in this order, and dried at 60 ^{o}C under vacuum.

Fourier transform infrared (FTIR) spectroscopy

The FTIR spectra of these microspheres were measured with an attenuated total reflection FTIR (ATR-FTIR) instrument (Perkin-Elmer, GB). Spectra were acquired with accumulation of 32 scans and a resolution of 4 cm^{-1}. Samples were prepared by KBr pellet method.

Elemental analysis

Elemental analysis was performed on a Varian MicroCube Analyzer with burning temperature of 1150 ^{o}C.

Differential Scanning Calorimetry studies

Calorimetric studies were performed with a Perkin-Elmer Differential Scanning Calorimeter Pyris 1 and analyzed with the Pyris 1 software (version 6.0.0.033) included. These studies were conducted with sample weights of approximately 8 mg, under a nitrogen dynamic flow of 20.0 mL min^{-1} and heating-cooling speed of 10 ºC min^{-1}. [25] Samples were deposited in aluminium capsules and hermetically sealed. Indium was used for calibration. Enthalpy (ΔH in J g^{-1} dry weight) and peak temperature were computed automatically. The samples were heated and cooled from -30 to 300 ºC.

Optical and electron microscopy

Microspheres size and size distribution were determined with a Nikon Eclipse E-400 optical microscope. The morphology of microspheres was studied with a JEOL JSM 6300F scanning electron microscope. Samples were sputtered on a graphite plate and analyzed without coating.

In-vitro drug release of the CS microspheres

25 milligrams of linked steroids-CS microspheres were placed in volumetric flask containing PBS solution at total volume of 25 mL and incubated at 30 ^{o}C with constant agitation at 100 rpm. 1 mL of solution was periodically withdrawn of the flask and replaced with equal volume of fresh solution to maintain sink conditions. The amount of released steroids was calculated by recording the UV absorbance of aliquots at 250 nm (DI-31 and S-7 monoesters) and 280 nm (diosgenin monoesters).

RESULTS AND DISCUSSION

Preparation of diosgenin and BS monoesters linked CS microspheres

The method employed to prepare the CS-steroid conjugates involved mild and not destructive conditions affording steroid contents between 11-57 wt-% (Table 1). The steroid content was generally higher employing CS1 microspheres.

The CS and steroid-linked CS particles obtained had spherical shape. After drying in vacuum

at 60 ^{o}C their size was significantly reduced and some of them showed an irregular shape when inspected at the optical microscope. The size distribution of the microspheres was evaluated after measuring the diameter of 85–90 particles. The size of CS microspheres showed an important dependence of the selected preparation method. The mean values for CS1 microspheres varied from 250 to 790 μm, while for CS2 microspheres they ranged from 40 to 280 μm. These particle sizes are consistent with those reported in other studies, [5, 26, 27] but smaller than free steroids loaded CS microspheres.[23] CS2 microspheres containing MID and MMD showed bimodal size distributions. This was probably due to a variation of experimental parameters during the microspheres preparation or the linking process.

Table 1. Steroid content (wt-%) by elemental analysis. CS1: chitosan microspheres obtained by simple coacervation-precipitation-cross-linking with sodium tripolyphosphate. CS2: chitosan microspheres obtained by water-in-oil emulsion glutaraldehyde cross-linking-evaporation.

	%		%		%
MSD-CS1	20	MSDI31-CS1	19	MSS7-CS1	23
MID-CS1	44	MIDI31-CS1	55	MIS7-CS1	57
MMD-CS1	18	MMDI31-CS1	31	MMS7-CS1	25
MSD-CS2	15	MSDI31-CS2	18	MSS7-CS2	21
MID-CS2	41	MIDI31-CS2	38	MIS7-CS2	29
MMD-CS2	17	MMDI31-CS2	27	MMS7-CS2	31

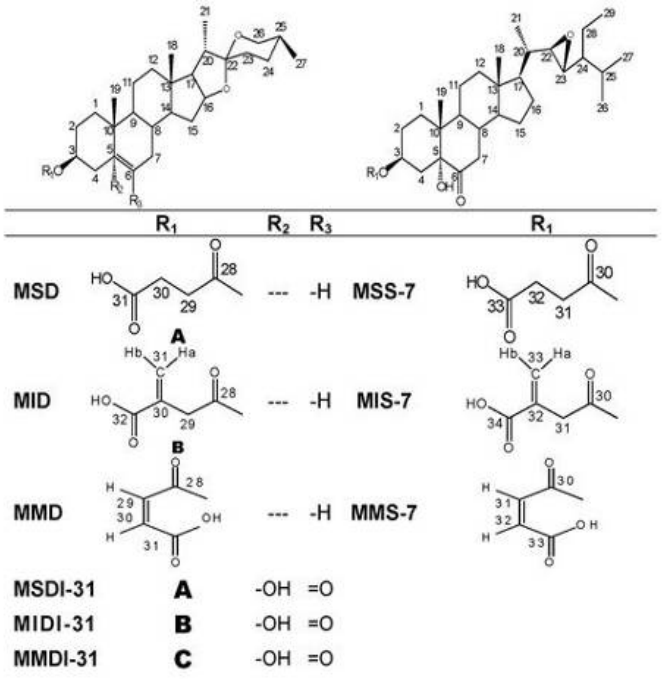

Figure 1. Structure of steroids linked to CS.

Fig. 2 shows the SEM images of linked diosgenin-CS1 and CS2 microspheres. The linked CS1 microspheres presented some wrinkles on the surface and a porous surface at higher

magnifications. The linked CS2 microspheres had smooth surface morphologies exhibiting a more compact surface at higher magnifications. These differences in surface morphology may be attributed mainly at the preparation method for obtaining the CS particles. This porosity of CS1 microspheres can explain the higher substitution by steroid during the linking process, affording superior steroid contents as shown (Table 1).

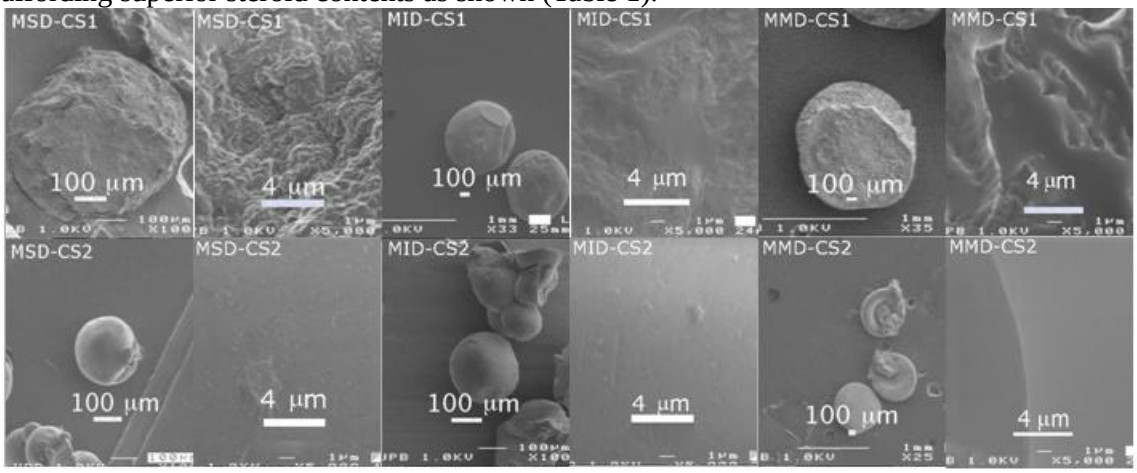

Figure 2. SEM micrographs of linked steroid-chitosan microspheres at 100 and 5000 magnifications.

Structural analysis

The FTIR spectra of linked steroids-CS1 microspheres between 2250- 1250 cm^{-1} are shown in Fig. 3. The spectrum of placebo CS microspheres is also included for comparison.

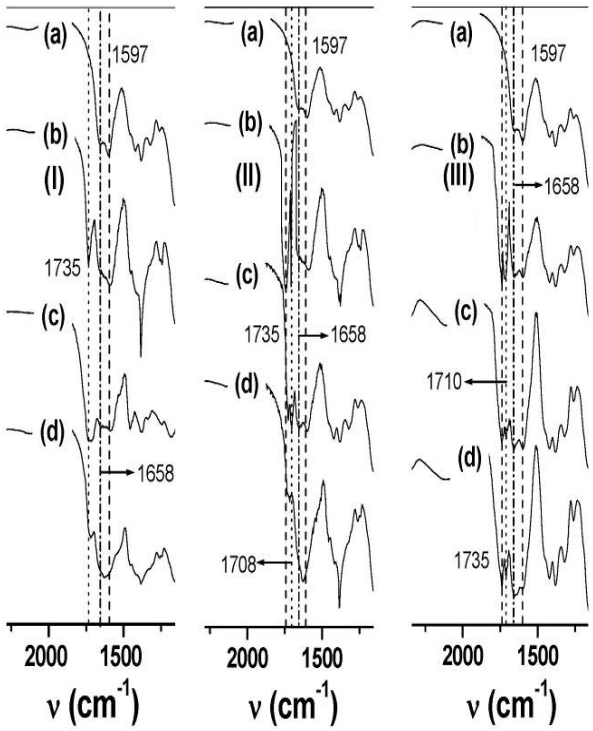

Figure 3. Infrared spectra of I:(a) CS1, (b) MSD-CS1, (c) MID-CS1, (d) MMD-CS; II: (a) CS1, (b) MSDI31-CS1, (c) MIDI31-CS1; III (a) CS1, (b) MSS7-CS1, (d) MMDI31-CS1, (c) MIS7-CS1, (d) MMS7-CS1.

The IR spectrum of CS microspheres presented characteristics absorption peaks at 2942-2784 cm^{-1} (aliphatic C-H stretching band), 1658 cm^{-1} (Amide 1) and 1597 cm^{-1} (-NH_2) bending and 1321 cm^{-1} (Amide III). The absorption peaks at 1154 cm^{-1} (antisymmetric stretching of the C-O-C bridge), 1082 and 1032 cm^{-1} (skeletal vibrations involving the C-O stretching) are due to its saccharide structure. [23, 28]

The spectra of steroids-chitosan microspheres are dominated by the intense and broad CS peaks; however the distinctive C=O peaks of ester linkage are present at 1735-1720 cm^{-1} (see Fig. 3). These peaks are overlapping the Amide I and -NH_2 peaks at 1658 and 1597 cm^{-1}. The peaks at 1712 – 1708 cm^{-1} of carbonylic ketone can be observed in DI-31 and S7-Chitosan microspheres.

Differential Scanning Calorimetry

The thermal behaviour of CS samples has been shown to be strongly dependent on the natural source, [25] the purity of samples and the preparation conditions.[29] However, the main thermal effects presented by a chitosan from a particular source can be interpreted on the basis of the behaviour of CS from other sources.

The DSC of cross-linked CS1 microspheres present three endothermic peaks at 105.5, 167.4, and 181.1 ^oC, while the CS2 microspheres showed two endothermic peaks at 170.4 and 187.0 ^oC, respectively. Their onset and completion temperatures are listed in Table 2, together with their associated peak enthalpy which is 115.1 J g^{-1} for CS1 particles and 124.1 J g^{-1} for CS2 microspheres. These endothermic effects must result mainly from the melting and dissociation of chitosan crystals, by comparison with reports for crab CS. [25, 29, 30]

Table 2. Thermal properties of steroids-CS linked microspheres, main endothermal effects.

	Endotherm (ºC)			
	Onset	Peak	Comp	ΔH Jg^{-1}
CS1	127.9	150.5	155.7	10.2
	155.7	167.4	177.2	26.2
	177.2	181.1	195.3	78.9
CS2	167.2	170.4	174.1	3.5
	181.5	187.0	197.8	120.6
MSD-CS1	177.2	196.3	229.4	145.1
MID-CS1	199.1	208.4	214.6	123.9
	155.1	165.0	180.4	82.9
MMD-CS1	154.9	160.7	171.4	29.9
	178.1	183.7	192.6	108.7
MSD-CS2	183.4	190.7	197.6	106.2
	152.4	166.5	176.2	57.3
MID-CS2	218.2	224.8	232.9	146.0
MMD-CS2	160.5	197.4	250.0	122.4

The DSC of the steroids-linked CS microspheres present an intense endothermic peak between 165-209 ^oC (see Table 2) with associated ΔH of 83–146 J g^{-1}. These peaks can be result from the melting of chitosan with the linked steroid and dissociation of CS chains.

Release profiles

The UV absorption spectra of linked diosgenin monosuccinate-CS1 microspheres (25 mg) in buffer solutions (25 mL) at different acidic pH measured 30 min after preparation of the suspension compared with the spectrum of 3.9×10^{-4} mol L^{-1} and the release profiles in PBS

solution (pH 6.0) are presented in Fig. 4.

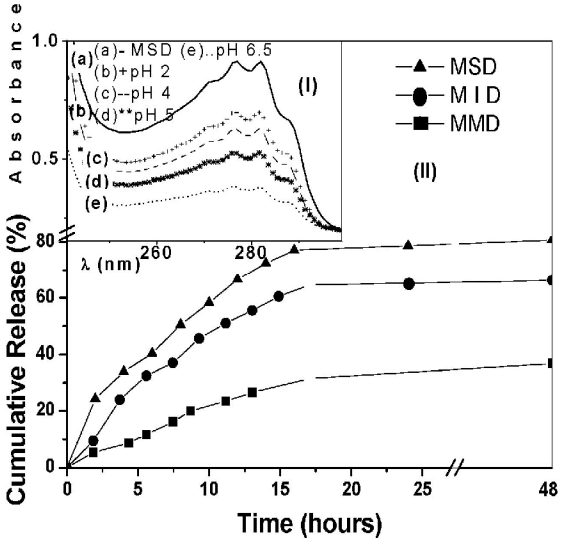

Figure 4. (I) UV spectra at several pH of linked MSD-CS1 microspheres; (II) Release profiles at 30 ^{o}C of linked diosgenin-CS1 microspheres in PBS solution(pH 6.0).

This release is mainly pH dependent and is controlled by the ester hydrolysis of the linkage between the steroid and the chitosan. It permits to control the kinetic release as a pH function. The release profile was also affected by the employed dicarboxylic linker between steroid and CS. In all cases a sustained release of steroids is obtained, which is characterized by an almost constant release rate (zero order kinetics) during the first 15 h. The different release patterns obtained might be the result of different strength of the steroids-CS link. The observed general trend of release rate was MSD>MID>MMD. This trend was different that the reported for the free steroids encapsulated in CS microspheres. [23]

CONCLUSIONS

CS microspheres were successfully linked to diosgenin and BS monoesters with agrochemical activity as confirmed by FTIR and elemental analysis. The steroid contents found were between 15-57 wt-% and showed a dependence on the employed carboxylic linker and the CS microspheres preparation method. Particle sizes ranged from 40 to 790 μm and the morphology was dependent on the method of microspheres obtaining. The linking process was somewhat more efficient in the more porous CS1 particles. The in vitro release studies performed in water at different acidic pH indicated a drug release dependence on the employed as linker, the steroid content and the acidity of solution. Sustained release profiles were obtained for all the studied steroids.

ACKNOWLEDGEMENTS

The authors wish to thank the Deutscher Akademischer Austauschdienst (DAAD) for a research grant to Javier Pérez and the Department of Chemistry of University of Paderborn. Also is acknowledged the Faculty of Chemistry at University of Havana.

REFERENCES

1. Rinaudo M, *Prog Polym Sci* 31: 603 (2006).
2. Minami S and Shigemasa Y, *Biotech & Gen Eng Rev* 13: 383 (1995).
3. Keshavayya J, Kulkarni PV and Kulkarni VH, *J Appl Polym Sci* 103: 211(2007).
4. D'ath L, Kosaraju SL and Lawrence A, *Carbohydr Polym* 64: 163 (2006).

5. Acosta N, Argüelles-Monal W, Peniche C and Peniche H, *Macrom Biosci* 3: 511 (2003).
6. Shtilman MI, Tsakalof AK, Tsakiris IN, Tsatsakis AM, Tzatzarakis MN and Voskanyan PS, *J Plant Growth Regul* 25 (3): 211 (2006).
7. Shtilman MI, Tsatsakis AM, *Plant GrowthRegul* 14 (1): 69 (1994).
8. Dunn EJ, Goosen MFA, Hunter BK, Li Q, Paterson WJ and Teixeira MA, *Ind & Eng Chem Res* 29 (7): 1205 (1990).
9. Rúnarsson ÖV, Holappa J, Nevalainen T, Hjálmarsdóttir M, Järvinen T, Loftsson T, Einarsson JM, Jónsdóttir S, Valdimarsdóttir M, Másson M, *Eur Polym J* 43: 2660(2007).
10. Fristensky B, Hadwiger LA and Riggleman RC. Academic Press Inc. J. P. Zikakis (Editor). Orlando, Florida 291- (1984).
11. Hewajulige IGN, Sivakumar D, Sultanbawa Y, Wijesundera RLC and Wilson-Wijeratnam RS, *Acta Hort* 740: 245 (2007).
12. Bumgardner JD, Chesnutt BM, Haggard WO, Ong JL, Utturkar G and Yang Y, *Carbohydr Polym* 68: 561 (2007).
13. Alonso E, Cabrera M, Coll F, Jomarrón I and Robaina C, *PTC Int. Appl.*, WO 97 13; 780 [CA 126: 343720] (1995).
14. Asami T, Bacic A, Clouse SD, Fujioka S, Pereira-Netto AB, Roessner U and Yoshida S, *Tree Physiology* 29(4): 607 (2009).
15. Bhardwaj R, Khurma UR, Ohri P and Sohal SK, *Indian J Nemat* 37: 2 (2007).
16. Agüero G, Alonso E, Bernardo Y, Coll F and Pérez C, *J Chem Res* 3: 176 (2006).
17. Dinan L, Voigt B and Whiting P, *Cell Molec Life Sci* 58: 1133 (2001).
18. Li F, Fernandez PP, Rajendran P, Hui KM, Gautam Sethi G, *Cancer Lett* (2010) In Press. doi: 10.1016/j.canlet.2009.12.003
19. Ando J, Ikeda T, Miyazono A, Nohara T, Tsumagari H, Uyeda M, Yokomizo K and Zhu X-H, *Biol Pharm Bull* 23 (3): 363 (2000).
20. Ju Y, Liu M-J, Wang Z, Wong RN Wu QY, *Cancer Chemother Pharm* 55: 79 (2005).
21. Tao H and Yu B, *J Org Chem* 67: 9099 (2002).
22. Covas CP, Quiñones JP, Szopko R and Schmidt C, *Steroids* Submitted (2010).
23. Covas CP, Curiel H, García YC and Quiñones JP, *Carbohydr Polym* (2010) In Press. doi: 10.1016/j.carbpol.2010.01.006
24. Karewicz A, Nowakowska M, Szczubialka K, Zomerska K, *J Control Release* 116 (2): 13 (2006).
25. Dockal ER, Santos JE, Soares JP, *Polimeros: Ciencia e Tecnologia* 13 (4): 242 (2003).
26. Aminabhavi TM, Patil SS, Rokhade AP, Shelke NB, *Carbohydr Polym* 69: 678 (2007).
27. Amaral IF, Barrias CC, Borges JP, Granja PL and Silva AIN, *Key Eng Mater* 254-256: 573 (2004).
28. Argüelles W, Davidenko N, Gallardo A, Peniche C, San Román J and Sastre R, *Biomaterials* 20: 1869 (1999).
29. Mau J-L, Yang J and Yen M-T, *Carbohydr Polymers* 75: 15 (2009).
30. Chao-Hua Z, Cheng-Peng L, Chun-Yan O, Lei Yang, Peng-Zhi H, Si-Dong L, *J Appl Polym Sci* 105: 547 (2007).

Chitosan activity on *Ramularia cercosporelloides* isolated from infected safflower leaf in Mexico

Eber A Quintana-Obregón*[1] Maribel Plascencia-Jatomea[1], Mario O Cortez-Rocha[1]

[1] Department of Research and Graduate Program in Food, Universidad de Sonora, Hermosillo, Sonora Mexico.
*E-mail: eberaddi@gmail.com

Abstract
The growth inhibitory properties of chitosan on *Ramularia cercosporelloides* were studied.

Keywords: Fungi; spores; growth radial; viscosity

INTRODUCTION

Fungus *Ramularia cercosporelloides* is the causative agent of the disease known in Mexico as the false mildew of safflower.[1] The disease control in field is difficult and requires the application of increasing doses of commercial fungicides (up to three times the recommended dose), increasing production costs and environmental risk. Chitosan, a polymer of natural origin, non-toxic and biodegradable,[2] represents a natural alternative to control the fungus. The aim of this study was to evaluate the effectiveness of chitosan on growth of *R. cercosporelloides* by *in vitro* analysis of spore germination and radial growth.

MATERIALS AND METHODS

Commercial chitosan solutions of low (QB) and high viscosity (QA) (Fluka, Biochemika) in 0.05 M acetic acid, were added to v8 agar (15 g base agar, 3 g CaCO3, 200 mL v8 juice, graduated to 1000 mL).[3] The final concentration of chitosan in the medium was 3.4 g L^{-1}. Using as control v8 agar with pH adjusted to 5.4 with acetic acid and agar v8 unadjusted pH. Individual effect of each of the biopolymers on spore germination and radial growth of *R. cercoporelloides* from spores with morphological characteristics of the genus *Ramularia* was determined. It was incubated at 25 °C and photoperiod of 12 h light-dark.

Germination of Spores. 10 mL of culture medium in Petri dishes 5 cm in diameter were deposited. The culture media with chitosan and controls were inoculated with 10^5 spores, the same that were placed in the center of the plate and distributed over the entire surface using a sterile glass rod. They were incubated at 25 °C and photoperiod of 12 light-dark. At different time intervals random samples were taken from the Petri dishes inoculated with the spores until the control reached more than 90% of spores germinated. With an optical microscope, 200 spores were counted at random from each plate, determining the number of germinated and ungerminated spores per plate giving the germination percentage. A spore was considered germinated when the length of the germinal tubule reached half the total diameter of the spore.[4] The percentage of ***germinatory*** inhibition described by the equation Plascencia-Jatomea *et al.,*[5] was determined.

Radial Growth. The technique of inoculation of spores in well was applied. For which drilling of 6 mm (well) in the center of each plate using a glass Pasteur pipette were made. The interior of each well was inoculated with 10^5 spores, incubated at 25° C and photoperiod of 12 h light-dark, starting with the presence of light. The diameter of the colony was manually measured and radial growth kinetics was obtained, by calculating the radial extension velocity of colony (m h^{-1}).[6]

RESULTS AND DISCUSSION

It was observed that acetic acid inhibited spore germination in 30% at 26 h and found no

significant difference (P≤0.05) with respect to control without adjusted pH. However, it did not affect significantly the radial growth (Fig. 1).

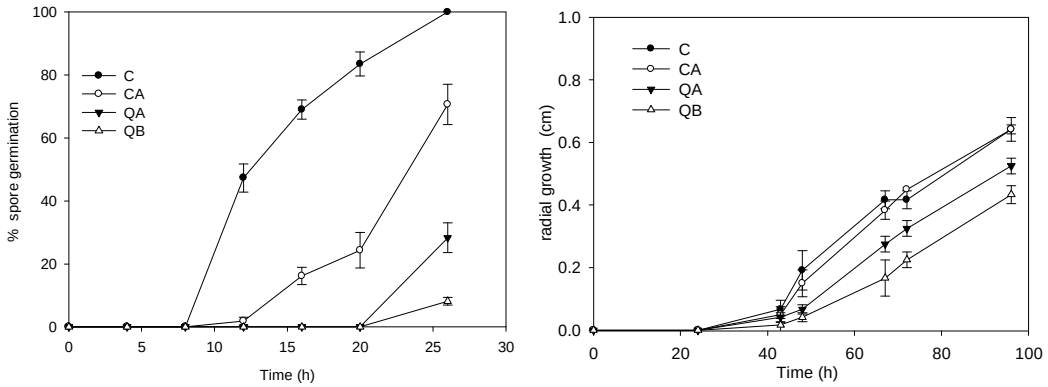

Figure 1. Percentage of spore germination and radial growth of *Ramularia cercosporelloides* in v8 medium with and without chitosan (3.4 g L^{-1}) at 25 °C and photoperiod of 12 h light-dark. C= control; CA= control acid; QA= chitosan of high viscosity; QB= chitosan of low viscosity.

The inhibitory effect of acetic acid in phytopathogenic fungi has been reported previously and also that once it has evaporated, the fungus is able to grow normally.[7-8] The addition of 3.4 g L^{-1} of chitosan with high and low viscosity, slowed significantly (P≤0.05) the germination of spores at 26 h with respect to control, finding percentages of inhibition of 60 ± 4 and 88 ± 1% for the Chitosan of high and low viscosity, respectively. Regardless of viscosity, both chitosan affected the development of the fungus in the stage of germination (Fig. 1). It was also noted that in the presence of chitosan, ungerminated spores have an increased size compared with the control before germinating, it might indicate morphological changes of the spore by the effect of the interaction between spore-chitosan (Fig. 2). There were no significant differences found (P≥0.05) in the radial extension velocity (data not shown) from vegetative growth of the fungus to 96 hours with respect to control (Fig. 1). This indicates that chitosan affects the early development of the fungus, particularly spore germination, delaying the germinal tubule elongation. According to estimated speeds, chitosan does not reduce the capacity expansion of the mycelium of the colony, which is of interest because there are no reports documenting the use of chitosan *in vitro* and *in vivo* over *R. cercosporelloides.* However, its effect on germination of spores on a variety of fungal pathogens has been observed using different concentrations and sources of chitosan. Chitosan inhibited spore germination up to 100% in fungi such as *Fusarium* sp*., Aspergillus niger*, *Verticillium dahlia.*[9,5,10] While *in Fusarium oxysporum*, *Penicillium digitatum* and *Rhizopus stolonifer* partially inhibit its growth in the presence of chitosan has been achieved.[11]

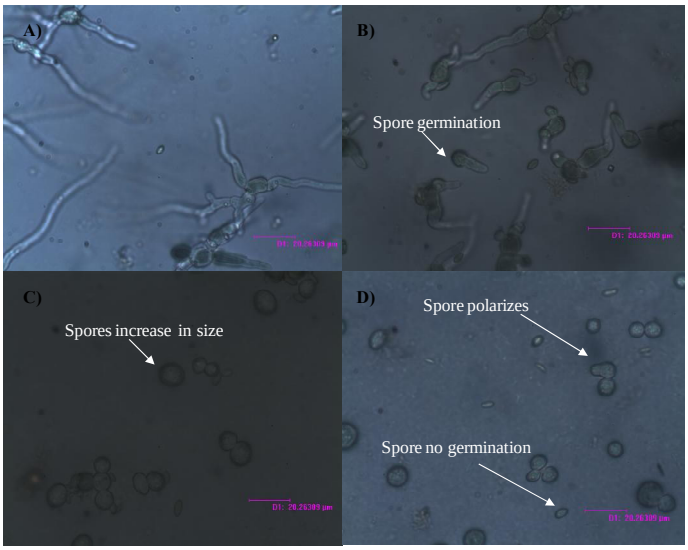

Figure 2. Spores observed at 20 h (400x) of the spore germination test of *Ramularia cercosporelloides* expressing as gender *Ramularia* in v8 medium. A) Control. Over 80% of spores germinated in plate, B) Control acid. Over 20% of spores germinated in plate, C) Chitosan of high viscosity. No spores germinated in plate, D) Chitosan of low viscosity. No spores germinated in plate.

Inhibition of germination and increased spore size may be due to morphological abnormalities that affect the polarization and elongation of the tubule germ.[5] These alterations are associated with increased vacuolation, shrinkage and changes in the plasma membrane or cell wall thickening and including cytoplasmic aggregation.[12]

CONCLUSIONS

In the process of prevention fungal contamination on agricultural crops, primarily the prevention of spore germination and subsequent development is desired. Based on the results of this study concluded that chitosan should be adequate to prevent the development of spores of *Ramularia cercosporelloides* in safflower crops. Though, it is necessary to study in detail the mechanism of action of chitosan on *Ramularia*, to establish the effective dose and type of chitosan, depending on the viscosity and molecular weight that can prevent the development of the fungus in the plant.

ACKNOWLEDGMENTS

CONACYT for the funding provided through key project No. 58249 and No. 53493 J1, and graduate scholarship No. 202460 to Quintana-Obregón, EA

REFERENCES

1 Huerta-Espino J, Constantinescu O, Velazquez C, Herrera-Foessel SA, and Figueroa-López P, *Plant Dis* **90:**1552 (2006).
2 Rabea EI, Badawy MET, Stevens CV, Smagghe G, and Steurbaut W, *Biomacromolecules*. **4:** 1457-1465 (2003).
3 ATCC, ATCC medium: 343 v8 juice agar, http://www.lgcpromochem-atcc.com/common/documents/mediapdfs/343.pdf. [accessed 1 January 2008].
4 El Ghaouth A, Arul JG, and Asselin A, *Phytopathology* **82:**398-402 (1992).
5 Plascencia-Jatomea M, Viniegra G, Olayo R, Castillo-Ortega MM, and Shirai K, *Macromol Biosci* **3:** 582-586 (2003).

6 Holmes G.J. and J.W. Eckert, *Phytopathology* **89:** 716-721 (1999).
7 Abd-Alla MA, *Egyptian Journal of Phytopathology* **29:** 79-87 (2001).
8 Kang HC, Park YH, and Go SJ, *Microbiology Research.* **158:** 321-326 (2003).
9 Rivero D, Cruz A, Martinez B, Ramirez MA, Rodriguez TA, and Cardenas RM, *Plant Protection Journal* **19:** 140-144 (2004).
10 Palma Guerrero J, Jansson HB, Salinas J, and López-Llorca LV, *J Appl Microbiol* **104:** 541–553 (2008).
11 Bautista-Baños S, Hérnandez-López M, and Bosquez-Molina E, *Revista Mexicana de Fitopatología* **22:** 178-186 (2004).
12 Laflame P, Benhawov N, Bussieres G, and Dessureauit M, *Canadian Journal Botanic* **77:**1460-1468 (1999).

Removal of 2,4-dichlorophenoxyacetic acid herbicide from water using chitosan

A. Nunes, A. Moura, M. Holanda and A.G.S. Prado*

QuiCSI Team, Instituto de Química, Universidade de Brasília, Caixa Postal 4478, 70904-970 Brasília, Distrito Federal, Brazil
*E-mail: agspradus@gmail.com, Fax: + 55 61 273 414

ABSTRACT

Chitosan has been applied in removing 2,4-dichlorophenoxyacetic acid herbicide from water. The series of adsorption isotherms were adjusted to a modified Langmuir equation. The maximum number of moles of 2,4-D adsorbed was 4.02 10^{-5} mol per gram of chitosan. The ΔH values for the interaction were determined to be -1.4 kJ mol^{-1} for 2,4-D. All interaction processes were spontaneous and were accompanied by an increase of entropy.

Keywords: chitosan, 2,4-D adsorption

INTRODUCTION

Herbicides are applied to eliminate different undesirable forms of life in agriculture and in urban areas. The use of herbicides is associated with the pollution of the soil and the water.[1] The application of the concentrations exceeding those required for control of the target organisms has caused the surface water contamination due to the runoff and leaching. The toxic effect of the herbicides on the environment can disturb the natural ecological equilibrium and presents risks to human and animal health. [2,3]

The harmful effects of herbicides on the environment have stimulated research to develop efficient technologies for water treatment in order to remove and/or degrade organic contaminants from water. Among these methods, the adsorption can be highlighted. [4,5,6] Low-cost adsorbents as sawdust, chitosans, clays, zeolites, soils, coals, natural oxides, humic substances, have been used to remove contaminants from water in recent years. [6,7,8,9] Chitosan is a biodegradable and a nontoxic polysaccharide, presenting a potencial hability to remove contaminants as dyes and metal of water. [7,10]

In this work, chitosan was used as host to remove the 2,4-dichlorophenoxyacetic acid (2,4-D), a herbicide commonly used in Brazilian sugar cane plantations.[11]

MATERIALS AND METHODS

Materials

The chitosan was produced by Polymar Science and Nutrition S.A. The degree of deacetylation (DD) was determined by infrared spectroscopy and ^{1}H nuclear magnetic resonance spectrum. Its obtained DD was 86.15%[12]. 2,4-dichlorophenoxyacetic acid – 2,4,D (Sigma) was used without purification.

Herbicide adsorption

The adsorption process was followed batchwise in aqueous solution of 2,4-D. For this process, a series of samples of about 50.0 mg of Chitosan were suspended in 50.0 mL of aqueous herbicide solutions of different concentrations, varying from zero to 1.0 x 10^{-4} mol L^{-1}. The amount of adsorbed herbicide was determined by the difference between the initial concentration in aqueous solution and the one found in the supernatant, by using a Spectrophotometer Varian at 227 nm. In every case, all samples were analyzed in triplicate.

Calorimetric analyses

Herbicide adsorption interactions were followed calorimetrically by titration using a Calorimeter. In a typical process, 0.50 g of chitosan suspended in 100.0 mL of water were incrementally titrated with an 2,4-D ethanolic solution 0.05 mol L^{-1}, under stirring. Herbicide solutions were added in increments of 0.5 mL up to saturation of the active surface sites of the modified material. For each increment, the heat flux ($\Delta_{tit}Q$) was recorded, as indicated by a constant heat flux at the end of each operation. The same procedure was employed to monitor the heat flux due to pesticide dilution ($\Delta_{dil}Q$) without the solid and also the heat flux of solvation on the suspended modified material ($\Delta_{sol}Q$)

RESULTS AND DISCUSSION

Herbicide removal

The chitosan was applied to remove 2,4-dichlorophenoxyacetic acid herbicide from water. The adsorption capacity was evaluated by measuring the sorption isotherms. The number of moles of the herbicides adsorbed per gram of adsorbent (N_f; mol g^{-1}) was obtained from equation 1:

$$Nf = \frac{n_i - n_s}{m} \quad (1)$$

where n_i is the initial number of moles of metal ion added to the system, n_s is the number of moles at equilibrium after adsorption, and m is the mass (g) of chitosan. The adsorptive behavior represented by the number of moles adsorbed (Nf), versus the number of moles at equilibrium per volume of solution (Cs) is presented in Figure 1. [6,7,13]

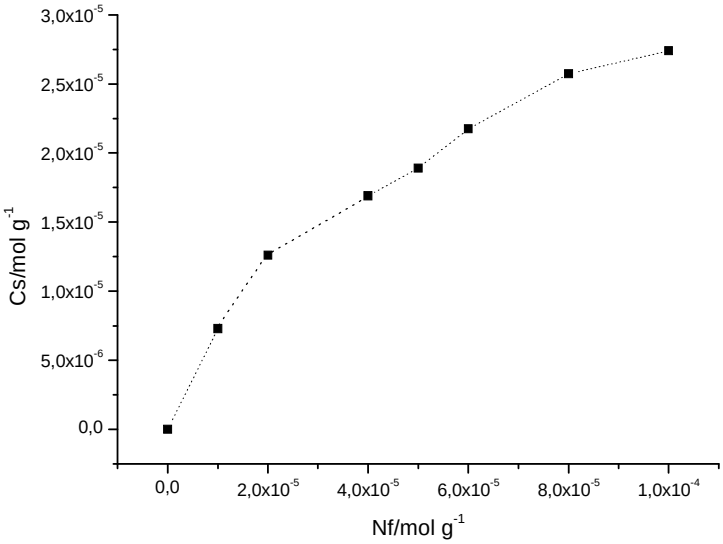

Figure 1. Adsorption isotherm of 2,4-D in chitosan

The experimental data were applied into the general equation of the modified Langmuir model presented in equation 2.

$$\frac{Cs}{Nf} = \frac{Cs}{Ns} + \frac{1}{Ns.K} \quad (2)$$

where C_s is the concentration (mol dm^{-3}) of the solution at equilibrium, N_s is the maximum amount of herbicide adsorbed per gram of adsorbent (mol g^{-1}), which depends on the number of adsorption sites, and K is a equilibrium constant (mol dm^{-3}). The linear form of the adsorption isotherm, i.e. from plots of C_s/N_f *versus* C_s, in which N_s and K are represented by

the slope and intercept, respectively, is shown in Figure 2. The maximum amount of 2,4-D herbicide that could be adsorbed per gram of chitosan was determined to be 4.02 10^{-5} mol g^{-1}. [9,7,13]

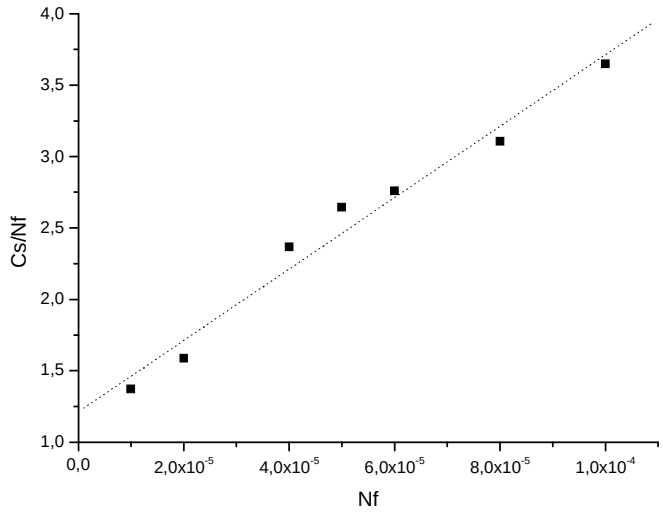

Figure 2. Linear form of isotherm of Langmuir in adsorption of 2,4-D (■) in chitosan.

Chitosan was calorimetrically titrated with 2,4-D herbicide in order to obtain more information about the adsorption processes at solid/liquid interface. The thermal effects of the interaction of herbicide with chitosan were determined from a series of calorimetric experiments. The complete thermodynamic cycle can be summarized as follows:

$$Chitosan_{(aq)} + 2,4\text{-}D_{(eth)} \longrightarrow [Chitosan \cdots 2,4\text{-}D]_{(sol)} \quad (a)\ Q_{tit}$$

$$H_2O + Chitosan_{(s)} \longrightarrow Chitosan_{(aq)} \quad (b)\ Q_{sol}$$

$$2,4\text{-}D_{(eth)} + H_2O \longrightarrow 2,4\text{-}D_{(sol)} \quad (c)\ Q_{dil}$$

$$Chitosan_{(s)} + 2,4\text{-}D_{(sol)} \longrightarrow [Chitosan \cdots 2,4\text{-}D]_{(sol)} \quad (d)\ Q_{int}$$

Three separate titration experiments were carried out in order to determine the component parts, namely: (a) the heat evolved by the host/Herbicide interaction (Qtit), (b) the heat of solvation of the solid Chitosan(Qsol), and (c) the heat of dilution of herbicide solution (Qdil). The net interaction heat change Qint (d) is given by the equation 3. [5,7,13]

$$\Sigma Q_{\text{int}} = \Sigma Q_{tit} + \Delta Q_{sol} - \Delta Q_{dil} \tag{3}$$

Since the heat of solvation of the aqueous suspended modified material was zero, the expression was reduced to equation 4.

$$\Sigma Q_{int} = \Sigma Q_{tit} - \Delta Q_{dil} \tag{4}$$

The net resultant heat output for this interaction in the solid/liquid interface obtained was illustrated in Figure 3.

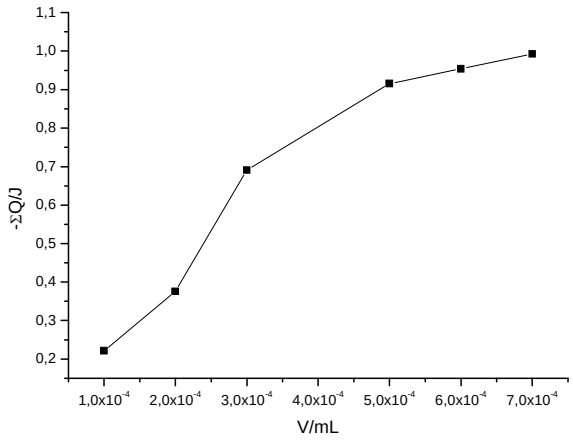

Figure 3. Calorimetric titration of 2,4-D against chitosan .

Using the net resultant heat output from the reaction, adjusted to a modified Langmuir equation, the integral enthalpies involved in the formation of a monolayer per unit mass of adsorbate, $\Delta_{mono}H$, were calculated through the equation 5.

$$\frac{\Sigma X}{\Sigma \Delta_R H} = \frac{1}{(K_{ap} - 1)\Delta_{mono} H} + \frac{\Sigma X}{\Delta_{mono} H} \quad (5)$$

where $\sum X$ is the sum of the molar fractions of the herbicide remaining in solution after adsorption and X values are obtained for each addition of titrant, using the modified Langmuir equation, whose behavior was shown to be a good adjustable model for such heterogeneous systems, K_{ap} is a proportionality constant that also includes the equilibrium constant and $\sum \Delta_R H$ is the integral enthalpy of adsorption (J g^{-1}) obtained from the net thermal effect of adsorption and the number of moles of the adsorbate. Based on the Langmuir equation, it is possible to calculate the reaction enthalpy of the monolayer formed, $\Delta_{mono}H$, from plots of $\sum X/\sum \Delta_R H$ *versus* $\sum X$. [6,7,11]

The molar enthalpy, ΔH, of the interaction process was calculated from $\Delta_{mono}H$ and the maximum number of moles inserted, N_s, using equation 6.

$$\Delta H = \frac{\Delta_{mono} H}{Ns} \quad (6)$$

The Gibbs free energy changes may be calculated from equation 7.

$$\Delta G = -RT \ln K \quad (7)$$

where R is universal gas constant and T is the temperature.in Kelvin. [6,7,13]

The entropy values, ΔS, were determined from equation 8. All thermodynamic data are listed in Table 1.

$$\Delta G = \Delta H - T\Delta S \quad (8)$$

Table 1. Maximum adsorbed amount of 2,4-D (Ns) per gram of chitosan and thermodynamic data for interactions at 298.1 K

Thermodynamic data	Values
Ns (mol g^{-1})	4.02 10^{-5}
ΔG (kJ mol^{-1})	-24.62
ΔH (kJ mol^{-1})	-1.4
ΔS (J mol^{-1} K^{-1})	77.93

The set of thermodynamic data obtained for the adsorption process indicated that the reaction between 2,4-D herbicide and chitosan was spontaneous since it was enthalpically and entropically favored. These data show the high ability of chitosan in removing 2,4-D herbicide from water.

CONCLUSION

The adsorption data showed that chitosan is efficiency in removing herbicide from water. The maximum number of moles of 2,4-D adsorbed was 4.02 10^{-5} mol per gram of chitosan. The 2,4-D herbicide-chitosan interaction process was spontaneous accompanied by an increase in entropy and with exothermic enthalpy values.

ACKNOWLEDGMENTS

The authors thank FAPDF for financial support and CNPq for fellowships.

REFERENCES

1 DeOliveira, E., *J. Colloid Interface Sci.* **323**: 98-104 (2008) .
2 Abate, G., Masini, J. C., *J. Agric. Food Chem.* **53**:12-15 (2005).
3 Legrouri,A., Lakraimi, M.; Barroug, A., De Roy, A., Besse.J.B., *Water Research* **39**: 3441-3448 (2005).
4 Prado, A.G.S., Faria, E.A., Souza De, J.R., and Torres, J.D., *J. Mol. Catal. A* **237**: 115-119 (2005).
5 Prado, A.G.S., Airoldi, C*., Fresenius J Anal Chem **371**: 1028-1030 (2001).*
6 Prado, A.G.S., Moura, A.O., Andrade, R. D.A., Pescara, I.C., Ferreira, V. S., Faria, E. A., Oliveira De, A. H. A., Okino,E. Y. A., Zara, L.F., *J Therm Anal Calorim* **99**: 681-687 (2010).
7 Prado, A.G.S., Torres, J.D., Faria, E.A., Dias, S. C.L., *J. Colloid Interface Sci.* **277:** 43-47 (2004).
8 Jianfa, Li., Yimin, Li., Jinhong, Lu., *Applied Clay Science* **46** :341-318(2009) .
9 Prado, A.G.S., Miranda, B. S., and Jacintho,G.V.M., *Surf. Sci.* **542**: 276-282 (2003)
10 Guinesi, L.S., Esteves, A. A., Cavalheiro, E. T. G., *Quím. Nova* **30 nº4**: 809-814 (2007).
11 Prado,A.G.S., Airoldi, C., *Thermochimica Acta* **349**: 17-22 (2000).
12 Prado,A.G.S., Pescara, I.C., Albuquerque,R.D.A., Honorato, F.N. and Almeida, C.M., *J.Analytica* **44**: 62-67 (2009).
13 Prado, A.G.S.; DeOliveira, E.; *J. Colloid Interface Sci.* **291**: 53-58 (2005).

Use of inoculants with chitin for the bioremediation of hydrocarbon-contaminated soils

Alejandro Gentili[1], María Cubitto[1] and María S. Rodríguez[2]

[1] Departamento de Biología, Bioquímica y Farmacia, Universidad Nacional del Sur. Bahía Blanca, Buenos Aires, Argentina
[2] INQUISUR UNS - CONICET, Bahía Blanca, Buenos Aires, Argentina

Keywords: Chitin, Chitosan, Bioaugmentation, Hydrocarbon-degrading bacterial strain, Soil bioremediation, Immobilization

Abstract
In this study the potential of inoculants developed at our laboratory for the bioremediation of hydrocarbon contaminated soils was examined. The inoculant was made using chitin flakes obtained from shrimp wastes as carrier material for a hydrocarbon-degrading bacterial strain, *Rhodococcus corynebacterioides*, isolated from Bahía Blanca coastal soils. It was assayed in two different microcosms: a typical soil for agronomic use polluted with petroleum and an aged- hydrocarbon contaminated soil of the landfarming of a local petroleum refinery. The inoculants formulated with chitin as carrier material improved the survival and the activity of the immobilized strain in the microcosms.

INTRODUCTION

Petroleum hydrocarbons are major pollutants of marine and terrestrial environments. Ultimate and complete degradation is accomplished by microorganisms. Thus, hydrocarbon contaminated soils show a large and diverse microbial community which can exhibit degradative capacities, and can detoxify the polluting compounds (Atlas, 1981; Oudot, 1984). A popular option for clean up of hydrocarbons polluted environments is biostimulation. This process consist in the addition of nutrients to stimulate the enrichment of the indigenous hydrocarbons-degrading microbial community. However, it may not be appropriated to relay on the natural response of members of the indigenous microbial community. Bioaugmentation, the addition of either indigenous or exogenous microorganisms to expedite the remediation process, is an useful alternative (Jansson et al., 2000; Cunningham et al., 2004). Bioaugmentation has met with varying degrees of success (Leavitt and Brown, 1994; Vogel, 1996) and there has been a considerable debate over its efficacy. Since natural environment is hostile to the introduced cells, the use of inoculant formulations involving carrier materials for the delivery of microbial cells to natural ecosystems, is an attractive option. Carrier materials provide protective niche to microbial inoculants. An optimal carrier should provide favorable conditions for survival as well as functioning of the inoculant cells (van Veen *et al*., 1997). The carrier should, further, be nontoxic, nonpolluting, biodegradable and have a constant quality and be locally available at low price (Ballati and Freire, 1996). Poor information have been reported about inoculants with natural carrier materials for soil bioremediation process. Since shrimp exoeskeletons are an abundant residue of the local fishing industry, chitin obtaining technology is available in our university, the material is nontoxic, nonpolluting and biodegradable, the flakes of chitin could be considered an alternative carrier material for immobilizing microorganisms for bioremediation purposes. Therefore, the aim of this study was to evaluate the potential of the strain immobilized on chitin flakes for the clean up of crude oil-contaminated soils.

MATERIALS AND METHODS

Two different soil microcosms were prepared. The first one was a typical agronomic use soil amended with 4 % of autoclaved crude oil . The treatments, assayed by triplicate, were: a) controls: hydrocarbon contaminated soil without inoculant and b) inoculated microcosms: hydrocarbon contaminated soil fertilized (to correct C:N:P relation with a fertilizer with nitrogen and phosphorus) and with 0.25 % of the inoculant. The second microcosms was an aged-contaminated soil of the landfarming of a local refinery. The different treatments, assayed by triplicate, were a) controls: contaminated soil without fertilizer. b) fertilized: contaminated soil fertilized c) indigenous microbiota: bioaugmented with an indigenous microbiota culture and d) inoculated microcosms: contaminated soil with 0,25% of the inoculant. All the microcosms were irrigated periodically and roturated weekly to provide adequate aireation. They were incubated at 18 ± 2 ºC for 120 days and humidity was controlled by a dispositive that measures soil conductivity. Periodically samples were taken and biological activity of hydrocarburolytic bacteria (BA) and total hydrocarbon concentrations (%TH) were determinated. To determine hydrocarbon concentration 10 g soil portions of each sample were taken and the residual hydrocarbons were then Soxhlet-extracted for 6 h with 200 mL hexane. The extracts were concentrated to 2 mL by rotary vacuum evaporation. The amount of residual hydrocarbons recovered was determined gravimetrically. The biological activity of hydrocarburolitic bacteria was determined by Girard and Rovieux technique (1964), using petroleum as unique source of carbon and energy. Serial decimal dilutions of the homogenized samples were prepared in Locke solution (NaCl 1,5 % (p/v); $MgCl_2$ 0,04 % (p/v); KCl 0,01 % (p/v). pH: 7,2). One ml of the different dilutions was poured in tubes containing 5 mL Winodgrasky solution (Pochón, 1962), and 0,5 % of petroleum was added to each tube. Control tubes without petroleum inoculated with the lower dilution were used to determine the microbial growth produced by the nutrients incorporated with the inocula and control tubes, without inocula were used to diferenciate abiotic changes of the sustrate. All tubes were incubated at 25ºC for 45 days. Turbidity and visible changes in the oily phase were considered as positive. Biological activity was graphicated placing days in abcises versus $\log_{10}$ of the highest positive dilution.

RESULTS

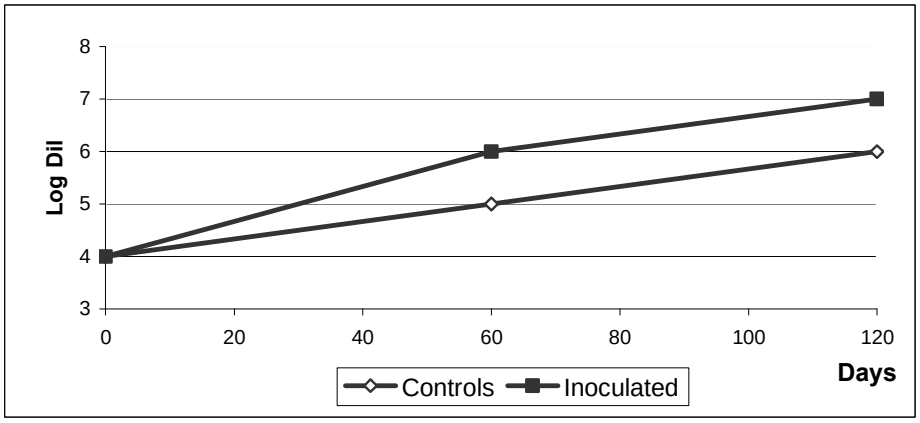

Figure 1. Biological Activity in agronomic use soil.

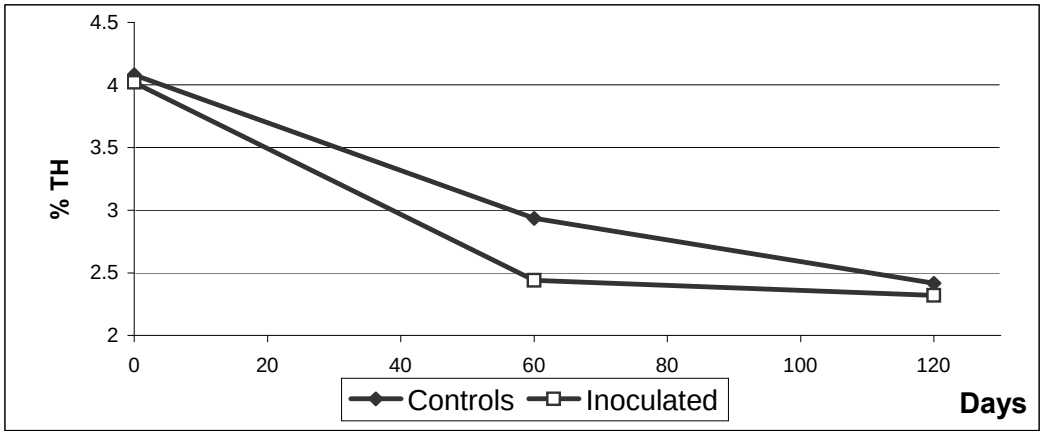

Figure 2. % Total Hydrocarbon in agronomic use soil.

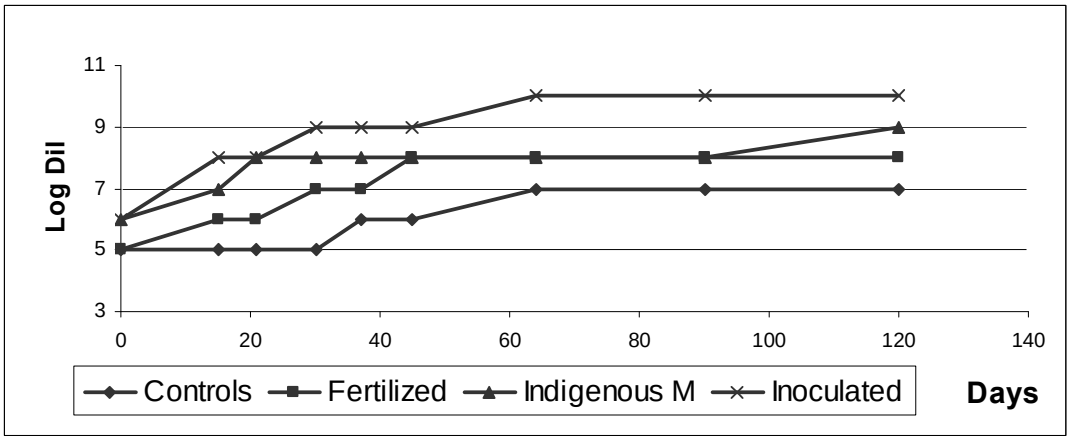

Figure3. Biological Activity in aged contaminated soil

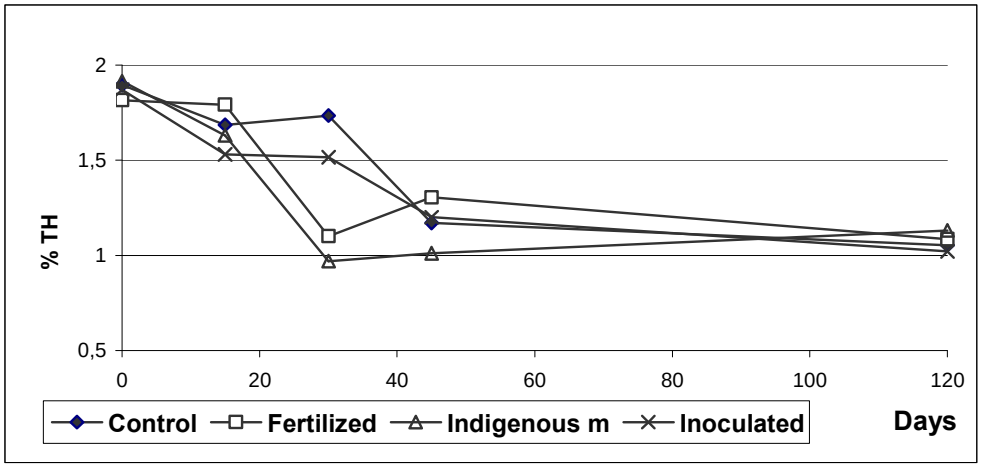

Figure 4. % Total Hydrocarbon in aged contaminated soil

DISCUSSION

In the first case, as it is shown in Fig. 1, biological activity in inoculated microcosms reach highest values, in one order of magnitude, than controls.The greater activity was observed during the first two months of the experience. The results of % total hydrocarbons (Fig.2) at 60 days show significative diferences ($p < 0,05$) between treatments. At 120 days the

achieved values are similar for both treatments.
In the age contaminated soil the results show that the inoculated microcosmos reach the higher values of BA (Fig. 3), although the fertilized and bioaugmented with indigenous microbiota showed more biodegradation (Fig. 4) than controls and inoculated. These results agree with bibliography that consider bioagumentation with inoculants, a process not convenient for cronic contaminated soils (Bento y col. 2005). In this cases, environment selects the more active and capable microbiota for biodegradation, and when the optimun conditions are present (nutrients, oxigen and humidity) the biodegradation process takes place in its best perfomance.

CONCLUSIONS

In the first soil the use of the inoculant improved the bioremediation process acelerating the degradation speed. In the aged contaminated soil, in agreement with international bibliography, it is demonstrated that the bioaugmentation with inoculants does not represent an advantage in the bioremediation of cronic contaminated soils. These results open a new perspective in the use of a contaminant residue at the same time that allow to treat soils impacted by industrial and portuary activity in Bahía Blanca zone.

REFERENCES

1 Atlas RM.,. *Microbiol Rev* **45**: 180-209 (1981).
2 Ballatti A. and Freire J. *Legume Inoculants. Selection and Characterization of Strain. Production, Use and Management* ed by Ballatti, A, Freire, J, La Plata, Buenos Aires, p. 39 – 54 (1996).
3 Bento FM., Camargo FAO, Okeke BC and FrankenbergerWT,. *Bioresource Technology*, **96**: 1049 – 1055 (2005).
4 Cunningham CJ, Ivshina IB, Losinsky VI., Kusukina MS and Philp JC, *Int Biodet Biodeg* **54** : 167 – 174 **(**2004).
5 Girard H., Rouvieux R.,*Técnicas de Microbiología Agrícola*. Ed Acribia, Madrid, España. (1964).
6 Jansson JK, Björkolöf K, Elvang AM. and Jorgensen S, *Environ Pollut* **107** : 217 – 223 (2000).
7 Leavitt ME, Brown, KL, *Hydrocarbon Bioremediation* ed by Hinche R, Alleman ME.
8 Hoeppel, RE. and Miller, RN CRC Press, Boca Raton, Fl., pp 72 – 79. (1994**).**
9 Pochon J, Tardieu L, Techniques d'analysis en microbiologie du sol. Ed De la Tourelle, Paris (1962).
10 Oudot J, *Mar Environ Res* **13**: 277-302 (1984).
11 Van Veen, JA, van Overbeek and van Elsas JD, *Microbiol Mol Biol Rev* Vol. **61**,No.2: 121 – 135 (1997).
12 Vogel TM., *Curr Opin Biotechnol* **7**: 311 – 316 (1996).

Immobilization of calcium oxide onto chitosan beads as a heterogeneous catalyst for biodiesel production

Chun-Chong Fu,[1] Tien-Chieh Hung,[2] Chia-Hung Su,[3*] Devi Suryani,[1] Wen-Teng Wu,[1] Wei-Chen Dai,[3] Yea-Tyam Yeh[3]

[1] Department of Chemical Engineering, National Cheng Kung University, No.1, Ta-Hsueh Road, Tainan 701, Taiwan
[2] Department of Biological and Agricultural Engineering, University of California, One Shields Av., Davis, CA 95616, USA
[3] Graduate School of Biochemical Engineering, Ming-Chi University of Technology, No. 84 Gung-Juan Road, Taishan, Taipei 24301, Taiwan
*E-mail: chsu@mail.mcut.edu.tw

Abstract
Calcium oxide (CaO), immobilized and stabilized onto chitosan beads, was employed as a heterogeneous catalyst to produce biodiesel catalytically by transesterification of soybean oil with methanol. The operating conditions were optimized for CaO immobilization with high stability, and CaO loading of the immobilized catalyst was obtained around 12% (w/w). The immobilized catalyst was further employed to investigate the transesterification reaction of soybean oil with methanol. The response surface methodology was applied to determine the optimal catalytic reaction conditions at 60°C with a molar ratio of methanol to oil of 1:13.4 and catalyst loading of 13.78 wt%. Under the optimal reaction conditions, the equilibrium conversion of soybean oil was 97% after 3 h of reaction time. In addition, the immobilized catalyst can be reused at least five times. The process for making CaO-based catalyst is easy, energy efficient, and repeatable, and is promising for application in biodiesel production.

Keywords: Calcium oxide, Chitosan, Immobilization, Biodiesel

INTRODUCTION

Biodiesel, an alternative biofuel, is produced from the transesterification of plant oils or animal fats with alcohols.[1] This reaction can be catalyzed by several heterogeneous alkali catalysts, among which CaO is commonly selected due to its higher activity, higher basic strength, and lower cost for application.[2] However, several studies have reported that a fraction of the CaO leaches into the reaction mixtures of biodiesel, reducing the reusability of the CaO catalyst and requiring additional processes to remove the dissolved catalyst from the product phase.[2,3] CaO supported on several inorganic materials under high operating temperatures has been investigated to overcome these problems.[3,4] In this study, chitosan, a biopolymer, was employed as a novel support for the immobilization of CaO under mild operating conditions. An easy method of preparing a stable CaO-based catalyst is demonstrated. The physical properties of the immobilized catalyst were determined, and the immobilized catalyst was tested in the transesterification of soybean oil with methanol.

MATERIALS AND METHODS

Catalyst preparation and characterization

Chitosan solution was prepared by dissolving 2% (w/v) chitosan powder in 1% (v/v) acetic acid solution. A suspended CaO solution was prepared by mixing 3 g CaO in 90 ml methanol containing 1 N NaOH. Chitosan solution was extruded at a flow rate of 0.85 ml/min through a syringe needle into a coagulant bath of suspended CaO solution under stirring to form spherical beads. The beads were collected, rinsed extensively with methanol to remove

residual NaOH, and dried at 60°C for 4 h to obtain dry CaO/chitosan beads. The beads were further modified by a crosslinking treatment. The parameters of the crosslinking treatment, the glutaraldehyde concentration and crosslinking time, were investigated in the ranges of 0.02 to 0.2 N and 10 to 50 min, respectively. One gram of dry CaO/chitosan beads was added to 20 ml of tetrahydrofuran (THF) containing a given dose of glutaraldehyde. The crosslinking treatment was carried out at 25°C for a certain period of time. Then, the crosslinked beads were filtered, rinsed with THF, and dried at 60°C overnight. The CaO loading, CaO leaching, and crystal structures of these crosslinked beads were examined by a titration procedure, determined by atomic absorption spectroscopy (AAS), and characterized by X-ray diffraction (XRD).[3,4]

Optimization of transesterification reaction using response surface methodology

A three-level three-factorial Box-Behnken design (BBD) was applied to investigate the reaction parameters affecting oil conversion from the transesterification of soybean oil. Experiments with varying molar ratios of methanol to oil (9:1 to 15:1), catalyst loading (5 to 15 wt%), and temperature (40 to 60°C) were conducted in 50 ml stoppered conical flasks. The conversion of soybean oil, analyzed by gas chromatography, was the performance index.[5]

RESULTS AND DISCUSSION

In this study, CaO immobilized onto chitosan beads was employed as a catalyst for biodiesel production. The CaO loading on the immobilized catalysts was about 12% (w/w), as measured by a titration method. During preparation, the immobilized catalysts were further crosslinked using glutaraldehyde to stabilize the active sites and avoid lixiviation of the CaO. The glutaraldehyde concentration and crosslinking time were optimized at 0.15 N and 30 min, respectively. Under these optimal conditions, less than 1% of the total CaO immobilized onto chitosan beads would be released into the reaction mixtures of biodiesel. An immobilized catalyst with the lowest CaO leaching was subsequently obtained.

The crystal structures of the chitosan support and several CaO-based catalysts were characterized by XRD (Figure 1). The chitosan support showed an atypical diffraction signal occurring at a 2θ of 20°. The broad peak represented the structural framework of the chitosan support and indicated that it was amorphous in form.[6] The strong reflections of the commercial CaO at 2θ of 32.3°, 37.4°, and 54° were assigned to CaO (lime).[4] A peak of $Ca(OH)_2$ was also observed because the commercial CaO was partially hydrated.[7] Once commercial CaO was immobilized onto chitosan beads, no CaO peaks disappeared, indicating the presence of active CaO on the immobilized catalyst. Moreover, a decrease in the diffraction peak of the chitosan support suggested that the chitosan structure was modified through the glutaraldehyde-based crosslinking treatment. This result shows evidence that CaO has been immobilized and stabilized onto chitosan beads.

The immobilized catalyst was employed to catalyze the transesterification of soybean oil and methanol. The reaction parameters affecting biodiesel production were optimized using response surface methodology. The optimal methanol/oil molar ratio, catalyst loading, and reaction temperature were 13.4:1, 13.78 wt% and 60°C, respectively. Under these optimal reaction conditions, the conversion of oil reached 97% after 3 h of reaction time. The result is similar to previous reports using CaO-based catalysts.[2-4]

Table 1 compares oil conversion and CaO lixiviation into reaction mixtures for several CaO-based catalysts. Several studies have reported the development of stable CaO catalysts using inorganic materials as supports.[3, 4] However, the preparation of such CaO-based catalysts is energy intensive because high temperatures are required for calcining CaO with inorganic supports.[3, 4] This study represents an easy, energy-efficient process for preparing a CaO-based catalyst using chitosan as the support. The proposed catalyst exhibited catalytic performance comparable to that of other CaO-based catalysts. In addition, only slight CaO leaching of the

proposed catalyst was observed because CaO was immobilized and stabilized onto chitosan beads followed by a crosslinking treatment using glutaraldehyde. The proposed catalyst was successfully recycled five times and maintained high catalytic performance in a biodiesel reaction (oil conversion of at least 80%). Further study to improve the catalyst is needed.

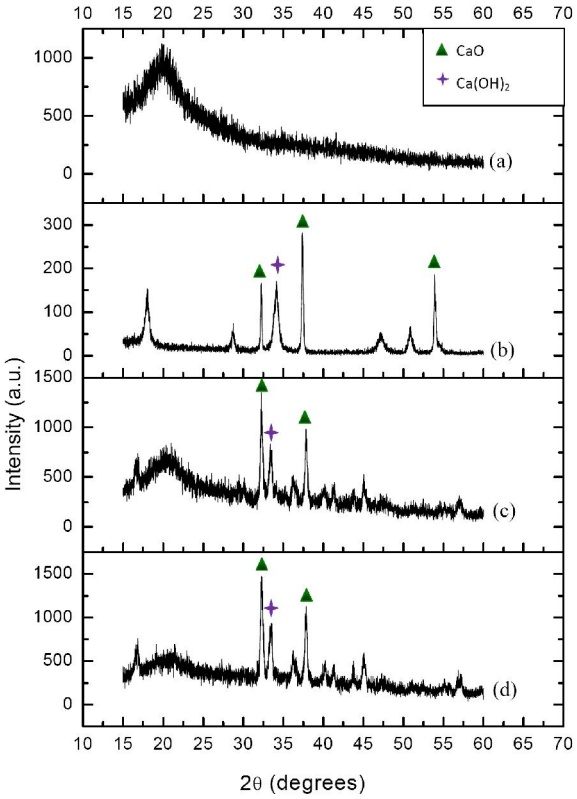

Figure 1. XRD patterns of (a) chitosan, (b) commercial CaO, (c) CaO immobilized onto chitosan beads without crosslinking treatment, and (d) CaO immobilized onto chitosan beads with crosslinking treatment.

Table 1. Oil conversion and CaO lixiviation into reaction mixtures for several CaO-based catalysts

Catalyst/support	**Maximal conversion of the transesterification reaction (%)**	**Leached CaO concentration in reaction mixtures (ppm)**	**Percentage of CaO from fresh catalyst leached into reaction mixtures (%)**	**Reference**
Commercial CaO	99	n.d.	25	2
Commercial CaO	98	22192.96 ± 1842.02	18.25 ± 1.51	The present study
CaO/MgO	92	n.d.	leaching without detection	3
CaO/SBA-15	95	n.d.	no leaching	4
CaO/chitosan	97 ± 6.43	166.21 ± 10.32	1.39 ± 0.09	The present study

CONCLUSIONS

A new family of alkali catalysts has been prepared by immobilizing CaO onto chitosan beads. The operating conditions of glutaraldehyde concentrations and crosslinking time were optimized to stabilize the catalyst, and a catalyst with the least CaO leaching was subsequently obtained. The immobilized catalyst exhibited catalytic performance comparable to that of other CaO-based catalysts and can be reused at least five times to drive transesterification at a conversion of 80%. This process for making a CaO-based catalyst is easy, energy efficient, and repeatable, and seems promising for application in biodiesel production.

ACKNOWLEDGEMENTS

This research was supported by grant (NSC 98-2218-E-131-004) from National Science Council of Taiwan.

REFERENCES

1 Su CH, Fu CC, Gomes J, Chu IM and Wu WT, *Aiche J* **54:**327-336 (2008).

2 Arzamendi G, Arguinarena E, Campo I, Zabala S and Gandia LM, *Catal Today* **133:**305-313 (2008).

3 Yan SL, Lu HF and Liang B, *Energy Fuels* **22:**646-651 (2008).

4 Albuquerque MCG, Jimenez-Urbistondo I, Santamaria-Gonzalez J, Merida-Robles JM, Moreno-Tost R, Rodriguez-Castellon E, Jimenez-Lopez A, Azevedo DCS, Cavalcante CL and Maireles-Torres P, *Appl Catal A-Gen* **334:**35-43 (2008).

5 Chen JW and Wu WT, *J Biosci Bioeng* **95:**466-469 (2003).

6 Yang D, Li J, Jiang ZY, Lu LY and Chen X, *Chem Eng Sci* **64:**3130-3137 (2009).

7 Granados ML, Alonso DM, Sadaba I, Mariscal R and Ocon P, *Appl Catal B-Environ* **89:**265-272 (2009).

TiO_2 immobilized on microspheres of chitosan for heterogeneous photocatalysis of 2,4-dichlorophenoxyacetic acid herbicide from water

G.W. Tavares, M.S. Holanda, A.R. Nunes, A.O. Moura, A.G.S. Prado*

QuiCSI Team, Instituto de Química, Universidade de Brasília, Caixa Postal 4478, 70904-970 Brasília, Distrito Federal, Brazil
*E-mail: agspradus@gmail.com, Fax: + 55 61 273 414

ABSTRACT
TiO_2 immobilized on microspheres of chitosan has been applied in photodegradation of 2,4-dichlorophenoxyacetic acid herbicide. This material showed be capable to degrade 2,4-D herbicide in aqueous solution and can be used in the purification of water.

Keywords: chitosan, 2,4-D, photodegradation

INTRODUCTION
The indiscriminate application of pesticides in agriculture leads to increase amounts of these compounds in the surface and underground waters. The presence of the pesticides can pollute the surface and ground water resources due to the runoff and leaching.[1,2] A tool to decrease the pollution of the soil and the water for pesticides is the heterogeneous photocatalysis using semiconductors. This technology is based in the generation of hydroxyl radicals that oxidizes a broad range of organic pollutants quickly. [3,4]
In this work, TiO_2 immobilized on microspheres of chitosan were utilized as photocatalyst to degrade the 2,4-dichlorophenoxyacetic acid (2,4-D) from water. The investigation of the photodegradation of the 2,4-dichlorophenoxiacetic acid (2,4-D) is due to frequent use of this systemic herbicide in Brazilian agriculture, mainly in sugarcane plantations.[5]

MATERIALS AND METHODS
Materials: The microspheres of chitosin were been prepared using the methods described by Prado et al.[6] The titanium isopropoxide was immobilized in microspheres of chitosin by sol-gel method, the material obtained was named TiO_2/microspheres of chitosan. 2,4-dichlorophenoxyacetic acid – 2,4,D (Sigma) was used without purification.
2,4-dichlorophenoxyacetic acid herbicide photocatalytic degradation: Photolysis of 2,4-dichlorophenoxyacetic acid herbicide (2,4-D) was carried out in a homemade photo-reactor (Figure 1)[7] using 250.0 mL of a 1.0×10^{-5} mol/L 2,4-D solution and 1.0 gL^{-1} of the TiO_2/microspheres of chitosan catalyst. These solutions were illuminated with a 125 W mercury-vapour lamp OSRAM HQL and the temperature of the reactor was kept at 30 °C. The solution irradiation was followed by an Instrutherm MRU-201 radiometer, which was maintained at 970 $\mu W/cm_2$ during the reaction. The herbicide degradation was followed on a UV-Vis Varian Cary 50 spectrophotometer.

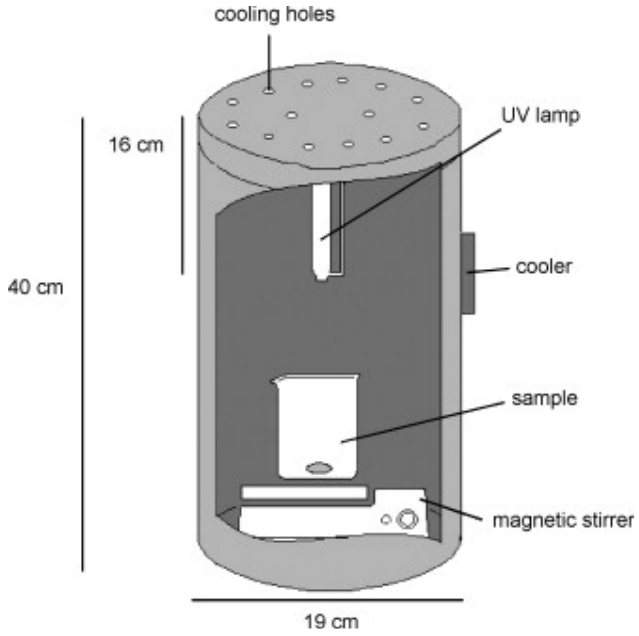

Figure 1. Schematic draw of home-made photo-reactor.

RESULTS AND DISCUSSION

Photocatalytic activity of TiO_2/microspheres of chitosan: The heterogeneous photocatalytic oxidation using semiconductors as catalysts becomes an alternative for organic pollutant degradation into innocuous final products (e.g., CO_2 and H_2O). Among the semiconductors, TiO_2 is the most suitable for the photodegradation of contaminants due to its chemical stability, low cost and low band gap value (3.2 eV). The band gap of TiO_2 allows that this oxide generate free hydroxyl radicals in water by UV irradiation which leads the contaminants degradation. [7,8]

The attachment of this oxide on microspheres of chitosan can allow the easy recuperation of the catalyst and increase its contact with water in order to generate more free hydroxyl radicals capable of degrading contaminants from water. [9]

The photodegradation of 2,4-dichlorophenoxyacetic acid herbicide was followed as a function of time, as represented in Figure 2. It can be observed that 2,4-D degraded quickly up to 50 min in the presence of TiO2/microspheres of chitosan.

These results suggest that TiO_2 immobilized on microspheres of chitosan can be explored as a photocatalyst to degrade contaminants from water.

CONCLUSION

These data showed TiO_2 immobilized on microspheres of chitosan can be applied in the water treatment, presenting high ability to degrade pesticides from water.

ACKNOWLEDGMENTS

The authors thank FAPDF for financial support and CNPq for fellowships.

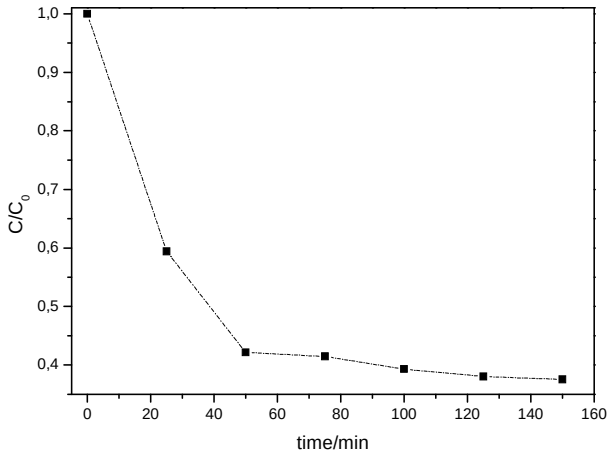

Figure 2. Kinetics of photocatalytic degradation of 2,4-D solution using of TiO_2/microspheres of chitosan.

REFERENCES

1. Prado, A.G.S., Airoldi, C*., Fresenius J. Anal Chem **371***: 1028-1030 (2001).
2 Bandala, E. K.; Peláez, M. A; Dionysiou, D. D.; Gelover, S.; Garcia, J.; Macías, D.; *J. Photochem. Photobiol. A* **186**: 357–363 (2007)
3 DeOliveira, E.;Neri, C. R.; Ribeiro, A. O.; Garcia, V.S.; Costa, L. L; Moura, A. O.; Prado, A.G.S. Serra, O. A.;Iamamoto, Y. *J. Colloid Interface Sci.* **323**: 98-104 (2008)
4. Cristante, V. M.; Prado, A.G.S.; Jorge, S. M. A.; Valente, J. P. S.; Florentino, A. O.; Padilha, P. M. *J. Photochem. Photobiol. A* **195**: 23–29 (2008).
5 Prado,A.G.S., Airoldi, C., *Thermochimica Acta* **349**: 17-22 (2000).
6. Prado,A.G.S., Pescara, I.C., Albuquerque,R.D.A., Honorato, F.N. and Almeida, C.M., *Analytica* **44**: 62-67 (2009).
7. Prado, A. G. S. ; Bolzon, L. B.; Pedroso, C. P.; Moura, A. O.; Costa, L. L. *Appl. Catal. B* **82**: 219-224 (2008).
8. Daneshvar, N.; Salari, D.; Khataee, A. R. *J. Photochem. Photobiol. A* **162** 317–322 (2004).
9. Prado, A. G. S.; Faria, E.;SouzaDe, J.R.; Torres, J. *J. Mol. Catal. A* **237**: 115–119 (2005).

Chitosan intelligent film: a fast detection of H_2S

Edison T. Kator Jr.,[1] Christiana M.P. Yoshida,[1,2] and Telma T. Franco[1]

[1] School of Chemical Engineering –State of University of Campinas, UNICAMP – P.O. Box 6066, Cep.13083-970, Campinas – SP, Brazil
[2] Federal University of São Paulo, UNIFESP – Professor Artur Riedel Avenue, 275, Cep. 09.972-270, Diadema – SP, Brazil
E-mail: kato_imel@yahoo.com.br

Abstract
An intelligent indicator system was developed combining chitosan as tridimensional biopolymer matrix and colorimetric indicator hydrogen sulfide gas (H_2S), that can be poisonous at high concentrations, it can be generated in different industrial sectors (petrochemical, paper mills, food, etc). Products as canned vegetables, minimally processed food and vacuum packaged meat are potentially exposed to contamination. A biodegradable and intelligent system was developed based on chitosan film containing H_2S colorimetric indicator. Colour variation on the system was measured along exposition time to H_2S gas. The indicator was able to produce black colour as a rapid response to the presence of H_2S.

Key words: Chitosan film, Intelligent packaging, Colorimetric indicator, Biodegradable

INTRODUCTION

Solid waste is a world problem and the improved management of wasted packaging has stimulated the development of biodegradable materials. The advantage of using natural polymers in packaging industry is the possible rapid biodegradation under composting and landfilling conditions[1],[2].

Several advantages were associated to biodegradable film, according to Srinivasa *et al.*[3], since they are generally prepared by using natural materials such as polysaccharides, proteins and their derivatives, which are abundantly available. Polysaccharides, proteins and lipids constitute a group of biomaterials that readily form biofilms[4] , which have been investigated for their ability to retard the transport of moisture, gases, flavour and lipids[5]. They can be used effectively as an alternative to synthetic plastics as long as the desirable overall mechanical and barrier properties are attended.

Chitosan is a polysaccharide derived from chitin by removing acetyl groups with alkali. Chitin is very abundant in nature, being found in fungal walls and exoskeletons of crustaceans and insects[6]. Chitosan is an excellent film-forming linear polymer with a backbone consisting of β-(1-4)- 2-acetamido-2-deoxy-D-glucose (*N*-acetyl glucosamine - GlcNAc) residues and glucosamine residues (GlcN). It is characterized by the degree of acetylation (DA) and average molecular weight (Mw), among other properties, e.g. degree of polymerization[7], viscosity and solubility. Chitosan is low toxic, biodegradable and depending on its molecular structure, size and concentration, may inhibit the growth of fungi, bacteria and yeasts[8]. It is soluble in dilute acid as it contains free amine groups ($-NH_2$) protonated in acidic solutions, which form ammonium groups ($-NH_3^+$)[9]. These useful properties make chitosan a promising biodegradable polymer for active food packaging application [10],[11]. Chitosan showed different useful film properties (water vapour transmission rate and mechanical properties such as tensile strength and elongation at break) when different additives, e.g. palmitic acid, beeswax or carnauba wax, were added in the mixture of the film-forming solutions[12].

Intelligent packaging can be defined as a packaging system capable of carrying smart

functions, e.g. detecting, sensing, recording, tracing, communicating, and applying scientific logic to facilitate decision making to extend shelf life, enhance safety, improving quality, providing information, and warning about possible problems. When integrated to science based principles, is a useful tool for tracking products and monitoring their conditions, facilitating real-time data access and exchange, and enabling rapid response and timely decision making[13].

A colorimetric sensor may be defined as a substance that indicates the presence of another substance or the degree of reaction between two or more substances by a colorimetric change. In contrast indicators do not comprise receptor and transducer components and communicate information through direct visual change[14].

The aim of this study was to develop biodegradable and intelligent system based on chitosan film containing a H_2S colorimetric indicator.

MATERIALS and METHODS

Raw materials: Chitosan (Primex, degree of acetylation, DA, of 18%, Island), acetic acid (Synth, Brazil), H_2S indicator (Synth, Brazil), sodium carbonate (Synth, Brazil) and card paper, Triplex TP 250 (Suzano Papel e Celulose, Brazil).

Intelligent system formation: Film solutions were prepared following the methodology proposed by Yoshida *et al.*[12] dispersing chitosan (3.0%, w/w) in aqueous acetic acid. The stoichiometric amount of acetic acid was calculated from weight of sample and the DA, to achieve the protonation of the NH_2 sites. Chitosan solutions were homogenized by magnetic stirring at room temperature for 60 minutes and 2.0% (w/w) of the colourimetric indicator then added and well mixed to the filmogenic solution. Two grams of the prepared solution of chitosand and indicator were coated on card paper sheets (16.5 x 27.5 cm) using a bar coater of 25μm of thickness manufactured by TKB Erichsen Instruments. The systems were dried in an oven at 150°C for a period of 90 seconds.

System response efficiency: The H_2S indicator response was measured submitting the coated paper sheets to different time exposition of H_2S gas, generated at room temperature by the reaction of 0.012g of FeS with HCl 1M (equation 1) in a closed chamber and slightly heated to accelerate the chemical reaction:

$$FeS + 2HCl \underset{\leftarrow}{\rightarrow} H_2S + FeCl_2 \qquad (1)$$

The amount of H_2S generated was determined stoichiometrically taking into account the volume of the chamber, 8000mL, and the purity of FeS informed by the manufacturer, as shown in Equations 1 and 2.

$$n_{H_2S} = \rho.V \qquad (Eq.\ 1)$$

With: ρ = 0,04079 mol/dm^3[15]; V = 8x10^{-4} dm

$$m_{FeS} = MM_{FeS}.n_{H_2S} \qquad (Eq.\ 2)$$

With: MM_{FeS} = 87,92 g/mol.

The color lightness parameter (L*) of the intelligent system was measured using a colorimeter (Konica Minolta Chroma Meter CR-400), according to Sobral *et al.*[16].

Evaluation of the microstructure of the intelligent system

Scanning Electron Microscopy (SEM): SEM analysis was performed on fractured cross-sections and the surface of gold-sputtered chitosan system using a LEO 440i scanning electron microscope (LEO Electron Microscopy Ltda.). SEM analysis was performed with

voltage and amperage of 10kV and 50pA, respectively.
Energy Dispersive X-ray Spectroscopy (EDS): Interaction of the primary beam with atoms in the sample causes shell transitions which result in the emission of an X-ray. The emitted X-ray has an energy characteristic of the parent element. Detection and measurement of the energy permits elemental analysis (EDS). An energy-dispersive (EDS) detector is used to separate the characteristic X-rays of different elements into an energy spectrum, and EDS system software is used to analyze the energy spectrum in order to determine the abundance of specific elements. EDS analysis was performed with voltage and amperage of 10kV and 600pA respectively.

RESULTS AND DISCUSSION

Intelligent chitosan system of H_2S presence was developed. Chitosan films obtained in our laboratory had a slightly yellow appearance (Figure 1a). The presence of the indicator induce a colour change of the chitosan films to a dark yellow colour (Figure 1b). Similar colour change was observed when the solution was applied as coating on the card paper surface (Figures 2a and 2b).

(a) (b)

Figure 1 - Images of (a) film without indicator, (b) intelligente film with H_2S indicator.

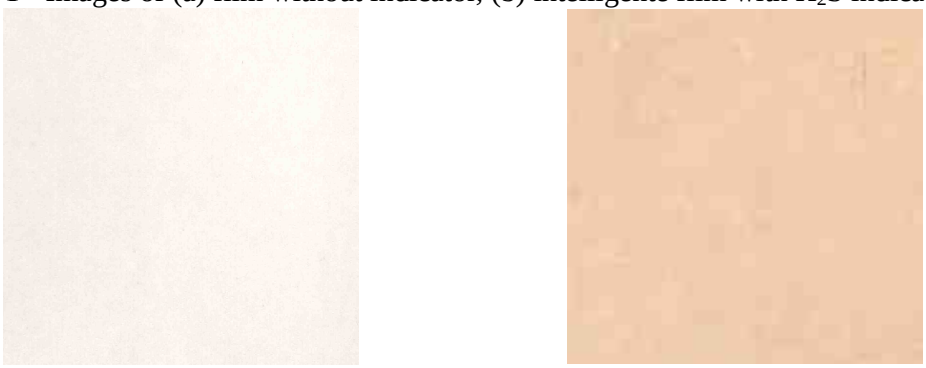

(a) (b)

Figure 2 - Images of (a) card paper coating with chitosan without H_2S indicator and (b) intelligente indicator with H_2S indicator.

A compact and cohesive structure without pores or cracks was observed on SEM analysis (Figure 3) confirming the visual appearance. According to Li, Du and Xu [17], chitosan is almost completely adsorbed onto the surface of cellulosic fibers, and that the adsorption increases with the degree of deacetylation. The possible ways of interaction between chitosan and cellulose substrates can be hydrogen bonding, electrostatic interaction, van der Waals forces, covalent bonds and aggregation or association. The EDS analysis shows the H_2S indicator was uniformly distributed into chitosan matrix films represented by red points

through chitosan matrix (Figure 3b).

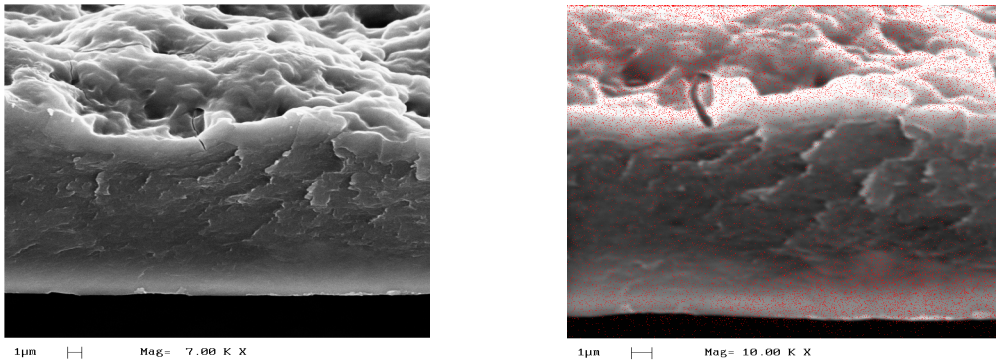

(a) (b)

Figure 3 - SEM Micrographs for chitosan intelligent system (a) and (b) elemental analysis.

Indicator response efficiency: The intelligent system developed in this study showed an initial response at 30 seconds of exposure changing the colour from yellow to black. Figure 4 illustrates the colour variation under different exposition time with H_2S gas contact. The L* parameter value, indicating luminosity, was measured and its standard deviation in function of H_2S exposition time was shown in Figure 5, where is denoted that variation on L* parameter value after 90 seconds has no statistically significance difference at $p \leq 0.05$.

Sen *et. al.*[18] developed a colorimetric sensor for detection of H_2S based on an inexpensive chemical sensor array (CSA) consisted of an array of chemoresponsive dyes manufactured by ChemSensing Inc.[19] that undergoes a color change upon interacting with gases and vapors. They obtained to the lowest H_2S concentrations studied (50, 100, 250, 500 ppb) differences in magnitude of color change after 30 min of exposure, while 2 and 5ppm produce a initial response and reached saturation at 15 min.

There are several applications for this kind of intelligent system, from the petrochemical to food industries (e.g. indication of gas leaking of petrol processes to detection of H_2S a microbial metabolite released in conditions of anaerobiosis). The system communicates the presence of H_2S in case of leaks in the line of recovery, in critical points (e.g. joints, valves, connections), or informs the consumer about microbiological changes in the product during transportation and/or storage, indicating the state of freshness of the product.

The H_2S detection in low concentration is extremely important due to its effects on humans and animals. Concentrations of 10 ppm and above, causes conjunctival irritation, because sulfide and hydrogen sulfide anions are strong bases. Hydrogen sulfide affects the sensory nerves in the conjunctivae, so that pain is diminished rapidly and the tissue damage is greater. Serious eye damage is caused by a concentration of 50 ppm [20]. Hydrogen sulfide causes odour nuisance at concentrations far below those that cause health hazards. On the basis of the scientific literature, it is not possible to state a specific concentration of hydrogen sulfide at which odour nuisance starts to appear. Half-hour average concentration exceeding 0.005 ppm is likely to produce substantial complaints among persons exposed[21],[22], however, at high concentrations, a person might lose their ability to smell it, this can make H_2S seriously dangerous[23], so that the odour can no longer be recognized as a warning signal. At higher concentrations there is strong stimulation of the central nervous system (CNS)[24], with hyperpnoea leading to apnoea, convulsions, unconsciousness, and death. At concentrations of over 940 ppm there is immediate collapse. In fatal human intoxication cases, brain oedema, degeneration and necrosis of the cerebral cortex and the basal ganglia have been observed[20].

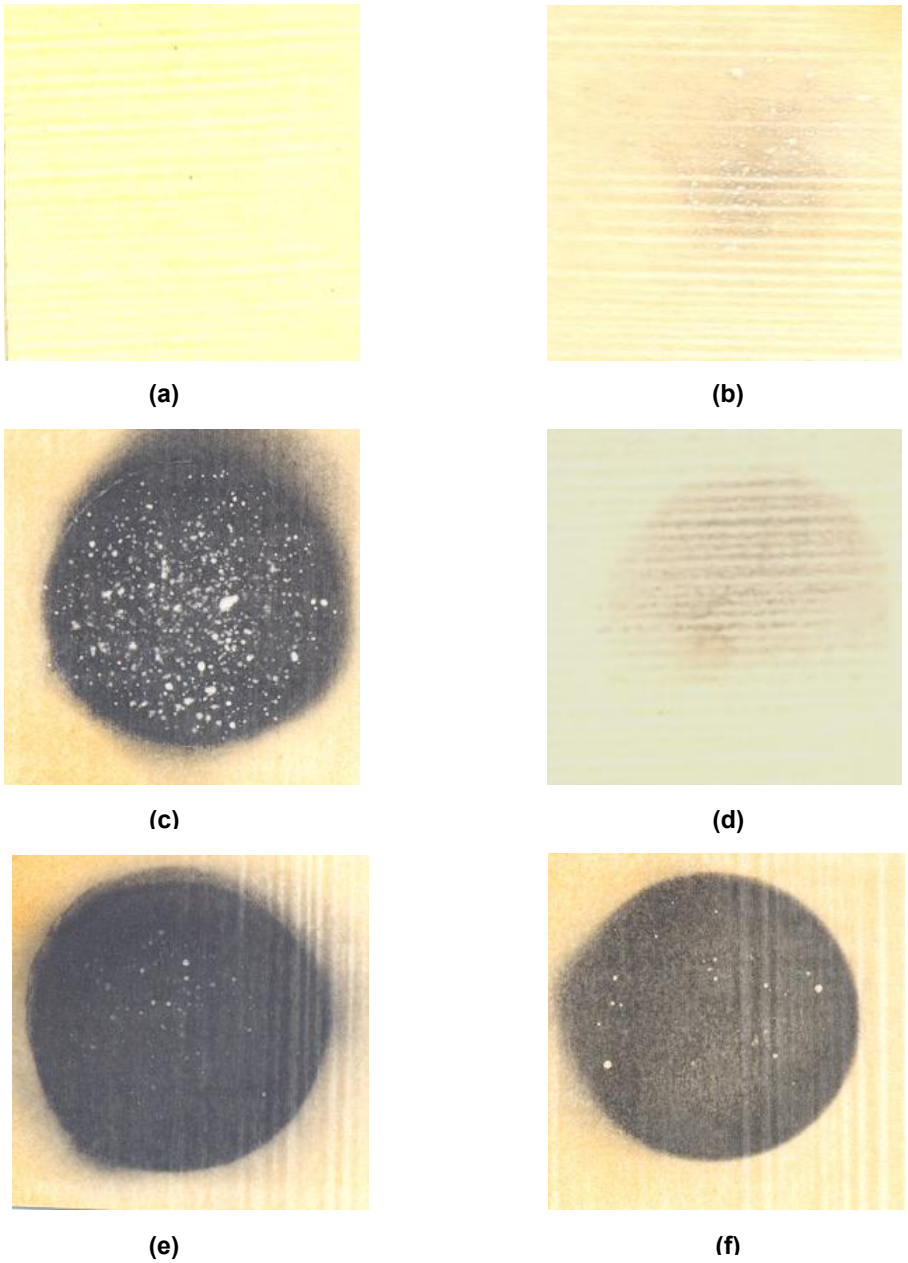

Figure 4. Colour response of chitosan intelligent films at different H_2S gas exposition time (a) 0; (b) 30; (c) 60; (d) 90; (e) 120; (f) 180s.

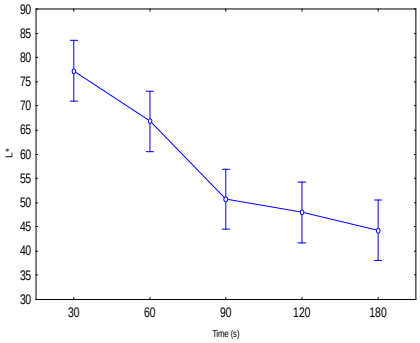

Figure 5 - L* parameter value vs. exposure time.

CONCLUSIONS

New intelligent, biodegradable and fast indicator system was obtained to H_2S gas detection, comparing to methylene blue methodology which require longer times for response, the time needed just to sampling, in concentrations equal or larger than $7mg/m^3$, is 300 seconds and the reaction time can take up to an hour. This new intelligent system is at least 130 times faster. Chitosan intelligent system presents colour variation, from light yellow to black, in function of the H_2S gas contact. The chitosan intelligent system could offer an efficient alternative to petrochemical, chemical and foods industries to communicate the presence of H_2S.

ACKNOWLEDGEMENTS

This work was financially supported both by FAPESP, CNPq and CAPES. The authors thank Primex for providing them chitosan samples.

REFERENCES

1 Ahvenainen R, Woodhead Publishing Ltd, Cambridge, UK, pp.5-21 (2003).

2 Rijk R, *Plastics & Polymers in Contact with foodstuffs*. Edinburgh, Scotland: Pira Intl (2002).

3 Srinivasa PC, Ramesh MN, Kumar KR and Tharanathan RN, *J. Food Eng.*, **63(1)**: 79-85 (2004).

4 Garcia MA, Pinotti A, Martino MN and Zaritzky NE, *Carbohydr. Polym.,* **56**: 339-345 (2004).

5 Pérez-Gago MB, Nadaud P, and Krochta JM, *J. Food Sci.,* **64 (6)**: 1034-1037 (1999).

6 Peter MG, in A. Steinbüchel (ed.) Biopolymers, Vol. 6. *Weinheim: Wiley-VCH*, 123-157 (2002).

7 Muzzarelli RAA, *Carbohydr. Polym.*, **29**: 306-316 (1996).

8 Tikhonov VE, Stepnova EA, Babak VG, Yamskov IA, Palma-Guerrero J, Jansson H-B, Lopez-Llorca LV, Salinas J, Gerasimenko DV, Avdienko ID and Varlamov VP, *Carbohydr. Polym.*, **64**: 66-72 (2006).

9 Hon DN-S, *Medicinal Applications*, ed by Dumitriu S. Marcell Decker. New York, pp.794 (1996).

10 Aider M, *LWT - Food Sci. Technol.*, **43**: 837–842 (2010).

11 Yoshida CMP, Bastos CEN and Franco TT, *LWT - Food Sci. Technol.*, **43**: 584–589 (2010).

12 Yoshida CMP, Oliveira-Junior EN and Franco TT, *Packaging Science and Technology*, **22**: 161-170 (2009).

13 Yam KL, Takhistov PT and Miltz J, *J. Food Sci.*, **70**: n.1 (2005).

14 Kerry JP, O'Grady MN and Hogan SA, *Meat Sci.*, **74**: 113-130 (2006).

15 Poling BE, Thomson GH, Friend DG, Rowley RL and Wilding WV, *The McGraw-Hill Companies*, Inc., USA (2008).

16 Sobral PJA, Menegalli FC, Hubinguer MD and Roques MA, *Food Hydrocolloids*, **3-4**: n.15, 423-32 (2001).

17 Li H, Du Y, and Xu Y, *J. Appl. Polym. Sci.*, **91**: 2642-2648 (2004).

18 Sen A, Albarella JD, Carey JR, Kim P and McNamara III WB, *Sens. Actuators, B*, **134**: 234-237 (2008).

19 Rakow NA and Suslick KS, *Nature*, **406**: 710-713 (2000).

20 Savolainen H, *Arbeta och hdlsa,* **31**: 1-27 (1982).

21 Lindvall T, *Nordisk hygienisk tidskrift,* **51**(Suppl. 2): 36-39 (1970).

22 National Research Council. *Odors from stationary and mobile sources.* Washington, DC, National Academy of Sciences, 1979, p. 491.

23 ASTDR - Agency for toxic substances and desease registry (2006), *Toxicological*

profile for hydrogen sulfide, US. Department of health and human services, Public Health Service Agency for Toxic Substances and Disease Registry. http://www.atsdr.cdc.gov/toxprofiles/tp114.html. [Accessed in 28 april 2009].
24 *Hydrogen sulfide.* Geneva, World Health Organization, 1981 (Environmental Health Criteria, No. 19).

Chitosan intelligent film: time-temperature indicator

Vinícius Borges V. Maciel[a], Cristiana M. P. Yoshida[a,b], Telma T Franco[a]*

[a] School of Chemical Engineering, Laboratory of Biochemical Engineering, Bioprocesses and Renewable Products, UNICAMP, State University of Campinas, SP, Brazil
[b] Federal University of São Paulo, UNIFESP, Diadema, SP, Brazil
*E-mail: franco.feq@gmail.com

Abstract
Natural thermal-sensitive pigment (anthocyanin) was incorporated into chitosan matrix films as a time-temperature indicator forming the intelligent films. These films could be applied as external packaging material to control the temperature conditions during transportation and storage. Anthocyanin (0.25g/100g) was incorporated into chitosan matrix films (2.0g/100g). The temperature (10°C and 50°C) and luminosity (0 and 1000 Lux) effects on chitosan intelligent films (ATH-CF) were analyzed using an experimental design of 2 variables, measuring the colour parameters (L*, a*, b*) and mechanical properties (tensile strength, elongation break and Young's modulus) as responses. The ATH-CF became darker after being submitted at temperature above 50°C and luminosity of 1000 Lux for 72 h, indicating a potential use as time-temperature indicator.

Keywords: chitosan films, anthocyanin, time-temperature indicators, chitosan intelligent films

INTRODUCTION

Biodegradable films continue to be an important packaging research target, owing their very significant commercial potential applications. Natural polymer films have been investigated for their ability to retard the moisture, gas, flavor and lipids transport. Many studies had been developed to produce and characterize of biodegradable films based on natural macromolecules, such as whey proteins[1,2], gelatin[3], zein[4], chitosan[5] and others. However, these material applications are still scarce according to the literature. Natural polymer use at flexible packaging has been largely studied, aiming at partial synthetic polymer substitution, due to environmental waste accumulation problem[6]. Among natural polymers, chitosan is biodegradable, obtained from renewable source, flexible forms and resistant films with an efficient oxygen barrier[5].

Intelligent packaging system is a concept that detects and monitors packaged products conditions to provide information, facilitate decision making, extend shelf-life, enhance safety, improve quality and warn about possible problems over the distribution chain[7-9]. These systems can involve sensor or indicators incorporation that shows, through signals (e.g. electric, colorimetric), any initial packaging condition changes[10,11].

Temperature control is an important variable in food and drug product quality and safety[12]. Appropriate packaging promotes effective barrier to gases and moisture, but temperature control strongly depends on the transport and storage conditions. Monitoring temperature could promote a more accurate product shelf-life, consequently increasing quality control and reducing waste[13].

Some natural pigments are thermal-sensitive, which have their structure and colour changed under heat exposition, e.g.: anthocyanin is thermically stable to 60°C according to Woodward *et al.*[14]. Natural pigment application as a time-temperature indicator was not found in literature.

At this study, the objective was to develop an intelligent film system based on anthocyanin incorporated into chitosan matrix. Efficient time-temperature indicator system response was analyzed by colour parameter changes. Mechanicals properties of films were measured.

MATERIALS AND METHODS

Materials

Chitosan (Primex, Finland), acetic acid (Synth, Brazil), anthocyanin (Christian Hansen, Brazil) and card paper triplex TP 250 g/m^2 (Suzano Papel e Celulose Ltd., Brazil).

Methods

Chitosan intelligent films (ATH-CF). Film suspensions were prepared by dispersing chitosan (2.0g/100g) in aqueous acetic acid[5]. The stoichiometric amount of acetic acid was calculated from weight sample, taking in account the value of DA to achieve the protonation of the NH_2 sites. The suspensions were homogenized by magnetic stirring at room temperature for 45 minutes. Then, 0.25g/100g of ATH was homogenized at filmogenic suspension and 9.0ml of aliquots were poured into Petri dishes (diameter=9.5cm). Films were dried at room temperature for 36 followed by 28°C in an incubator with forced air circulation for 24 h. As the solution mass applied onto Petri dishes was maintained constant, then the total solid content per gram of dried films were 28.2g/m^2 for ATH-CF.

Anthocyanin kinetic degradation. Anthocyanin kinetic degradation at ATH-CF was studied based on the colour parameter (L*,a*,b*) variations, at different time periods (0, 12, 24, 48 and 72 h) at temperature and luminosity conditions using a controlled chamber (TE-391, Tecnal, Brazil).

Experimental Design. Temperature and luminosity effects on ATH-CF were studied using an experimental design (Table 1). Luminosity range was from dark exposition (0 Lux) to supermarket light simulation (1000 Lux). The exposition time to temperature and luminosity conditions was established for 72 h.

Table 1. Values range used in experimental design of two variables.

Variables	-1	0	+1
Temperature (^{o}C)	10	30	50
Luminosity (Lux)	0	500	1000

ATH-CF characterization

Colour evaluation. For the colour determinations, ATH-CF was analyzed using a colorimeter Chroma Meter CR 400 (Konica Minolta, Japan). Before each measurement, the apparatus was calibrated with a white calibration plate. Measurements were performed in the CIE L*a*b* system. The lightness value, L*, indicates how dark/light the sample is (varying from 0, black, to 100, white), a* is a measure of greenness/redness (varying from -60 to +60), and b* is the grade of blueness/yellowness (also varying from-60 to +60). Transforming a* and b* values into geometric values can be a better predictor of sensory perception[15]. Thus, to describe the colour behavior of ATH-CF submitted at temperature and luminosity different, the hue angle, h_{ab} (0-360°), obtained by arctan b*/a*, expressing the characteristic/dominant colour, were used[16-18]. Data were obtained in triplicate.

Mechanical properties. Tensile strength (Ts), elongation at break (ε) and Young's Modulus (E) were determined based on ASTM D882[19]. Films were cut into 25.4 × 100.0 mm strips and then preconditioned at 50% RH and 25 ± 2ºC for 48h. Mechanical properties were measured with a TA.XT2 texture analyzer (Stable Micro Systems, Godalming, UK). The initial grip separation was set at 50mm and crosshead speed at 1mm/min. There were at least ten replicates per experiment. Film thickness was measured using a micrometer (Mitutoyo Mfg

Co. Ltd., Japan) and measurements were taken at five random positions on the film. Average values were used to calculate film properties.

Scanning electron microscopy (SEM). SEM analysis was performed on fractured cross-sections and the surface of gold-sputtered chitosan films using a LEO 440i scanning electron microscope (LEO Electron Microscopy Ltda., England), operating at 10 kV and 100 pA. Chitosan films (CF) without anthocyanin was studied as reference.

Cardpaper tests. After total solubilization of chitosan (2g/100g) in aqueous acetic acid under continuous agitation, 0.25g/100g of ATH was homogenized in filmogenic dispersion. Sheets of cardpaper (0.045m^2) were coated with filmogenic suspensions of ATH-CF equivalent to 0.081g/m^2 using a 80 μm wire bar coater (TKB Erichsen, Brazil). The coated paper sheets were dried in oven at T=150°C for 90 seconds.

Anthocyanin kinetic degradation. The cardpaper coated with ATH-CF were submitted at temperature and luminosity conditions using a controlled chamber (TE-391, Tecnal, Brazil), according to Table 2. The anthocyanin kinetic degradation in cardpaper was analized based on the colour parameters (L*,a*,b*) variations, at different periods of time (0, 12, 24, 48 and 72 h).

Table 2. Temperature and luminosity conditions for colour kinetic degradation in cardpaper coated with ATH-CF.

Conditions	Temperature (°C)	Luminosity (Lux)
1	75	0
2	60	0
3	50	1000
Control	25	0

Water absorption – Cobb Test. Cardpaper uncoated and coated with ATH-CF were cut into 125.0 x 125.0 mm and preconditioned at 50% RH and 25°C for 48h. Water absorption capacity was determined in accordance with standard ASTM D3285[20]. The weight gain was measured in analytical balance (AND HR-200 model, Japan). The results were expressed in g/m^2. There were at least fifteen replicates per experiment.

Taber Stiffness. Taber stiffness was determined according to the standard method ASTM D5342[21]. Uncoated and coated cardpaper were cut in dimensions of 38.1 mm x 70 mm in the machine direction (MD) and the cross direction (CD) using a guillotine (Regmed, Brazil) and preconditioned 50% RH and 25°C for 48h. Taber stiffness was measured at angle 15° using Taber stiffness equipment (RI 5000 model, Regmed, Brazil). Results were expressed in mN.m. There were at least fifteen replicates for experiment.

Statistical Analysis. Statistical analysis was carried out with Statistic version 5.0 program (Statisc Inc., USA) and differences between the means were detected by the Tukey multiple comparison test.

RESULTS AND DISCUSSION

Chitosan intelligent films. Homogeneous, transparent, dark violet films were obtained. Following the drying steps, films were easily removed from the support plates, forming a flexible and resistant matrix.

Anthocyanin kinetic degradation. The kinetic curves of colour parameters (L*, a*, b*) of ATH-CF were obtained in different time periods (0, 12, 24, 48, 72 h) after temperature and light expositions.

The parameters L* and a* did not change significantly after temperature and light exposition according to Tukey test ($p \leq 0.05$). Only the parameter b* increased proportionally to the

temperature (Figure 1). Parameter b* was characterized by colour change in a range of -b (blue) to +b (yellow).

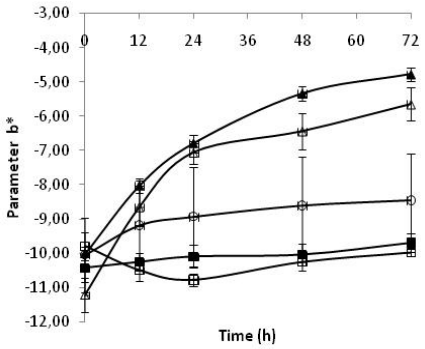

Figure 1. Kinetic curve of parameter b* colour change of ATH-CF submitted at different temperature and light conditions: 30°C and 500 Lux (○); 50°C and 1000 Lux (Δ); 10°C and 1000 Lux (■); 50°C and 0 Lux (▲) and 10°C and 0 Lux (□).

Luminosity did not affect the colour films at 10°C, confirming anthocyanin structure stability at refrigerator temperature condition. ATH-CF submitted at 50°C reduced b* values significantly, after exposition at 0 Lux and 1000 Lux, compared to initial conditions of, 52,3% and 49,6% lower, respectively.

Shaked-Sachray *et al.*[22] and Bolivar and Cisveros-Zevallos[23] observed that higher temperatures increased anthocyanin pigment degradation and discoloration. Significant changes in b* values were also found by Alighourchi and Barzegar[24] for anthocyanins in pasteurized pomegranate juice, stored at 4°C, 20°C and 37°C for 210 days. In this study, L*, a* and b* values decreased, and the most significant colour change was observed after storage at 20°C and 37°C. This change was attributed to the anthocyanin degradation or polymerization when submitted to high temperatures, making juice coloration into brown colour, at the end of evaluation period.

Thermal anthocyanins degradation can result into a variety of species depending upon the severity and nature of heating. Anthocyanins degradation mechanisms is still relatively unknown but chemical structure and presence of other organic acids have a strong influence[25]. Markakis *et al.*[26] suggested opening of pyrylium ring and chalcone formation as a first degradation step for anthocyanins. Chalcone is derived from three acetates and from one derived from cinnamic acid. It has a yellow pigmentation and is a precursor flavonoid biosynthesis. Adams[27] proposed hydrolysis of sugar moiety and aglycone, an isoflavone, formation as initial degradation step, possibly due to cyclic-adducts formation. The author also reported that anthocyanin would decompose upon heating into a chalcone structure, the latter being further transformed into a coumarin glucoside derivative from a loss of the B-ring.

Recent studies[25,28-31] have been published, confirming the results found in this study on anthocyanin colour change. According to Lauro and Francis[32], the anthocyanins could interact with temperature, light, oxygen presence, pH, sugars, enzyme presence, proteins and metal ions[28,29,33,34], producing polymers that have decreased their stability.

ATH-CF characterization. Films were characterized after 72 h of exposition at different temperature and luminosity conditions.

L* and Hue angle (h_{ab}) colour parameters of ATH-CF are presented in Table 3. At experimental design, the parameters of a* and b* had not to be analyzed on independent form, due to interactive relationship existing between them. This parameter has measured the colour saturation. Then, according to Choubert and Baccaunaud[16], Gonçalves *et al.*[17] and Wyszecki

et al.[18], it was necessary to convert these parameters into a single parameter known as Hue angle – h_{ab}.

Table 3. Matrix of experimental design 2^2 and responses of colour parameters and mechanicals properties.

Tests	Independent Variables		Responses				
	Temperature (°C)	Luminosity (Lux)	L*	h_{ab} (°)	ε (%)	Ts (MPa)	E (GPa)
1	-1 (10)	-1 (0)	45.52	274.13	3.215	60.714	3.123
2	+1 (50)	-1 (0)	48.73	307.29	2.911	66.511	3.152
3	-1 (10)	+1 (1000)	45.16	298.08	3.607	60.62	2.5
4	+1 (50)	+1 (1000)	45.85	323.19	3.38	50.039	2.71
5	0 (30)	0 (500)	45.77	312.29	2.56	67.644	3.138
6	0 (30)	0 (500)	45.7	311.45	2.53	67.675	3.14
7	0 (30)	0 (500)	46.09	312.01	2.558	67.628	3.145

Temperature and luminosity variables effects obtained on L* parameter at ATH-CF are shown in Figure 2.

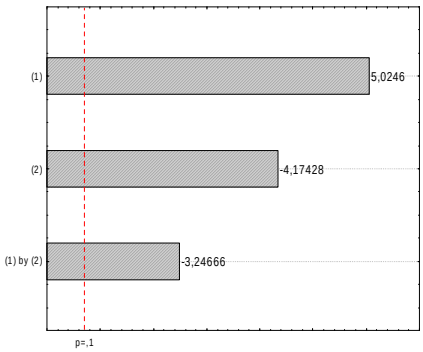

Figure 2. Pareto chart evaluating the effects on L* parameter at ATH-CF. (1) Temperature; (2) Luminosity; (1) by (2) Temperature and Luminosity interaction.

All factors were significant for a confidence level of 90%. Increasing the temperature from 10 to 50°C, a darkening on film was observed in order of 5.04. Luminosity caused a contrary effect, an increase from 0 to 1000 Lux, promoting an ATH-CF discoloration, making them lighter. The interaction between the two variables reduced L* value in order of 3.2.
For the h_{ab} colour response of ATH-CF, only the temperature effect was observed (Figure 3). At increase of temperature from 10 to 50°C, the h_{ab} values were higher in order 3.40, indicating that the films became darker. The same tendency was observed for luminosity, increasing from 0 to 1000 Lux, higher h_{ab} values, which was favorable whereas the films showed colour changing.

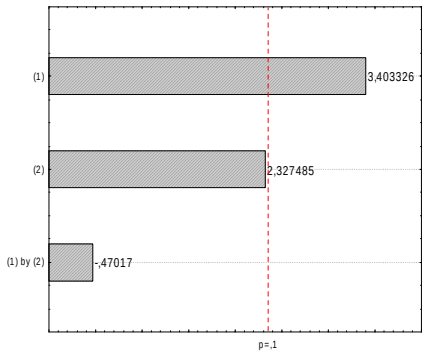

Figure 3. Pareto chart evaluating the effects on h_{ab} parameter at ATH-CF. (1) Temperature; (2) Luminosity; (1) by (2) Temperature and Luminosity interactions.

Mechanical Properties. Mechanical properties could indicate material rigidity and flexibility. The ε, Ts and E of ATH-CF were required after temperature and luminosity conditions of experimental design measured (Table 3).

Temperature and luminosity have not influenced ε and Ts significantly. For E, only the luminosity had a slightly significant effect ($p \leq 0.1$), as shown in Figure 4. Maintaining it at constant temperature (10° or 50°C), E decreased in order of 19.9% and 14.0%, respectively, as luminosity increased from 0 to 1000 Lux.

These results are indicating that flexibility and strength of ATH-CF remaining the same throughout product transport and storage process.

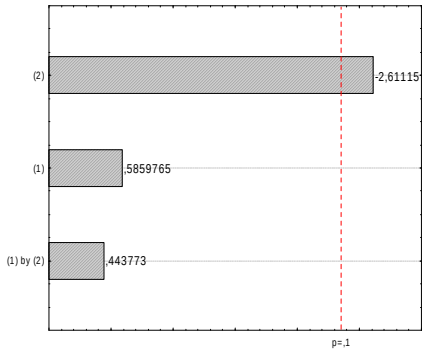

Figure 4. Pareto chart evaluating the effects on Ts at ATH-CF. (1) Temperature; (2) Luminosity; (1) by (2) Temperature and Luminosity interaction.

Scanning electron microscopy (SEM)- A compact and cohesive structure without pores or cracks was observed in CF (Figure 5a). No significant difference was observed between ATH-CF and CF structures (Figure 5b), since the natural pigment anthocyanin were entrapped in the film matrix. The absence pores in structure of film matrix is advantageous, in view that the formation of pores interferes directly in the mechanical properties of films.

Cardpaper Tests. Coating cardpaper with ATH-CF could be a commercial alternative to apply these films in an industrial making form. Chitosan presented biocompatibility with cardpaper surface, forming a homogenous film without any bubbles or defects.

The grammage results of uncoated and coated cardpaper were 3.79 ± 0.02 g/m^2 and 3.81 ± 0.04 g/m^2, respectively, indicating that no were observed significant difference.

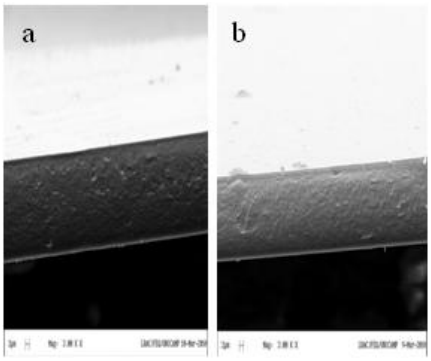

Figure 5. SEM Micrographs for (a) CF, (b) ATH-CF (0.25g/100g of ATH).

Water resistance is an important property, which can determine the behavior of cardpaper in various applications including food and drug packaging. The water absorption results obtained on the cardpaper uncoated and coated with chitosan films were 35.0 ± 0,63 g/m^2 and 31.6 ± 1,58 g/m^2, respectively. Despite the high sensitivity of CF to water[35], the cardpaper coated with these films decreased significantly the water absorption in order 9.71%. This reduction it makes the cardpaper more resistant. According to Aider[36], chitosan films have abilities to avoid moisture loss or water absorption and could be regarded as a reinforcement layer. Bordenave *et al.*[37] studied the potentiality of bioactive food packaging based on chitosan-coated papers, revealed that chitosan film improved the paper water absorption despite the very low amount of total solids. Chitosan from concentrations of 0.1, 0.25, 0.50 and 0.75 % were applied as a coating additive in paper and paperboard, observing that increasing chitosan concentration from 0.1 to 0.75%, reduced, significantly, the water absorption values[38]. The greaseproof paper coated with chitosan films, did not provide extra barrier against water absorption[39].

The Taber stiffness evaluates as a material is rigid after being subjected to a given force. Uncoated and coated cardpaper with ATH-CF were analyzed in the CD (cross-direction) and the MD (machine direction) of the cardpaper (Table 4).

Taber Stiffness results obtained for uncoated and coated cardpaper were statistically significant different ($p \geq 0.05$), presenting higher Taber stiffness for coated cardpaper. Higher Taber stiffness is better because this system proposed become more resistant. According to Vartiainen *et al.*[40] it is very seldom used coating in paper sheets to improve tensile properties. Kuusipalo *et al.*[38] also studying the stiffness of paper and paperboard founded that in the MD, the increase coating weight of chitosan does not show as pronounced a reinforcing effect as in the CD, which is contrary to the results found in this study.

Table 4. Stiffness values of cardpaper uncoated and coated with ATH-CF.

Analysis	CD (mN.m)		MD (mN.m)	
	Cardpaper uncoated	**Cardpaper coated**	**Cardpaper uncoated**	**Cardpaper coated**
Stiffness	5,64 ± 0,08^b	6,15 ± 0,13^b	12,44 ± 0,18^a	13,88 ± 0,51^a

a, b – statistically significant difference between the average in same section ($p<0.05$) calculated for Tukey Test through of Statistic software version 7.0

Anthocyanin kinetic degradation. The kinetic curves of colour parameters (L*, a*, b*) of cardpaper coated with ATH-CF were obtained in different periods of time (0, 12, 24, 48, 72 h) after temperature and light exposition, according to Table 2.
Parameters L* and a* did not change significantly ($p \leq 0.05$) after temperature and light exposition. Although parameter b* increased with the temperature and luminosity exposition (Figure 6).

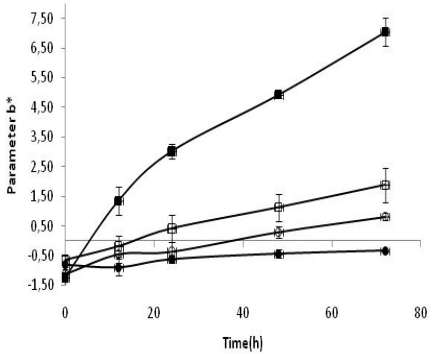

Figure 6. Kinetic curve of parameter b* colour change of cardpaper coated with ATH-CF submitted at different temperature and light conditions: Control (♠); 50°C and 1000 Lux (□); 60°C and 0 Lux (○); 75°C and 0 Lux (■).

The colour cardpaper coated with ATH-CF in control condition did not affect significantly ($p \leq 0.05$), confirming good stability of anthocyanin structure in low temperature[24,25] and dark condition. The cardpaper coated submitted at 75°C changed b* values significantly from -1.24 to 7.04. The conditions of 60°C and 50°C both in dark exposition, changed the parameter b* values from -1.14 to 0.82 and from -0.59 to 1.24, respectively. The colour changes observed in the cardpaper coated with ATH-CF are present in Figure 7.
Independent of temperature and luminosity used, the cardpaper coated with ATH-CF showed the tendency to become yellow, the same behavior observed on ATH-CF. This colour change, according to Patras *et al.*[25] and other authors[26,27] could be associated the anthocyanin degradation or polymerization when subjected to high temperatures, forming degradation products as chalcone and coumarin glucoside. Several authors[22-24] observed that the anthocyanins when exposed to temperatures above 50°C show discoloration. And exposing to high luminosities, the discoloration process is accelerate[28,29].
The colour change was more significant on cardpaper coated than ATH-CF. This probably occurred due to the ATH-CF thickness on cardpaper to be lower when compared with ATH-CF. A smaller thickness could promote the greater of anthocyanin molecules and increase its degradation.

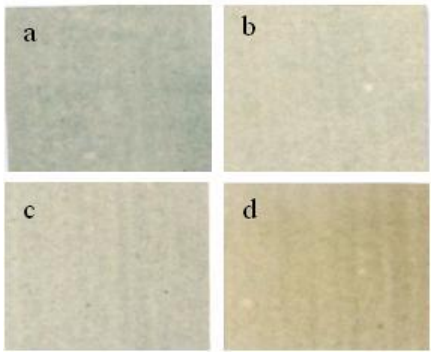

Figure 7. Change colour in cardpaper coated with ATH-CF. (a) Control; (b) 50°C and 1000 Lux; (c) 60°C and 0 Lux; (d) 75°C and 0 Lux.

CONCLUSIONS

ATH-CF films show potential to apply as a time-temperature indicator device. The system became darker after 72h under T=50°C, independently of luminosity. Colour parameter b* values have changed significantly. Increasing the temperature, films become darken (black colour - L* parameter) and increasing luminosity, films tended to discoloration.

Mechanicals properties ε and Ts did not change significantly after temperature and luminosity exposition. Only for E, luminosity had significant effect.

ATH-CF coating on cardpaper change the colour after temperature and luminosity conditions and decreased the water absorption and increased Taber stiffness.

ACKNOWLEDGEMENTS

The current study has been performed with the support of CNPq, FAPESP and CAPES.

REFERENCES

1 McHugh TH and Krochta JM, Permeability properties of edible films, in *Edible Coatings and Films to Improve Quality*, ed Krochta J.M, Baldwin EA and Nisperos-Carriedo MO. Technomic Publishing, New York, pp 30-55 (1994).

2 Yoshida CMP, Aplicação de concentrado protéico de soro de leite na elaboração de filmes comestíveis. Campinas (São Paulo): *UNICAMP*, 227p. (Tese de doutorado em Engenharia de Alimentos), 2002.

3 Carvalho RA and Grosso CRF, *Braz J Chem Eng* **23:** 45-53 (2006).

4 Gennadios A and Weller CL, CFW *Cereal Food World Review* **36:** 1004-1009 (1991).

5 Yoshida CMP, Oliveira-Junior EN and Franco TT, *Packag Technol Sci* **22:** 161-170 (2009).

6 Cuq B, Gontard N and Guilbert S, *Cereal Chem*, **75:** 1-9 (1998).

7 Yam KL, Takhistov PT and Miltz J, *J Food Sci*, **70:** R1-R10 (2005).

8 Rijk R. *Proceedings of a Conference on active and intelligent packaging development*. 19th International Conference: Plastics & Polymers in Contact with Foodstruffs. Edinburgh, Scotland: Pira Intl, 2002.

9 Ahvenainen R. In: R. Ahvenainen (Ed.), *Novel food packaging techniques*. Finland: CRC Press (2003).

10 Brody AL, Strupinsky ER and Kline LR, Active packaging for food applications, in *Active Packaging Opportunities*. Technomic Publishing, New York, pp 1-26 (2001).

11 Dainelli D, Gontard N, Spyropoulos D, Zondervan-van den Beuken E and Tobback P, *Trends Food Sci Technol,* **19:** S103-S112 (2008).

12 Tsai P, Mcintosh J, Pearce P, Cardem B and Jordan BR, *Food Research Int*, **35:** 351-356 (2002).

13 Shimoni E, Anderson EM and Labuza TP, *J Food Sci* **66**: 1337-1340 (2001).

14 Woodward G, Kroon P, Cassidy A and Kay C, *J Agric Food Chem* **57:** 5271-5278 (2009).

15 Ross EW, Shaw CP and Mary Friel, *J Food Quality*, **20:** 427-439 (1997).

16 Choubert G and Baccaunaud M, *Food Sci Technol*, **39:** 1203-1213 (2006).

17 Gonçalves EM, Pinheiro J, Alegria C, Abreu M, Branda TRS and Silva CLM, *J Agric Food Chem*, **57:** 5370-5375 (2009).

18 Wyszecki G and Stiles WS. *Color science*. Nova Iorque, EUA: J. Wiley & Sons, Inc., 1967.

19 ASTM. Tensile properties of thin plastic sheeting. Annual Book of ASTM Standards. *American Society for Testing and Materials*, Philadelphia, D882 (1995).

20 ASTM. Water Absorptiveness of nonbibulous paper and paperboard (Cobb Test). *American Society for Testing and Materials*, Philadelphia, D3285 (1999).

21 ASTM. Resistance to Bending of Paper and Paperboard (Taber- Type Tester in Basic Configuration). Annual Book of ASTM Standards. *American Society for Testing and Materials*, Atlanta, D5342 (2002).
22 Shaked-Sachray L, Weiss D, Reuverin M, Nissim-Levi A and Oren-Shamir M, *J Plant Physiol* **114:** 559-565 (2002).
23 Bolivar ACC and Cisveros-Zevallos L, *Food Chem* **86:** 66-97 (2004).
24 Alighourchi H and Barzegar M, *J Food Eng* **90:** 179-185 (2009).
25 Patras A, Brunton NP, O'Donnell C and Tiwari, BK, *Trends Food Sci Technol*, **21:** 3-11 (2010).
26 Markakis P, Livingstone GE and Fillers GR, *Food Research*, **22:** 117-130 (1957).
27 Adams JB, *J Sci Food Agric*, **24:** 747-762 (1973).
28 Patras A, Brunton NP, Da Pieve S and Butler F, *Inn Food Sci Emerg Technol* **10:** 308-313 (2009).
29 Rein M, Copigmentation reactions and color stability of berry anthocyanins. *University of Helsinki*, Helsinki, pp 10-14 (2005).
30 Wallace TC and Giusti MM, *Food Chem*, **73:** 241-248 (2008).
31 Aramwit P, Bang N and Srichana, T, *Food Research Int*, doi:10.1016/j.foodres.2010.01.022 (2010).
32 Lauro GJ and Francis JF, Natural Food Colorants, in *Anthocyanins*. Marcel Dekker, Inc., New York, pp 237-252 (2000).
33 Rhim JW, *Food Sci Biotechnol*, **11:** 361-364 (2002).
34 Mazza G and Miniati E, Introduction, in: *Anthocyanins in fruits, vegetables, and grains*, CRC Press, Boca Raton, pp. 1–28 (1993).
35 Fernandez-Saiz P, Ocio MJ and Lagaron JM, *Carbohydrate Polym*, **80:** 874-884 (2010).
36 Aider M, *Food Sci Technol,* **43:** 837-842 (2010).
37 Bordenave N, Grelier S, Pichavant F and Coma V, *J Agric Food Chem*, **55:** 9479-9488 (2007).
38 Kuupisalo J, Kaunisto M, Laine A and Kellomäki M, *Tappi J,* **4:** 17-21 (2005).
39 Kjellgren H, Gällstedt M, Engström G and Järnström L, *Carbohydrate Polym*, **65:** 453-460 (2006).
40 Vartiainen J, Motion R, Kulonen H, Rättö M,Skyttä E and Ahvenainen R, *J Appl Polym Sci*, **94:** 986-993 (2004).

Effects of chitosan coating on kraft barrier properties

Arlete B. Reis[*1,2], Cristiana M. P. Yoshida[1,3], Telma T. Franco[1]

[1] School of Chemical Engineering – State University of Campinas ,UNICAMP, – P.O. Box 6066, 13083-970, Campinas – SP, Brazil
[2] Federal University of Vale do Jequitinhonha and Mucuri, UFVJM – Institute of Science and Technology, Diamantina-MG, Brazil
[3] Federal University of São Paulo, UNIFESP – Department of exact and Earth Science, Av. Prof.Artur Riedel, 275, Diadema-SP-Brazil
*E-mail: arlete.reis@ufvjm.edu.br, Phone: +55-38-35321214

Abstract
The effects on chitosan-lipid coating on Kraft paper were studied. Different chitosan concentrations and lipid additions were evaluated for moisture barrier and structure properties of chitosan Kraft paper systems. The novelty of this paper is the formation of its packaging system, which conbines a biodegradable polymer (chitosan) and a hydrophobic compound (palmitic acid and stearic acid) with a widely used packaging paper (Kraft paper).

Keywords: Chitosan, lipid, coating, Kraft paper, barrier properties

INTRODUCTION

Chitosan is an abundant, natural polysaccharide obtained from fishing industry waste and a good candidate for partial replacement of synthetic polymers due to its renewable source and biodegradability, capacity to form resistant, elastic and flexible films[1]. Chitosan films also provide an efficient oxygen barrier; however, they are a poor water vapor barrier, which can be improved by incorporation of a hydrophobic compound (i.e. lipid), forming an emulsified film. Lipids, stearic, oleic, linoleic and palmitic acids in chitosan films reduces the matrix affinity for water molecules[2-5]. Kraft paper is widely used in packaging applications but its porous structure makes it highly permeable to gases[6] and it is formed of a structural matrix that connects cellulose and non cellulose chains (hemicellulose and lignin) by H-bondings. Its low cost favors its application in the packaging sector (electronics, food, pharmaceuticals, etc.). The aim of this work was to develop combining chitosan emulsified film and Kraft paper and to analyze the effects of chitosan concentration and lipid concentration on bilayer packaging properties (coating homogeneity, moisture barrier properties, and water absorption capacity).

MATERIALS AND METHODS

Materials

Chitosan (Primex, ChitoClear®, lot TM 2227, Iceland, DD=82%, Mw=171.492g/mol, acetic acid (Synth, Brazil), stearic acid (Synth, Brazil), palmitic acid (Synth, Brazil) and Kraft paper sheet grammage of 200g/m^2 (Klabin, Brazil).

Methods

Chitosan solubilization - The chitosan filmogenic suspensions were prepared by dispersing 3.0% and 4.0% chitosan (w/w) in aqueous acetic acid under continuous agitation. The dispersion was stirred until the chitosan was fully dissolved.

Chitosan emulsion - The emulsified filmogenic suspension of 4% chitosan (w/w) was obtained by adding palmitic acid (PA) at different concentrations (0.25, 1.00, and 2.00% w/w)

under continuous agitation. Lipids were liquefied by heating to temperatures above their melting points (90°C). The solution was emulsified in a power stirrer (Fisaton Mod.713D, São Paulo, Brazil) at 5.000 rpm for 10 minutes.

Kraft Paper/Film Packaging Systems - Sheets of Kraft paper (0.045m^2) were coated with filmogenic suspensions of chitosan equivalent to 2.6 or 3.5g/m^2 (each coated sheet) using a 40µm wire bar coater (TKB Erichsen, Brazil). The coated paper sheets were dried at over T=200ºC for 1 minute.

Coating Evaluation – Colored Solution Penetration - Uncoated and coated Kraft paper was cut in a 10x10 cm sheets 0.5% of rhodamine in isopropanol solution was applied to the whole coated paper sheet, using a cotton swab held by metallic tweezers. The uniformity of coating was evaluated by the presence of reddish spots on the opposite surface, indicating leak or capillary penetration of the solution[7].

Scanning Electron Microscopy - Kraft paper sheets, both uncoated and coated with 3.5g/m^2 chitosan, were cut and the microstructure was analyzed using Scanning Electron Microscopy (SEM) with LEO equipment, model LEO 440i, under the following conditions: tension = 15KV, distance = 25mm, current = 200pA.

Pre-conditioning - The uncoated and coated Kraft paper sheets were previously conditioned at 23±1ºC and 50±2% relative humidity had been before analysis, in accordance with ASTM D 685-93 standard method[8].

Water Vapor Permeability Rate (WVPR) - WVPR was determined based on standard gravimetric method E96-05[9]. The results were expressed in gH_20/(m^2 day). There were at least five replicates per experiment and one control.

Water Absorption – Cobb Test - Water absorption capacity was determined in accordance with standard T 441 om-90[10]. The results were expressed in g/m^2. There were at least ten replicates per experiment.

RESULTS AND DISCUSSION

Coating Evaluation. The homogeneity and uniformity of chitosan coating on the Kraft paper surface were investigated by evaluating the permeation of the paper of the colored solution of rhodamine B. A larger number of colored spots was observed on the back of the surface of Kraft C3 than on the back surface of the Kraft C4 (Figure 1), since after one contained a higher load of chitosan 3.5g/m^2 than Kraft C3. Chitosan films applied on Kraft papers improved paper surface properties[11].

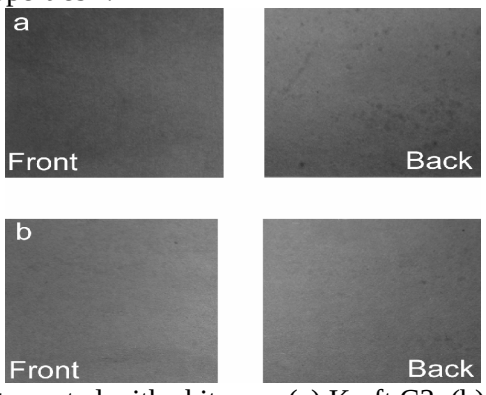

Figure 1: Kraft paper sheets coated with chitosan: (a) Kraft C3, (b) Kraft C4.

Microstructure

Image analysis by SEM was initially employed to observe the surface of uncoated and coated Kraft paper sheets. The effect of chitosan coating on Kraft paper was clearly observed through the SEM image analysis (Figure 2). Chitosan was deposited on the heterogeneous surface of

the original uncoated Kraft paper sheet, characterized by a cellulose fiber interlacement (Kraft CF, Figure 2a, 2b and 2c). However, the increase in the concentration of chitosan suspension from 4% led to a higher solids concentration on the paper (from 3.5g/m^2 (wet basis), Kraft C4). The paper coated shows a uniform and homogeneous surface (Figure 2d, 2e and 2f).

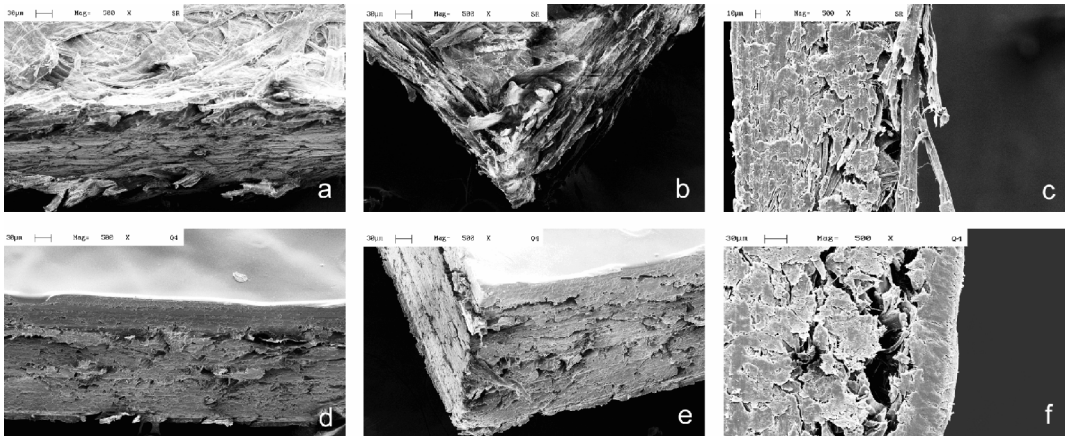

Figure 2. Micrographic images of Kraft paper packaging systems: series a, b, c – uncoated paper; series d, e, f – coated Kraft C4.

Water Vapor Permeability Rate

Coating with plain chitosan was able to reduce the WVPR from 1073 gH_2O/m^2 day for the uncoated Kraft paper to 710 gH_2O/m^2 day for the Kraft C3 and 606 gH_2O/m^2 day for the Kraft C4, representing a 34% and a 44% reduction, respectively (Table 1). The WVPR analyses were performed at 23ºC and 75%rh. First, the concentration of chitosan was evaluated for the Kraft CF, Kraft C3 (2.6g/m^2), and Kraft C4 (3.5g/m^2). This effect could be explained by the microstructure of the coated papers and the pores filled with chitosan. The total solid per unit of area influenced the WVPR of chitosan films[4]. Similar value was obtained by Vartiainen *et al*.[12] that applying 1.5g/m^2 of chitosan solution on a 80g/m^2 of copy paper, the WVTR was 681 gH_2O/m^2 day determined at typical storage conditions for apples and kiwis.

Water Absorption Capacity-Cobb

In cellulosic materials, water absorption depends on either the type of cellulose when used the applied coating. The water absorption indicates the water resistance of coated paper when it directly contacts with water. Cobb tests were performed on the Kraft CF and the coated Kraft C3, Kraft C4, Kraft C4+SA 0.2, Kraft C4+PA 0.2, Kraft C4+PA 0.9 and Kraft C4+PA 1.8 (Table 1). Chitosan coating was able to reduce water capacity up to 35%, when using 2.6 g/m^2 for Kraft paper. Good results were obtained by Matsui *et al*.[13] by impregnating recycled Kraft paper with starch acetate with a fourfold improvement in the water absorption rate. Here in our work, the incorporation of both lipids, stearic and palmitic acids, into the formulation did not statistically reduce water absorption values.

Table 1. WVPR and water absorption of coated and uncoated Kraft paper packaging systems.

Paper Samples	WVPR (gH_2O/m^2 day)	Water absorption (g/m^2)
Kraft CF	1074.32 ± 51.09 [a]	38.98 ± 4.06 [a]
Kraft C3	710.14 ± 70.09 [b]	24.67 ± 3.37 [b]
Kraft C4	606.03 ± 31.82 [c]	30.06 ± 5.05 [c]
Kraft C4+SA 0.2	658.91 ± 31.79 [bc]	27.07 ± 1.97 [c]
Kraft C4+PA 0.2	527.36 ± 31.15 [c]	26.24 ± 3.45 [c]
Kraft C4+PA 0.9	627.57 ± 32.10 [bc]	25.59 ± 1.29 [c]
Kraft C4+PA 1.8	553.18 ± 32.15 [c]	23.01 ± 1.63 [d]

[a-d] Means in the same column with different superscripts differ significantly ($p \leq 0.05$) according to Tukey's test.
SA – Stearic acid, PA – Palmitic acid
Kraft CF – Kraft Chitosan free (uncoated paper)
Kraft C3 – Kraft Chitosan 3.0%
Kraft C4 – Kraft Chitosan 4.0%

CONCLUSIONS

The application of chitosan coating (3.5g/m^2, wet basis) on Kraft paper sheets provided a significantly lower. The incorporation of PA into the chitosan film solutions at 1.8g/m^2 improved the properties of Kraft paper even more by further reducing the WVPR and water absorption capacity by 48% and 40%, respectively. Therefore, the chitosan emulsion coating on Kraft paper improved the water barrier properties as compared to uncoated Kraft paper that could be considered an interesting ecofriendly alternative. In comparison with synthetic polymers coated Kraft paper (as polyethylene), the biobased coated package properties.

ACKNOWLEDGMENTS

We are be grateful to Fundação de Amparo à Pesquisa do Estado de São Paulo (Fapesp), Conselho Nacional de Desenvolvimento Científico e Tecnológico (CNPq), Coordenação de Aperfeiçoamento de Pessoal de Nível Superior (CAPES),the Alpha POLYLIFE for funding the research expenses. We also express our gratitude to Fundação de Amparo à Pesquisa do Estado de Minas Gerais (FAPEMIG).

REFERENCES

1. John,M.J.,Thomas,S. Biofibres and biocomposites.*Carb. Pol* **71**, pp.343-364, (2008).
2. Signini, R., Desbrières, J., Campana Filho, S.P. On the stiffness of chitosan hydrocholoride in acid-free aqueous solutions. *Carb Pol* , **43:**4, pp. 351-357 (2008).
3. Cárdenas, G., Amaya, P., Plessing, C., Rojas, C., Sepúlveda, J. Chitosan composite films. Biomedical applications. *J Mat Sci: Mat Med*, **19**, pp. 2397-2405 (2008).
4. Yoshida, C.M.P., Oliveira-Junior, E.N., Franco, T.T. Chitosan Tailor-made films: The effects of additives on barrier and mechanical properties. *Packaging Technology Science*, **22**:3, pp 161-170 (2009).
5. Domard, A., Espuche, E., Despond, S., Cartier, N. *Support covered with chitosan-based coating and method for the production*. Patent Application Publication Unit States US 2005/0084677 A1, (2005).
6. Despond S., Espuche,E.,Cartier, N., Domard, A., Barrier properties of paper-chitosan and paper-chitosan-carnauda wax films. *J Appl Polym Sci*, **98**, pp 704-710 (2005).
7. Matsui, K.N., Lorotonda, F.D.S., Paes, S.S., Luiz, D.B., Pires, A.T.N., Laurindo, J.B. Cassava bagasse-Kraft paper composites: Analysis of influence of impregnation with

starch acetate on tensile strength and water absorption properties. *Carb Polym*, **55**, pp 237-243 (2004).
8. Marcy, J.E. Integrity testing and biotest for heat-sealet containers In: Blakistone, B. Plastic package integrity testing: assuring seal quality *Hemdon.IoPP*, 17p. (1995).
9. ASTM D 685-93- Conditioning paper and paper products for testing, *ASTM Book of Standards*, Philadelphia, PA, (1997).
10. ASTM E96-05 - Standard test methods for determining gas permeability characteristics of plastic film and sheeting, *ASTM Book of Standards*, Philadelphia, PA, (1995).
11. Tappi Test Methods T 441 om-90- Water absorptiveness of sized (non-bibulous) paper and paperboard (Cobb test), *Tappi-Technical Association of The Pulp And Paper Industry*, Atlanta, (1994).
12. Ashori A, Raverty W.D, Vanderhoek N, Ward JV. Surface topography of kenaf (Hibiscus cannabinus) sized papers. *Biores Tech*, **99**, pp 404–410 (2008).
13. Vartiainen, J.;Motion, R.; Kulonen, H.; Ratto, M.; Skytta, E.; Ahuenainen, R. Chitosan-coated paper: Effects of nisin and different acids on the antimicrobial activity. *J Appl Polym Sci*, **94**, pp. 986-993 (2004).

Effect of chitosan on growth and development of highbush blueberry plants

Gustavo Cabrera[1*], Denisse González[2], Carola Silva[2], Yamilé Bernardo[1], Manuel Gidekel[1], Jennifer Osorio[1], Edelio Taboada[3], Juan Carlos Cabrera[4]

[1] VentureLab, Escuela de Negocios, Univ. Adolfo Ibáñez, Santiago de Chile, Chile
[2] Escuela de Agronomía, Facultad de Recursos Naturales, Universidad Católica de Temuco, Temuco, Chile
[3] Escuela de Ingeniería Ambiental, Facultad de Ingeniería, Universidad Católica de Temuco, Temuco, Chile
[4] Unité de Recherche en Biologie Cellulaire Végétale, Facultés Universitaires Notre-Dame de la Paix, Namur, Belgium
*E-mail: gustavo.cabrera@uai.cl.

Abstract
Chitosan is a linear polysaccharide composed of units of glucosamine and N-acetyl-glucosamine linked by β-(1-4) bond, with a predominance of the former. This biopolymer is of natural origin and has become a promising alternative to be used in sustainable agriculture systems. The purpose of this work was to assess the effect of chitosan on the growth and development of highbush blueberry (*Vaccinium corymbosum*) cv. O'Neal when applied in young plants before transplanting. For this purpose a greenhouse trial was carried out using chitosan (DA 94%, Mw 120 kDa) obtained from prawn shell wastes. The polysaccharide was employed at the following concentrations 0.5% (w/v), 1% (w/v) and 1.5% (w/v). Data showed that chitosan application at 1% (w/v) improved stem and root length, bud number, number of leaves, root and shoot dry weight.

INTRODUCTION

Chitosan is a cationic linear polysaccharide composed essentially of β-(1→4) linked glucosamine units together with some proportion of N-acetylglucosamine units. It occurs in nature but it is generally obtained by extensive deacetylation of chitin. Chitin is also a linear polysaccharide composed by β-(1→4) linked N-acetyl-D-glucosamine units, it is present in the shells of crustaceans, mollusks, the cell walls of fungi, and the cuticle of insects [1].
Chitosan is biocompatible, biodegradable, nontoxic and water soluble under acid conditions, which makes it attractive for applications in agriculture. In addition, chitosan can inhibit the growth of an important number of fungal pathogens [2-4], elicit defensive responses [5-6], protect against pathogens in plants [7] and regulates plant growth [8-9].
Northern Highbush blueberry (*Vaccinium corymbosum*) is a species of blueberry native to eastern North America which was cultivated for commercial purposes in Chile. Blueberries are interesting fruit for potential health benefits due to their bioactive compounds (anthocyanins, flavonoids, polyphenols and ascorbic acid) and it's one of the most important export specie from Chile. That is why it's necessary to keep a sustainable production of plants to supply the international growing market. Actually, one of the mayor issues to be solved in order to keep rising the blueberry production in Chile is the necessity of good quality highbush blueberry plantlets producers. One of the problems observed for this crop was the high mortality obtained during plantlets transplantation, which is mainly due to the lack of a good radical system in plants or to the poor shoot development.
The purpose of the current study was to evaluate the growth and development of Highbush blueberries *(Vaccinium corymbosum*) cv. O´Neal plantlets when different concentrations of chitosan were applied to the roots of plantlets.

MATERIALS AND METHODS

Chitosan (DA 94%, Mw 120 kDa) was obtained by extensive deacetylation of chitin isolated from shells of the Chilean prawn shell wastes [10]. The polymer was dissolved in acetic acid and pH adjusted to 5,6 with diluted NaOH (0,5 M).

Completely randomized block assay was carried out using 10 plants per treatment having three replicates per each treatment. The experiment was carried out in 2009 season at the greenhouse of the farm Agrícola Bosbes Ltda, sited in Santiago of Chile. For this purpose, 60 days old Highbush blueberries *(Vaccinium corymbosum*) cv. O´Neal plantlets were selected. The plant roots were washed with water and then dipped in chitosan solutions during 20 seconds. After that, the plants were planted in plastic containers of 1L capacity using sterilized soil. The control treatment (T0) was fertilized with the same fertilizer mixture (complete N, P, K) used for production conditions in this farm. Chitosan concentrations used in greenhouse experiments were 0,5 % (w/v) (T1), 1,0 % (w/v) (T2) and 1,5 % (w/v) (T3). The stem length (SL), the buds number per plant (BN) and the leaves number per plant (LN) were measured using 30 plants per treatment. The root length (RL), the root dry weight (RDW), the leaves area index (LA) and the shoot dry weight (SDW) were measured using five plants per each replicate.

The results were statistically analyzed using SPSS for Windows version 15.0 software. A simple ANOVA and the Duncan´s Multiple Range Test comparison procedures were carried out in order to compare the different treatments used. In tables, different letters denote statistically significant difference at the 95% confidence level.

RESULTS AND DISCUSSION

The chitosan effects on the number of leaves per plant (LN) are shown in Fig. 1. It could be observed that plants which received the T2 treatment showed 40% more leaves per plant than control. Besides, it showed significant differences with all treatments. However, the other chitosan treatments didn´t show differences with control.

The chitosan effects on the leaves area are shown in Fig. 2. In this case all chitosan treatments showed higher leaf area index than control (T0) and a significant difference with T0 was observed. Both results indicates a foliar stimulating activity of chitosan which is in agreement with previously published results [11].

The chitosan effects on BN are shown in Fig. 3. The T2 treatment showed the best performance stimulating the production of higher amount of buds per plant. This treatment also showed significant differences with T0 and T1 treatments producing one bud more per plant than both of them.

Table 2 shows the results obtained for the root length (RL), stem length (SL), root dry weight (RDW) and shoot dry weight (SDW) for treated and control blueberry plants. The average root length of plants treated was slightly higher than untreated ones being T3 the best treatment; however, no significant enhancements were obtained among treatments.

Regarding the SL parameter all treated plants were higher than control but no significant difference was obtained among them. However, it is worth to note than differences higher than 3cm in stem length were obtained for chitosan treated plants respect to T0 treatment.

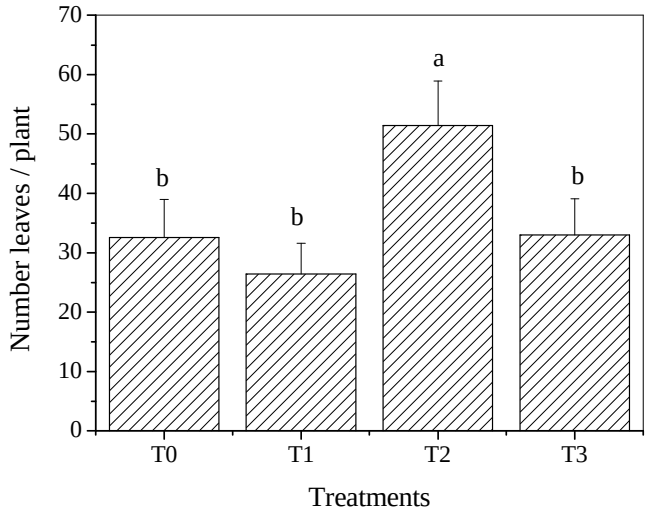

Figure 1. Effect of chitosan on the number of leaves per plant (LN) 60 days after applying chitosan to blueberry roots.

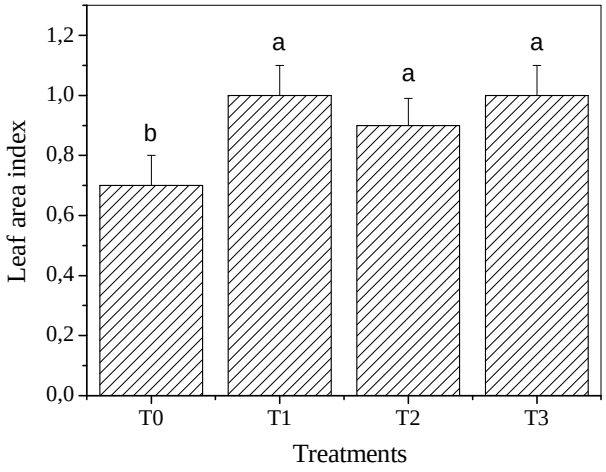

Figure 2. Effect of chitosan on leaf area index at 60 days after applying chitosan to blueberry roots.

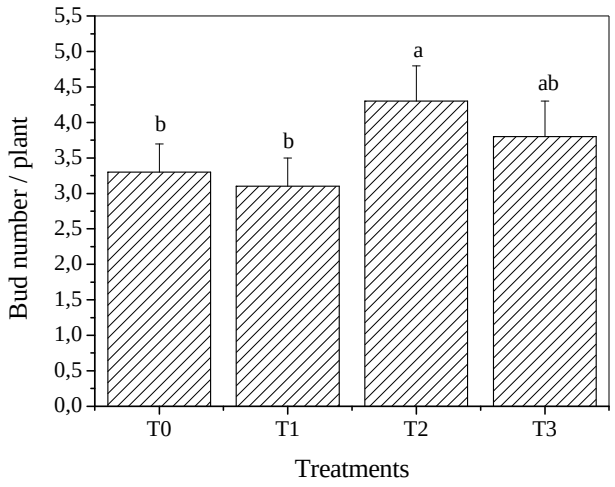

Figure 3. Effect of chitosan on the bud number per plant at 60 days after applying the product in blueberry roots.

Table 2: Development parameters measured at 60 days after applying chitosan to the blueberry roots

Treatments	RL	SL (cm)	SDW (g)	RDW (g)
T0	21,2 ± 1,4 a	25,6 ± 3,6 a	2,8 ± 0,2 a	0,8 ± 0,1 b
T1	21,4 ± 1,7 a	28,1 ± 3,2 a	2,1 ± 0,2 b	0,7 ± 0,1 b
T2	21,5 ± 1,5 a	29,2 ± 3,1 a	3,1 ± 0,3 a	1,2 ± 0,2 a
T3	22,6 ± 1,5 a	29,4 ± 3,5 a	2,9 ± 0,2 a	1,1 ± 0,1 a

Different letters denote statistically significant difference at the 95% confidence level according to Duncan test.

In case of shoot dry weight (SDW), T2 was the best treatment showing significant differences with T1 but not with T0 and T3 treatments, respectively. This result is in agreement with those presented in figures 1 and 2. Both factors (higher number of leaves and leaf area) could contribute to a more photosynthesate production which reflects on higher shoot dry weight in T2 treated blueberry plants [11].

Regarding the RDW parameter it could be observed that chitosan treatments at concentrations higher than 1% (w/v) (T2 and T3) showed significant differences with T0 and T1, respectively. This fact indicates that treated blueberry plants increase the overall radical system at the same time of promoting plant growth. A highly developed radical system allow blueberry plants to increase mineral, vitamins and water uptake from soil and thus producing plants of higher quality before transplanting; which in turn should contribute to increase the surviving rate of blueberry plants.

These data agrees with previously published results in which a positive effects of chitosan incorporated into the soil on early growth stages of soybean, mini-tomato, upland rice and lettuce was reported [12]. These improvement included plant height, leaf area, and dry weight of plants. A similar trend was recently obtained by other authors [11], which observed that leaf area and plants dry weight increased in strawberry plants treated with chitosan. Furthermore, it had been reported that chitosan also promoted growth of various crops such as cabbage [13], soybean sprouts [14] and sweet basil [15].

Finally, it was observed that the degree of plants responses differed according to the applied concentration of chitosan, being better at 1% (w/v) polymer concentration in this work. This response was also known to differ by crop, chitosan molecular weight and concentration [12, 15-17], respectively.

CONCLUSIONS

The results suggest the beneficial effect of using chitosan at 1% (w/v) concentration to treat blueberry plants growth under greenhouse conditions because it promotes plant vegetative development. Such effect was account by improving both the blueberry plant foliage and rooting system. A higher production of buds per plant was also observed suggesting this treatment could be a good alternative for blueberry plantlets treatment before transplanting.

REFERENCES

1. M. Rinaudo (2006), *Progress in.Polymer Science*, 31, 603–632.
2. El Gaouth A, Arul J, Asselin A, Benhamou N (1992). *Mycological Research* 9:769–779.
3. Park R, Kyu-Jong J, You-Young J, Yu-Lan J, Kil-Yong K, Jae-Han S, Yong-Woong K (2002). *Journal of Microbiology and Biotechnology*. 12:84–88.
4. A. Falcón, J.C. Cabrera, D. Costales, M. Ramírez, G. Cabrera, M.A. Martínez-Téllez (2008).. *World Journal of Microbiology and Biotechnology* 24, 103-112.
5. Kauss H, Jeblick W, Domard A (1989). *Planta* 178:385–392.
6. A. Falcón-Rodríguez, J. C. Cabrera, E. Ortega and M. Martínez-Téllez (2009). *American Journal of Agricultural and Biological Sciences* 4 (3): 192-200,.
7. Ben-Shalom N, Ardi R, Pinto R, Aki C, Fallik E (2003). *Crop Protection* 22:285–290.
8. Ohta K, Morishita S, Suda K, Kobayashi N, Hosoki T (2004). *Journal of Japan Society of Horticultural Science*, 73:66–68.
9. Chibu H, Shibayama H, Arima S (2002). *Japan Journal of Crop Science*, 71:206–211.
10. E. Taboada, G. Cabrera, R. Jimenez, G. Cárdenas (2009). *Journal of Applied Polymer Science* 144 (4), 2043-2052.
11. Abdel-Mawgoud AMR, Tantawy AS, El-Nemr MA, Sassine YN (2010). *European Journal of Scientific Research*, 39 (1), 161-168.
12. Chibu H, Shibayama H, (2001). *in*: T. Uragami, K. Kurita, T. Fukamizo (Eds.), *Chitin and Chitosan in Life Science, Yamaguchi,* pp. 235–239.
13. Hirano S (1988). *Nippon Nogeikagaku Kaishi*, 62, 293-295.
14. Lee YS, Kim YH, Kim SB (2005). *HortScience* 40, 1333-1335.
15. Kim HJ, Chen F, Wang X, Rajapakse NC (2005). *Journal of Agricultural and Food Chemistry* 53, 3696-3701.
16. Walker R., Morris S., Brown P., Gracie, A. (2004). *Publication No. 04.of Rural Industries Research and Development Corporation. Australia.* pp. 55.
17. Quang L. L., Naotsugu N., Masao T., Tomoko N. (2006). *Radioisotopes* 55 (1):23-27.

Characterization of quaternized chitosan-stabilized iron-oxide nanoparticles as a novel potential MRI contrast agent for cell tracking

Chia-Rui Shen[1,2], Shu-Ting Wu[1], Zei-Tsan Tsai[2], Tzu-Chen Yen[2], Jin-Sheng Tsai[3] and Chao-Lin Liu[4*]

[1] Department of Medical Biotechnology and Laboratory Science, Chang Gung University, Taoyuan, Taiwan.
[2] Molecular Imaging Center, Chang Gung Memorial Hospital, Taoyuan, Taiwan.
[3] National Synchrotron Radiation Research Center, Hsinchu, Taiwan.
[4] Department of Chemical Engineering and Graduate School of Biochemical Engineering, Ming Chi University of Technology, Taipei, Taiwan.
*E-mail: f2402002@ms16.hinet.net

Abstract
The polymer-stabilized iron-oxide nanoparticles could be used as contrast agents in magnetic resonance (MR) imaging due to their unique superparamagnetism. Here we demonstrate a quaternized chitosan (N-[(2-hydroxy-3-trimethylammonium) propyl] chitosan chloride) encapsulating superparamagnetic iron oxide (SPIO), with very low toxicity and less effect on cell growth. N-[(2-hydroxy-3-trimethylammonium) propyl] chitosan chloride has quaternary amino groups introduced into the chitosan chain, and such modification on chitosan should render it soluble in water. Most importantly, such preparation of SPIO present the great ability to accelerate the MR relaxation processes of surrounding water protons, resulting in enhanced MR imaging contrast (R2: y = 0.1076x - 0.0092; R1: y = 0.008x - 0.0005) . Also, the intracellular iron content was quantified by Prussian blue staining as well as MR imaging, and revealed the positive correlation between Prussian blue positive cells and the changing of MR intensity signals. Transmission electronic microscopy (TEM) analysis and element mapping confirmed the intracellular metal-like spots as the internalized iron oxide. Such findings support these quaternized chitosan-stabilized iron-oxide nanoparticles with potential as a MR contrast agent.

Keywords: cell tracking, contrast agent, iron-oxide, MRI, nanoparticles, quaternized chitosan

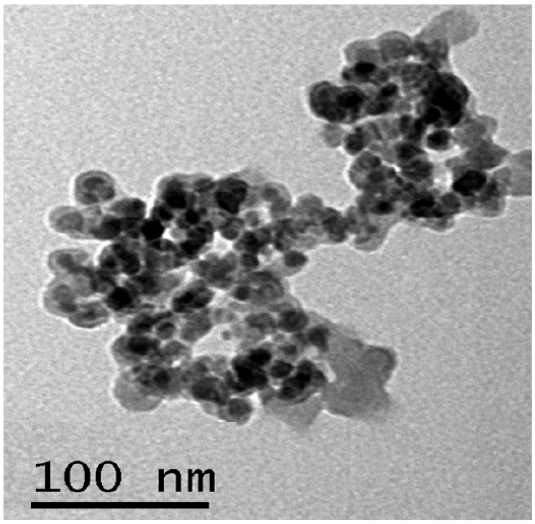

Figure 1. TEM analysis of N-[(2-hydroxy-3-trimethylammonium) propyl] chitosan chloride encapsulated-SPIO.

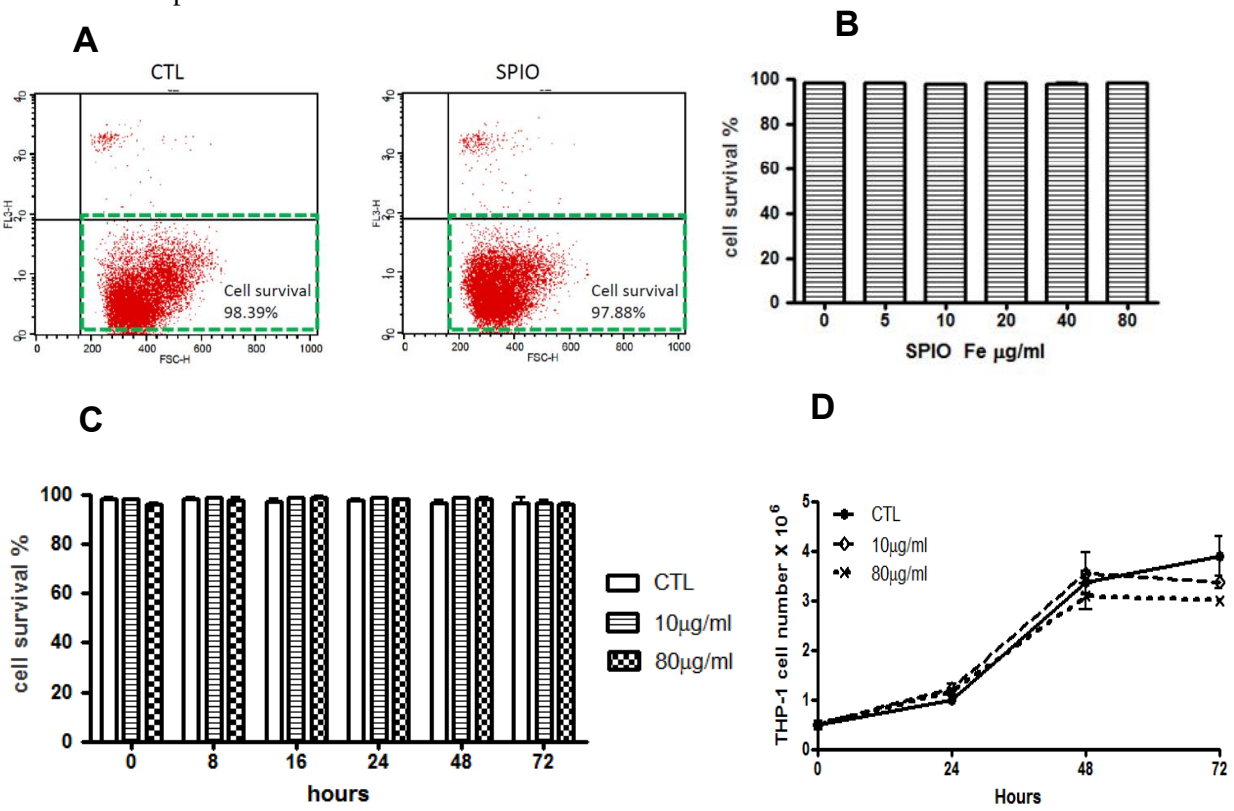

Figure 2. Minimal effects of HTCC-SPIO loading on cell survival and growth. (A) The representative flow cyometric analysis on cell survival by propidium iodide (PI) staining. (B) Less or none effect of different doses of SPIO loading on cell survival. (C) Time-kinetic studies revealed the addition of 10 or 80µg/ml of SPIO with very low toxicity or effect on cell survival and (D) cell growth.

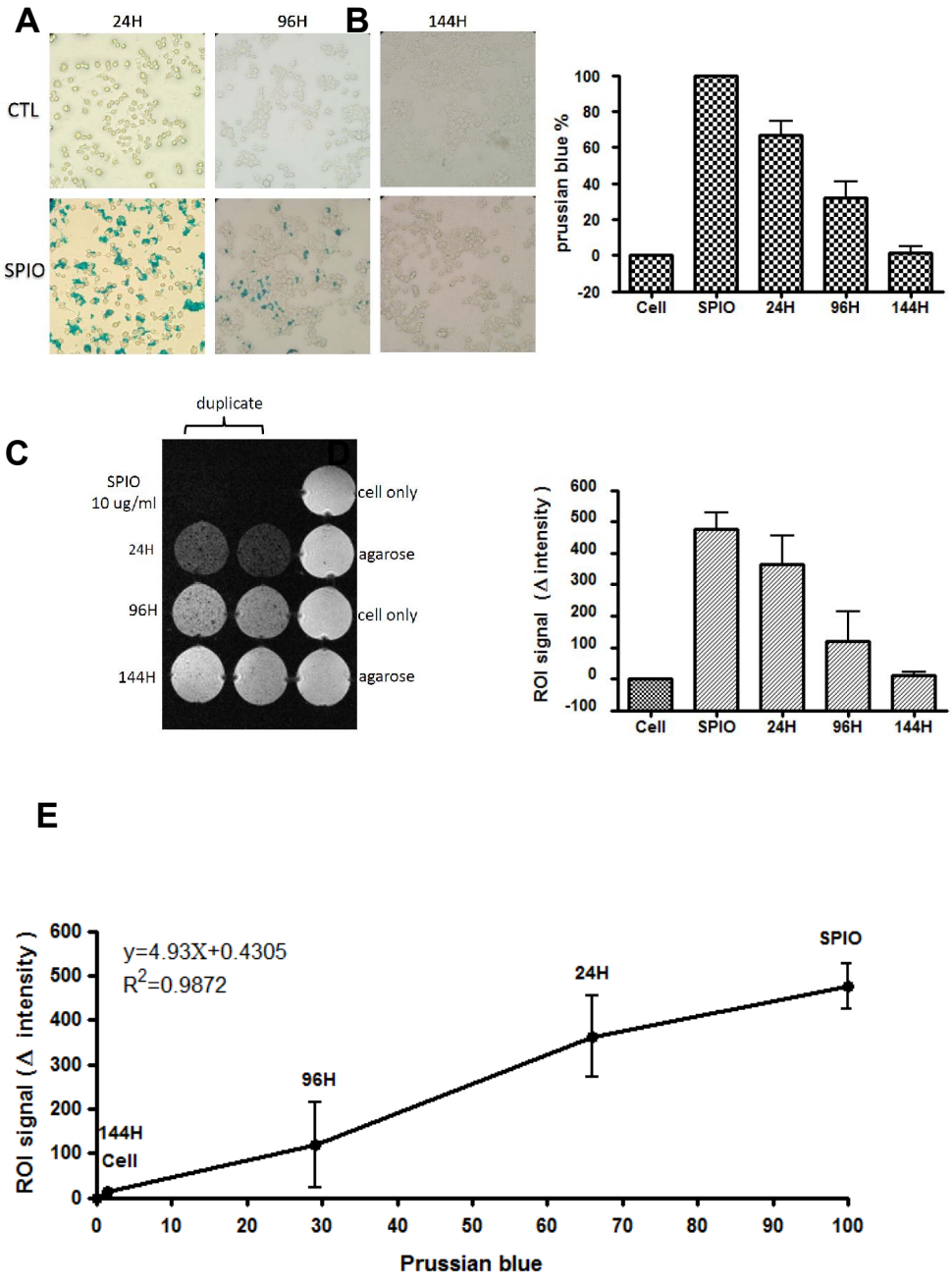

Figure3. The positive correlation on intracellular iron content and MR signals. (A) The intracellular iron content analyzed by Prussian blue staining. (B) The decreasing percentage of Prussian blue positive cells associating with the intracellular iron content in SPIO loaded cells following cell division. (C) The intracellular iron content quantified by MR imaging. (D) The reducing ROI (region of interest) intensity of MR signal correlating with SPIO loaded cells following cell division. (E) Correlation analysis on Prussian blue positive cells and the intensity changing of MR imaging signals.

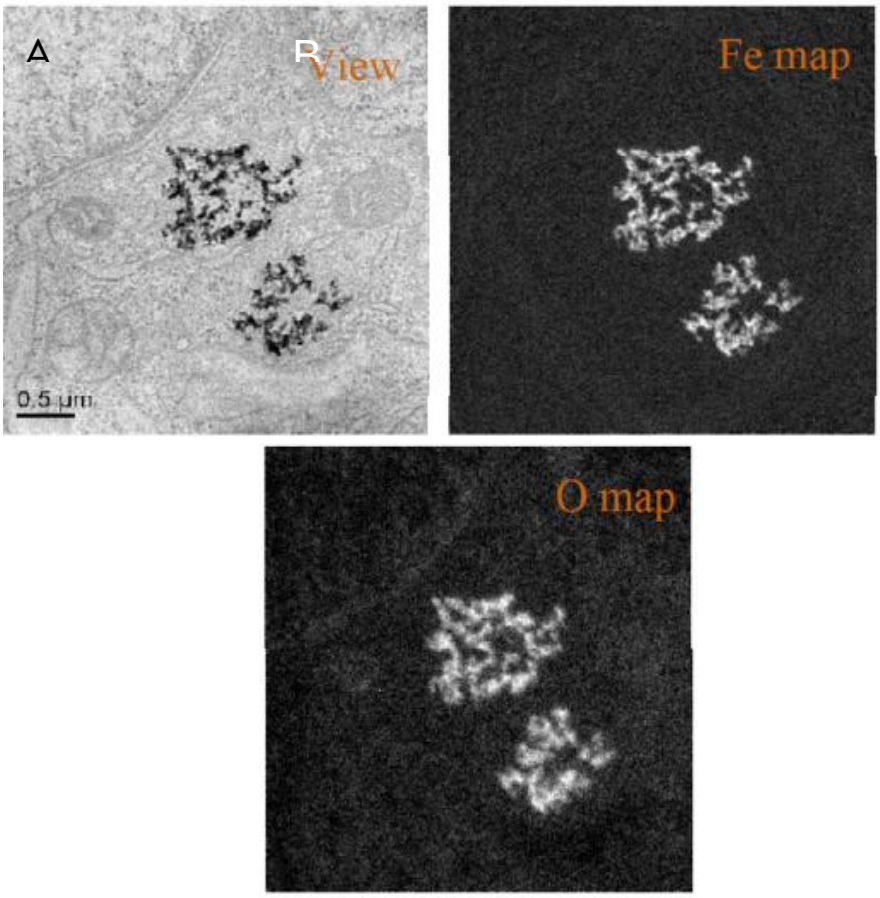

Figure 4. TEM analysis and element mapping of intracellular iron oxide in the cells loaded with SPIO. (A) TEM analysis of the cells loaded with SPIO. (B) Fe mapping and (C) O mapping of intracellular iron oxide in the cells loaded with SPIO.

REFERENCES

1 Ravi Kumar MNV, Muzzarelli RAA, Muzzarelli C, Sashiwa H and Domb A, *Chem Rev* **104:** 6017-6084 (2004).
2 Lim SH, and Hudson SM, *Carbohydr Polym* **339:** 313-319 (2004).
3 Xu Y, Du Y, Huang R and Gao L, *Biomaterials* **24:** 5015-5022 (2004).
4 Belessi V, Zboril R, Tucek J, Mashlan M, Tzitzios V and Petridis D, *Chem Mater* **20:** 3298-3305 (2008).
5 Tsai ZT, Wang JF, Kuo HY, Shen CR, Wang JJ, Yen YC, *J Magn Magn Mater* **322:** 208–213 (2010).

Platelet lysate formulation based on chitosan for the treatment of buccal lesions: in vitro evaluation

C.M. Caramella[1,*], F. Ferrari[1], M.C. Bonferoni[1], S. Rossi[1], G. Sandri[1], M. Mori[1], C. Perotti[2], C. Delfante[2]

[1] Department of pharmaceutical chemistry, University of Pavia, Viale Taramelli 12, Pavia, Italy

[2] Immunohaematology And Transfusion Service, Apheresis And Cell Therapy Unit, Fondazione IRCCS Policlinico S. Matteo, Viale Golgi 19, Pavia, Italy

***E-mail:** Carla.caramella@unipv.it

INTRODUCTION

Platelets are specialized secretory cells that release, in response to activation, a large number of biologically active substances from intracellular alpha-granules. Among these substances, a very important category is represented by growth factors (GFs). They in fact initiate and modulate tissue repair mechanisms such as chemotaxis, cell proliferation, angiogenesis, extracellular matrix depositing and remodelling [1]. A large number of platelet GFs have been until now isolated, studied and characterized. Among these, most intensively investigated are PDGF (platelet derived growth factor), TGF-α and β (transforming growth factors alpha and beta), PDEGF (platelet-derived epidermal growth factor), EGF (epidermal growth factor), VEGF (vascular endothelial growth factor), IL-8 (inteleukin-8), TNF-α (tumor necrosis factor alpha). Some of these GFs are available in purified form, but it has been pointed out that tissue repair cannot be effectively mediated by a single agent, as multiple signals are required to complete the regeneration process (1). To better exploit the whole potential of the naturally occurring platelet GFs, the therapeutic employment of platelet rich preparations has been suggested. These are hemoderivatives from which platelets can release their complete pull of biologically active substances.

For these reasons platelet lysate (PL) and platelet rich plasma (PRP) are proposed in the treatment of soft and hard-tissue surgical conditions and in the management of non-healing wounds.

Aim of the work was to develop a formulation suitable to maintain PL in contact with injured tissues for a time suitable to treat lesions of oral cavity. This represents a challenge because of salivation and its washing effect. Therefore the residence time of the formulation is crucial to assure the contact of the actives with the injured tissues for a sufficient time duration so as to exert the therapeutic effect.

Chitosan was proposed as a gel base because of its well known mucoadhesive and wound healing properties [2, 3].

Rheological and mucoadhesive properties were featured to improve the resistance towards the removal effect of salivary flux. The healing enhancement properties of the vehicle with the PL were evaluated on fibroblast cell line in an in vitro wound healing model.

MATERIALS AND METHODS

Polymers: Chitosan glutamate 213 (CSG) (MW: 300 kDa, acetylation degree: 15%, acid glutammic content: 35-50%) (Protasan G213, Pronova Biomedical AS, Oslo, Norway); Hydroxy propyl methyl cellulose (HPMC), Methocel K100M CR, Premium, Colorcon Limited).

Platelet Lysate (PL): Pool of platelet aliquots (sterile connection technique) was obtained by platelet apheresis procedures performed on regular blood donors (high platelet concentration

in little plasma volume and minimal leukocyte contamination). Platelet pool was frozen at –80°C for at least 5 hours and subsequently defrozen in a sterile water bath at 37°C, then was diluted 1:1 with saline solution to obtain a final platelet concentration ≅500-600x10^3/µl.

Preparation of vehicle and formulation: CSG vehicle was prepared in saline solution (0.9% w/v NaCl) using CSG at 6% w/w and HPMC at 2% w/w (Ph 5.5). The vehicle was sterilized using steam sterilization at 121°C for 15 minutes (Alpha Junior, PBIInternational, I). The formulation was based on 1:1 mixture of vehicle and PL obtaining a final concentration of CSG and HPMC of 3% w/w and 1% w/w respectively. The concentration of platelet derived growth factor PDGF AB in the formulations was evaluated by means of ELISA test (Human PDGF-AB Quantikine PharmPak, R&D systems, Minneapolis, MN, USA; assay range: 31.2-2000 pg/ml).

Rheological characterization: The viscosity of formulation was measured using a rotational rheometer (Rheostress 600, Haake, I) equipped with a cone plate combination (C35/1°) at 25°C at 100 s^{-1}.

Mucoadhesion measurements: The mucoadhesive properties of the vehicle and the formulation were investigated by TA-XT2 Plus Texture Analyser (Stable Micro Systems, I). The samples were layered on a filter paper fixed with double sided adhesive tape on the bottom of the upper probe. Either buffer solution pH 6.4 mimicking saliva or 8% (w/w) mucin (type II crude, Sigma Aldrich, I) solution in the same buffer was placed on a filter paper attached to the lower probe. After a prefixed time contact at a prefixed pre-load between the two surfaces, the upper probe was moved upwards at a prefixed rate and the detachment force was determined.

In vitro wound healing test: Fibroblasts were seeded in the 2 chambers (at 10^5 cells/cm^2) of an insert that are divided by a septum of 500 µm ± 50 µm.

After 24 h, at confluence, the insert was removed displaying 2 distinct areas of cell substrates divided by the prefixed gap. Cell substrates were put in contact with 200 µl of PL at 1/20 concentration and PL CGS diluted to have the same PL concentration of PL. At prefixed times (0, 24, 48, 72 h) microphotographs were taken to evaluate cell growth in the gap.

RESULTS AND DISCUSSION

The viscosity of CGS vehicle at 100 s^{-1} is 11.21 Pa.s (sd±0.39) and that of the formulation is 2.34 Pa.s (sd±0.20). These properties should allow a good resistance of the formulation towards the mechanical effect of salivary flux and an easy spreading on the buccal mucosa.

The mucoadhesive parameter Fmax measured for the vehicle is 2469.9 mN (sd±204.5) in presence of mucin and 1109.4 mN (sd±238.3) in blank measurements and that of the formulation is 2377.5 (sd±101.9) in presence of mucin and 1005.4 (sd±217.3) in blank measurements indicating that both the vehicle and the formulation are characterized by good mucoadhesive properties and that the dilution of the vehicle with PL does not impair CGS capability to form the mucoadhesive joints.

PL batch used to prepare formulation contained PDGF AB at 23701±1105 pg/ml. In the formulation the concentration of PDGF AB was 27760±2096 pg/ml and not significantly different from PL, which indicates that the presence of CGS did not affect PDGF AB concentration.

This result suggests that the presence of the polymers did not alter the structure of PDGF AB and so it is conceivable that they do not alter the activity of PDGF AB. It could be argued that the effect of the polymers on the other growth factors would be similar.

Figure 1 shows the microphographs of the gaps in fibroblast substrates in contact with: a) PL at 1/20 concentration, b) PL CGS at PL concentration of 1/20 after 24, 48 and 72 h of contact time. At 24 h fibroblasts started to invade the gap both in the substrate in contact with PL and

in the substrate in contact with the formulation. At 48 h the invasion of the fibroblasts was complete and the gap could not be seen any more in either substrates. At 72 h the cells were subconfluent in both substrates.

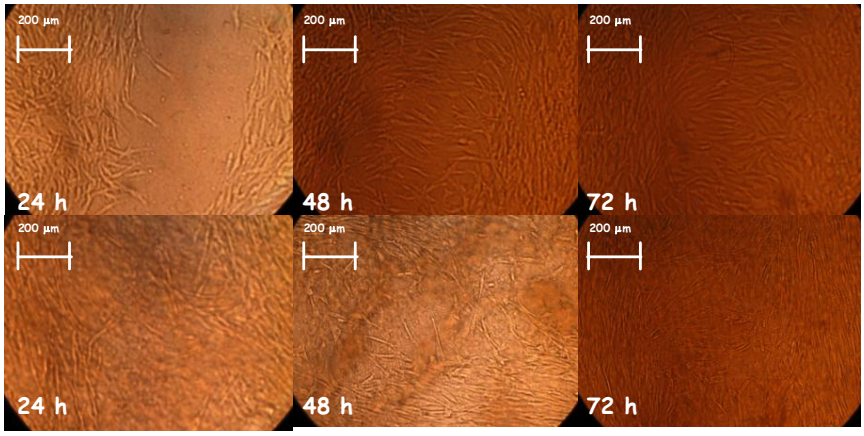

Figure 1: Microphotographs of gaps in fibroblast substrates after 24, 48 and 72 h contact with: PL at 1/20 concentration (upper series of microphotographs) and PL CGS at PL concentration of 1/20 (lower series of microphotographs)

CONCLUSIONS

The rheological and mucoadhesive properties of PL CGS formulation suggest that it should possess suitable properties to hinder removal action of salivary flux and to maintain and prolong the contact of PL with the damaged mucosa of the oral cavity. Chitosan vehicle was compatible with PDGF AB growth factor. The wound healing effect induced by PL CGS formulation was fast and analogous to that of PL. These in vitro studies indicate that platelet lysate loaded in chitosan vehicle has a positive effect on regeneration properties.

ACKNOWLEDGEMENT

The authors wish to thank Cariplo Foundation for the financial support (Project title: "Platelet gel bioadhesive systems for mucositis in chemio/radio therapy and stem cell trasplantation" call 2006).

REFERENCES

1. Anitua E, Sanchez M, Nurden AT, Nurden P, Orive G, Andia I. Trends in Biotechnology 24 (2006) 227.
2. Ueno H, Mori T, Fujinaga T. Adv Drug Del Rev 52 (2001) 105.
3. Minagawa T, Okamura Y, Shigemasa Y, Minami S, Okamoto Y. Carbohydr Polym 67(2007) 640.